Transmitter Based Techniques for ISI and MAI Mitigation in CDMA-TDD Downlink

Stamatis L. Georgoulis

A thesis submitted for the degree of Doctor of Philosophy.
The University of Edinburgh.
January 2003

Abstract

The third-generation (3G) of mobile communications systems aim to provide enhanced voice, text and data services to the user. These demands give rise to the complexity and power consumption of the user equipment (UE) while the objective is smaller, lighter and power efficient mobiles. This thesis aims to examine ways of reducing the UE receiver's computational cost while maintaining a good performance.

One prominent multiple access scheme selected for 3G is code division multiple access. Receiver based multiuser detection techniques that utilise the knowledge of the downlink channel by the mobile have been extensively studied in the literature, in order to deal with multiple access and intersymbol interference. However, these techniques result in high mobile receiver complexity.

Recently, work has been done on algorithms that transfer the complexity from the UE to the base station by exploiting the fact that in time division duplex mode the downlink channel can be known to the transmitter. By *linear precoding* of the transmitted signal the user equipment can be simplified to a filter matched to the user's spreading code. In this thesis the problem of generic linear precoding is analysed theoretically and a method for analytical calculation of BER is developed. The most representative of the developed precoding techniques are described under a common framework, compared and classified as bitwise or blockwise. Bitwise demonstrate particular advantages in terms of complexity and implementation but lack in performance. Two novel bitwise algorithms are presented and analysed. They outperform significantly the existing ones, while maintain a reduced computational cost and realisation simplicity. The first, named inverse filters, is the Wiener solution of the problem after applying a minimum mean squared error criterion with power constraints. The second recruits multichannel adaptive algorithms to achieve the same goal. The base station emulates the actual system in a cell to converge iteratively to the pre-filters that precode the transmitted signals before transmission. The advantages and the performance of the proposed techniques, along with a variety of characteristics are demonstrated by means of Monte Carlo simulations.

Declaration of originality

I hereby declare that the research recorded in this thesis and the thesis itself was composed and originated entirely by myself in the Department of Electronics and Electrical Engineering at the University of Edinburgh.

The software used to perform the simulations was written by myself with the following exceptions:

- The routines used to generate uniform and Gaussian distributed pseudo-random samples were obtained from *Numerical recipes in C*[1].

Stamatis Georgoulis

to my parents Leandros and Margarita.

στους γονείς μου Λέανδρο και Μαργαρίτα.

Acknowledgements

First and foremost, I wish to thank my supervisor Dr. Dave Cruickshank whose continuous and patient guidance as well as his timely advice contributed greatly to the completion of this thesis. Also, my second supervisor Prof. Stephen McLaughlin for his advice and guidance when Dr. Cruickshank was away, and for reviewing the manuscript.

I would like to thank the Faculty of Science and Engineering at Edinburgh University for providing the financial support without which I would not have been in the position to commence and complete this Ph.D. project.

Special thanks to my colleagues and friends in the *Signals and Systems Group* for sharing their knowledge and a pleasant time in our office.

I express my sincere gratitude to my grandfather Apostolos and my uncle Antonis for their small financial help that added quality in my life during the three years in Edinburgh.

Last but not least, I wish to thank my parents Leandros and Margarita for their relentless support, priceless guidance and boundless love.

Contents

List of figures

List of tables

Acronyms and abbreviations

3G	Third-Generaration
3GPP	Third-Generaration Partnership Project
AMPS	Advanced Mobile Phone Services
ARQ	Automatic Repeat Request
AWGN	Additive White Gaussian Noise
BER	Bit Error Ratio
BPSK	Binary Phase Shift Key
BS	Base Station
CDMA	Code Division Multiple Access
DPF	Decorrelating Prefilters
DS	Direct Sequence
ETACS	European Total Access Communication System
ETSI	European Telecommunications Standards Institute
FDD	Frequency Division Duplex
FDMA	Frequency Division Multiple Access
FEC	Forward Error Control
FH	Frequency Hopping
FIR	Finite Impulse Response
FPLMTS	Future Public Land Mobile Telecommunications Service
FTF	Fast Transerval Filter
GSM	Global System for Mobile communications
IMT	International Mobile Telecommunications
INVF	Inverse Filters
IS	Interim Standard
ISI	Intersymbol Interference
ITU	International Telecommunications Union
JD	Joint Detection
JOS	Jointly Optimised Sequences
JT	Joint Transmission

JTACS	Japanese Total Access Communication System
KKT	Karush-Kuhn-Tucker
LAN	Local Area Network
LMS	Least Mean Squares
MAI	Multiple Access Interference
MC	Multichannel
MC-LMS	Multichannel-Least Mean Squares
MC-RLS	Multichannel-Recursive Least Squares
MLSE	Maximum-likelihood Sequence Estimation
MMSE	Minimum Mean Squared Error
MS	Mobile Station
MSC	Mobile Switching Center
MUD	Multiuser Detection
NMT	Nordic Mobile Telephone
NTT	Nippon Telephone and Telegraph
PDC	Personal Digital Cellular
PIC	Parallel Interference Cancellation
PN	Pseudo-Noise
QPSK	Quadrature Phase Shift Keying
SD	Single Detection
SIC	Serial Interference Cancellation
SNIR	Signal to Noise plus Interference Ratio
SNR	Signal to Noise Ratio
SS	Spread Spectrum
TACS	Total Access Communication System
TDD	Time Division Duplex
TDMA	Time Division Multiple Access
TH	Time Hopping
TP	Transmitter Precoding
UE	User Equipment
UMTS	Universal Mobile Telecommunications System
UTRA	UMTS Terestial Radio Access
W-CDMA	Wideband-Code Division Multiple Access

XOR	EXclusive OR
ZF	Zero Forcing
rms	Root Mean Square

Nomenclature

$\mathbf{A}_k$	general matrix for the description of the detected data at the receiver's output
$\mathbf{A}_v$	general matrix that describes the noise after being filtered by the receiver
$\tilde{\mathbf{A}}_k$	matrix that consists of $\gamma_{kj}(n)$ for $j = 1 \dots K$
$\mathbf{B}$	block-diagonal matrix of $\mathbf{B}_k$
$\mathbf{B}_k$	matrix whose columns are the spreading code of kth user plus zeros
$\tilde{\mathbf{B}}$	matrix that consists of $z_k(n)$ samples for $k = 1 \dots K$
$\mathbf{C}$	block-diagonal matrix of $\mathbf{C}_k$
$\mathbf{C}_k$	matrix whose columns are the spreading code of kth user
$\mathfrak{D}_k$	all-zero vector except for a unity entry at position k
$E[\cdot]$	expectation of $\cdot$
$\mathcal{E}_g$	transmission power per user per symbol of a conventional CDMA (no precoding)
E_g	transmission power per user per symbol of a CDMA with precoding
$\sqrt{\mathcal{F}}$	scaling factor to normalise the transmission power of the precoding techniques
G	length of the expanded symbol at the k-user pre-filter output
G_γ	length of expanded symbol of filtered reference outputs
$\mathbf{G}$	arrangement of K matrices $\mathbf{G}_k$
$\mathbf{G}_k$	matrix whose columns are the vector $\mathbf{g}_k$
$\mathbf{H}$	$\mathbf{H}_k$ matrices arranged in a column
$\mathbf{H}_k$	matrix whose columns are the channel impulse response $\mathbf{h}_k$ of kth user
$\mathbf{I}$	identity matrix
J	cost function
J_c	cost function with power constraint
K	total users active in a cell
$\mathbf{K}(T_s^n)$	auxiliary matrix used in the MC-RLS
L	chip-rate sampled length of the channel impulse response
L_s	length of optimally designed signature sequence $\boldsymbol{\zeta}_k$
M	number of bits responsible for intersymbol interference
$\mathbf{M}(T_s^n)$	matrix used in the MC-RLS
N	block of data addressed to one user

N_o	power spectral density
P	pre-filter length
$P_e(\hat{d}_k^m)$	error probability of detected symbol d_k^m
$\bar{P}_e(\hat{d}^m)$	K users system average theoretical error probability
Q	spreading gain
$\mathbf{R}_d$	covariance matrix of data vector $\mathbf{d}$
$\mathbf{R}_v$	covariance matrix of noise vector $\mathbf{v}$
$\mathbf{R}$	matrix that contains all filtered reference signals in an INVF system
Re	denotes the real part of a complex number
T_c	chip period
T_s	symbol period
T_{ss}	sampling time on the receiver
T_s^n	sampling time sequence on the receiver
$\boldsymbol{\mathcal{T}}$	general transformation matrix for precoding
$\boldsymbol{\mathcal{T}}_{TP}$	transformation matrix for TP
$\boldsymbol{\mathcal{T}}_{JT}$	transformation matrix for JT
$\mathbf{U}_k$	matrix whose columns vectors are the $\mathbf{c}_k$, used for power calculation
$\mathbf{V}(n)$	filtered reference matrix used in MC-RLS algorithm
$\mathbf{U}$	block-diagonal matrix of K $\mathbf{U}_k$
$\mathbf{W}$	block-diagonal matrix of $\mathbf{W}_k$
$\mathbf{W}_k$	diagonal matrix with diagonal elements the kth user's transmission amplitude
Z	length of a FIR filter which results by cascaded channel and matched filter receiver
$\mathbf{c}_k$	k-user's spreading code in a vector form of length Q
c_k^q	rectangular chip waveform, $c_k^q = \pm 1$
$c_k(n)$	spreading code in discrete time, $0 \leq n \leq Q$
$c_k(t)$	spreading code in continuous time, $0 \leq t \leq T_s$
d_k^m	the mth bit transmitted for kth user
$\hat{d}_k^m$	soft decision on the receiver of the mth bit transmitted for kth user
$\mathbf{d}_0$	vector of K data-bits d_k^0
$\hat{\mathbf{d}}_0$	estimated received vector of K data-bits d_k^0
$\mathbf{d}$	vector of a block of KN data-bits assigned to all users
$\mathbf{d}_k$	vector of a block of N data-bits assigned to user k

$\hat{\mathbf{d}}$	vector of a block of KN receiver estimated data-bits assigned to all users
$\hat{\mathbf{d}}_k$	vector of a block of N receiver estimated data-bits assigned to user k
$e_k(n)$	discrete time received signal on k-user's receiver
$e_k(t)$	continuous time received signal on k-user's receiver
$\mathbf{e}$	arrangement in a vector of K $\mathbf{e}_k$
$\mathbf{e}_k$	received signal on k-receiver in vector form of length $Q+L-1$
f_o	carrier frequency
$\mathbf{g}_k$	vector of the expanded symbol at the k-user pre-filter output
$g_c(t)$	the chip waveform
$\mathbf{h}_k$	channel impulse response in a vector form, of length L
$h_k(n)$	chip-rate sampling of channel impulse response
$h_k(t,\tau)$	time-varying linear channel impulse response for downlink with k-user
$h_k(\tau)$	time-invarying linear channel impulse response for downlink with k-user
k	denotes a particular user index
m	index for transmitted bit
n	discrete time index $n=1,2,3,....$, chip rate sampling
$\mathbf{p}$	arrangement of K vectors $\mathbf{p}_k$ in a vector of length KP
$\mathbf{p}_k$	k-user pre-filter FIR in vector form of length P
$p_k(n)$	continuous time k-user's pre-filter impulse response
$p_k(t)$	discrete time k-user's pre-filter impulse response
q	index for the chips in a spreading sequence, $q=0\ldots Q-1$
$r_{ij}(n)$	filtered reference signal
$\mathbf{r}_{ij}$	vector of P length associated with filtered reference signal $r_{ij}(n)$
$\mathbf{s}$	transmitted vector of length NQ with no precoding
$\mathbf{s}_p$	transmitted vector of length NQ with precoding
$s(n)$	discrete time transmitted signal with no precoding from the BS
$s(t)$	continuous time transmitted signal with no precoding from the BS
$s_p(n)$	discrete time transmitted signal with precoding from the BS
$s(t)$	continuous time transmitted signal with precoding from the BS
$\underline{s}(t)$	bandpass transmitted signal with no precoding from the BS
t	continuous time index
$v(n)$	additive Gaussian noise at the receiver
$\tilde{v}(n)$	noise at the receiver's output

$\mathbf{v}$	additive Gaussian noise vector on the receiver
$x_k^m(n)$	spread symbol d_k^m
$\mathcal{Y}$	complex symbol alphabet set
$\mathcal{Y}_i$	complex symbols from data alphabet $i = 1 \dots \ell$
w_k^m	transmission amplitude of kth user's mth data-bit
$z_k(n)$	convolution of kth user channel impulse response and its matched filter receiver
$\mathbf{\Gamma}$	expectation of $\mathbf{R}^T\mathbf{R}$
$\mathbf{\Gamma}_{ij}$	matrix whith columns the vector $\boldsymbol{\gamma}_{ij}$
Δ	delay in sampling
Φ_s^x	SNIR spread
$\Omega_{bitwise}$	computational cost of bitwise precoding techniques
$\Omega_{blockwise}$	computational cost of blockwise precoding techniques
β	roll-off factor for the raised cosine pulse shaping
$\boldsymbol{\gamma}$	expectation of $\mathbf{R}^T\mathbf{d}_0$
$\boldsymbol{\gamma}_{ij}$	expanded symbol that corresponds to the filtered reference signal $r_{ij}(n)$
$\gamma_{ij}(n)$	convolution of ith user spread. code with jth user channel and matched filter FIR
$\bar{\boldsymbol{\gamma}}_{ij}$	vector of P length with elements $[\mathbf{\Gamma}_{ij}]^{p,(M+1)}$, where $p = 1 \dots P$
δ	small positive constant for MC-RLS
$\boldsymbol{\zeta}_k$	optimally designed signature sequence of length L_s
θ	forgetting factor for MC-RLS algorithm
ϑ/ϑ	first order gradient
λ	Lagrange multiplier
$\lambda(T_s^n)$	time variant Lagrange multiplier
$\underline{\boldsymbol{\lambda}}$	diagonal matrix of Lagrange multipliers
μ	step-size parameter for MC-LMS algorithm
ρ_{ij}	crosscorrelation of spreading codes $c_i(t)$ and $c_j(t)$
σ^2	AWGN variance
τ	time delay in propagation time
τ_{max}	maximum time delay in propagation time, delay spread
τ_r	half the chip-period, used for the raised cosine pulse shaping
$\phi(\hat{d}_k^m)$	SNIR associated with data-bit d_k^m

$\check{\psi}(\cdot)$	minimum eigenvalue of a matrix
$\tilde{\psi}(\cdot)$	maximum eigenvalue of a matrix
$*$	convolution operator
$.^T$	transpose operator
$.^*$	conjugate operator
$\|\mathbf{x}\|$	norm: $\sqrt{\mathbf{x}^T\mathbf{x}}$
$\|\mathbf{X}\|_s$	spectral norm: sq. root of maximum eigenvalue of $\mathbf{X}^T\mathbf{X}$
$[.]^{i,j}$	element in the ith row and jth column of a matrix
$[.]^i$	ith element of a vector

Chapter 1
Introduction

The radio age began just over 100 years ago with the invention of the radio telegraph by Gulielmo Marconi. This event gave birth to a large number of deployments, many of which operate widely even today (representative examples include the transmission of speech, music and/or images by radio and TV stations). The development of wireless communication systems continued through the years and their design and implementation was both aided and influenced initially by the invention of the triode cathode tube, and later by the advent of the semiconductor technology in the form of the transistor. Continuous advances in this technology have greatly benefited wireless communications systems, which have been increasingly capable of handling such demanding tasks as video, multimedia transmission and teleconferencing among individuals who are physically thousands of kilometers apart. A modern and very interesting aspect of wireless communications is that of mobile communications or cellular communications.

The cellular concept was invented by Bell Laboratories and the first commercial analog voice system was introduced in Chicago in October 1983 [3, 4]. The first generation analog cordless phone and cellular systems became popular using the design based on a standard known as Advanced Mobile Phone Services (AMPS). Similar standards were developed around the world including Total Access Communication System (TACS), Nordic Mobile Telephone (NMT) 450, and NMT 900 in Europe; European Total Access Communication System (ETACS) in the United Kingdom; C-450 in Germany; and Nippon Telephone and Telegraph (NTT), JTACS and NTACS in Japan [5].

In contrast to the first generation analog systems, second generation systems are designed to use digital transmission. These systems include the Pan-European Global System for Mobile Communications (GSM) and DCS 1800 systems, North American dual-mode cellular system Interim Standard (IS)-54, North American IS-95 system, and Japanese personal digital cellular (PDC) system [3, 6].

The third-generation (3G) mobile communications systems are being studied worldwide, under the names of Universal Mobile Telecommunications System (UMTS) and International Mobile

Telecommunications (IMT)-2000 [7]. The aim of these systems is to provide users advanced communication services, having wideband capabilities, using a single standard. In 3G communications systems, satellites are going to play a major role providing a global coverage. Furthermore, future generation systems promise even more reliable and higher speed communication, which is expected to enable additional services like mobile multimedia, real-time mobile video transmission, mobile access to Internet resources and even shopping, making these systems increasingly indispensable.

The remaining of this Chapter is organised in the following sections: Section 1.1 presents a general overview of the cellular fundamentals and section 1.2 a brief history of the third-generation wireless systems. In section 1.3 the open problems are given along with the motivation and the goal of this thesis. Finally, the layout of this thesis is given in section 1.4.

1.1 Cellular fundamentals

Nowadays wireless communications are used widely in many communication systems: mobile telephony, satellite networks, digital radio/television broadcasting, fixed wireless local loops, etc. The success of mobile communications lies in the ability to provide instant connectivity anytime and anywhere and the ability to provide high speed data services to the mobile users. The quality and speeds available in the mobile environment must match the fixed networks if the convergence of the mobile wireless and fixed communication networks is to happen in the real sense. So, the challenges for the mobile networks lie in making the movement from one network to the another as transparent to the user as possible and the availability of high speed reliable data services along with high quality voice. A range of successful technologies exists today in various parts of the world and every technology must evolve to fulfill all these requirements. In this work we are particularly interested in the cellular mobile environment, therefore, our attention will be primarily focused on this research area.

The area served by mobile phone systems is divided into small areas known as cells. Each cell contains a base station (BS) that communicates with mobiles in the cell by transmitting and receiving signals on radio links. The transmission from the base station to a mobile station (MS) is typically referred to as downstream, forward-link or downlink. The corresponding terms for the transmission from a mobile to a base station are upstream, reverse-link and uplink. Each base station is associated with a Radio Network Controller (RNC) and each RNC is connected

with a mobile switching center (MSC) that connects calls to and from the base stations to mobiles in other cells and the public switched telephone network. A typical setup depicting a group of base stations and a MSC is shown in Figure 1.1.

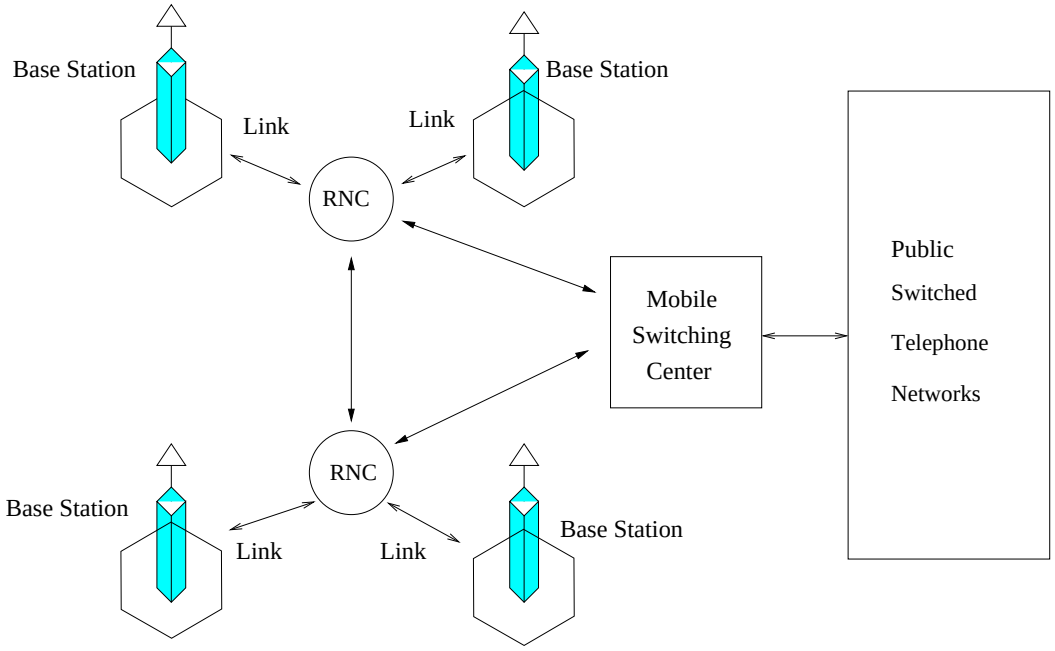

Figure 1.1: *A typical cellular system setup*

A base station communicates with mobiles using two types of radio channels, control channels to carry control information and traffic channels to carry messages. Each base station continuously transmits control information on its control channels. When a mobile is switched on, it scans the control channels and tunes to a channel with the strongest signal. This normally would come from the BS located in the cell in which the mobile is also located. The mobile exchanges identification information with the BS and establishes the authorization to use the network. At this stage the mobile is ready to initiate and receive a call. Important elements that describe a cellular mobile system are the channel characteristics, the multiple access scheme and the channel reuse.

1.1.1 Channel characteristics

In the study of communication systems the classical (ideal) additive Gaussian noise channel, with statistically independent Gaussian noise samples corrupting data samples, is the usual starting point for understanding basic performance relationships. The primary source of per-

formance degradation is thermal noise generated in the receiver. However, for most practical channels, where signal propagation takes place in the atmosphere and near the ground, the free space propagation model is inadequate to describe the channel and predict the system performance. In the following a brief description of the channel characteristics is given. More details about channel characterization and interference mitigation can be found in [8–10].

1.1.1.1 Fading channels

The propagation of radio signals on both the forward (BS to mobile) and reverse (mobile to BS) links is affected by the physical channel in several ways. The signal arriving at the receiver is a combination of many components arriving from various directions as a result of multipath propagation. These paths arise from scattering, reflection, refraction or diffraction of radiated energy off the objects that lie in the environment as it is illustrated in Figure 1.2. The terrain conditions and local buildings and structures cause the received signal power to fluctuate randomly as a function of distance. Fluctuations of the order of 20dB are common within the distance of one wavelength. This phenomenon is called fading. One may think this signal as a product of two variables. The first component, also referred to as the short-term fading com-

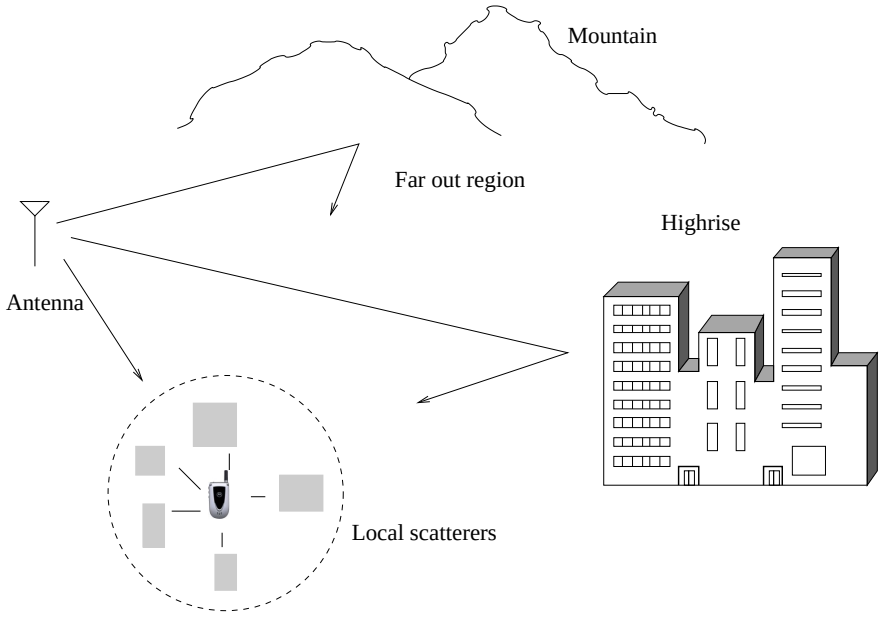

Figure 1.2: *A mobile multipath environment*

ponent, changes faster than the second one and can be modeled with a Rayleigh distribution. The second component is a long term or slow-varying quantity modeled with a log-normal distribution. In other words, the local mean varies slowly with lognormal distribution and the fast

variation around the local mean has a Rayleigh distribution.

1.1.1.2 Doppler spread

The movement of a mobile causes the received frequency to differ from the transmitted frequency because of the Doppler shift resulting from its relative motion. As the received signals arrive along many paths, the relative velocity of the mobile with respect to various components of the signal differs, causing the different components to have different Doppler shifts. This can be viewed as Doppler spreading of the transmitted frequency and is referred to as the Doppler effect. The width of the Doppler spread in the frequency domain is closely related to the rate of fluctuations in the observed signal. Fast fading results in Doppler spread and is often referred to as time-selective fading, since signal amplitude varies with time. Time-selective fading can be characterised by the coherence time of the channel. Coherence time represents the maximum time separation for which the channel impulse responses at two time instants remain strongly correlated. The coherence time is inversely proportional to the Doppler spread [11, 12].

1.1.1.3 Delay spread

In a multipath propagation environment, several time-shifted and scaled versions of the transmitted signal arrive at the receiver. That results in spreading of the signal in time. A double-negative exponential model is typically observed: the delay separation between paths increases exponentially with the path delay and the path amplitudes also fall exponentially with delay [12]. This spread of path delays is called delay spread. Delay spread causes frequency-selective fading, which implies that fading now depends on the frequency. It can be characterized in terms of coherence bandwidth, which represents the maximum frequency separation for which the frequency domain channel responses at two frequency shifts remain strongly correlated. The coherence bandwidth is inversely proportional to the delay spread [11]. This is the bandwidth over which the channel is flat; that is; it has a constant gain and linear phase. For a signal bandwidth above the coherence bandwidth the channel loses its constant gain and linear phase characteristic and becomes frequency-selective. Roughly speaking, a channel becomes frequency selective when the root mean square (rms) delay spread is smaller than the symbol duration and causes *intersymbol interference* (ISI) in digital communications. Frequency-selective channels are also known as dispersive channels whereas the nondispersive channels are referred to as flat-fading channels.

1.1.1.4 Link budget and path loss

Link Budget is a name given to the process of estimating the power at the receiver site for a microwave link taking into account the attenuation caused by the distance between the transmitter and the receiver. This reduction is referred to as the path loss. In free space the path loss is proportional to the second power of the distance. In other words, by doubling the distance between the transmitter and the receiver, the received power at the receiver reduces to one fourth of the original amount. In a non-free space the attenuation can be higher or lower than that.

1.1.2 Multiple access scheme

The available spectrum bandwidth is shared in a number of ways by various wireless radio links. The ways in which this is done are referred to as multiple access schemes. There are basically three principle schemes. These are frequency division multiple access (FDMA), time division multiple access (TDMA) and code division multiple access (CDMA) [5]. Figure 1.3 shows how the calls are distributed into the spectrum according to the multiple access scheme used.

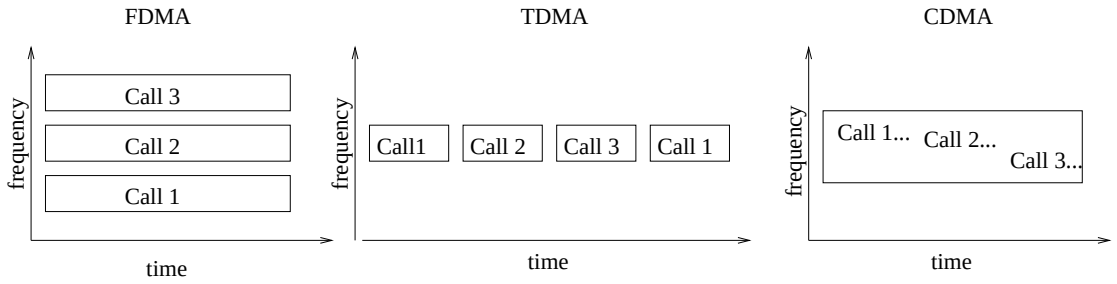

Figure 1.3: *Call allocation in the spectrum with different multiple access schemes*

1.1.2.1 FDMA

In a FDMA scheme the available spectrum is divided into a number of frequency channels of certain bandwidth and individual calls use different frequency channels. All first-generation cellular systems use this scheme.

1.1.2.2 TDMA

In a TDMA scheme several calls share a frequency channel. The scheme is useful for digitized speech or other digital data. Each call is allocated a number of time slots based on its data rate within a frame for uplink as well as downlink. Apart from the user data, each time slot also carries other data for synchronisation, equalisation, guard times and control information. The traffic in two directions is separated either by using two separate frequency channels or by alternating in time. The two schemes are named as frequency division duplex (FDD) and time division duplex (TDD), respectively.

1.1.2.3 CDMA

CDMA is a spread spectrum (SS) method [13]. The main characteristic of any spread spectrum system is that the transmitted signal has a bandwidth much larger than the bandwidth of the baseband representation of the original signal. CDMA is classified depending on the modulation method used to obtain a wideband signal. This division leads to three types of CDMA: direct sequence (DS), frequency hopping (FH), and time hopping (TH). In DS-CDMA, spectrum is spread by multiplying the information signal with a pseudo-noise sequence, resulting in a wideband signal. In FH-CDMA a pseudo noise sequence defines the instantaneous transmission frequency. The bandwidth at each moment is small but the total bandwidth over, for example, a symbol period is large. In TH-CDMA a pseudo noise sequence defines the transmission moment. Furthermore, combinations of these techniques are possible. In the current thesis we focus on DS-CDMA because it is the technique used for the third-generation wideband CDMA (W-CDMA) proposals. Wideband CDMA is defined as direct sequence spread spectrum multiple access scheme where the information is spread over a bandwidth significantly more than the coherence bandwidth of the channel.

DS-CDMA uses linear modulation with wideband pseudonoise (PN) sequences to generate signals. These sequences, also known as codes, spread the spectrum of the modulating signal over a large bandwidth, simultaneously reducing the spectral density of the signal. Various CDMA signals occupy the same bandwidth and appear as noise to each other. Each user is assigned an individual code at the time of call initiation. This code is used both for spreading the signal at the time of transmission and despreading it at the time of reception. Cellular systems using CDMA [14–16] schemes can utilise FDD or TDD for the forward and reverse link separation. The principle of DS-CDMA is that the codes are orthogonal between each other to

allow for decoupling at the receiver. On downlink the BS transmits to all users synchronously and this preserves the orthogonality of various codes assigned to different users. The orthogonality, however, is not preserved between different components arriving from different paths in multipath propagation or when the users transmit asynchronously, in the uplink, for instance.

Hence, although the spreading codes are designed to be orthogonal with each other, there are scenarios under which the orthogonality cannot be controlled. This results in interference from user to user. This type of interference is called *multiple access interference* (MAI) and imposes a limitation to CDMA systems. The reason for selecting CDMA over TDMA is that in a high number of users scheme the transmission on time slots, that TDMA provides, is a limitation factor for the development of high rate data transmission. The full bandwidth should be utilised in this scenario, which is feasible with CDMA.

1.1.3 Channel reuse

The generic term *channel* is normally used to denote a frequency in FDMA system, a time slot in TDMA system and a code in CDMA or a combination of these in a mixed system. Two channels are different if they use different combinations of these at the same place. For an allocated spectrum and a given performance aim the number of channels in a system is limited. This limits the capacity of a system to sustain simultaneous calls and may only be increased by using each traffic channel to carry many calls simultaneously. Using the same channel again and again is one way of doing it and this is the concept of channel reuse.

The concept of channel reuse can be understood from Figure 1.4(a). It shows a cluster of three cells. These cells use three separate sets of channels. Each set is indicated by a letter. In Figure 1.4(b) this cluster of three cells is repeated to indicate that three sets of channels are being reused in different cells.

Let F channels be available over a given geographical area and there be N cells in a cluster to use the available channels. In the absence of the channel reuse this cluster covers the whole area and the system can sustain simultaneously F calls. If the cluster on N cells is repeated M times over the same area, then the system capacity increases to MF as each channel is used M times. Of course the re-use factor would be chosen to ensure that the level of co-channel interference is low enough that the system can operate satisfactorily. The co-channel interference results from neighboring cells and it is referred to as *intercell* interference and it is another factor that

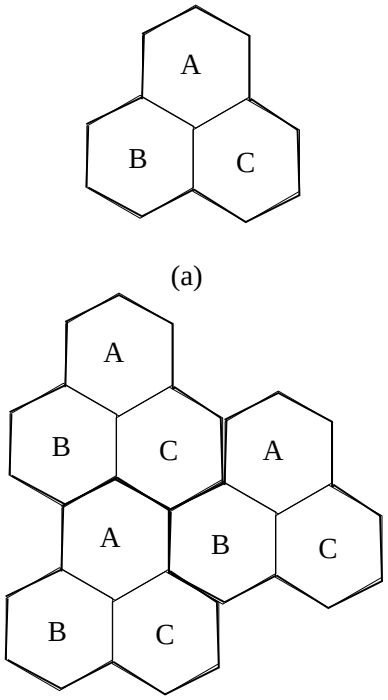

Figure 1.4: *(a) A cluster of three cells (b) Channels reuse concept using a three cell cluster*

limits the cellular system's performance.

1.2 Third-Generation systems

The emphasis and the contribution of this thesis is on techniques to be applied on WCDMA-TDD which is one of the air interface selected for the third-generation mobile telecommunications system. Thus, a brief reference on the development of these systems is given in this section.

The third-generation systems aim to provide a network that can provide user voice, data, multimedia and video services regardless of their location on the network: fixed, cordless, cellular, satellite and so on. These networks support global roaming while providing high-speed data and multimedia applications of up to 144Kbps on the move and up to 2Mbps in a local area[17]. WCDMA, in FDD mode, can achieve up to 3.84 Mcps in contrast with IS-95 than cannot exceed the chip rate of 1.2288 Mcps. In TDD mode WCDMA can achieve chip rates up to 1.28 Mcps. Some type reference channels are refered in the 3GPP Technical Specifications 25.xxx

series [18–21]. Third-generation systems are currently being defined by both the International Telecommunications Union (ITU) and regional standardization bodies. Globally, the ITU has been defining third-generation systems since the late 1980s through work on the IMT-2000 system, formerly called the Future Public Land Mobile Telecommunications Service (FPLMTS) [5]. The ITU sought and evaluated candidate technologies in accordance with agreed guidelines. The European proposal for IMT-2000 is known as the UMTS and is being defined by the European Telecommunications Standards Institute (ETSI), which has been responsible for UMTS standardization since the 1980s. UMTS will provide significant changes for customers and technologies and it will be fully deployed within a short time frame.

IMT-2000 defines systems capable of providing continuous mobile telecommunications coverage for any point on the earth's surface. Access to IMT-2000 is via either a fixed terminal or a small, light, portable mobile terminal. More details and informations about UMTS can be found in [22–24].

1.3 Open problems-Motivation of the thesis

A third-generation wireless system designer is faced with a number of challenges. These include a complex multipath time-varying propagation environment; limited availability of radio spectrum; limited energy-storage capability of batteries in portable units; user demand for higher data rates, better voice quality, fewer dropped calls, enhanced in-building penetration and longer talk times, and operator demand for greater area coverage by base stations, increased subscriber capacity and lower infrastructure and operating costs. A number of different technologies have been used to meet such diverse requirements, including advanced multiple access schemes, bandwidth-efficient source coding, and sophisticated signal-processing techniques. Cellular-radio signal processing includes modulation and demodulation, channel coding and decoding, equalization, and diversity combining.

In a CDMA scheme the major problems encountered are already mentioned in this Chapter and are the MAI, due to simultaneous usage of the bandwidth by many users and ISI due to multipath channels. MAI and ISI are often added to the background thermal noise modeled as additive white Gaussian noise (AWGN). Thus, the system's utility is limited by the amount of total interference instead of the background noise exclusively as in other cases. In other words, the signal to noise plus interference ratio (SNIR) is the limiting factor for a mobile

communications system instead of the signal to noise ratio (SNR).

Therefore, in systems applying CDMA the two problems of equalisation and signal separation have to be solved simultaneously to increase the SNIR and achieve a good performance. In the state of the art for CDMA systems this is addressed by *multiuser detection* (MUD) techniques. MUD has been studied extensively and a number of solutions have been proposed. These techniques are all receiver based, they usually require channel estimation, knowledge of all the active users spreading codes and they have considerable computational cost. While this is feasible for the base station (for the uplink scheme), it contrasts with the desire to keep portable units (for the downlink scheme), like mobile phones, simple and power efficient. This will be shown in Chapter 2. An alternative to multiuser detection is to precode the transmitted signal such that the ISI and MAI effects are minimised before transmission in the downlink. The extra computational cost is transfered to the base station where power and computational resources are more readily available. This is the motivation and the goal of this thesis.

Recently, work has been done on algorithms that move towards that goal. They all exploit the fact that in a TDD scheme the downlink channel is known to the transmitter. This is true because in TDD mode the same channel impulse response is valid for both the uplink and the downlink, if the time elapsing between uplink and downlink transmissions is sufficiently small compared to the coherence time of the mobile radio channel[1]. In these algorithms, the multiuser detection and channel equalisation can be carried out at the transmitter. This can be achieved with *linear precoding* of the transmitted signal. The receiver structure at the user equipment is then simplified when compared to a multiuser detection receiver, and can be a conventional matched filter (which only requires knowledge of the desired user's spreading code). Thus no channel estimation or adaptive equaliser is required at the mobile receiver. Techniques which only require a matched filter receiver also enhance the downlink system capacity since no system resources have to be allocated for the transmission of training signals on the downlink.

In this thesis the problem of linear precoding in a CDMA scheme is generally examined. An analytical framework for the theoretical calculation of the performance of any precoding algorithm is presented. A basic assumption to apply these algorithms is that the downlink channels remain constant during transmission and perfect knowledge of them is assumed at the BS. The

[1]Channel reciprocity also pressumes that the same antenna configuration is used in both uplink and downlink directions and the temporar changes are negligible.

state of the art precoding algorithms are thoroughly examined under this common framework and they are compared in terms of bit error ratio performance (BER) and computational cost. They are also compared with their receiver based counterparts and the results are discussed. This work classifies the precoding techniques into *blockwise* and *bitwise*. It is shown that the existing blockwise techniques demonstrate a superior performance compared to the existing bitwise techniques at the cost of increased complexity. It emerges then the need for a new bitwise technique that combines low complexity with a good performance.

Thus, we propose and analyse a new bitwise technique, called *inverse filters* (INVF) that achieves a BER performance equivalent to or better than the blockwise techniques. The implementation of this method can be described as applying an individual linear finite impulse response (FIR) filter to each user signal after the spreading process and before transmission. The advantage of low complexity now is combined with a very good BER performance. Furthermore, adaptive multichannel feed-forward algorithms are examined for the first time in the mitigation of MAI and ISI in a CDMA system. Three different algorithms are appropriately modified and applied to wireless telecommunications.

1.4 Thesis layout

This thesis is organised as follows:

In Chapter 2 we derive the discrete time vector-matrix description of a CDMA downlink system. The major air interface components of a CDMA system are briefly described. The receiver based conventional reception technique is given along with the multiuser detection schemes and the reasons why they are difficult to be applied at the MS for the downlink are explicitly explained. Complexity and performance issues are also addressed in Chapter 2.

Chapter 3 presents the problem of linear precoding in a CDMA system from a general and theoretical point of view. The assumptions and the scenarios under which linear precoding can give the desired results are discussed. A classification, in terms of realisation and implementation, of the linear precoding algorithms is given and the advantages and disadvantages of each are also presented. Furthermore, a theoretical analysis results in a general analytical expression that calculates the BER performance of any precoding method.

The state of the art major linear precoding techniques are described in Chapter 4. The different

criteria applied by different algorithms are written under a common framework and notation. They are classified as blockwise or bitwise while their performance and computational cost is analysed. A comparison by means of Monte Carlo simulations follows along with a discussion. The discussion leads to the conclusion that there is space for the development of a new bitwise technique that applies more efficient criteria and that should give better performance.

A new bitwise technique is developed in Chapter 5. It is called inverse filters and it is proved that the mitigation of MAI and ISI is more efficient compared with the other bitwise techniques. The criteria applied are minimum mean squared error (MMSE) plus power constraint and the theoretical analysis is fully presented in Chapter 5. The derivation of the Wiener solution is also given in a closed form, while a detailed discussion on the power constraint term follows. Finally, the performance of the INVF algorithm is demonstrated and compared to the state of the art precoding techniques and the receiver based MUD ones.

In Chapter 6 adaptive feed-forward algorithms are appropriately modified and applied for the first time on the CDMA downlink. The idea and the motivation for investigating such techniques is given along with the area that they derived from. Metrics such as convergence speed and BER performance are demonstrated by means of Monte Carlo simulations. The results are presented and a discussion on them is following.

Chapter 7 summarises the work and the results of this thesis. Furthermore, future extensions and fields to be further investigated are presented.

Chapter 2
System model - Multiuser detection

In this Chapter a CDMA system model is described in section 2.1 and some of CDMA's fundamental functions are presented in section 2.2. Section 2.3 gives an overview of the RAKE receiver and section 2.4 presents the receiver based multiuser detection techniques. It is also explained why receiver based MUD algorithms are not appropriate to be applied on the user equipment for the downlink transmission due to high complexity cost, capacity and hardware requirements. Section 2.5 describes the assumptions made for the simulations of this thesis and the simulation results of the receiver based MUD techniques BER performance are displayed.

2.1 System model

In this section, a discrete-time model to describe the transmission in a CDMA system is derived from the continuous-time model under certain assumptions. The emphasis is given to the DS-CDMA downlink scheme. The model is a further development of the models presented in [25, 26] associated with a flat-fading channel and [27] extended to multipath propagation. Furthermore, the matrix-vector description of the system is deduced from the discrete-time model.

2.1.1 Continuous-time model

As mentioned in Chapter 1 in DS-CDMA communication systems the information-bearing signal is multiplied directly by a spreading code (also known and as signature waveform or spreading sequence) with a much larger bandwidth than the data. The general transmitter-receiver block diagram of such a system is given in Figure 2.1. After transmission of the signal, the receiver despreads the SS-signal using a locally generated code sequence. To be able to perform the despreading operation, the receiver must not only know the code sequence used to spread the signal, but the code of the received signal and the locally generated code must also be synchronised. This synchronisation must be accomplished at the beginning of the reception and maintained until the whole signal has been received [2]. This operation is performed by the

synchronisation/tracking block. In this work perfect code synchronisation/tracking is assumed and thus the corresponding block in Figure 2.1 is omitted. We will get into more details about the transmitter and receiver operations in sections 2.1 and 2.3. In this section, we will restrict our description to the data spreading and transmission over a radio channel.

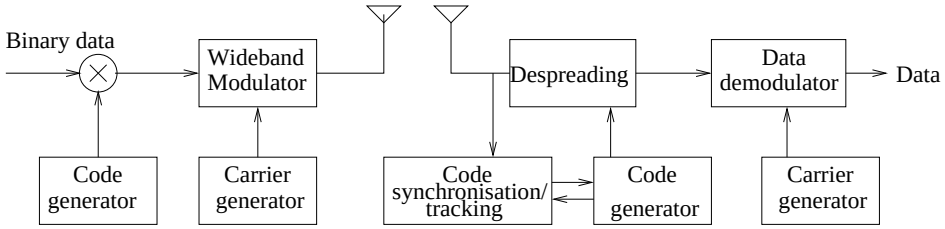

Figure 2.1: *Transmitter-receiver DS-CDMA block diagram*

For the derivation of the continuous time model of a CDMA system we start from the general block diagram as presented in Figure 2.2. In every cell of a modern mobile communications system there are K active users. Values and functions related to user k, where k takes the values $1 \dots K$ are marked with subscript k. In this model the base station has one omnidirectional antenna element. The bandpass signal $\underline{s}(t)$ transmitted from the BS to K mobile stations is

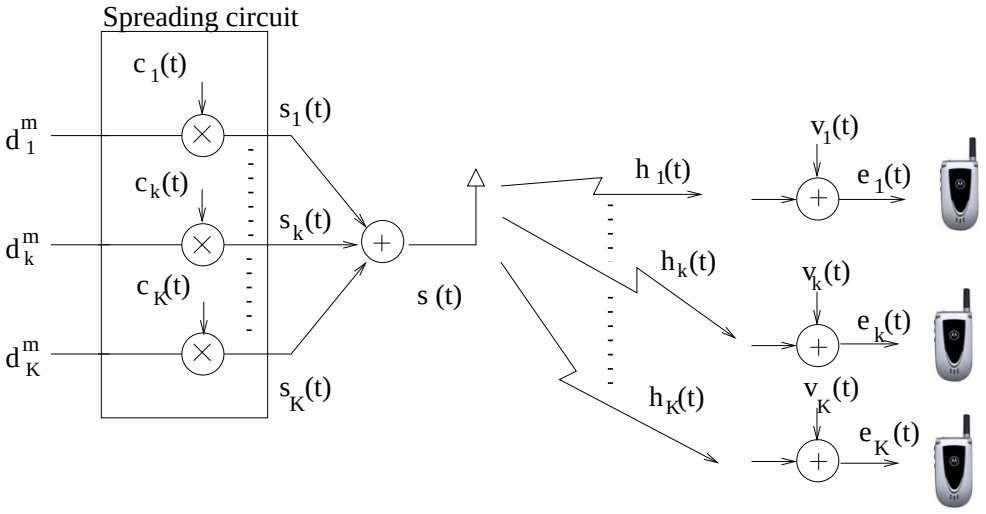

Figure 2.2: *Continuous-time downlink model for multiple access*

given by eq.(2.1). In eq.(2.1) Re denotes the real part of a complex number and f_o is the carrier frequency.

$$\underline{s}(t) = Re\{s(t)e^{j2\pi f_0 t}\} \tag{2.1}$$

The analysis throughout this thesis will be simplified by representing all signals with their complex lowpass equivalents. Thus, $s(t)$ is transmitted over K time-varying linear radio channels

with impulse response $h_k(\tau, t)$, where τ denotes the delay time and t denotes the absolute time [8, 9, 11, 28]. The delay time τ is the delay in excess of the minimum propagation time between transmitter and receiver and characterises the time spread introduced by multipath propagation when an impulse is transmitted over the channel. The delays arise from scattering, reflection, refraction or diffraction of radiated energy off the objects that lie in the environment, as explained in Chapter 1. The minimum delay time is zero and the maximum delay time is denoted as τ_{max}. The maximum delay time is also known as the *delay spread*. At site k the received signal $e_k(t)$ is the result of the convolution of $s(t)$ with the channel impulse response $h(\tau, t)$. The convolution product is:

$$e_k(t) = \int_0^{\tau_{max}} s(t-\tau) h_k(\tau, t) d\tau + v(t) \tag{2.2}$$

In Figure 2.2 the received signal is disturbed by an additive noise signal $v(t)$. The additive noise signal $v(t)$ is mainly determined by intercell interference as the same frequency band is reused in adjacent cells according to a CDMA cellular system. Adjacent channel intracell interference and thermal noise is also present in $v(t)$ as in the case of CDMA the K signals are neither disjoint in frequency domain, as in FDMA, nor in the time domain, as in TDMA, but are only separable by means of different spreading sequences. An essential assumption that simplifies our notation is that the time duration of the signal $s(t)$ is short enough that the channel impulse response $h_k(\tau, t)$ may be considered time-invariant during the transmission of $s(t)$, i.e.

$$h_k(\tau, t) = h_k(\tau) \tag{2.3}$$

The case of time-invariant channels $h_k(\tau)$ is relevant for the CDMA-TDD system concept and is valid for low mobility users as will be explained in Chapter 3.

In order to describe the continuous model of the transmitted downlink lowpass signal $s(t)$ for multiple access, as depicted in Figure 2.2, the spread signals $s_k(t)$ addressed to each user should be:

$$s_k(t) = \sum_{m=-M}^{M} w_k^m d_k^m c_k(t - mT_s) \tag{2.4}$$

The data symbols transmitted are denoted as d_k^m, $m = -M \ldots M$. The block of transmitted data has a length of $N = 2M + 1$ data. They are taken from a complex symbol alphabet $\mathcal{Y} = \{\mathcal{Y}_1 \ldots \mathcal{Y}_\ell\}$ of length ℓ. Each one of the K users transmits data symbols scaled by the amplitude w_k^m determined by power control algorithms. The data symbols are spread before

transmission with specific signature waveforms. The symbol duration is T_s and the signature waveform designated for kth user is denoted as $c_k(t)$:

$$c_k(t) = \begin{cases} \sum_{q=0}^{Q-1} c_k^{(q)} g_c(t - qT_c), & t \,\epsilon\, [0, T_s] \\ 0, & \text{otherwise} \end{cases} \tag{2.5}$$

The chips $c_k^{(q)}$, of duration T_c are taken from the alphabet $\{-1, +1\}$ and $g_c(t)$ is the chip waveform which is assumed to be the same for each of the K users. An example of a direct-sequence chip waveform is a rectangular pulse:

$$g_c(t) = \begin{cases} 1, & \text{if } 0 \leq t \leq T_c \\ 0, & \text{otherwise} \end{cases} \tag{2.6}$$

The magnitude of the Fourier transform of the rectangular pulse waveform displays considerable frequency content beyond the spectral null $1/T_c$. For the sake of spectral efficiency some CDMA systems choose a smooth chip waveform with very little energy beyond the chip rate. Such typical chip waveforms can be the raised cosine pulse shaping [11] with a roll off factor $\beta = 0.22$ and $\tau_r = T_c/2$.

$$g_c(t) = \frac{\sin(\frac{\pi t}{\tau_r}) \cdot \cos(\frac{\pi \beta t}{\tau_r})}{(\frac{\pi t}{\tau_r}) \cdot (1 - 4(\frac{\beta t}{\tau_r})^2)} \tag{2.7}$$

For every symbol of duration T_s, there is a corresponding number Q of weighted chip impulses $g_c(t)$ with the weighting factors $c_k^{(q)}$ forming the kth user's specific spreading sequence. The ratio

$$Q = \frac{T_s}{T_c} \tag{2.8}$$

by which the chip rate $1/T_c$ is increased over the symbol rate $1/T_s$ is the spreading factor or processing gain related to a data symbol [13]. In frequency domain this means that the spectrum of the source signal is increased by a factor of Q times. An example of a direct sequence spread spectrum (DS-SS) signal $s_k(t)$ is shown in Figure 2.3. In this example 14 code chips per information symbol are transmited (the chip rate is 14 times the data rate).

Returning to Figure 2.2 the resulting transmitted signal from the BS to the K mobile active

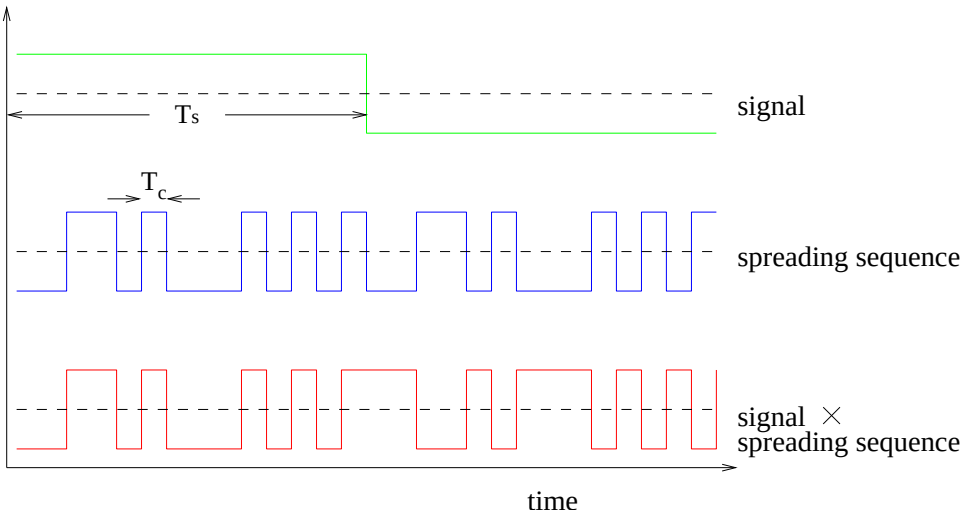

Figure 2.3: *Generation of a SS signal*

users is written as the superposition:

$$s(t) = \sum_{k=1}^{K} s_k(t) \tag{2.9}$$

In the next section the discrete-time model for the downlink of CDMA will be produced based on the continuous model.

2.1.2 Discrete-time downlink transmission model

For the derivation of the discrete-time model, it is assumed that $h_k(\tau)$, eq (2.3), has finite duration and is causal. These assumptions are common in the case of mobile radio applications [28]. Under these assumptions, $h_k(\tau)$ sampled at the chip rate yields a finite number L of samples or multipath components.

$$h_k(n) = \begin{cases} h_k\big(lT_c\big), & 0 \leq l \leq L-1 \\ 0, & \text{otherwise} \end{cases} \tag{2.10}$$

These samples are in general not equal to zero, whereas the samples $h(lT_c)$ for $l < 0$ and $l > L-1$ are zero. The channel impulse response $h_k(\tau)$ can be reconstructed perfectly from the samples $h_k(l)$, $l = 0 \ldots L-1$, if the bandwidth of $h_k(\tau)$ is smaller than or equal to the sampling rate $1/T_c$. Most of the effective energy of the transmitted signal $s_k(t)$, and thus of the $h_k(\tau)$ is concentrated in a frequency bandwidth of $1/T_c$. The energy portion outside the the

bandwidth $1/T_c$ is assumed to be negligible.

In the same way, the spreading sequence, as described in eq. (2.5), sampled at the chip rate is:

$$c_k(n) = \begin{cases} c_k\big(qT_c\big), & 0 \leq q \leq Q-1 \\ 0, & \text{otherwise} \end{cases} \tag{2.11}$$

In this work the rectangular pulse chip waveform is adopted and therefore it turns out regarding eq. (2.5) that:

$$c_k\big(qT_c\big) = c_k^{(q+1)} \ , q = 0 \dots Q-1 \tag{2.12}$$

The number Q of chips per bit and the chip waveform are common to all users in a direct-sequence spread-spectrum CDMA system. The difference among the signature waveforms is the assignment of binary "sequence" or "code" $\{c_k^0 \dots c_k^{Q-1}\}$, which is different for each user. As mentioned in Chapter 1 multiple access capability in CDMA requires low crosscorrelations of different spreading sequences. In subsection 2.2.3 a brief introduction to spreading codes design and classification is given. Throughout this research the period of the pseudonoise waveform is equal to the symbol period, although in some practical CDMA systems it can be larger ($Q \geq T_s/T_c$).

The total transmitted downlink signal $s(n)$ for the conventional CDMA downlink scenario in discrete-time mode is derived directly from equations (2.4) and (2.9) and can be:

$$s(n) = \sum_{m=-M}^{M} \sum_{k=1}^{K} w_k^m d_k^m c_k(n - mQ) \tag{2.13}$$

Similarly, the received signal $e_k(t)$, eq. (2.2), on kth mobile terminal takes the following discrete-time description:

$$e_k(n) = \sum_{l=0}^{L-1} s(n-l)h(l) + v(n) \tag{2.14}$$

The discrete-time transmission model of eq. (2.14), which describes the transmission in a CDMA system, is illustrated in Figure 2.4. In this representation the channel has been replaced by a tapped delay line transversal filter or finite impulse response filter with delays equal to the chip duration T_c and tap-coefficients equal to $h_k(n)$, $n = 0 \dots L-1$ [11]. A representative model of the channel profile (tap delays and statistical properties) can be provided by the UMTS

specifications [29].

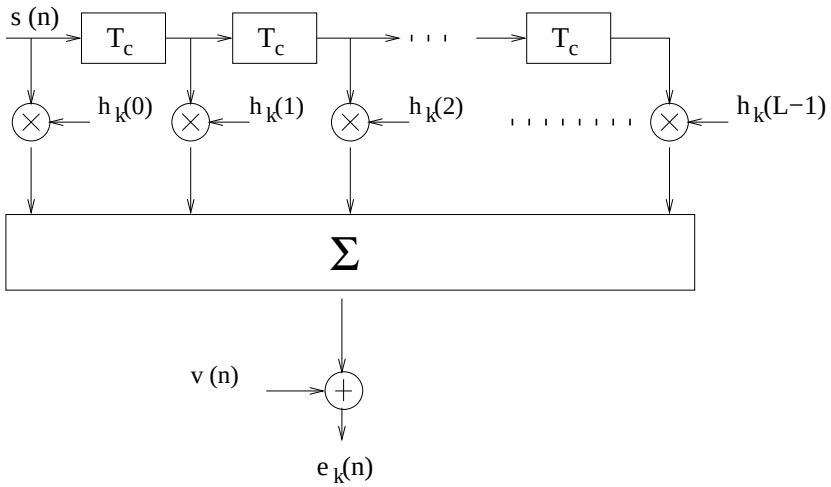

Figure 2.4: *Discrete-time CDMA channel model*

2.1.3 Matrix-vector notation for the discrete-time transmission model

Based on the aforementioned assumptions and notations of the discrete-time transmission model, the matrix-vector notation is introduced in this section. For the sake of clarity we state, at this point, that for any vector $\mathbf{x}$, $\|\mathbf{x}\|^2$ denotes the inner product $\mathbf{x}^T\mathbf{x}$ and $[\mathbf{x}]^j$ the jth element of the $\mathbf{x}$ vector. For any matrix $\mathbf{X}$, $[\mathbf{X}]^{i,j}$ denotes the element in the ith row and jth column. Furthermore, vectors are represented by boldface lower case letters and matrices by boldface upper case letters while symbols $\mathbf{x}^*/\mathbf{X}^*$ and $\mathbf{x}^T/\mathbf{X}^T$ indicate complex conjugation and transposition of vector/matrix $\mathbf{x}/\mathbf{X}$ respectively.

The spreading code consists of Q chips and it is described by the vector:

$$\mathbf{c}_k = [c_k(0) \cdots c_k(Q-1)]^T \tag{2.15}$$

The channel vector $\mathbf{h}_k$ consists of the tap-coefficients of the FIR filter that represents the channel:

$$\mathbf{h}_k = [h_k(0) \cdots h_k(L-1)]^T \tag{2.16}$$

Let $\mathbf{d}_k$ be a vector sequence of $N = 2M + 1$ transmitted bits for user k

$$\mathbf{d}_k = [d_k^{-M} \cdots d_k^0 \cdots d_k^M]^T \tag{2.17}$$

The column vector $\mathbf{d}$ of length KN is a block of data that contains the bits of all the users and is defined as :

$$\mathbf{d} = \left[\mathbf{d}_1^T \cdots \mathbf{d}_k^T \cdots \mathbf{d}_K^T\right]^T \tag{2.18}$$

By defining now the $NQ \times N$ matrix $\mathbf{C}_k$:

$$\mathbf{C}_k = \{[\mathbf{C}_k]^{i,j}\} \quad ; \quad i = 1...NQ, j = 1...N$$

$$[\mathbf{C}_k]^{i,j} = \begin{cases} c_k(i - Q(j-1) - 1), & \text{for} \quad 0 \leq i - Q(j-1) - 1 \leq Q - 1 \\ 0, & \text{otherwise} \end{cases} \tag{2.19}$$

and the $NQ \times NK$ matrix $\mathbf{C}$:

$$\mathbf{C} = \left[\mathbf{C}_1 \cdots \mathbf{C}_k \cdots \mathbf{C}_K\right] \tag{2.20}$$

the NQ-length vector form for signal $\mathbf{s}$, in eq. (2.13), for a conventional CDMA system is:

$$\mathbf{s} = \mathbf{CWd} \tag{2.21}$$

where $\mathbf{W}$ is a $NK \times NK$ diagonal matrix with the diagonal elements the amplitude of each transmitted symbol d_k^m. $\mathbf{W}$ is defined as:

$$\mathbf{W} = \text{blockdiag}\left(\mathbf{W}_1 \ldots \mathbf{W}_k \ldots \mathbf{W}_K\right) \tag{2.22}$$

and $N \times N$ matrix $\mathbf{W}_k$ as:

$$\mathbf{W}_k = \{[\mathbf{W}_k]^{i+M+1,j+M+1}\} \quad ; \quad i = -M...M, j = -M...M$$

$$[\mathbf{W}_k]^{i+M+1,j+M+1} = \begin{cases} w_k^i, & i = j \\ 0, & i \neq j \end{cases} \tag{2.23}$$

The received signal $e_k(n)$ at the kth MS is the result of the convolution $s(n) * h_k(n)$ or in vector form the vector $\mathbf{e}_k$ of length $NQ + L - 1$:

$$\mathbf{e}_k = \mathbf{H}_k\mathbf{s} + \mathbf{v} = \mathbf{H}_k\mathbf{CWd} + \mathbf{v} \tag{2.24}$$

where channel matrix $\mathbf{H}_k$ is of size $(NQ + L - 1) \times (NQ)$

$$\mathbf{H}_k = \{[\mathbf{H}_k]^{i,j}\} \quad ; \quad i = 1 \dots NQ + L - 1, j = 1 \dots NQ$$

$$[\mathbf{H}_k]^{i,j} = \begin{cases} h_k(i-j), & \text{for} \quad 0 \le i - j \le L - 1 \\ 0, & \text{otherwise} \end{cases} \tag{2.25}$$

and $\mathbf{v}$ is a noise vector of length $(NQ + L - 1)$. The components $[\mathbf{v}]^i$ are assumed to be statistically independent from the data symbols d_k^m. The noise vector $\mathbf{v}$, in eq. (2.26), has a covariance matrix $\mathbf{R}_v$. The matrix $\mathbf{R}_v$ is Hermitian and in the case of stationary noise it has a Toeplitz structure. In eq. (2.26) $E[\cdot]$ denotes expectation or mean.

$$\mathbf{R}_v = E\big[\mathbf{v}\mathbf{v}^{*^T}\big] = \tag{2.26}$$

$$\begin{bmatrix} E\big[[\mathbf{v}]^1[\mathbf{v}]^{1^*}\big] & E\big[[\mathbf{v}]^1[\mathbf{v}]^{2^*}\big] & \cdots & E\big[[\mathbf{v}]^1[\mathbf{v}]^{(NQ+L-1)^*}\big] \\ E\big[[\mathbf{v}]^2[\mathbf{v}]^{1^*}\big] & E\big[[\mathbf{v}]^2[\mathbf{v}]^{2^*}\big] & \cdots & E\big[[\mathbf{v}]^2[\mathbf{v}]^{(NQ+L-1)^*}\big] \\ \vdots & \vdots & \ddots & \vdots \\ E\big[[\mathbf{v}]^{(NQ+L-1)}[\mathbf{v}]^{1^*}\big] & E\big[[\mathbf{v}]^{(NQ+L-1)}[\mathbf{v}]^{2^*}\big] & \cdots & E\big[[\mathbf{v}]^{(NQ+L-1)}[\mathbf{v}]^{(NQ+L-1)^*}\big] \end{bmatrix}$$

Data symbols d_k^m, $k = 1 \dots K, m = -M \dots M$, have also zero mean and the covariance matrix of the vector $\mathbf{d}$ is $\mathbf{R}_d$.

$$\mathbf{R}_d = E\big[\mathbf{d}\mathbf{d}^T\big] \tag{2.27}$$

For instance, in the case of $Q = 3, L = 2, N = 3, K = 2, M = 1$ eq. (2.21) takes the form:

$$\mathbf{s} = \underbrace{\begin{bmatrix} c_1(0) & 0 & 0 & c_2(0) & 0 & 0 \\ c_1(1) & 0 & 0 & c_2(1) & 0 & 0 \\ c_1(2) & 0 & 0 & c_2(2) & 0 & 0 \\ 0 & c_1(0) & 0 & 0 & c_2(0) & 0 \\ 0 & c_1(1) & 0 & 0 & c_2(1) & 0 \\ 0 & c_1(2) & 0 & 0 & c_2(2) & 0 \\ 0 & 0 & c_1(0) & 0 & 0 & c_2(0) \\ 0 & 0 & c_1(1) & 0 & 0 & c_2(1) \\ 0 & 0 & c_1(2) & 0 & 0 & c_2(2) \end{bmatrix}}_{\mathbf{C}} \underbrace{\begin{bmatrix} w_1^{-1} & 0 & 0 & 0 & 0 & 0 \\ 0 & w_1^0 & 0 & 0 & 0 & 0 \\ 0 & 0 & w_1^1 & 0 & 0 & 0 \\ 0 & 0 & 0 & w_2^{-1} & 0 & 0 \\ 0 & 0 & 0 & 0 & w_2^0 & 0 \\ 0 & 0 & 0 & 0 & 0 & w_1^1 \end{bmatrix}}_{\mathbf{W}} \underbrace{\begin{bmatrix} d_1^{-1} \\ d_1^0 \\ d_1^1 \\ d_2^{-1} \\ d_2^0 \\ d_2^1 \end{bmatrix}}_{\mathbf{d}}$$

(2.28)

and $\mathbf{H}_k$ of eq. (2.24) is :

$$\mathbf{H}_k = \begin{bmatrix} h_k(0) & 0 & 0 & 0 & 0 & 0 & 0 & 0 & 0 \\ h_k(1) & h_k(0) & 0 & 0 & 0 & 0 & 0 & 0 & 0 \\ 0 & h_k(1) & h_k(0) & 0 & 0 & 0 & 0 & 0 & 0 \\ 0 & 0 & h_k(1) & h_k(0) & 0 & 0 & 0 & 0 & 0 \\ 0 & 0 & 0 & h_k(1) & h_k(0) & 0 & 0 & 0 & 0 \\ 0 & 0 & 0 & 0 & h_k(1) & h_k(0) & 0 & 0 & 0 \\ 0 & 0 & 0 & 0 & 0 & h_k(1) & h_k(0) & 0 & 0 \\ 0 & 0 & 0 & 0 & 0 & 0 & h_k(1) & h_k(0) & 0 \\ 0 & 0 & 0 & 0 & 0 & 0 & 0 & h_k(1) & h_k(0) \\ 0 & 0 & 0 & 0 & 0 & 0 & 0 & 0 & h_k(1) \end{bmatrix} \tag{2.29}$$

2.2 Air interface structure

The design of an air interface presupposes good understanding of the system's requirements. Target data rates, bit error rate, delays along with the channel models define the radio environment. The radio environment sets the constraints on the system design and therefore it has to be carefully modeled. More issues that have to be taken into account when designing an air interface are the spectrum availability, the synchronisation constraints, signaling requirements and complexity restrictions. The IMT-2000 system requirements have been specified in [30] and described in more detail in [31]. Corresponding ETSI documents for UMTS are [32, 33]. The CDMA radio interface involves several areas, as shown in table 2.1, that sometimes contradict with each other. The desire, for example, for minimisation of equipment and complexity cost leads in general to poorer performance since the later demands more advanced and complex receivers. Figure 2.5 shows that the air interface functions are divided into protocol layers [34]. The *physical layer* performs error control, modulation, spreading, interleaving, transmitting and receiving data for the physical channels. The *medium access layer* coordinates the resources provided by the physical layer and the *link access layer* sets up, maintains and releases the logical link connection. The *network layer* includes call control, mobility manager and the radio resource management, part of which are the handover and power control. A brief description of some of the above functions that depend on the underlying multiple access method (CDMA) follows next. Data detection and recovery at the receiver will be examined in details in the next sections.

System requirements	Radio interface design
data rates	physical channels
BER, delay	spreading codes design
radio environment	modulation
bandwidth availability	error control schemes
synchronisation need	packet data transmission
complexity aspects	transceiver
	handover
	power control
	channel estimation

Table 2.1: *Air design procedure for CDMA*

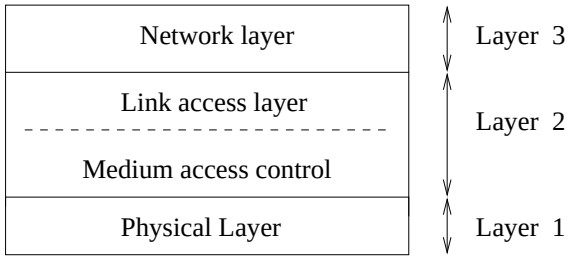

Figure 2.5: *Layer structure of CDMA air interface*

2.2.1 Frame length design

The service requirements and desired radio performance determine the frame length of the data transmitted, e.g. in a fading channel the frame length has to be long enough to support a reasonable interleaving depth but it cannot exceed the transmission delay requirement of service. For third generation wireless systems the delay requirement for speech is specified to be $30-40$ms and hence, a frame length of 10ms is short enough if interleaving is spanning only one frame. On the other hand, for data services a longer interleaving period is often tolerable.

2.2.2 Pilot signals

A pilot channel is useful in order to obtain a phase reference for the coherent detection of the data modulated signal. User dedicated pilot symbols can be used as a reference for channel estimation and initialisation of the RAKE receiver fingers.

2.2.3 Spreading code design

In a DS-CDMA transmitter the information signal is modulated by a spreading code and in the receiver it is correlated with a replica of the same code. Thus, low crosscorrelation between the desired and the interfering users is important to reduce the multiple access interference. Moreover, adequate autocorrelation properties are required for reliable initial synchronisation. Large sidelobes of the autocorrelation function can easily lead to erroneous code synchronisation decisions. Good autocorrelation properties of the spreading code result in a better resolution of the multipath components of a spread spectrum signal. Crosscorrelation and autocorrelation properties are connected in such a way that both cannot be adequate simultaneously [2]. For example, random codes exhibit good autocorrelation properties but worse crosscorrelation than the deterministic ones. Spreading codes can be divided into *pseudo-noise* codes and *orthogonal codes*.

Pseudo-noise sequences are generated with a linear feedback shift register generator. The outputs of the shift register cells are connected through a linear function formed by exclusive-or (XOR) logic gates into the input of the shift register. A two-tap linear binary shift register is displayed in Figure 2.6. Three of the basic classes of pseudo-noise sequences are:

- Maximum length sequences (M-sequences)
- Gold sequences
- Kasami sequences

Figure 2.7 displays the autocorrelation function of an M-sequence and the crosscorrelation function of two randomly selected M-sequences. The autocorrelation properties of M-sequences are very good, in contrast with their crosscorrelation properties. Orthogonal sequences are completely orthogonal for zero delay but for other delays they have very bad crosscorrelation properties and thus they are suitable only for synchronous applications.

In any case the correlation properties and the number of codes needed are two important selection criteria in order to design and select the most appropriate code family for a particular air interface design. For a more detailed description of spreading codes design, analysis and usage readers can refer to [13, 35–40].

The spreading codes for UTRA are called channelisation codes. Channelisation codes are used

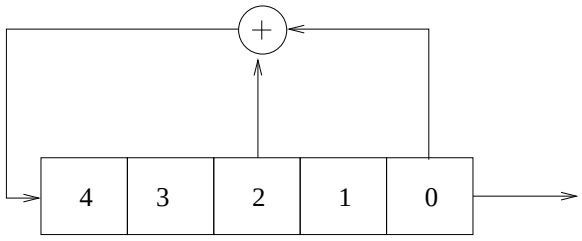

Figure 2.6: *Two-tap linear binary shift register*

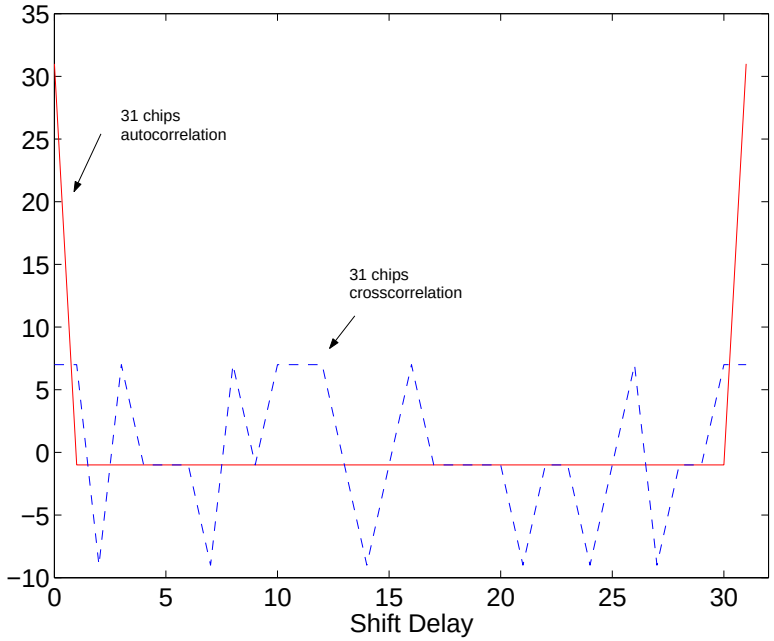

Figure 2.7: *The autocorrelation function of an* 31*-chips long M-sequence and the crosscorrelation function of two randomly selected M-sequences with the same length.*

from a single source to seperate transmissions, i.e. downlink connections within one sector and the dedicated physical channel in the uplink from one terminal. The spreading/channelisation codes of UTRA are based on the Orthogonal Variable Spreading Factor (OVSF) technique, which was originally proposed in [41]. The use of OVSF codes allows the spreading factor to be changed and orthogonality between different spreading codes of different lengths to be maintained. The codes are picked from the code tree, which is illustrated in Figure 2.8. In case the connection uses a variable spreading factor, the proper use of the code tree also allows despreading according to the smallest spreading factor. This requires only that channelisation codes are used from the branch indicated by the code used for the smallest spreading factor. In downlink the only impairment of channelisation codes is their limited number which reduces the number of active users. For examble for channelisation of length $Q = 16$, only 16 users can be active simultaneously. The problem is solved with random codes at the cost of orthogonality.

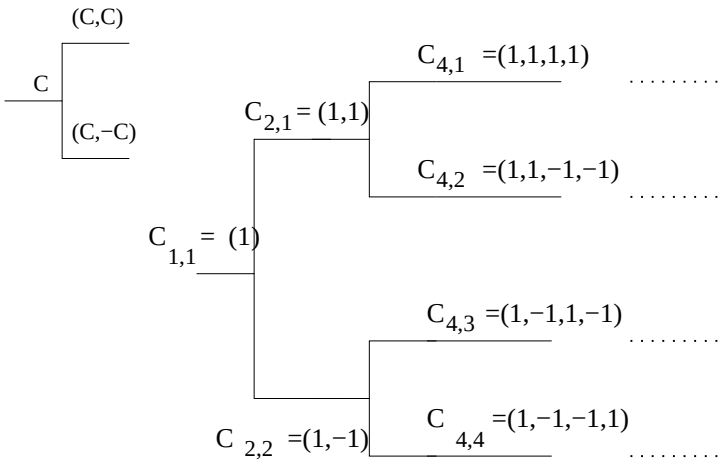

Figure 2.8: *Beginning of the channelisation code tree.*

The loss of orthogonality, on the other hand can be of minimum effect by means of multiuser detection or pre-coding techniques. The second is the subject of this thesis and, therefore, random generated codes are used.

2.2.4 Scrambling

In addition to spreading, part of the process on the transmitter is the scrambling operation. This is needed to separate terminals or base stations from each other. Scrambling is used on top of spreading, so it does not change the signal bandwidth but only makes the signals from different sources separable from each other. With the scrambling it would not matter if the actual spreading were done with identical code for several transmitters. The scrambling codes at the uplink seperate the terminals and at the downlink seperate the sectors.

2.2.5 Modulation

The *data modulator* maps the incoming coded data bits into one of $M = 2^m$ possible real or complex valued transmitted symbols. Binary data modulation follows the rule: $(1 \Rightarrow +1)$, $(0 \Rightarrow -1)$ or quaternary, like Gray encoding, that follows the rule: $(00 \Rightarrow +1 + j)$, $(01 \Rightarrow -1 + j)$, $(10 \Rightarrow 1 - j)$, $(11 \Rightarrow -1 - j)$. Quaternary modulation does not give any advantage over binary modulation in a power limited DS-CDMA system [2]. On the contrary, it is actually slightly more sensitive to phase errors due to crosscoupling of the I and Q channels. Demodulation can be noncoherent, differentially coherent or coherent. The coherent reception gives a 3-dB advantage over noncoherent in a AWGN channel. The phase reference, required

for coherent demodulation, can be provided by a data bearing signal or an auxiliary source such as a pilot symbol.

The modulated data are transmitted with binary, quaternary or complex spreading via *spreading circuits*. The binary DS-spreading circuit has a simple transmitter structure, as in Figure 2.2, with only one PN sequence per symbol. Its drawback is that it is more sensitive to MAI than the balanced and the dual-channel quaternary transmitter. The balanced quaternary DS-spreading spreads the same data signal onto I and Q channels using two spreading sequences, while in the dual-channel QPSK spreading circuit the symbol streams on the I and Q channels are independent of each other. Both spreading circuits are depicted in Figure 2.9.

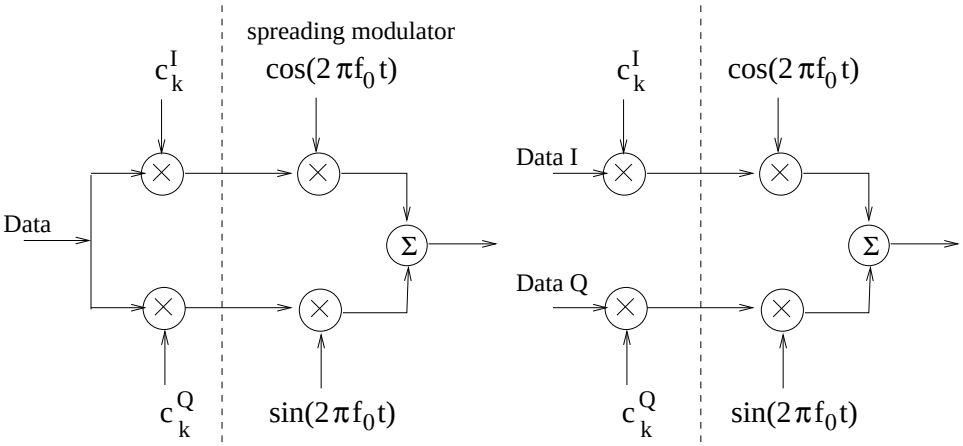

(a)Balanced spreading circuit (b)Dual−channel spreading circuit

Figure 2.9: *Spreading circuits*

The spreading circuit is followed by the *spreading modulator*. Linear modulation methods (BPSK, QPSK, and offset QPSK) have been proposed for WCMDA on the grounds that they offer good modulation efficiency. The modulated signal should be able to tolerate as much as possible the fact that nonlinear power amplifiers (preferred over linear) on the transmitter result in spectrum leakage to adjacent carriers. Thus, in practice, after the modulation is fixed, pulse shaping, eq. (2.7), determines the final spectrum properties of the modulation scheme. The BPSK, QPSK and O-QPSK constellation diagrams are illustrated in the Figure 2.10.

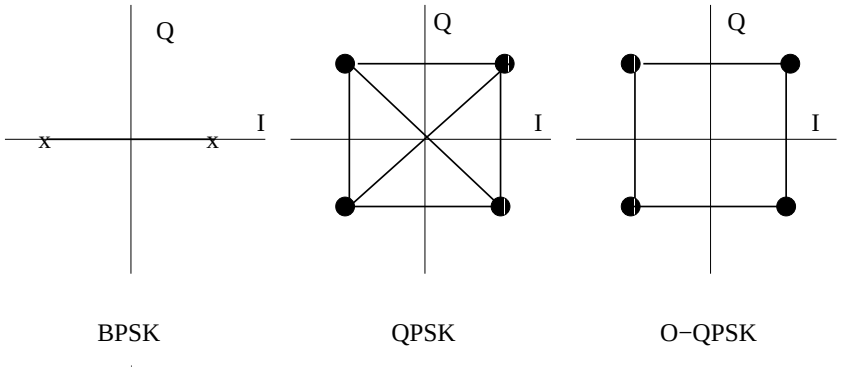

Figure 2.10: *Constellation diagrams of linear modulation methods*

2.2.6 Error control schemes

Error control schemes, used in wireless telecommunications, are divided in two major categories: the forward error control (FEC) and automatic repeat request (ARQ) [42]. A hybrid scheme is a combination of these two. In FEC, the error correcting code, sometimes referred to as the channel code, is used to combat transmission errors in a fading radio channel, while in ARQ the error detecting is used together with a retransmission protocol. Among the different error control schemes the right choice is a function of the required quality of service (data rate, delay and BER) and the radio channel. Error ratios without any error correcting algorithms in a fading channel are of the order of 10^{-1} to 10^{-2}. After using *convolutional codes* [11] (standard coding for all cellular systems) the resulting error ratio drops down to the order of 10^{-2} to 10^{-3} which is sufficient for speech transmission. However, this performance is not sufficient for data transmission, where the required BER is 10^{-6} or better. This can be achieved with a concatenated coding scheme using a convolutional and a block code, typically a *Reed-Solomon* code [43]. A recently developed FEC coding scheme is turbo coding [44–47]. *Turbo codes* are parallel or serial concatenated recursive convolutional codes, whose decoding is carried out iteratively [47] and they demonstrate performance close to the Shannon capacity limit on both AWGN and Rayleigh fading channels. Another scheme used for controlling errors is *interleaving* that is mostly effective against burst errors. The interleaving scheme can either be block or convolutional interleaving [11].

2.2.7 Power control

The power control problem arises particularly in the uplink of a DS-CDMA system and it is due to multiple access interference. The signal received by the BS from a user terminal close to

the BS will be stronger than the signal received from another terminal located further. [2, 48]. Therefore, the remote users will be dominated by the close users. This is called the *near-far effect*. To overcome this problem the signals should arrive at the BS with the same mean power. The power control mechanism achieves a near constant received mean power for each user. In addition to these, this mechanism may improve the overall performance of a DS-CDMA system against fading channels by compensating for the fading dips.

In the downlink, in contrast to the uplink all signals are transmitted through the same channel and they are received by a given MS with equal powers. Thus, power control is not required to eliminate the near-far problem. However, the power control is still needed to minimise the interference to other cells and to compensate for the interference of other cells. The worst-case scenario occurs when the MS is located at the cell's edge, equidistant from more than one BS.

There are two types of power control: open loop and closed loop [49]. In the open loop power control, the receiver measures the interference conditions from the channel and consecutively adjusts the transmission power to meet the desired error rate. This method presumes that the uplink and the downlink channels are correlated, otherwise a closed loop algorithm is necessary. In closed loop power control, the receiver measures the signal to interference ratio and sends the information to the transmitter.

2.2.8 Handover

In a CDMA system the neighboring cell frequency bands are arranged as mentioned in Chapter 1. With this type of approach a mobile performs a *hard handover*, when the signal strength of a neighboring cell exceeds the signal strength of the current cell by a given threshold. In order to avoid this kind of interference, an instantaneous handover from the current cell to the new cell would be required but this is not feasible in practice. The solution that allows the MS to be connected into a cell from which it receives the highest power is *soft handover*. In accordance with that the mobile terminal is connected simultaneously to two or more base stations thereby its transmission power can be controlled according to the cell whose signal arrives with the strongest power. A mobile station enters the soft handover state when the signal strength of a neighboring cell exceeds a certain threshold but is still below the current base station's signal strength. We should mention here that, typically, soft handover is only applied in FDD systems while it is more difficult to be applied in TDD systems.

2.2.9 Discussion

From the above we conclude that a CDMA system is more complex than the simple version presented in Figure 2.1. A more elaborate version of the transmitter, for instance, is illustrated in Figure 2.11. The data before transmission are passing through the blocks for framing, channel coding, interleaving and multiplexing with other services if necessary. Parameters like the spreading factor, the data rate and the power factor by which the transmitted data are scaled are determined by the control block. In this section only a general idea was given of the variety of operations that take place in a CDMA air interface. In reality, the system is much more complicated and depend on the actual CDMA (WCDMA, cdma2000,...) specifications. For more details on the 3G partnership project (3GPP) wideband CDMA physical layer, for instance, the TS25 series of 3GPP specifications should be studied.

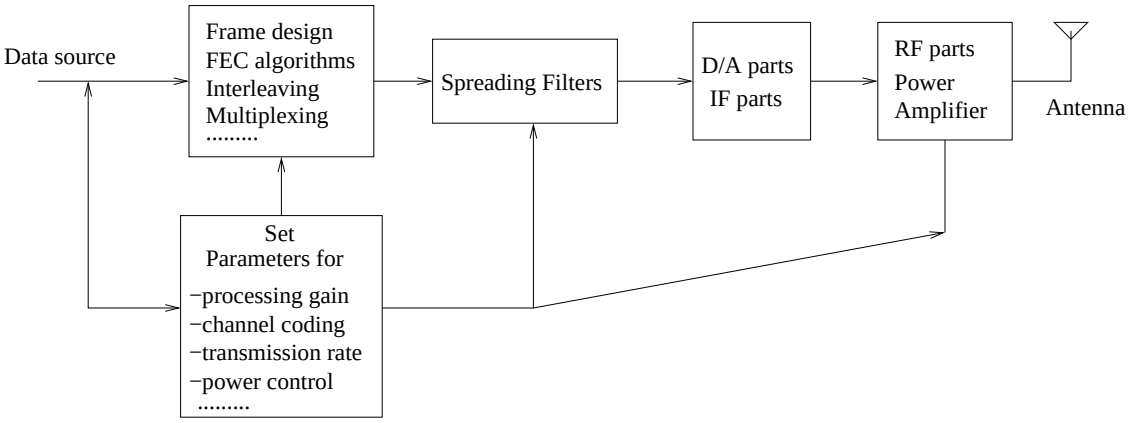

Figure 2.11: *Transmitter block diagram*

2.3 RAKE receiver

If a synchronous AWGN channel is assumed in conjuction with orthogonal codes it is adequate for the receiver to correlate the received signal with the spreading code of the user of interest. The correlator can be replaced by a filter matched to the spreading code [11]. Setting $\|\mathbf{c}_k\| = 1$ the output of the correlator will be:

$$y_k = \int_0^{T_s} e_k(t)c_k(t)dt = d_k + \sum_{\substack{i=1 \\ i\neq k}}^{K} \rho_{ik}d_i + \int_0^{T_s} c_k(t)v(t), \qquad 1 \leq k \leq K \tag{2.30}$$

where by ρ_{ik} we denote the crosscorrelation between the spreading codes $c_i(t)$, $c_k(t)$

$$\rho_{ik} = \int_0^{T_s} c_i(t)c_k(t)dt, \rho_{ik} = \mathbf{c}_i^T \mathbf{c}_k \tag{2.31}$$

Thus, if $\rho_{ik} = 0$, $i \neq k$, then the output of the matched filter consists of the decoupled desired symbol perturbated by the filtered noise. However, in Chapter 1 it was mentioned that radio channels usually include multipath propagation where, several time-shifted and scaled versions of the transmitted signal arrive at the receiver, reflected by mountains, buildings and other obstacles. The presence of multipath fading environment or even random time offsets between signals destroy the orthogonality among the spreading sequences of the received user signals. Lack of orthogonality leads to cross interference or multiple access interference between the signals of different users while the multipath imposes intersymbol interference to the transmitted signal. In Figure 2.12 the multipath effect is illustrated. Equation (2.30) is extended to (2.32) for the multiple access in multipath.

$$y_k = \int_0^{T_s} e_k(t)c_k(t)dt = d_k + \text{MAI} + \text{ISI} + \int_0^{T_s} c_k(t)v(t) \tag{2.32}$$

Correlation with the kth user gives rise to the recovered data term, a correlation term from all the other users (MAI), and correlation with the thermal noise $v(t)$ yields the noise term. The signal to noise-plus-interference ratio was defined in Chapter 1 as the the desired signal energy over the sum of the power of all kinds of interferences. For data detection in systems applying CDMA, the two problems of channel equalisation and of signal separation have to be solved simultaneously. A simple correlator or a matched filter is not adequate any more as it detects only one user while the signals of the other users are treated as noise and it can't cope with the intersymbol interference. We will examine next the single-user scenario of a DS-CDMA system in a frequency selective channel.

As shown in section 2.1 a multipath channel can be modeled as a tapped delay line with statistically independent tap weights that provides us with L replicas of the same transmitted signal at the receiver. Hence, a receiver that processes the received signal in an optimum manner will achieve the performance of an equivalent Lth-order diversity communications system. The signals are resolvable when they arrive more than one chip apart in time from each other. In frequency domain, it means that the bandwidth of the transmitted signal should be larger than the coherence bandwidth of the channel. This is the case when a spread spectrum signal is assumed, as in a DS-CDMA system. In DS-CDMA, multipath has both a positive and a negative

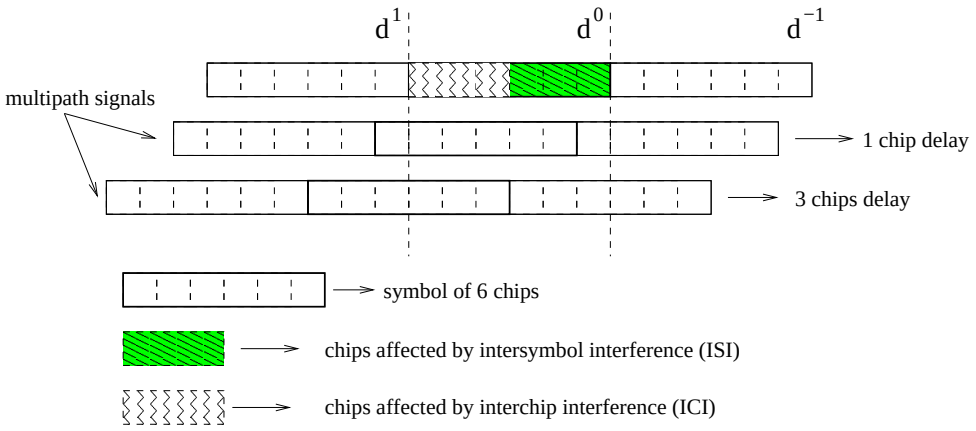

Figure 2.12: *Intersymbol interference (ISI): how bit d^{-1}'s multipath replicas affect the next bit d^0. Interchip interference (ICI) : within one symbol by delayed replicas of itself.*

effect. On one hand, the independent paths can be a valuable source of diversity and on the other hand impose intersymbol interference.

A popular single-user receiver in the presence of multipath is the RAKE combiner proposed by Price and Green in 1958 [50, 51]. The RAKE receiver uses multiple correlators, one for each path, and the outputs of the correlators are combined into a single output to maximise the signal to noise ratio. The combination method is usually maximal ratio combining in accordance to which each of the replicas of the signal is weighted by its own complex conjugated path gain (attenuation factor). In Figure 2.13 the configuration for a RAKE receiver is given. It is a tapped delay line whose tap-coefficients correspond to the multipath channel illustrated in Figure 2.4. In effect, the tapped delay line receiver structure attempts to collect the signal energy from all the received signal paths that fall within the span of the delay line and carry the same information. In the configuration of Figure 2.13 the correlators can be replaced by filters matched to the k-user's spreading code $\mathbf{c}_k$. The outputs are sampled at bit times, which yields "soft" estimates of the transmitted data. The final ± 1 "hard" data decisions are made according to the signs of the soft estimates.

While the RAKE receiver gives good results and increases the signal to interference ratio for the single-user case it doesn't do the same in the multiuser DS-CDMA scenario. Orthogonal codes lose their properties when passed through different multipath channels. It is clear that the conventional RAKE receiver follows a single-user detector strategy; it detects one user without regard to the existence of other users, which are treated as noise. Thus, there is no sharing of multiuser information or joint signal processing. The success of this detector depends on the

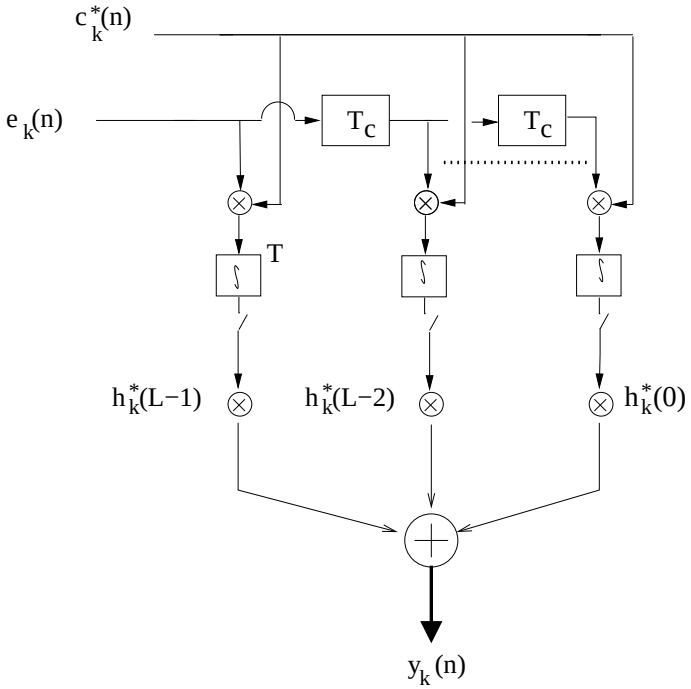

Figure 2.13: *RAKE receiver configuration*

properties of the correlation between codes. Thus eq. (2.32) is also valid for the RAKE receiver. As the number of interfering users increases, the MAI increases and consequently the signal to (MAI+ISI+noise) reduces. Therefore, the overall performance of the system is dramatically decreased. On the top of that, the conventional detector is very sensitive to the near-far problem as weaker users may be overwhelmed by stronger users. All of these give rise to the *multiuser detection* problem which will be discussed in the next section.

The matrix description of the conventional detector will be described. The output of the kth user's matched filter is:

$$\hat{\mathbf{d}}_k = \mathbf{B}_k^T \mathbf{e}_k \tag{2.33}$$

where the $(NQ + L - 1) \times N$ matrix $\mathbf{B}_k$ is defined as

$$\mathbf{B}_k = \left[\mathbf{C}_k^T \ \mathbf{O}\right]^T$$

and $\mathbf{O}$ is a $N \times (L-1)$ zero matrix. For a AWGN channel, when $L = 0$, $\mathbf{B}_k = \mathbf{C}_k$. The output of a RAKE receiver is written as:

$$\hat{\mathbf{d}}_k = \left(\mathbf{H}_k \mathbf{C}_k\right)^T \mathbf{e}_k \tag{2.34}$$

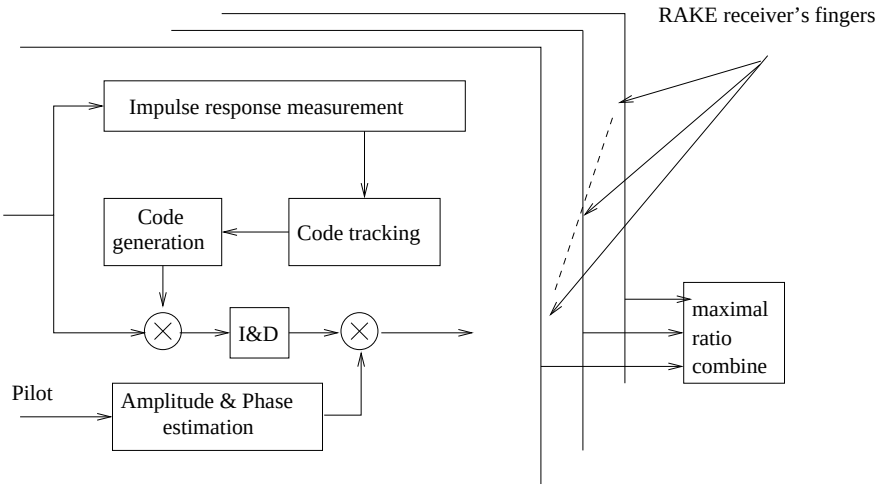

Figure 2.14: *RAKE receiver's fingers*

The RAKE receiver involves several more functions that become even more complicated when it comes to actual implementation. Figure 2.14 illustrates some of the functions that take place in each finger of the RAKE-receiver in addition to the despreading correlator and the maximal ratio combining. The impulse response measurement correlates the received signal with different phases of the pilot code to find the multipath components. Whenever the delays of the impulse response change, the impulse response measurement block allocates new code phases for the code tracking block that tracks the small changes. The RAKE receiver's weights must be updated, whenever the channel changes, with the complex conjugated channel coefficients. Therefore, the amplitude and phase estimation block is necessary. The channel estimate can be implemented using pilot symbols or adaptively with training sequences. More details about RAKE receiver implementation and extended bibliography can be found in [2].

2.4 Multiuser detection

The goal of the data detection in every mobile user k is to determine an estimate of the transmitted symbols addressed to the particular user. In other words, an estimate $\hat{\mathbf{d}}_k$ of the source data vector $\mathbf{d}$ has to be determined from the received vector $\mathbf{e}_k$, which is disturbed by the noise vector $\mathbf{v}$, eq. (2.24).

$$\hat{\mathbf{d}}_k = \left(\hat{d}_k^{-m} \dots \hat{d}_k^{0} \dots \hat{d}_k^{m}\right)^T = \mathbf{d}_k \tag{2.35}$$

The detection problem results from the fact that a number of signals, only distinguished by different codes arrive at the receiver at the same time in the same frequency band and the

orthogonality properties cannot be controlled in a multipath environment. As discussed in section 2.3, RAKE receivers fail to recover the data when MAI is present because there is no sharing of multiuser information or joint signal processing. Therefore, a more sophisticated receiver should be implemented. In Figure 2.15 the detection problem is illustrated for the uplink and the downlink. In the uplink the BS knows the codes of all users and the channels that link it with them, while in the downlink the MS should have an estimate of the channel and knowledge of all the spreading codes active in a cell. Vector $\mathbf{e}$ in Figure 2.15 denotes a superposition of all signals $\mathbf{e}_k$ arriving at the BS.

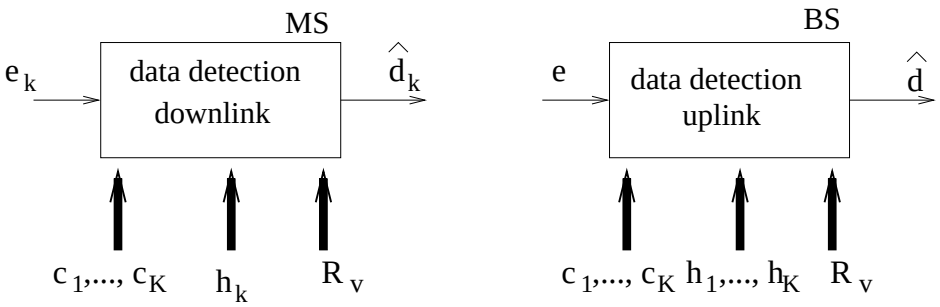

Figure 2.15: *Problem of data detection*

The optimum solution to the equalisation problem, under the assumption that all possible transmitted sequences are equally probable, is nonlinear maximum-likelihood sequence estimation (MLSE) implemented, for instance, by the Viterbi algorithm [26]. The detector which yields the most likely transmitted sequence, $\mathbf{d}$, chooses $\mathbf{d}$ to maximise the probability that $\mathbf{d}$ was transmitted given that $\mathbf{e}$ was received . This probability is reffered to as a *joint a posteriority probability* $P(\mathbf{d}|\mathbf{e})$[11]. The problem with the MLSE approach is that the complexity of the Viterby algorithm increases exponentially with the size of the symbol alphabet and the number of active users K. Actually, there are 2^{NK} possible $\mathbf{d}$ vectors that results in an exhaustive search for typical message sizes and number of users. Another disadvantage of the MLSE detector is that it requires knowledge of the received amplitudes and phases. These values, however, are not known a priori, and must be estimated. Despite the huge performance and capacity gains over conventional detection, the MLSE detector is not practical. A realistic direct-sequence system has a relatively large number of active users; thus an exponential complexity in the number of users makes the computational cost of this detector too high.

Therefore, several suboptimum algorithms for the multiuser detection problem have been developed. Figure 2.16 shows their classification. The proposed detectors can be classified in one of

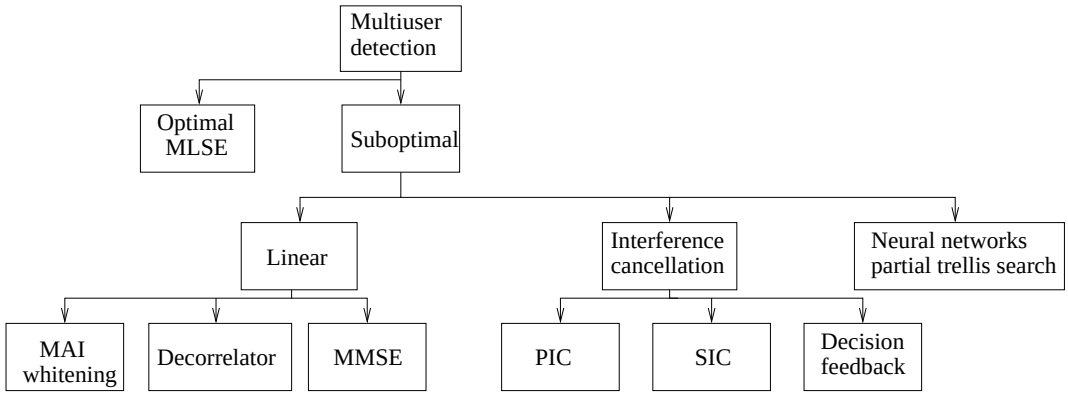

Figure 2.16: *Multiuser detection classification*

two categories: linear multiuser detectors and subtractive interference cancellation detectors. Representative and popular linear multiuser detection are the zero-forcing (ZF) and MMSE. In subtractive interference cancellation detection, estimates of the interference are generated and subtracted out. Successive interference cancellation can take place in serially (SIC) or in parallel stages (PIC). In extension to that, some interference cancellation algorithms that use decision feedback for improved performance create a new family of algorithms. An overview of the multiuser detection algorithms can be found in [28, 52–54]. Table 2.2 is a list of important contributions where various multiuser detection algorithms are derscibed in detail. In the "remarks" column we state if the algorithm is developed for a synchronous or asynchronous CDMA system, in a multipath Rayleigh or flat-fading radio-channel.

	References	**Remarks**
Linear	[55–57]	synchronous, flat channel
	[25, 58, 59]	asynchronous, flat-fading
	[60–63]	synchronous, frequency-selective, Rayleigh
	[64]	asynchronous, frequency-selective, Rayleigh
	[65]	asynchronous, frequency-selective, Rayleigh fading, antenna diversity
Non-linear	[26]	maximum likelihood, Gaussian, asynchronous
	[66, 67]	subtractive interference cancellation, multipath

Table 2.2: *Important contributions to multiuser detection algorithms*

A comparison by means of Monte-Carlo simulations of the above methods can be found in [68]. In addition to the algorithms named above, in the bibliography adaptive multiuser detection algorithms [69–75] or blind algorithms [55] can be found. Two linear multiuser detection algorithms applied for a frequency selective channel, will be presented in detail in this section.

The reason for selecting linear ones is to compare them with linear transmitter based precoding techniques, which is the main topic of this thesis. The synchronous case scheme is considered for simplicity and since in this thesis we are interested in the downlink of a CDMA system the algorithms are the ones that can be applied on the mobile receiver.

2.4.1 Zero-Forcing algorithm

The zero forcing block linear equalization is described for the uplink case in [28]. A modification applicable for the downlink is presented here. The estimate of the data vector $\mathbf{d}_k$ determined by the ZF algorithm is defined as:

$$\hat{\mathbf{d}} = \arg \quad \min_{\mathbf{d}} \big((\mathbf{e}_k - \mathbf{H}_k \mathbf{C}\mathbf{d})^H \mathbf{R}_v^{-1} (\mathbf{e}_k - \mathbf{H}_k \mathbf{C}\mathbf{d}) \big) \tag{2.36}$$

Note that all the transmitted data $\mathbf{d}$ are detected here and not only the desired ones $\mathbf{d}_k$. Thus, this is a joint detection zero forcing algorithm (ZF-JD). ZF minimises the quadratic form $\big((\mathbf{e}_k - \mathbf{H}_k \mathbf{C}\mathbf{d})^H \mathbf{R}_v^{-1} (\mathbf{e}_k - \mathbf{H}_k \mathbf{C}\mathbf{d}) \big)$ with respect to $\mathbf{d}$. If $\mathbf{R}_v = \sigma^2 \mathbf{I}$ this minimisation is equivalent to minimising the squared Euclidean distance $\|\mathbf{e}_k - \mathbf{H}_k \mathbf{C}\mathbf{d}\|^2$. The function to be minimised is the same for MLSE. However, while the minimisation in the case of MLSE is performed under the constrained that $\mathbf{d}$ is taken from the data vector alphabet, in the case of the ZF $\mathbf{d}$ may take any value. The ZF can be interpreted as an MLSE for unknown data vector alphabet. The solution of this criterion is

$$\hat{\mathbf{d}} = \big((\mathbf{H}_k \mathbf{C})^H \mathbf{R}_v^{-1} (\mathbf{H}_k \mathbf{C}) \big)^{-1} (\mathbf{H}_k \mathbf{C})^H \mathbf{R}_v^{-1} \mathbf{e}_k \tag{2.37}$$

By assuming that $\mathbf{R}_v = \sigma^2 \mathbf{I}$ the above equation is simplified to:

$$\hat{\mathbf{d}} = \big((\mathbf{H}_k \mathbf{C})^H (\mathbf{H}_k \mathbf{C}) \big)^{-1} (\mathbf{H}_k \mathbf{C})^H \mathbf{e}_k \tag{2.38}$$

As a presupposition for the ZF algorithm the matrix $\big((\mathbf{H}_k \mathbf{C})^H (\mathbf{H}_k \mathbf{C}) \big)$ has to be non-singular. When considering real world time-variant channel impulse responses $\mathbf{h}_k$ and when choosing the user specific CDMA codes $\mathbf{c}_k$ properly the matrix is singular with probability equal to zero if $K \leq Q$ [28]. The requirement $K \leq Q$ is deduced from the fact that the number $NQ + L - 1$ of samples of the received vector $\mathbf{e}_k$ (number of scalar equations forming the system of linear equations given in eq. (2.38)) has to be larger than the number KN of data symbols combined in $\mathbf{d}$, which have to be estimated. Independently of the number L of multipath components

of $\mathbf{h}_k$ this is fulfilled if $K \neq Q$. The JD-ZF algorithm is particularly useful in the downlink when non-orthogonal, e.g. pseudo-random spreading sequences, are used as it exploits fully the known crosscorrelation of all users. In case of orthogonal codes a single-detection ZF (ZF-SD) algorithm can be used as described in [28] where the mobile detector knowledge is restricted to its own spreading code and the channel link. The received signal is filtered by a channel equalizer $\left(\mathbf{H}_k^H \mathbf{H}_k\right)^{-1} \mathbf{H}_k^H$ and the codes' orthogonal properties are recovered. The performance of ZF-SD is worse than ZF-JD as shown in [28]. On the top of that, the number of users for a spreading gain Q that can be active is restricted to Q for orthogonal codes, while it increases up to 2^Q for non-orthogonal codes. The modified algorithm for ZF-SD is:

$$\hat{\mathbf{d}}_k = \left(\mathbf{C}_k^T \mathbf{C}_k\right)^{-1} \mathbf{C}_k^T \left(\mathbf{H}_k^H \mathbf{H}_k\right)^{-1} \mathbf{H}_k^H \mathbf{e}_k \tag{2.39}$$

If we replace $\mathbf{e}_k$ with the right-hand side of eq. (2.24) in equations (2.39) and (2.38) it becomes obvious that ZF algorithms eliminate the ISI and MAI perturbation term. The result output contains only the desired symbols and a noise term with enhanced covariance $\left((\mathbf{H}_k \mathbf{C})^H (\mathbf{H}_k \mathbf{C})\right)^{-1} \sigma^2$ (for ZF-JD), which is further reflected in the BER performance.

2.4.2 Minimum mean square error algorithm

The linear data detector based on MMSE block linear equaliser is presented here. The MMSE multiuser detection algorithm has been well analysed in [55] for a single path Gaussian channel and extended for multipath in [59, 61]. Again two versions can be employed. The joint detection (MMSE-JD) where the full construction of the downlink transmitted signal is taken into account and the single detection (MMSE-JD) that presupposes orthogonal spreading codes for sufficient performance. We note here that for the uplink only a joint detection can be applied as the different channels over which the mobiles transmit destroy the orthogonality. The criterion to be optimised is the following:

$$\hat{\mathbf{d}} = \underset{\mathbf{d}'}{\text{argmin}} E\left[\|\mathbf{d}' - \mathbf{d}\|^2\right] \tag{2.40}$$

The MMSE minimises the mean squared norm of the estimation error vector $\mathbf{d}' - \mathbf{d}$ with respect to $\mathbf{d}'$. With $\mathbf{R}_d$, as in eq. (2.27), the solution is:

$$\hat{\mathbf{d}} = \left((\mathbf{H}_k \mathbf{C})^H \mathbf{R}_v^{-1} (\mathbf{H}_k \mathbf{C}) + \mathbf{R}_d^{-1}\right)^{-1} (\mathbf{H}_k \mathbf{C})^H \mathbf{R}_v^{-1} \mathbf{e}_k \tag{2.41}$$

By adopting the assumptions that $\mathbf{R}_d = \mathbf{I}$ and $\mathbf{R}_v = \sigma^2\mathbf{I}$ eq. (2.41) is further simplified to:

$$\hat{\mathbf{d}} = \big((\mathbf{H}_k\mathbf{C})^H(\mathbf{H}_k\mathbf{C}) + \sigma^2\mathbf{I}\big)^{-1}(\mathbf{H}_k\mathbf{C})^H\mathbf{e}_k \tag{2.42}$$

While MMSE-JD depends on full knowledge of the spreading codes of all users MMSE-SD describes a single detection form of this algorithm where each mobile knows only its own signature waveform [28].

$$\hat{\mathbf{d}}_k = \big(\mathbf{C}_k^H\mathbf{C}_k\big)^{-1}\mathbf{C}_k^T\big(\mathbf{H}_k^H\mathbf{H}_k + \sigma^2\mathbf{R}_s^{-1}\big)^{-1}\mathbf{H}_k^H\mathbf{e}_k \tag{2.43}$$

where $\mathbf{R}_s = E\big[\mathbf{ss}\big]$, $\mathbf{s}$ as in eq. (2.21). As before the single detection algorithm can give sufficient performance only under the condition that the signature waveforms of the users are orthogonal and even under this assumption it is outperformed by its joint detection counterpart.

2.4.3 Discussion

The $NK \times NQ + L - 1$ dimension matrix $(\mathbf{H}_k\mathbf{C})^H$ in equations (2.38) and (2.42) implies a bank of RAKE receivers. The NK outputs of those receivers is transformed by the appropriate decorrelating matrices (ZF or MMSE) to yield the estimate transmitted data as shown in Figure 2.17. Another approach could be that each multipath component is used as an additional user and then a number of KNL of samples has to be taken at the chip rate at the outputs of matched filters. The later approach is described in [27].

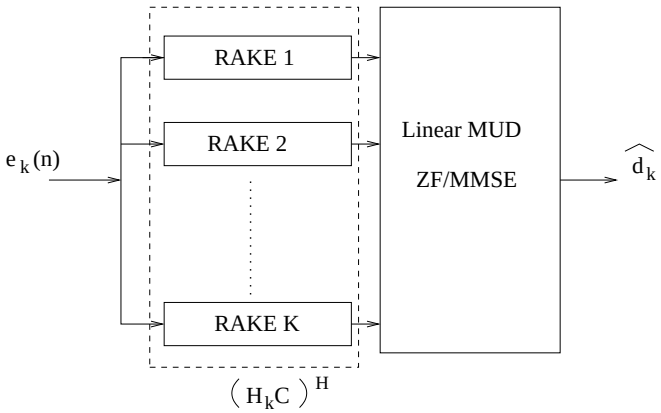

Figure 2.17: *Block diagram of linear receiver based multiuser detection scheme*

2.4.4 Complexity

From the previous section we can conclude that for the downlink CDMA the JD techniques are preferable over the SD in terms of performance and in the sense that they are the only recommended methods for the scenario of random spreading codes assigned to the users. This section examines the computational complexity of JD algorithms and explains why it is not practical to implement them at the mobile terminal for the CDMA downlink. To do so we examine what the terms in equations (2.38) and (2.42) imply.

- $\mathbf{C}$, spreading codes knowledge

  This implies that all the codes of all active users should be known to the mobile in order to construct the appropriate matrix $\mathbf{C}$ and uncouple the desired signal. To achieve this the BS station should send the information at the beginning of every transmission, which means extra capacity loss.

- $\mathbf{H}_k$, channel knowledge

  All the linear algorithms contain the matrix $\mathbf{H}_k$. The construction of this matrix presupposes channel knowledge, which can be acquired either by channel estimation algorithms for CDMA or by feedback information from the BS. This results in extra hardware and power consumption in the mobile terminal for performing the channel estimation algorithms while the later leads to capacity deterioration.

- Matrix inversion for MMSE-JD: $\left((\mathbf{H}_k\mathbf{C})^H(\mathbf{H}_k\mathbf{C})+\sigma^2\mathbf{I}\right)^{-1}$, ZF-JD: $\left((\mathbf{H}_k\mathbf{C})^H(\mathbf{H}_k\mathbf{C})\right)^{-1}$

  The transformation matrices are of size $NK \times NK$ and their inverse is required. A matrix inversion is the operation that requires the largest computational cost. Instead of matrix inversion Choleski decomposition can be used to alleviate the complexity cost. As described in [28], in some cases, a submatrix of the matrix to be inverted that still contains the whole information of the initial matrix but has smaller dimensions, can be inverted or decomposed.

From the above observations it becomes apparent that multiuser detection algorithms require hardware, power consumption and consequently size and weight. Because issues of cost, size and weight are much larger concerns for the mobiles than for the base station, it is not currently practical to include multiuser detection in mobiles [52]. Instead it has been primarily considered for use at the base station where detection of multiple users is required in any case. However,

improving the capacity of the uplink past that of the downlink does not improve the overall capacity of the system [54]. For these reasons in the next Chapters we will examine under a common framework techniques that simplify the mobile terminal and transfer the complexity to the BS.

2.5 Simulation results

2.5.1 General assumptions

The basic assumptions for the Monte Carlo simulations that are carried out in this thesis are listed in this section. The simulated systems are simplified in such a way that the objective of this research remains unaffected.

- The data symbols d_k^m, $m = -M \dots M$, are BPSK modulated thus $d_k^m = \pm 1$. They are uncorrelated and thus, $\mathbf{R}_d = \mathbf{I}$. In this work the data transmission is continual.
- For the implementation of receiver-based multiuser detection techniques for comparison purposes, perfect knowledge of the downlink channels is assumed at the MS. The BS has also perfect knowledge of the downlink channel that can be extracted from the uplink reception under certain conditions. Those conditions will be examined in Chapter 3. Thus, no pilot symbols or training sequences are required for channel estimation.
- The additive noise at the receiver is white Gaussian and uncorrelated. Hence, $\mathbf{R}_v = \sigma^2 \mathbf{I}$.
- The spreading codes for the users are random generated binary codes to allow for the worst case. The spreading gain selected is $Q = 16$.
- Throughout our research we focus on the downlink system and we consider only one cell. The intercell interference is modeled as AWGN.
- The channels are also assumed to have slow fading characteristics and are constant during the data-block transmission. The channels have a multipath profile that follows the delays of the vehicular environment A [29], shifted to be the nearer integer multiplier of the chip period $T_c = 0.26\mu$sec. The profiles of 5 of the channels used in this work, characterised as severe multipath, are given in table 2.3. For the scenario of more than five users, wherever examined in this thesis, the rest of the channels follow a similar pattern. The delay spead is $L = 11$ chip spaces taps. The tap coefficients are real and so is the

Delay in μsec	**Tap coefficients**				
	User 1	User 2	User 3	User 4	User 5
0.00	0.714206	-0.711388	0.712718	-0.742424	-0.700968
0.26	-0.614927	0.598559	-0.650006	0.596557	0.556799
0.52	0.000000	0.000000	0.000000	0.000000	0.000000
0.78	0.233789	-0.283209	-0.200871	-0.240244	0.351316
1.04	-0.201291	0.200496	0.142206	0.153339	-0.226829
1.30	0.000000	0.000000	0.000000	0.000000	0.000000
1.56	0.000000	0.000000	0.000000	0.000000	0.000000
1.82	0.100884	-0.112747	0.089726	-0.093466	-0.139862
2.08	0.000000	0.000000	0.000000	0.000000	0.000000
2.34	0.000000	0.000000	0.000000	0.000000	0.000000
2.60	-0.080135	0.050362	-0.030055	-0.054407	-0.064669

Table 2.3: *Severe multipath channels' profile*

Gaussian noise added at the receive point. In section 5.7 we also examine the scheme under which the tap-coefficients are complex and their power distribution follows random pattern (normalised). Another multipath delay profile used throughout this thesis is the mild one with $L = 3$ chips delay spread as presented in table 5.2. For both multipath schemes the channel length is less than one symbol period ($L \leq Q$) and thus ISI is extended only into the next transmitted symbol.

- The BS transmits all users signals with equal power normalised to $(w_k^m)^2 = 1$. Therefore, $\mathbf{W}$ in equations (2.21) and (2.23) is replaced by the $NK \times NK$ identity matrix $\mathbf{I}$. This is done mainly for simplicity reasons and for examining the spread in performance that the users may demonstrate even if transmitted with equal power depending on the precoding method used on the transmitter. The case of unequal powers and how this affects the system will also be addressed. The transmission of the users is synchronous.

- Error control coding is beyond the scope of this thesis.

- For simplicity reasons synchrononisation, tracking and coherent reception are considered to be perfect.

- In this work the issue of handover will not considered as we consider only one cell.

2.5.2 Receiver based JD performance

Following the assumptions described above, Monte Carlo simulations were implemented to examine the performance of the linear receiver based multiuser detection algorithms ZF-JD and MMSE-JD. Figure 2.18 shows the BER performance graphs versus E_b/N_o for a system of $K = 5$ users in a flat-fading channel. E_b is the transmitted energy per bit per user and $N_o/2$ the power spectral density of the noise. The corresponding graph for the conventional RAKE receiver is also illustrated. It is obvious that both multiuser detection schemes outperform the RAKE receiver. The MMSE-JD is slightly better than the ZF-JD which is expected as the MMSE algorithm takes into account the noise variance in conjunction with the MAI. Figure 2.19 shows the BER performance graphs versus E_b/N_o for a system of $K = 5$ users in a frequency selective propagation scheme. In both graphs the BER performance of the single user refers to the AWGN channel. The conclusions are similar to the ones drawn from Figure 2.18.

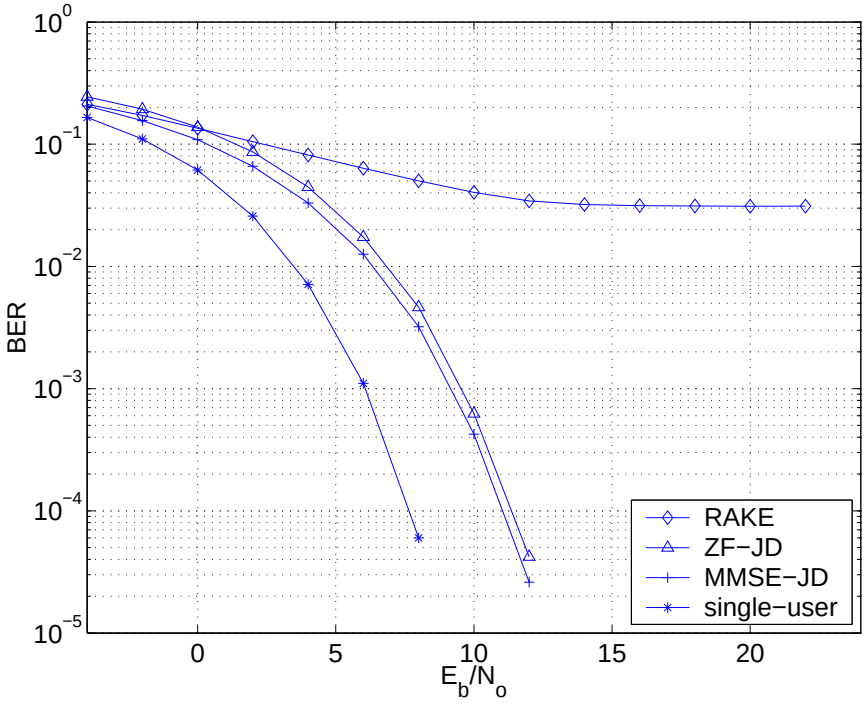

Figure 2.18: *Receiver-based MUD algorithms performance in AWGN channels.* $K = 5$ *users.*

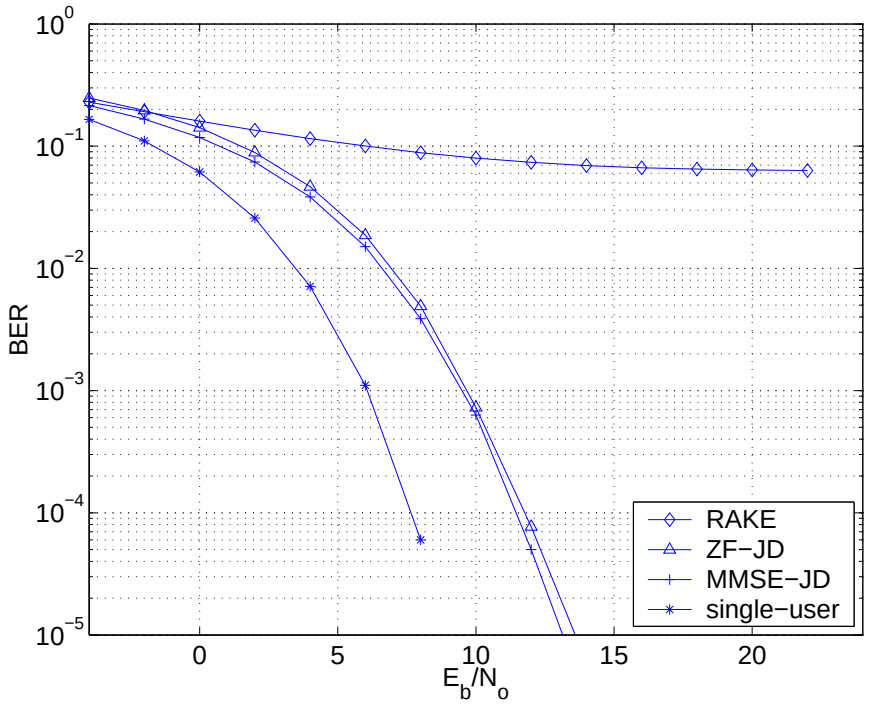

Figure 2.19: *Receiver-based MUD algorithms performance in frequency selective channels (Table: 2.3) when $K = 5$ users. Single user performance in AWGN channel.*

2.6 Summary

A mathematical vector-matrix description of a CDMA system was given along with some air-interface structure details. In a CDMA system the conventional RAKE receiver is not adequate to deal with the multiple access interference. Receiver based multiuser detection techniques that follow a bank of RAKE receivers are necessary for sufficient performance. Two linear multiuser detection algorithms were examined, ZF-JD and MMSE-JD. In the downlink mode these algorithms should be applied at the mobile terminal but the computional cost and the preliminary requirements, like downlink channel knowledge, make this application difficult. Hence, the need for techniques that remove the complexity from the MS emerges. These techniques are transmitter based (applied at the BS) and are called transmitter precoding techniques. In the following Chapter we will examine the general idea of transmitter precoding techniques and the conditions under which they are useful.

Chapter 3
Linear precoding - A general approach

The objective of this thesis is to propose techniques that remove the multiuser detection algorithms from the mobile terminal while maintaining satisfactory performance. After discussing the motivations for such an attempt in section 3.1 the special conditions that make this idea realistic in a WCDMA-TDD mode are given in section 3.2. Section 3.3 presents the precoding concept in theory and gives an analytical framework for the calculation of its bit error ratio performance . Section 3.4 classifies precoding techniques into two categories and some power issues are introduced in section 3.5.

3.1 Motivation

In the previous Chapter the problems of implementing multiuser techniques in mobile receivers and the need for their removal was underlined. The linearity of the conventional CDMA system, presented simplified in Figure 3.1, raises the question if we can somehow reverse the multiuser detection technique. The aim is to transfer the complexity and the computational load to the

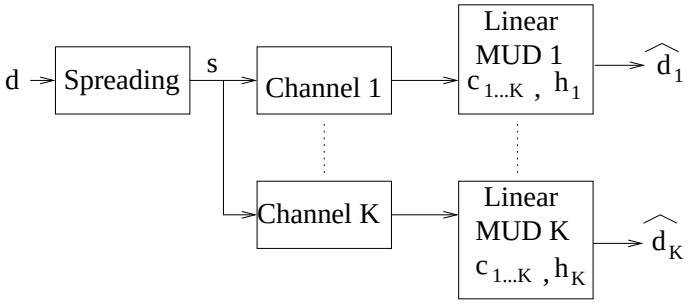

Figure 3.1: *Linearity of CDMA downlink*

transmitter (BS) where weight and size is not of concern and resources, like power and space for hardware are readily available while maintaining at least the same performance that the receiver based MUD techniques provide. The MS will be restricted to the knowledge of its own signature waveform. Therefore, the k-subscriber 's receiver shall consist of a simple correlator or a filter matched to the spreading sequence $\mathbf{c}_k$, ideal for single user in an AWGN channel and

no channel estimation, adaptive equaliser or feedback from the BS is required. In addition to that the overall capacity of the downlink in system is increased as no training sequences need be transmitted.

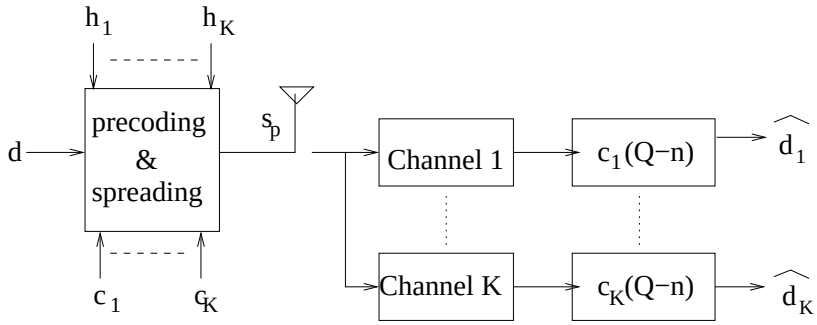

Figure 3.2: *Linear Precoding*

An answer to the question posed is to apply a linear transformation matrix, $\boldsymbol{\mathcal{T}}$, on the transmitted vector $\mathbf{d}$ (the data spreading is included in the $\boldsymbol{\mathcal{T}}$ matrix) in order to eliminate ISI and MAI, the major impairements of a CDMA system, before transmission. Under this scheme, the actual transmitted signal is distorted before transmission, in a way that after passing through the radio channel and the mobile receiver yields the desired data. In Chapter 2 we showed that each MS needs knowledge of the downlink channel impulse response $h_k(n)$ and the spreading codes of every user to apply a joint multiuser detection. If we take into account all mobile receivers, then the total information required is *all* K downlink channels and signature waveforms ($\mathbf{h}_k$, $\mathbf{c}_k$, $k = 1 \dots K$). The transformation matrix $\boldsymbol{\mathcal{T}}$ should be a function of the same knowledge in linear precoding. In other words, to achieve good performance the transmitted signals in the downlink must be jointly optimised based on the spreading code and the downlink channel impulse response of every user. The BS station obviously knows the spreading codes of all the active users in a cell and all it needs is the downlink channels impulse responses. The uplink channels can be estimated by the BS but this knowledge cannot be used for the downlink unless the principle of reciprocity is valid. Under certain conditions the downlink and uplink channels of a radio link are reciprocal. This can be assumed for the 3GPP WCDMA-TDD mode provided the time taken to switch between uplink and downlink is smaller than the coherence time of the channel [76].

3.2 WCDMA-TDD

The WCDMA [2] air interface, also referred as UMTS terrestrial radio access (UTRA), was developed by the 3GPP. WCDMA has two modes characterised by the duplex method used: frequency division duplex and time division duplex, for operating with paired and unpaired bands respectively. In FDD mode the uplink and the downlink are allocated different frequency bands separated by a significant gap in frequency, the guard frequency. In contrast in TDD mode, the uplink and downlink are time multiplexed into the same carrier. For IMT-2000 there exist two types of frequency band, paired and unpaired, and this means that both FDD and TDD modes are required to fully utilise the IMT-2000 spectrum. The principles of TDD and FDD are illustrated in the Figure 3.3.

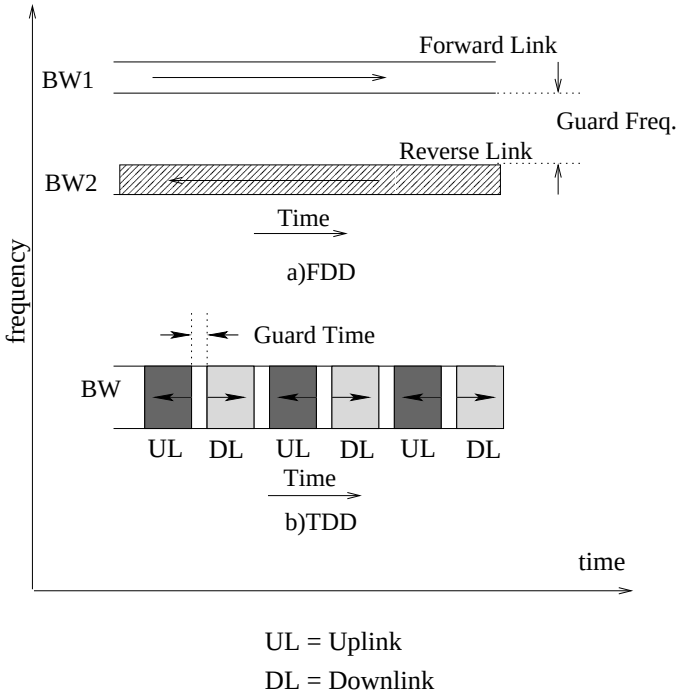

Figure 3.3: *TDD and FDD principles*

The fast fading due to multipath propagation depends on the frequency and so is uncorrelated between the uplink and the downlink in a FDD system. Therefore, the FDD transmitter cannot predict the fast fading that will affect its transmission. In TDD, where both uplink and downlink use the same frequency, the transmitter based on the uplink received signal is able to know the fast fading of the multipath channel, from the uplink and use this knowledge for precoding on the downlink. This presumes that the TDD frame length is shorter than the coherence time of the channel, as defined in Chapter 1. According to [77], Doppler frequencies up to 80Hz

(43km/h at 2-GHz carrier frequency) can be supported with a very small degradation if the uplink part of the TDD frame is 1.5ms. If the TDD system is intended only for slowly moving terminals then longer TDD frames could also be used. A possible scenario in which the above assumptions are satisfied would be a personal communication system with low mobility users such as pedestrians in an outdoor environment. Indoor and microcell environments are the most probable application areas for TDD communications. A second scenario could be a wireless local area network (LAN). In such a case the indoor RF channel has a small delay spread and a computer workstation environment has essentially stationary channels [78]. A slow variation of the channels could be addressed with a periodical update of the channel profile estimates in the BS.

The air interface structure specifications of a WCDMA-TDD system follow the general principles described in section 2.2. A brief description can be found in [2] and for a detailed explanation the 3GPP specification documents should be studied. The physical layer of WCDMA-TDD is a combination of TDMA and CDMA. Each TDD frame is of length 10ms and is divided into 15 time slots. The physical content of time slots are the bursts of corresponding length. There are two types of bursts: type 1 suitable for the uplink and type 2 for the downlink. They consist of two data symbol fields, a midamble and a guard period. In Figure 3.4(a) the structure of the burst type 2 is displayed. The TDD time slots can be allocated to either the uplink or the downlink. At least one time slot has to be allocated for the downlink and the same is valid for the uplink. In Figure 3.4(b) a multiple-switching-point configuration is illustrated. Downlink physical channels are using a spreading factor of 16, while multiple parallel physical channels transmitted using different channelisation codes can be used to support higher data rates. For the uplink physical channels the spreading factor can range from 16 down to 1.

In WCDMA-TDD mode power control is applied to limit the interference level within the system, thereby reducing the intercell interference level and the power consumption in the mobile station. Power control is performed on a frame basis (i.e. every 10ms). Based on the SNIR of the received signal, the transmitter is able to track the fast fading of the multipath channel. This assumption holds only if the frame length of 10ms is shorter than the coherence time of the channel. For the downlink a closed loop power control is used so that the mobile station can compare the estimated received SNIR with the target SNIR. This information can then be transferred to the BS, which accordingly adapts its transmitted power for that particular mobile station. We will not focus on power control issues in this work, as we assumed in

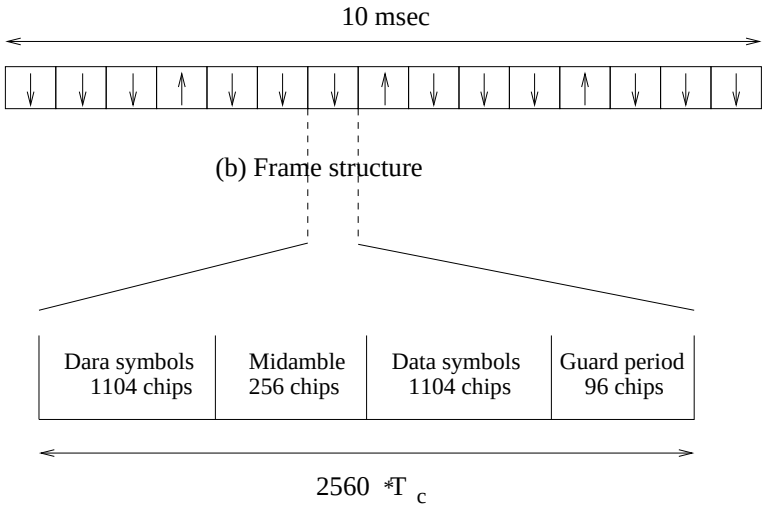

Figure 3.4: *TDD frames and bursts structure [2]*

section 2.5.1 that all users are transmitted with equal power. WCDMA downlink is synchronous transmission for all users and multiuser detection techniques can be applied for both uplink and downlink. The assumptions made for the analysis and the simulations that follow in the rest of this work are as presented in section 2.5.1.

3.3 Performance analysis of linear precoding

In a conventional CDMA model the transmitted vector is as in eq. (2.21) for $\mathbf{W} = \mathbf{I}$, $\mathbf{s} = \mathbf{Cd}$. After applying the transformation matrix $\boldsymbol{\mathcal{T}}$ on the data block $\mathbf{d}$ the resulted transmitted signal will be $\mathbf{s}_p$. Subscript p distinguishes the transmitted signal between the conventional CDMA system and the one with precoding.

$$\mathbf{s}_p = \boldsymbol{\mathcal{T}}\mathbf{d} \tag{3.1}$$

$\mathbf{s}_p$ is still of length NQ, like the original $\mathbf{s}$ and thereby matrix $\boldsymbol{\mathcal{T}}$ is of size $NQ \times KN$. The received vector $\mathbf{e}_k$ at each mobile site will now be:

$$\mathbf{e}_k = \mathbf{H}_k\boldsymbol{\mathcal{T}}\mathbf{d} + \mathbf{v}_k \tag{3.2}$$

It is desirable for the receiver of the mobile terminal k to be a filter matched to the spreading code $\mathbf{c}_k$. However, in Chapter 4 one precoding algorithm that requires a RAKE receiver will be

examined. Thus, in eq. (3.3) the output of the receiver is given for both cases:

$$\hat{\mathbf{d}}_k = \begin{cases} \mathbf{B}_k^T \mathbf{H}_k \boldsymbol{\mathcal{T}} \mathbf{d} + \mathbf{B}_k^T \mathbf{v}_k & , \quad \text{matched filter} \\ \mathbf{C}_k^T \mathbf{H}_k^T \mathbf{H}_k \boldsymbol{\mathcal{T}} \mathbf{d} + \mathbf{C}_k^T \mathbf{H}_k^T \mathbf{v}_k & , \quad \text{RAKE receiver} \end{cases} \tag{3.3}$$

From eq. (3.3) we can conclude that the detected signal at the output of the receiver has the general form:

$$\hat{\mathbf{d}}_k = \mathbf{A}_k \mathbf{d} + \mathbf{A}_v \mathbf{v}_k, \qquad k = 1 \dots K \tag{3.4}$$

where $\mathbf{A}_k$ is a $N \times KN$ matrix with elements $\{[\mathbf{A}_k]^{i+M+1,j}\}$, $i = -M \dots M, \;\; j = 1 \dots KN$ and $\mathbf{A}_v$ is also of dimensions $N \times KN$.

Based on eq. (3.4) we follow a general approach to calculate the theoretical BER performance of the precoding systems. The technique is similar to the one followed in [28] for receiver based linear multiuser detection techniques. Each component $\hat{d}_k^m, m = -M \dots M$, in $\hat{\mathbf{d}}_k$ consists of three contributions, the first determined by the desired symbol d_k^m, the second determined by ISI and MAI and the third determined by noise.

$$\hat{\mathbf{d}}_k = \underbrace{diag(\mathbf{A}_k)\mathbf{d}}_{desired\,symbol} + \underbrace{\overline{diag}(\mathbf{A}_k)\mathbf{d}}_{ISI\,and\,MAI} + \underbrace{\mathbf{A}_v^T \mathbf{v}_k}_{noise} \tag{3.5}$$

In eq. (3.5), $diag(\mathbf{A}_k)$ represents a diagonal matrix containing only the diagonal elements of the matrix $\mathbf{A}_k$ and $\overline{diag}(\mathbf{A}_k) = \mathbf{A}_k - diag(\mathbf{A}_k)$ represents a matrix with zero diagonal elements containing all but the diagonal elements of $\mathbf{A}_k$. The covariance matrix of the noise term, in eq. (3.5), is equal to

$$\mathbf{A}_v^T \mathbf{R}_v \mathbf{A}_v \tag{3.6}$$

A performance measure is the SNIR $\phi(\hat{d}_k^m)$ of $\hat{d}_k^m$ at the receiver's output. The SNIR $\phi(\hat{d}_k^m)$ is:

$$\phi(\hat{d}_k^m) = \frac{E\left\{\left|\text{symbol energy in } \hat{d}_k^m\right|^2\right\}}{E\left\{\left|\text{ISI and MAI in } \hat{d}_k^m\right|^2\right\} + E\left\{\left|\text{noise in } \hat{d}_k^m\right|^2\right\}} \tag{3.7}$$

The SNIR defined in eq. (3.7) takes into account the perturbation due to noise, ISI and MAI.

We can substitute the components from eq. (3.5) to obtain:

$$\phi(\hat{d}_k^m) = \frac{\overbrace{E\left\{|[diag(\mathbf{A}_k)\mathbf{d}]^m|^2\right\}}^{\text{desired symbol}}}{\underbrace{E\left\{\|[\overline{diag}(\mathbf{A}_k)\mathbf{d}]^m\|^2\right\}}_{\text{ISI and MAI}} + \underbrace{E\left\{|[\mathbf{A}_v\mathbf{v}]^m|^2\right\}}_{\text{noise}}} \tag{3.8}$$

Proceeding further to determine the desired and perturbation coefficients we write $\phi(\hat{d}_k^m) =$

$$\frac{\overbrace{\left|[\mathbf{A}_k]^{m',j'}\right|^2 E\left\{|d_k^{j'}|\right\}^2}^{\text{desired symbol}}}{\underbrace{[\mathbf{A}_k\mathbf{R}_d\mathbf{A}_k^T]^{m',j'} - 2Re\left\{[\mathbf{A}_k\mathbf{R}_d]^{m',j'}[\mathbf{A}_k^T]^{m',j'}\right\} + |[\mathbf{A}_k]^{m',j'}|^2 E\left\{|d_k^{m'}|^2\right\}}_{\text{ISI and MAI}} + \underbrace{[\mathbf{A}_v\mathbf{R}_v\mathbf{A}_v^T]^{m',j'}}_{\text{noise}}} \tag{3.9}$$

In eq. (3.9) and eq. (3.10) it is $m' = m + M + 1$ and $j' = M + 1 + N(k-1)$. For a matched filter receiver and after taking into account the assumptions previously made that $\mathbf{R}_d = \mathbf{I}$ and $\mathbf{R}_v = \sigma^2\mathbf{I}$ the expression in eq. (3.8) is simplified to:

$$\phi(\hat{d}_k^m) = \frac{\left([\mathbf{A}_k]^{m',j'}\right)^2}{\sum_{\substack{j=1 \\ j\neq j'}}^{KN} \left([\mathbf{A}_k]^{m',j}\right)^2 + \sigma^2} \tag{3.10}$$

The SNIR as given by eq. (3.10) can be used for calculating the error probability P_e for the detected BPSK bit $\hat{d}_k^0$. For $K \to \infty$ we can consider that ISI and MAI follow a Gaussian distribution as dictated by the central limit theorem. Therefore, the error probability $P_e(\hat{d}_k^0)$ is given by applying the Q function:

$$P_e(\hat{d}_k^m) = Q\left(\sqrt{\phi(\hat{d}_k^m)}\right) \tag{3.11}$$

For a system of K users the average theoretical error probability is

$$\bar{P}_e(\hat{d}^m) = \frac{\sum_{k=1}^{K} P_e(\hat{d}_k^m)}{K} \tag{3.12}$$

A critical issue in CDMA systems is to provide all users with equivalent performance assuming that signals of equal power are addressed to them. That means that the SNIR ϕ_k must be

approximately the same for every user. By defining the *SNIR spread* Φ_s^x as:

$$\Phi_s^x = \frac{\max\{\phi_i\}}{\min\{\phi_j\}} \quad i,j\epsilon\{1\cdots K\} \text{ for } E_b/N_o = x(dB) \tag{3.13}$$

we have a measure of the variety among the K individual performances for $E_b/N_o = x$dB. Ideal values for Φ_s^x are close to unity. SNIR spread behavior varies according to the precoding algorithm used and it will be considered in the following Chapters.

3.4 Precoding techniques-Classification

As shown in eq. (3.1) the precoded transmitted signal can be described in general with a linear transformation matrix $\boldsymbol{\mathcal{T}}$ applied on the data. In this section we will classify the realisation of this linear algorithm as either blockwise or bitwise. Although they can both be described by an appropriate matrix $\boldsymbol{\mathcal{T}}$ there are important differences.

3.4.1 Blockwise techniques

In blockwise algorithms, as will be explained in Chapter 4, the data is precoded and transmitted in blocks of N data bits for each of the K users in a cell. This means that transformation matrix $\boldsymbol{\mathcal{T}}$ is applied to a block of NK data bits. Furthermore, it is desirable for the resulting signal $\mathbf{s}_p$ to retain the same length NQ as produced by the conventional CDMA system. Thus, dimensions of the $\boldsymbol{\mathcal{T}}$ matrix shall be $NK \times NQ$. The block diagram of a blockwise precoding technique is shown in Figure 3.5.

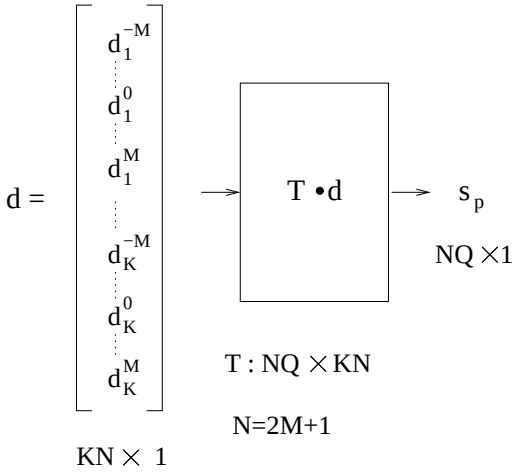

Figure 3.5: *Blockwise precoding diagram*

Matrix $\boldsymbol{\mathcal{T}}$ can be chosen according to different optimisation criteria and the complexity for determining it varies from algorithm to algorithm. Ignoring this complexity the multiplications required per bit per user for transmission of any blockwise technique results from $\mathbf{s}_p = \boldsymbol{\mathcal{T}}\mathbf{d}$, it is denoted as $\Omega_{\text{blockwise}}$ and is:

$$\Omega_{\text{blockwise}} = \frac{(KN)(NQ)(KN)}{KN} = N^2QK \tag{3.14}$$

Eq. (3.14) shows that the multiplications required for one symbol transmission are proportional to the square of a block length N^2 which for a real WCDMA-TDD can be excessively high. A not so apparent problem with the blockwise algorithms is the fact that in a multipath environment the end bits of each block are not correctly precoded and this deteriorates the overall performance. Each block is treated independently and the ISI, between the symbols of the block itself, is canceled. However, under the scenario of continual block transmission each block is extended in duration due to multipath and therefore it overlaps with the next one. The degree of damage (the number of symbols affected) depends on the channel's delay spread L. One solution to mitigate this problem is to increase the block length, but this results in increased complexity. A second solution is to neglect the number of affected symbols resulting in loss of capacity.

3.4.2 Bitwise techniques

In the bitwise techniques, the precoding realisation does not include blocks of data to be processed. The data of user k after being spread is pre-filtered by an FIR filter of length P with a discrete time impulse response $p_k(n)$ as shown in Figure 3.6. The resulting modified signals are summed to form the final transmitted signal $\mathbf{s}_p$. The filter is applied on the transmitted waveform, rather than the data symbols as in the blockwise techniques. Thus the multipath resolution afforded by the CDMA spreading is exploited. Moreover, since the filters are applied at the chip level and the derivation of the algorithms are restricted to consider only a few symbols (even one), the higher computation required for data-block solutions is eliminated. Pre-filters have also the advantage of not modifying the original CDMA structure directly as it is a simple addition of an array of FIR filters to the existing BS transmission system. Furthermore, the bitwise nature of the algorithms removes the undesirable effect of the end bock-bits as described in the previous section. The taps of the pre-filters are determined by the adopted technique. Ignoring the complexity of the algorithm used to determine the taps, the multiplications required

now per transmitted symbol per user $\Omega_{bitwise}$ is given by:

$$\Omega_{\text{bitwise}} = PQ \tag{3.15}$$

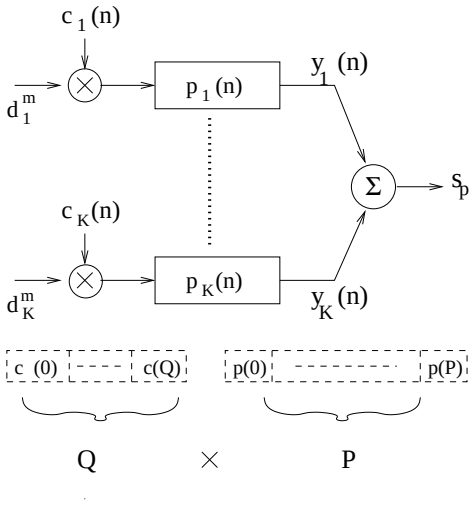

Figure 3.6: *Bitwise precoding diagram*

Comparing now equations (3.15) and (3.14) we calculate the relative complexity of blockwise and bitwise techniques.

$$\frac{\Omega_{\text{blockwise}}}{\Omega_{\text{bitwise}}} = \frac{N^2 K}{P} \tag{3.16}$$

In a CDMA system with linear MUD the users that can be accommodated do not outnumber the spreading gain : $K \leq Q$. If we set as a reasonable pre-filter length P as twice the spreading gain Q and $K = Q/2$ then :

$$\frac{\Omega_{\text{blockwise}}}{\Omega_{\text{bitwise}}} = \frac{N^2 Q/2}{2Q} = \frac{N^2}{4} \tag{3.17}$$

Apparently, for $N \geq 2$ (in a realistic system it is $N >> 2$) the multiplications required with a blockwise implementation of precoding outnumber the corresponding bitwise implementation by a large number.

It is essential for the derivation of theoretical BER to describe the bitwise techniques in the matrix form of eq. (3.1). This description is straight forward for the blockwise approach. Vector $\mathbf{p}_k$ represents the tap-coefficients of the k_{th} user specific FIR pre-filter.

$$\mathbf{p}_k = [p_k(0) \cdots p_k(P-1)]^T \tag{3.18}$$

The transmitted symbol is now expanded to $d_k^m c_k(n) * p_k(n) = d_k^m g_k(n)$, where $*$ denotes the convolution effect. The length of the pre-filter output symbol $\mathbf{g}_k$ in vector form is of length $G = Q + P - 1$ chips.

$$\mathbf{g}_k = [g_k(0) \cdots g_k(G-1)]^T \tag{3.19}$$

The pre-filters impose intersymbol interference on the system. This interference is caused by the symbols transmitted before and after the symbol under consideration. Without affecting the generality, for the bitwise techniques let us assume that the transmitted symbol under consideration is d_k^0. Let $y_k(n)$ be the signal at the output of the kth pre-filter as shown in Figure 3.6. In order to describe this signal in matrix form we must take into account M transmitted bits before and after. The right choice for M is $M = \langle (G-Q)/Q \rangle$ where $\langle x \rangle$ denotes that x is rounded up to the nearest integer. Thus, the G-length transmitted vector for user k, $\mathbf{y}_k$, is written as:

$$\mathbf{y}_k = \mathbf{G}_k \mathbf{d}_k \tag{3.20}$$

where the $G \times N$ matrix $\mathbf{G}_k$ is:

$$\mathbf{G}_k = \{[\mathbf{G}_k]^{i,(j+M+1)}\} \quad ; \quad i = 1...G, j = -M...M$$

$$[\mathbf{G}_k]^{i,(j+M+1)} = \begin{cases} g_k(i - jQ - 1), & \text{for} \quad 0 \leq i - jQ - 1 \leq G - 1 \\ 0, & \text{otherwise} \end{cases} \tag{3.21}$$

The summation of $\mathbf{y}_k$ for all the users gives the transmitted signal $\mathbf{s}_p$ which can be written as the G-length column vector:

$$\mathbf{s}_p = \sum_{k=1}^{K=1} \mathbf{y}_k = \mathbf{G}\mathbf{d} \tag{3.22}$$

where the $G \times NK$ matrix $\mathbf{G}$ is defined as:

$$\mathbf{G} = \begin{bmatrix} \mathbf{G}_1 \cdots \mathbf{G}_k \cdots \mathbf{G}_K \end{bmatrix} \tag{3.23}$$

From eq. (3.1) and eq. (3.22), it is obvious that matrix $\mathbf{G}$ corresponds to the $\boldsymbol{\mathcal{T}}$ for the bitwise algorithm matrix description. Matrix $\mathbf{G}$ is associated with the pre-filters taps and it is based on the optimisation method chosen to define the taps. Now we can apply $\mathbf{G}$ directly in the analysis of section 3.3 to calculate the theoretical BER of a bitwise precoding system.

3.5 Power scaling factor

All the precoding techniques, examined in the following Chapters, aim to mitigate the ISI and MAI impairements of a CDMA system before the transmission. In Figure 3.2, ignoring noise and assuming a unit gain channel, it is aparrent that the objective goal is $\hat{d}_k^m = d_k^m$. Depending on the method employed into the "precoding and spreading procedure" box , a certain transmit power is required for interference elimination which is usually greater than the one required for conventional spreading. In real systems however power is limited. Thus, the transmitted signal $\mathbf{s}_p$ must be scaled to maintain the total (for K users) average transmitted energy per bit interval to the desired level. The transmitted power may vary from user to user individually, according to the precoding algorithm employed, but the overall average energy per bit interval is constant. The reference power used is the one for the corresponding conventional CDMA system. The unscaled total transmission power per symbol produced by any algorithm is denoted as E_g.

For a precoding system that handles block of data the transmited energy per symbol [79] is given by the eq. (3.24).

$$E_g = \frac{\text{trace}\{\boldsymbol{\mathcal{T}}^T \boldsymbol{\mathcal{T}}\}}{N} \tag{3.24}$$

The average total transmitted energy E_g per symbol for a system using pre-filters is:

$$E_g = \sum_{k=1}^{K} \|\mathbf{c}_k * \mathbf{p}_k\|^2 \tag{3.25}$$

The conventional CDMA system model is described in section 2.1.3 in eq. (2.21). For that system the energy per transmitted symbol per user is denoted as $\mathcal{E}_g$ and for $\mathbf{W} = \mathbf{I}$ it is equivalent to:

$$\mathcal{E}_g = \text{trace}\{\mathbf{C}^T \mathbf{C}\} \tag{3.26}$$

The matrix $\mathbf{C}^T\mathbf{C}$ is the crosscorelation matrix of the spreading codes and in the case of signature waveforms normalised to $\|\mathbf{c}_k\| = 1$, $\mathcal{E}_g$ is equal to the number of users active in the system:

$$\mathcal{E}_g = K \tag{3.27}$$

At this point the vectors $\mathbf{p}_k$, $k = 1 \dots K$, (3.18), will be arranged in a KP-length vector $\mathbf{p}$ as in eq. (3.28). The reasons for doing that will become apparent when describing the derivation

of the inverse filters algorithm in Chapter 5.

$$\mathbf{p} = [\mathbf{p}_1^T \cdots \mathbf{p}_k^T \cdots \mathbf{p}_K^T]^T \tag{3.28}$$

The energy E_g of the transmitted signal $\mathbf{s}_p$, for a bitwise algorithm, will be expressed as a function of $\mathbf{p}$:

$$E_g(\mathbf{p}) = \mathbf{p}^T \mathbf{U}^T \mathbf{U} \mathbf{p} \tag{3.29}$$

where $\mathbf{U}$ is a matrix of size $K(Q+P-1) \times KP$:

$$\mathbf{U} = \text{blockdiag}\left(\mathbf{U}_1, \cdots, \mathbf{U}_k, \cdots \mathbf{U}_K\right)$$

and $\mathbf{U}_k$ is a matrix of dimension $(Q+P-1)\times P$, given in eq. (3.30) and illustrated in eq. (3.31).

$$\mathbf{U}_k = \{[\mathbf{U}_k]^{i,j}\}; \quad i = 1 \ldots Q+P-1, \quad j = 1 \ldots P$$

$$[\mathbf{U}_k]^{i,j} = \begin{cases} c_k(i-j), & \text{for} \quad 0 \le i-j \le Q-1 \\ 0, & \text{otherwise} \end{cases} \tag{3.30}$$

$$\mathbf{U}_k = \begin{bmatrix} c_k(0) & & & \\ \vdots & c_k(0) & & \mathbf{0} \\ c_k(Q-1) & \vdots & \ddots & \\ & c_k(Q-1) & & \\ & & \ddots & c_k(0) \\ \mathbf{0} & & & \vdots \\ & & & c_k(Q-1) \end{bmatrix} \tag{3.31}$$

The energy level of transmitted signal $\mathbf{s}_p$ cannot exceed $\mathcal{E}_g$. To control the energy of the output signal $\mathbf{s}_p$ of the precoding algorithms one of the following ways can be followed:

- scale the signal $\mathbf{s}_p$ before transmission with a scaling factor $\sqrt{\mathcal{F}}$

$$\mathcal{F} = \frac{\mathcal{E}_g}{E_g} \tag{3.32}$$

  This is called a global power normalisation technique and can be applied in both the bitwise and blockwise techniques. If this normalisation factor $\mathcal{F} < 1.0$, the scaling

results in a decrease in the SNR at the receiver decision point. With this in mind, the optimum precoding technique is one that minimises the MAI and ISI and maximises $\mathcal{F}$.

- In [78] the author applies a different power scaling technique for the bitwise algorithm, called decorrelating pre-filters. Each user is individually normalised to achieve a specified received SNR in contrast with the global normalisation derived in eq. (3.32). The data bit d_k^m is scaled before spreading with the factor $\frac{1}{\|\mathbf{c}_k * \mathbf{p}_k\|}$. Thus, after being filtered by $\mathbf{p}_k$ pre-filter its power is normalised to one.

- Power constraint optimisation criteria should be imposed on the algorithms that give the precoding solution. In this case the resulted power may not be exactly the intended $\mathcal{E}_g$ and a extra scaling step should take place, but the scaling step should be a small adjustment.

3.6 Summary

The linearity of a CDMA system with linear MUD gave birth to the idea of transfering the MUD complexity to the BS. Knowledge of the downlink channels is necessary for this idea and this problem is solved by assuming a WCDMA-TDD system where the reciprocity of the downlink and uplink channel is valid. The theoretical BER of a precoding system can be calculated assuming that ISI and MAI have Gaussian distribution and a new metric, called *SNIR spread* was introduced for testing if all the MSs are undergoing the same performance, given that signals of equal energies are transmitted to them. Precoding techniques can be classified in blockwise and bitwise with the later displaying particular advantages over the former, in terms of complexity and implementation. Linear transformation of transmitted data usually leads to an increased transmitted power and a scaling factor applied before transmission is necessary. An important conclusion is that the optimum precoding technique is one that minimises the MAI and ISI and maximises $\mathcal{F}$. In the next Chapter the state of the art of linear precoding techniques is presented.

Chapter 4
Linear precoding - State of the art

In the previous Chapter the idea of linear precoding in a TDD system for slow fading channels (where the rapidity of fading is slow relative to signaling rate) was supported. Such conditions can be encountered in indoor, microcellular and some satellite communications scenarios. By means of precoding, the multiuser detection problem is reduced to decoupled single user detection problems. In what follows we will describe recently developed linear precoding techniques. For all methods downlink channel knowledge is assumed at the BS. In the previous Chapter the precoding techniques were classified in blockwise and bitwise in accordance to their realisation and block diagram. Blockwise techniques like *joint transmission* (JT) and *transmitter-precoding* (TP) are given in sections 4.1 and 4.2, respectively. The bitwise ones as *decorrelating pre-filters* (DPF) and *pre-RAKE* are presented in sections 4.3 and 4.4. Section 4.5 deals with the complexity encountered by each technique while section 4.6 is a reference to a number of alternative algorithms. A discussion on the performance and a number of issues associated with precoding techniques is raised in section 4.7 and the conclusions are summarised in section 4.8.

4.1 Joint transmission

In joint transmission [80, 81] the algorithm seeks for a common signal $\mathbf{s}_p$, of length NQ, which gives the desired data at the output of every user's receiver. The received signal $\mathbf{e}_k$ at user site k is as described in eq. (2.24). The noiseless version of $\mathbf{e}_k$ is written as:

$$\mathbf{e}_k = \mathbf{H}_k \mathbf{s}_p \tag{4.1}$$

After arranging all K matrices $\mathbf{H}_k$ into the $K(NQ + W - 1) \times NQ$ matrix $\mathbf{H}$

$$\mathbf{H} = \left[\mathbf{H}_1^T \cdots \mathbf{H}_k^T \cdots \mathbf{H}_K^T\right]^T \tag{4.2}$$

and all $\mathbf{e}_k$, $k = 1 \dots K$, vectors to a total received vector $\mathbf{e}$:

$$\mathbf{e}^T = \left[\mathbf{e}_1^T \cdots \mathbf{e}_k^T \cdots \mathbf{e}_K^T\right]^T \tag{4.3}$$

it can be written:

$$\mathbf{e} = \mathbf{H}\mathbf{s}_p \tag{4.4}$$

The total received signal $\mathbf{e}$ of eq. (4.4) cannot be observed by a single MS. A MS can only observe $\mathbf{e}_k$ as described by eq. (2.24). The outputs $\hat{\mathbf{d}}_k$, $k = 1 \dots K$, at the decision variable of the K users are combined to form the vector $\hat{\mathbf{d}}$:

$$\hat{\mathbf{d}}^T = \left[\hat{\mathbf{d}}_1^T \cdots \hat{\mathbf{d}}_k^T \cdots \hat{\mathbf{d}}_K^T\right]^T \tag{4.5}$$

Recalling that the k-user's receiver is a filter matched to the user's spreading code as in eq. (2.33), $\hat{\mathbf{d}}$ can be written as in eq. (4.6).

$$\hat{\mathbf{d}} = \mathbf{B}^T\mathbf{e} = \mathbf{B}^T\mathbf{H}\mathbf{s}_p \tag{4.6}$$

In eq. (4.6) the $K(NQ + W - 1) \times KN$ block diagonal matrix $\mathbf{B}$ is defined as:

$$\mathbf{B} = \text{blockdiag}\left(\mathbf{B}_1, \cdots, \mathbf{B}_k, \cdots, \mathbf{B}_K\right) \tag{4.7}$$

The objective of any precoding algorithm is that the output of the mobile receiver yields the transmitted data :

$$\hat{\mathbf{d}} = \mathbf{d} \tag{4.8}$$

By substitution of eq. (4.8) into eq. (4.6) the problem of JT takes the form:

$$\mathbf{B}^T\mathbf{H}\mathbf{s}_p = \mathbf{d} \tag{4.9}$$

Matrices $\mathbf{B}$, $\mathbf{H}$ and vector $\mathbf{d}$ in eq. (4.9) are known at the BS and $\mathbf{s}_p$ is an unknown vector with length NQ . The condition

$$KN \leq NQ \tag{4.10}$$

is a basic assumption for TD-CDMA [28], and hence eq. (4.9) constitutes an optimisation problem [82], where the number of restrictions contained in the vector $\mathbf{d}$ of length KN, is smaller than the number NQ of degrees of freedom, expressed by the vector $\mathbf{s}_p$. Therefore, the validility of eq. (4.10) implies that eq. (4.9) has infinitely many solutions for $\mathbf{s}_p$. A constraint

criterion is necessary to be imposed to the system. It is desirable for the transmitted vector $\mathbf{s}_p$ to be of minimum energy and the approach to achieve that is by following standard Lagrange techniques [83]. The minimisation of the power $\mathbf{s}_p^T\mathbf{s}_p$ using the constraints as expressed in eq. (4.9) is described with the following Lagrange function:

$$F(\mathbf{s}_p) = \mathbf{s}_p^T\mathbf{s}_p - \underline{\boldsymbol{\lambda}}^T(\mathbf{B}^T\mathbf{H}\mathbf{s}_p - \mathbf{d}) \tag{4.11}$$

where $\underline{\boldsymbol{\lambda}}$ is the $KN \times 1$ vector of Lagrange multipliers. The minimisation of eq. (4.11) can be achieved by taking the gradient of $F(\mathbf{s}_p)$:

$$\frac{\vartheta F(\mathbf{s}_p)}{\vartheta \mathbf{s}_p} = 2\mathbf{s}_p - \mathbf{H}^T\mathbf{B}\underline{\boldsymbol{\lambda}} = 0 \tag{4.12}$$

The solution is straightforward:

$$\mathbf{s}_p = \mathbf{H}^T\mathbf{B}\underline{\boldsymbol{\lambda}} \tag{4.13}$$

The factor 2 in eq. (4.12) has been absorbed by $\underline{\boldsymbol{\lambda}}$. By replacing $\mathbf{s}_p$ in eq. (4.9) with the right-hand part of eq. (4.13) the Lagrange multipliers can be calculated:

$$\underline{\boldsymbol{\lambda}} = \left(\mathbf{B}^T\mathbf{H}\,\mathbf{H}^T\mathbf{B}\right)^{-1}\mathbf{d} \tag{4.14}$$

Hence, returning back and manipulating eq. (4.13) the final solution for signal $\mathbf{s}_p$ is proved to be:

$$\mathbf{s}_p = \mathbf{H}^T\mathbf{B}\left(\mathbf{B}^T\mathbf{H}\,\mathbf{H}^T\mathbf{B}\right)^{-1}\mathbf{d} \tag{4.15}$$

Recalling the general linear precoding eq. (3.1) it is obvious that the joint precoding matrix $\boldsymbol{\mathcal{T}}$ for JT can be written as:

$$\boldsymbol{\mathcal{T}}_{JT} = \mathbf{H}^T\mathbf{B}\left(\mathbf{B}^T\mathbf{H}\,\mathbf{H}^T\mathbf{B}\right)^{-1} \tag{4.16}$$

Equation (4.13) shows that joint transmission can be considered as a set of independent pre-RAKEs ($\mathbf{H}^T\mathbf{B}$) applied on the modified information signal given by $\underline{\boldsymbol{\lambda}}$, which is a linear transformation of the data vector $\mathbf{d}$ [84]. The same equation for linear transformation of the transmitted signal has been derived through different methods in [85, 86]. The conclusions reached for a system with a conventional receiver apply also when a RAKE receiver is employed, in which case the channel matrix $\mathbf{H}$ in eq. (4.15) should be substituted by the matrix $\mathbf{H}'$ that represents the cascaded channel and RAKE receiver $\mathbf{H}' = \mathbf{H}^T\mathbf{H}$. In case the K channels are

AWGN channels $\mathbf{H} = \mathbf{I}$ and $\mathbf{B}$ is equal to $\mathbf{C}$. Consequently $\boldsymbol{\mathcal{T}}_{JT}$ becomes:

$$\boldsymbol{\mathcal{T}}_{JT} = \mathbf{C}\big(\mathbf{C}^T\mathbf{C}\big)^{-1} \tag{4.17}$$

4.2 Transmitter precoding

Transmitter precoding is presented in [79]. It represents a linear transformation technique of transmitted data, such that the mean squared errors at all receivers are minimised. The author describes both a power unconstrained and constrained optimisation. However, the case of power constrained precoding is given only for a flat fading channel. In the unconstrained algorithm the transmitted signal is scaled with an appropriate factor in order to maintain the transmit power the same as in the case without precoding. The author in [79] considers transmitter precoding with either a conventional matched filter receiver or a RAKE receiver.

4.2.1 Unconstrained optimisation

In the scheme of a conventional CDMA system the matched filter outputs of all mobile receivers can be jointly expressed by defining the following $NK \times NK$ matrix $\mathbf{U}$:

$$\hat{\mathbf{d}} = \underbrace{\begin{bmatrix} \mathbf{B}_1^T\mathbf{H}_1\mathbf{C} \\ \vdots \\ \mathbf{B}_k^T\mathbf{H}_k\mathbf{C} \\ \vdots \\ \mathbf{B}_K^T\mathbf{H}_K\mathbf{C} \end{bmatrix}}_{\mathbf{U}} \mathbf{d} + \underbrace{\begin{bmatrix} \mathbf{B}_1^T \\ \vdots \\ \mathbf{B}_k^T \\ \vdots \\ \mathbf{B}_K^T \end{bmatrix}}_{\grave{\mathbf{v}}} \mathbf{v} \tag{4.18}$$

where $\grave{\mathbf{v}}$ is a zero-mean Gaussian noise vector with covariance matrix equal to diag$\{\sigma^2\}$, if $\|\mathbf{c}_k^2\| = 1$. To reduce the effect of MAI and ISI the author in [79] applies a linear transformation matrix $\mathbf{T}$, of dimension $NK \times NK$ on the block of data, before the spreading process. Therefore, after precoding and spreading, the vector at the outputs of the MS receivers will be:

$$\hat{\mathbf{d}} = \mathbf{UTd} + \grave{\mathbf{v}} \tag{4.19}$$

In order to calculate $\mathbf{T}$ the MMSE criterion is employed. The cost function J that has to be

minimised is defined as:

$$\begin{aligned} J &= E_{\mathbf{d},\grave{\mathbf{v}}}\left[\|\mathbf{d}-\hat{\mathbf{d}}\|^2\right] \\ &= E_{\mathbf{d},\grave{\mathbf{v}}}\left[\|\mathbf{d}-(\mathbf{UTd}+\grave{\mathbf{v}})\|^2\right] \end{aligned} \tag{4.20}$$

$E_{\mathbf{d},\grave{\mathbf{v}}}[\cdot]$ represents the expectation with respect to the data block vector $\mathbf{d}$ and noise vector $\grave{\mathbf{v}}$. The matrix $\mathbf{T}$, that minimises J is given in eq. (4.21). The derivation is given in [79].

$$\mathbf{T} = \mathbf{U}^{-1} \tag{4.21}$$

Hence, eq. (4.19) becomes:

$$\hat{\mathbf{d}} = \mathbf{d} + \grave{\mathbf{v}} \tag{4.22}$$

The multiuser detection problem that normally should have taken place in the receiver has been decoupled into NK separate single user detection problems, by means of precoding. An additional advantage is that the noise is not enhanced at the receiver, due to the lack of a receiver based decorrelating process. The cost is an increase in the transmitted energy which may neutralise the benefit described before.

The author of [79] gives the precoding matrix solution when a RAKE receiver is employed. Under this scenario $\mathbf{T}$ is still equal to $\mathbf{U}^{-1}$ but now $\mathbf{U}$ is defined as:

$$\mathbf{U} = \begin{bmatrix} \mathbf{C}_1^T\mathbf{H}_1^T\mathbf{H}_1\mathbf{C} \\ \vdots \\ \mathbf{C}_k^T\mathbf{H}_k^T\mathbf{H}_k\mathbf{C} \\ \vdots \\ \mathbf{C}_K^T\mathbf{H}_K^T\mathbf{H}_K\mathbf{C} \end{bmatrix} \tag{4.23}$$

Hereafter, we will denote the TP with matched filter receiver as TP-MAT to distinguish it from the TP with RAKE receiver, which in turn will be denoted as TP-RAKE.

From both definitions of $\mathbf{U}$ in eq. (4.18) and eq. (4.23) $\mathbf{C}$ can be taken out to write $\mathbf{U} = \mathbf{U}'\mathbf{C}$. $\mathbf{C}$ spreads the data after precoding and $\mathbf{U}'$ corresponds to the cascaded channel and receiver. Observing eq. (4.19) and after replacing $\mathbf{U}$ with $\mathbf{U}'\mathbf{C}$ it is easy to write $\mathbf{s}_p$ as:

$$\mathbf{s}_p = \mathbf{CTd} \tag{4.24}$$

From eq. (4.24) and eq. (4.21) it is obvious now that the transformation matrix $\boldsymbol{\mathcal{T}}_{TP}$ for TP is:

$$\boldsymbol{\mathcal{T}}_{TP} = \mathbf{C}\mathbf{U}^{-1} \tag{4.25}$$

In the case of a single path channel matrix $\mathbf{U}$ is simplified as in eq. (4.26).

$$\mathbf{T} = \left(\mathbf{C}^T\mathbf{C}\right)^{-1} \tag{4.26}$$

which is the $NK \times NK$ crosscorrelation matrix of the spreading codes. The same result was produced in [87, 88] described as pre-decorrelating. For the scenario of a flat fading channel the precoding matrix for TP is $\boldsymbol{\mathcal{T}}_{TP} = \mathbf{C}\left(\mathbf{C}^T\mathbf{C}\right)^{-1}$ which is the same with $\boldsymbol{\mathcal{T}}_{JT}$ in eq. (4.17). The later shows that for a single path channel the JT and TP transformation matrices are identical.

4.2.2 Constrained optimisation

The transmitter precoding technique was also extended in [79] to include a power constraint. However, this is done only for the scenario of a single path AWGN channel. Under this scheme eq. (4.19) is written as $\hat{\mathbf{d}} = \mathbf{C}^T\mathbf{C}\mathbf{T}\mathbf{d} + \mathbf{C}^T\mathbf{v}$. A direct approach to find the optimum linear transformation matrix $\mathbf{T}$, of dimensions $NK \times NK$, under the average power constraint can be formulated as

$$\min_{\mathbf{T}} E_{\mathbf{d},\hat{\mathbf{v}}}\left[\|\mathbf{d} - \hat{\mathbf{d}}\|^2\right] \tag{4.27}$$

under the constraint

$$E_g(\mathbf{T}) = \text{trace}\{\mathbf{T}^T\mathbf{C}^T\mathbf{C}\mathbf{T}\} = \mathcal{E}_g \tag{4.28}$$

where $E_g(\mathbf{T})$ is the total average transmit energy with precoding and $\mathcal{E}_g$ the corresponding power of a non-precoding equivalent CDMA system. For the AWGN channel there is no inter-symbol interference and the analysis is sufficient for the block-length of one data ($N = 1$). In that case, the total average transmit energy per bit interval $E_g(\mathbf{T})$ should be equal to $\mathcal{E}_g = K$, assuming that $\|\mathbf{c}_k\|^2 = 1$. This problem can be solved by means of the Lagrange multiplier. The precoding matrix $\mathbf{T}$ should minimise the constrained cost function J_c:

$$J_c = E\left\{\|\mathbf{d} - \hat{\mathbf{d}}\|^2\right\} + \lambda E_g(\mathbf{T}) \tag{4.29}$$

The solution is given in [79]:

$$\mathbf{T} = (\mathbf{C}^T\mathbf{C} + \lambda\mathbf{I})^{-1} \tag{4.30}$$

where $\mathbf{I}$ is the identity matrix and λ can be found from (4.29) and (4.30). It is shown in [79] that a unique $\lambda \geq 0$ exists as the desired solution where $\mathbf{C}^T\mathbf{C}$, is a positive defined matrix (property of cross correlation matrix [89]). The constrained transmitter precoding optimisation results in a worse performance than the unconstrained one with power scaling, as demonstrated in [79]. This fact in conjunction with the lack of an extension for the multipath environment will lead us into not examining this algorithm any further.

4.3 Decorrelating prefilters-Jointly optimized sequences

In [78] channel and multiple access effects are mitigated by jointly designing user transmit waveforms. It is an alternative approach to the one given in [79], but the implementation is different. Rather than relying on transmit data filtering and receiver RAKE or matched filter processing, the transmit waveforms themselves are modified. The methods described in [78] are named as *decorrelating pre-filters* (DPF) and *jointly optimized sequences* (JOS). They attempt to precompensate for the channel multipath and minimise the crosscorrelation of other users at the individual receivers simultaneously. The system is analogous to a system using a multiuser detector, specifically the decorrelator [28], at the receiver except that the processing is now at the transmitter.

4.3.1 Decorrelating prefilters

The block diagram of the DPF follows the bitwise precoding one as illustrated in Figure 3.6. The algorithm is similar to TP-MAT which calculates the best pre-filter to apply to the data symbols, filtering the data by blocks. DPF are applied to the transmit signal (instead of the data symbols directly, as in [79]), so that the filter can be applied externally and the multipath component resolution available from spread spectrum coding can be exploited.

Under the assumption of a synchronous CDMA system the received signal at mobile user j is written as:

$$e_j(n) = \sum_{k=1}^{K} d_k c_k(n) * p_k(n) * h_j(n) + v_j(n) \tag{4.31}$$

The pre-filters $p_k(n)$, $k = 1 \dots K$ are designed such that the signal meant for interfering users is orthogonal to the matched filter response for the desired user, irrespective of the received signals powers. Each user's pre-filter must be designed jointly taking into account the channel information and the transmit codes of all users. The approach taken in [78] is to design the pre-filters that maximise the signal to noise ratio at the receiver while reducing the MAI interference. This method is not a strict error probability minimizing scheme, but rather a zero forcing simultaneous multiuser interference rejecting and channel pre-equalization method. The problem formulation is stated as follows. The matched filter output at the receiver of user j is:

$$\hat{d}_j = \sum_{k=1}^{K} d_k c_k(n) * p_k(n) * h_j(n) * c_j(Q-n) + \tilde{v}_j(n) \tag{4.32}$$

$\tilde{v}_j(n)$ is the noise contribution to sample n of the receiver's output. To simplify the notation, let:

$$\gamma_{ij}(n) = c_i(n) * h_j(n) * c_j(Q-n);\ i,j = 1,\dots,K \tag{4.33}$$

Then eq. (4.32) becomes:

$$\hat{d}_j = \sum_{k=1}^{K} d_k p_k(n) * \gamma_{kj}(n) + \tilde{v}_j(n) \tag{4.34}$$

Now the pre-filter optimisation problem is written mathematically as:

$$\max_{\mathbf{p}_j} \big(p_j(n) * \gamma_{jj}(n)\big)|_{n=T_{ss}}$$

subject to constraints:

$$\begin{aligned} \big(p_k(n) * \gamma_{kj}\big)|_{n=T_{ss}} &= 0 \ \forall\ j \neq k \\ \|\mathbf{p}_k * \mathbf{c}_k\| &= 1 \end{aligned} \tag{4.35}$$

where T_{ss} is the decision sample. The second constraint in eq. (4.35) allows for proper normalisation. Each user is individually normalised to achieve a specified received SNIR in contrast with the global normalisation in eq. (3.32). Therefore the signal addressed to user k must be scaled by $1/\|\mathbf{c}_k * \mathbf{p}_k\|$. The solution is found by solving for the minimum two-norm vector $\mathbf{p}_k$

satisfying

$$\underbrace{\begin{bmatrix} \gamma_{k1}(T_{SS}) & \gamma_{k1}(T_{SS}-1) & \cdots & \gamma_{k1}(T_{SS}-P+1) \\ \gamma_{k2}(T_{SS}) & \gamma_{k2}(T_{SS}-1) & \cdots & \gamma_{k2}(T_{SS}-P+1) \\ & & \vdots & \\ \gamma_{kK}(T_{SS}) & \gamma_{kK}(T_{SS}-1) & \cdots & \gamma_{kK}(T_{SS}-P+1) \end{bmatrix}}_{\tilde{\mathbf{A}}_k} \times \mathbf{p}_k = \mathfrak{D}_k \tag{4.36}$$

where $\mathfrak{D}_k$ is an all-zero vector except for a unity entry at position k. This equation is solved using the pseudo-inverse of $\tilde{\mathbf{A}}_k$ and a solution is guaranteed to exist as long as the length of the pre-filter $P \geq K$ (if matrix $\tilde{\mathbf{A}}_k$ is full rank, an exact zero-forcing solution is obtained; otherwise, a least squares solution results). DPF carries all the advantages of the bitwise approach in terms of complexity and can be applied externally to an existing design, for the preprocessing matrix is applied to the output of the spread spectrum encoder. On the contrary, TP applies the linear transformation first and then the spreading.

4.3.2 Jointly optimised sequences

This method, also described in [78], is suitable for systems that can update the spreading codes adaptively. According to this algorithm the transmitted sequence itself is designed for each channel such that each desired received signal at the matched filter is orthogonal to the signals meant for all other users. The formulation of this problem is similar to the one for the decorrelating pre-filters except that the concatenated channel filter matrix previously defined as $\tilde{\mathbf{A}}_k$ is different.

The optimally designed signature sequence $\boldsymbol{\zeta}_k$, of length L_s, used for the signal intended for receiver k must now replace what was represented above as $\mathbf{c}_k * \mathbf{p}_k$. The user-to-user concatenated channel, denoted by $\gamma_{ij}(n)$ above, is defined now as

$$z_j(n) = h_j(n) * c_j(Q-n) \tag{4.37}$$

The channel filter matrix equation becomes

$$\underbrace{\begin{bmatrix} z_1(T_{SS}) & z_1(T_{SS}-1) & \cdots & z_1(T_{SS}-L_s+1) \\ z_2(T_{SS}) & z_2(T_{SS}-1) & \cdots & z_2(T_{SS}-L_s+1) \\ & & \vdots & \\ z_K(T_{SS}) & z_K(T_{SS}-1) & \cdots & z_K(T_{SS}-L_s+1) \end{bmatrix}}_{\tilde{\mathbf{B}}} \times \boldsymbol{\zeta}_k = \mathfrak{D}_k \tag{4.38}$$

The length L_s of the signature sequence must be at least K and $\tilde{\mathbf{B}}$ must be a full rank matrix, or the system will not have a direct solution. Again the minimum norm solution $\boldsymbol{\zeta}_k$ is found using the pseudoinverse of $\tilde{\mathbf{B}}$ and the unit-norm signature sequence for user k is $\boldsymbol{\zeta}_k/\|\boldsymbol{\zeta}_k\|$. The normalisation guarantees that the transmit power will be equal to a conventional CDMA system. Jointly optimised sequences could also be derived for a block of symbols in a manner similar to the derivation of TP in [79]. The solution for the best jointly optimised sequence would be found by modifying eq. (4.38) to include the transmitted symbols for the block data. Block processing has the advantage that the residual ISI is eliminated between symbols of the same block. However, the disadvantage is that the channel must remain stationary for the duration of the block and the end bits of the block are not correctly precoded.

4.4 Pre-RAKE diversity

This technique was initially described in [90] for DS-Spread spectrum systems and then extended in [76] for CDMA-TDD mobile communications. The algorithm for pre-RAKE origins from the diversity theory in frequency selective channels. In a mobile environment the combination of the received signals from diverse independent paths or mediums can improve the system performance. According to the central limit theorem as the number of independent paths increase, the combination of their signals will have less of a Rayleigh fading characteristic and more of a Gaussian one [89]. Hence in the radio mobile communications it is desirable to receive a signal from diverse independent paths and then combine their powers. This is what a RAKE receiver does as described in section 2.3.

The pre-RAKE technique is straight forward and takes direct advantage of the fact that in TDD the channel impulse response can be assumed the same for the uplink and the downlink. The idea is to transmit a number of signals that when received after the multipath channel merge to

a signal with the characteristics of a RAKE diversity signal. Each one of these transmissions should be then delayed according to the estimated relative path delay, and amplified according to the estimated path complex coefficient. In other words, in the downlink the BS multiplies the signal to be sent to user k by the time inverted complex conjugate of the uplink channel impulse response of the same user. When the signal is transmitted it is convolved with the channel impulse response of user k. This produces a strong peak at the output of the channel which is equivalent to the RAKE receiver's output. Therefore, the receiver of the MS does not need to estimate the channel impulse response and only uses a matched filter tuned to this peak. Figure 4.1 displays how the pre-RAKE combination affects an input signal (Dirac function) and the delayed peak produced at the output of the channel.

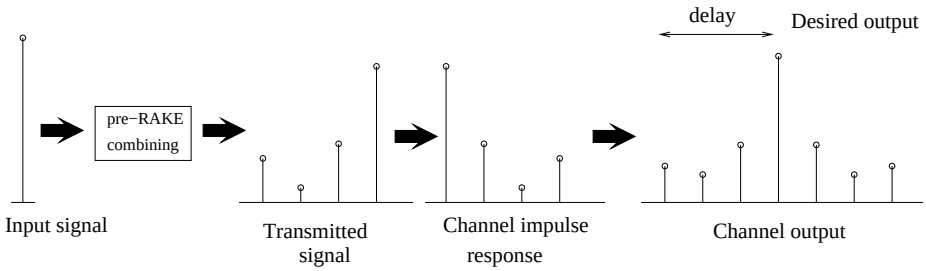

Figure 4.1: *Pre-RAKE combination process*

The analogy of RAKE and pre-RAKE concept for a single user scheme is illustrated in Figures 4.2 and 4.3, while it is mathematically explained in what follows. We begin with the SNR analysis at the output of the RAKE receiver. In Figure 4.2 the input signal is $x(n) = w_k d_k^m c_k(n)$ with a transmission power w_k^2. The signal at point 2 y_2 after passing from the multipath channel and being pertrurbated by AWGN is :

$$y_2 = \sum_{l=0}^{L-1} h(l)x(n - lT_c) + v(n) \tag{4.39}$$

The filter right after point 2 is matched to the spreading code. The RAKE combination follows and at point 3 we have:

$$y_3 = \sum_{l=0}^{L-1} h^*(L-1-nT_c)v(n-lT_c) + \sum_{l=0}^{L-1}\sum_{m=0}^{L-1} h(l)h^*(L-1-m)x(n-(l+m)T_c) \tag{4.40}$$

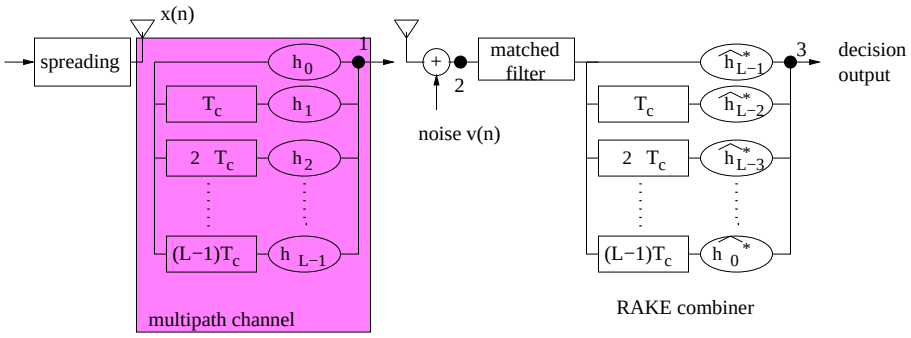

Figure 4.2: *RAKE combiner*

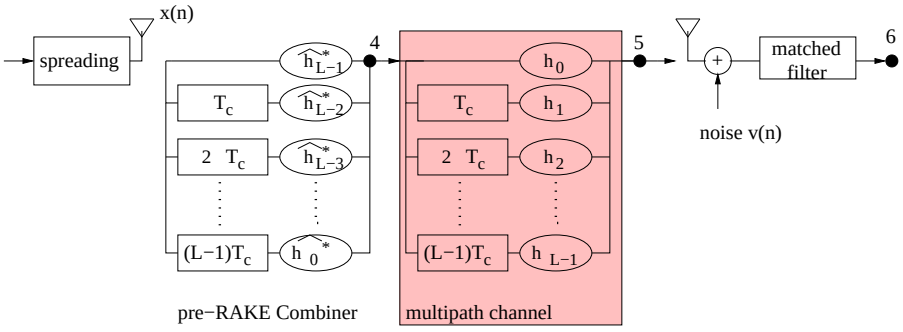

Figure 4.3: *Pre-RAKE combiner*

The desired output of the RAKE system is $\sum_{l=0}^{L-1} h(l)h^*(l)x(n-(L-1)T_c)$ and occurs at time $n=(L-1)T_c$ ($l+m=L-1$). This has a signal strength of

$$\left(\sum_{l=0}^{L-1} h(l)h^*(l)\right)^2 w_k^2 \tag{4.41}$$

Noise adds up incoherently and its power is:

$$\left(\sum_{l=0}^{L-1} h(l)h^*(l)\right)\sigma^2 \tag{4.42}$$

From equations (4.41) and (4.42) the SNR at the output of the RAKE receiver is equal to:

$$SNR_{RAKE} = \frac{w_k^2}{\sigma^2}\left(\sum_{l=0}^{L-1} h(l)h^*(l)\right) \tag{4.43}$$

In Figure 4.3 the block diagram of a pre-RAKE is illustrated. In order to make sure that the power of the signal at the output of the pre-RAKE transmitter is equal to w_k^2, a power scaling

factor should be chosen to compensate for the gains produced by $h(l)^*$. In [90] the scaling factor is:

$$\mathcal{F} = \frac{1}{\sqrt{\sum_{l=0}^{L-1} h(l)h^*(l)}} \tag{4.44}$$

In Figure 4.3 after pre-RAKE combining the signal at point 4 y_4 is :

$$y_4 = \mathcal{F} \sum_{l=0}^{L-1} h^*(n - lT_c)x(n - lT_c) \tag{4.45}$$

After transmission, convolution with the multipath channel and addition of AWGN the signal at point 6 of Figure 4.3 becomes:

$$y_6 = \mathcal{F}^2 \left(\sum_{l=0}^{L-1} \sum_{m=0}^{L-1} h^*(l)h(L-1-m)x(n-(l+m)T_c) \right) + v(n) \tag{4.46}$$

The desired signal occurs again at time $n = (L-1)T_c$ and has a power equal to

$$w_k^2 \mathcal{F} \left(\sum_{l=0}^{L-1} h(l)h^*(l) \right)^2 \tag{4.47}$$

The noise at the output of the matched filter has a power equal to σ^2. We replace $\mathcal{F}$ with the right-hand part of eq. (4.44) and thus the SNR is written as:

$$SNR_{pre-RAKE} = \mathcal{F}^2 \frac{w_k^2}{\sigma^2} \left(\sum_{l=0}^{L-1} h(l)h^*(l) \right)^2 = \frac{w_k^2}{\sigma^2} \left(\sum_{l=0}^{L-1} h(l)h^*(l) \right) \tag{4.48}$$

From equations (4.43) and (4.48) the SNR for the Pre-RAKE system is equal to that of the RAKE system, for a single user. This analysis holds only under the assumption that the channels parameters are estimated ideally [90] on the transmitter. The two systems have similar performance. In Figure 4.4 the noiseless RAKE receiver's output is illustrated and this corresponds to point 3 of Figure 4.2. The graph in Figure 4.5 shows the matched filter's output and corresponds to the noiseless pre-RAKE block diagram graph of Figure 4.3. In both Figures we mark the delay after which the peak is detected. The multipath channel has a length of $L = 11$ chips. The data has been spread with a signature waveform of $Q = 16$ chips. The similarities between a single user pre-RAKE and RAKE system are obvious and will be verified in the next section by means of a BER performance comparison.

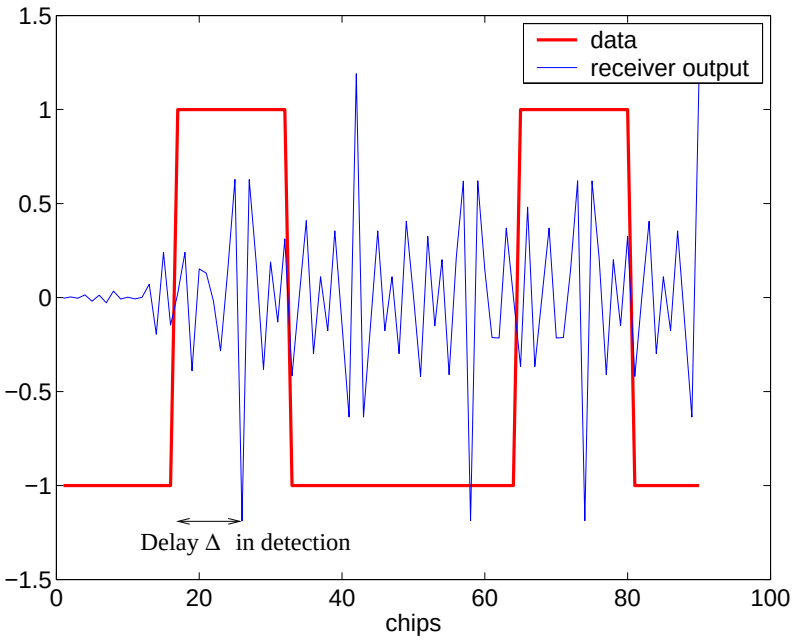

Figure 4.4: *Single user noiseless output of a RAKE receiver*

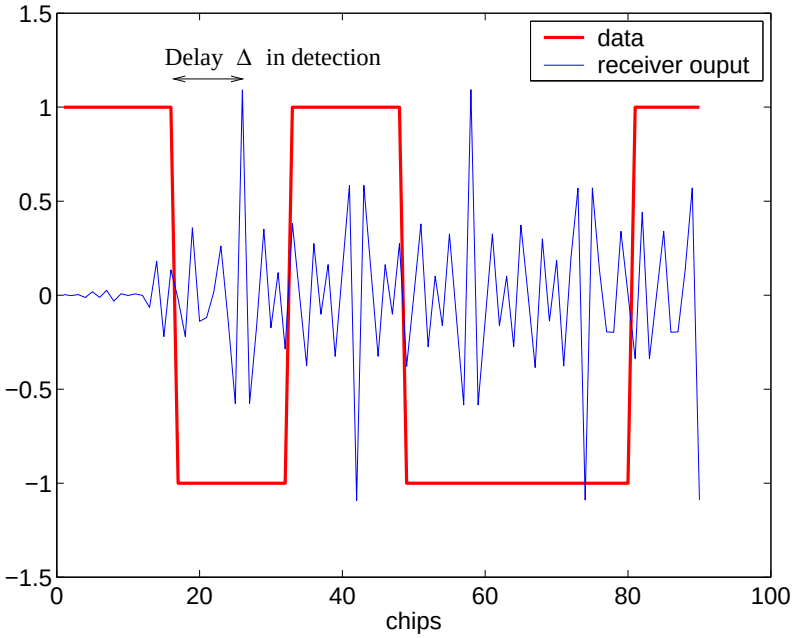

Figure 4.5: *Single user noiseless matched filter output after pre-RAKE processing*

In [76] the concept of pre-RAKE was extended to a multiuser CDMA-TDD system. The signal for user k after spreading is filtered by the time inverse complex conjugate impulse response of the k-user's channel and this process is repeated for every user before transmission. The

produced signals are appropriately scaled to maintain the power at the desired levels and then superimposed at the antenna element. The block diagram of the pre-RAKE technique applied in a CDMA-TDD is identical with the general description of a bitwise precoding technique as illustrated in Figure 3.6. Therefore, pre-RAKE has the advantages of a bitwise approach in terms of complexity and simplicity in implementation. Furthermore, the calculation of the pre-filter's tap coefficients don't require any complicated algorithm. Each pre-filter's impulse response is the time inverse conjugated of the corresponding uplink channel. The transmitted signal $s_p(n)$, under the multiuser scheme is:

$$s_p(n) = \sum_{k=1}^{K} \mathcal{F}_k \sum_{l=0}^{L-1} h^*(n - lT_c) x_k(n - lT_c) \tag{4.49}$$

The principle applied is that in the downlink the desired user's signal is maximal ratio combined by the channel itself while other user signals are not. In the analysis presented in [76] at the sampling time the matched filter output consists of the desired part of the transmitted bit, the intersymbol and multiple access interference and the noise. The mean and the variance of each one of these terms is calculated. Under the multiuser scenario the pre-RAKE is proved to be an insufficient technique unable to compensate for the multipath interference and MAI as shown in [76, 91].

4.5 Complexity

The precoding techniques described in this Chapter require excessive computational cost compared to the usual conventional spreading. The complexity is similar or exceeds the one demonstrated by the receiver based multiuser techniques as described in [28, 60, 62]. However, it is shifted to the BS, where the resources are more readily available and thus it is less critical. Table 4.1 summarises the computational cost for JT, TP-MAT, DPF, Pre-RAKE. The criteria used are the dimension of the matrix that needs to be inverted and the number of multiplications per transmitted symbol. The number of multiplications are calculated after the final transformation matrix $\boldsymbol{\mathcal{T}}$, for the blockwise techniques, as defined in Chapter 3, has been formulated. As expected the blockwise techniques JT and TP-MAT are more demanding in terms of complexity compared to the bitwise DPF and pre-RAKE.

It will be shown in the next section that JT outperforms in terms of performance the other techniques. Therefore, it is useful to emphasize on this technique. JT algorithm can be optimized

Precoding-algorithm	**Dimension of matrix to be inverted**	**Number of multiplications per symbol**
JT	$KN \times KN$	N^2QK
TP-MAT	$KN \times KN$	N^2QK
DPF	$K(P \times P)$	PQ
Pre-RAKE	none	LQ

Table 4.1: *Precoding algorithms computational complexity*

by taking advantage of two properties of matrix $\left(\mathbf{B}^T\mathbf{H}\,\mathbf{H}^T\mathbf{B}\right)$ [86]:

- $\left(\mathbf{B}^T\mathbf{H}\,\mathbf{H}^T\mathbf{B}\right)$ is Hermitian
- It consists of non-vanishing blocks of coefficients located near the diagonal which are repeated along the diagonal.

Property 1 allows for decomposing the matrix triangularly (Cholesky decomposition), which in turn allows efficient calculation of $\left(\mathbf{B}^T\mathbf{H}\,\mathbf{H}^T\mathbf{B}\right)^{-1}\mathbf{d}$ by back-substitution. On the other hand property 2 allows for decomposing $\left(\mathbf{B}^T\mathbf{H}\,\mathbf{H}^T\mathbf{B}\right)$ more efficiently than by the usual full Cholesky decomposition. The complexity of JT can be compared with the receiver based ZF-JD, described in 2.4.1. We reproduce here, for convenience, the basic equation of ZF-JD.

$$\hat{\mathbf{d}} = \left((\mathbf{H}_k\mathbf{C})^H(\mathbf{H}_k\mathbf{C})\right)^{-1}(\mathbf{H}_k\mathbf{C})^H\mathbf{e}_k \tag{4.50}$$

The matrices to be inverted for both receiver and transmitter based techniques are of dimension $KN \times KN$. Both have exactly the same structure with exactly the same non-vanishing elements. Both matrices can be inverted efficiently by taking into account properties 1 and 2. So inverting the matrices for ZF-JD and JT requires the same computational power. The only complexity difference between JT and ZF-JT arises from matrix multiplications $\mathbf{H}^T\mathbf{B}$ and $(\mathbf{H}_k\mathbf{C})^H$ respectively. The complexity of the joint predistortion techniques can be further reduced by exploiting the structure of the matrices as explained in [92]. However, the multiplications required per symbol after the matrix inversion outnumber the ones required by a bitwise technique, in a realistic system.

4.6 Other techniques

The precoding techniques described in this Chapter are only representative and most commonly used as a reference. In the recent bibliography there are alternative techniques for reducing the mobile complexity that may utilise smart antennas or even the frequency domain of a system. A comparison and review among different linear precoding techniques can be found in [91, 93]. The usage of antenna arrays can result in space-time (ST) algorithms that, when applied at the downlink, minimise the MAI and ISI. Such a ST precoding downlink transmission is described in [94, 95]. In [96–98] the authors develop a space-time zero-forcing pre-equalisation technique for interference cancellation in the TDD downlink, by transferring the analysis to the frequency domain. Moreover, an alternative blockwise precoding technique that incorporates a power constraint (JT with power constraint) is described in [84], named *joint signal precoding*. An extension of the pre-RAKE named *post-RAKE* is presented in [99]. The idea of post-RAKE is to maximise the signal to noise ratio at the MS by replacing the matched filter in the pre-RAKE block diagram with a receiver which is matched to the combination of the pre-RAKE filter and the channel. Finally, *joint transmitter-receiver optimisation* is also investigated in [100, 101]. The impairment of the post-RAKE and the transmitter-receiver optimisation algorithms is that the idea of the simplest possible receiver is not valid any more. The precoding techniques described so far induce distortion in the signal's spectral properties. A power constrained algorithm that acts on the amplitude of the transmitted signals by a simple scaling is demonstrated in [102]. This method is called *optimising precoder* and maintains the spectral properties of the initial designed signals. However, this method is developed only for a single path Gaussian channel and, on top of that, the determination of each user's power needs to be readjusted at each bit interval, which in turn results in excessive computational cost.

4.7 Simulation results

In Chapter 3 it was asserted that one of drawbacks of the blockwise techniques is that they do not allow for correct precoding of the end data, when a multipath channel occurs. Therefore, the overlapping of the signal's replicas affect the first and last transmitted bit(s). This results in a performance degradation which is more intense when the length of the transmitted block is small. This conclusion is illustrated in the Figure 4.6. The performance of JT versus the number of users is shown for block lengths 1, 3 and 20 data. Spreading gain is set to the default

for this thesis $Q = 16$ chips. The simulation corresponds to a system where the channels follow a severe multipath profile ($L = 11$ chips) and $E_b/N_o = 10$dB. Each curve represents an average over 60 different sets of random codes to smooth out the effect of codes with low or high crosscorrelation. As shown the performance is better for $N = 20$.

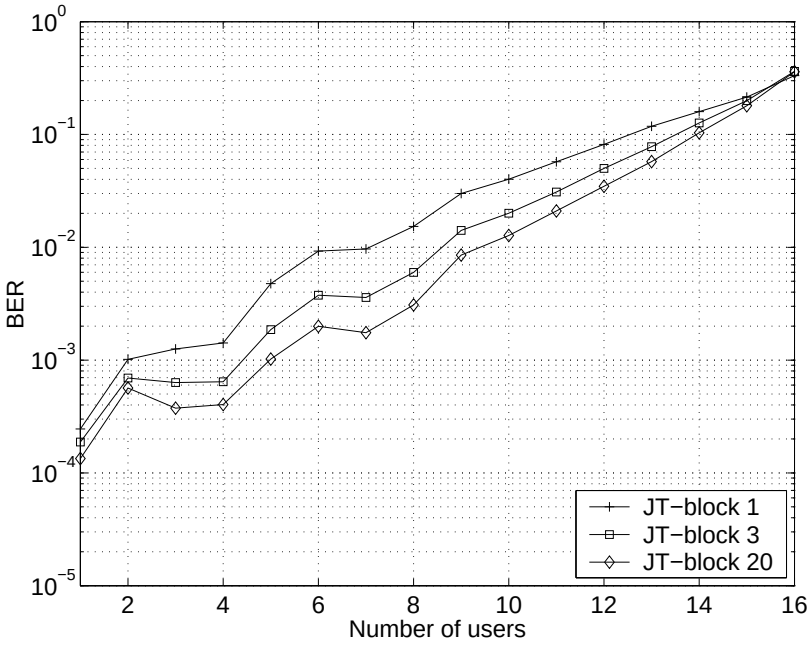

Figure 4.6: *Block-length effect on JT performance*

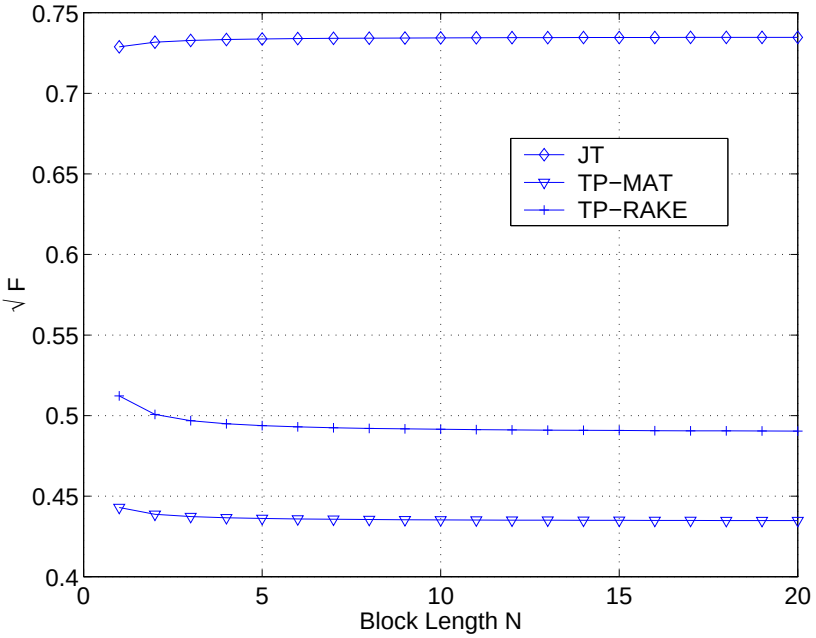

Figure 4.7: *Block-length effect on Transmitted Energy E_g*

In Figure 4.7 we investigate how the block length affects the scaling factor needed to maintain the total transmitted energy per symbol E_g equal to $\mathcal{E}_g$. The blockwise algorithms displayed are TP-MAT, TP-RAKE and JT. The same system is simulated for each curve and thus a conclusion of how the different methods affect the transmitted energy can be drawn. The system adopted is one of $K = 5$ users in a multipath environment. For each algorithm the scaling factor $\sqrt{\mathcal{F}}$ is almost flat versus N. For small N there is some differentiation but it can be assumed negligible. We recall here from Chapter 3 that ideally the scaling factor should be $\sqrt{\mathcal{F}} \geq 1.0$, otherwise it deteriorates the SNR at the receiver point. Comparing the three algorithms it is obvious that TP-MAT results in the highest increase of transmitted energy (it corresponds to the smallest $\sqrt{\mathcal{F}}$), while JT is the most modest and displays the least energy increase. TP-RAKE lies in between. The excess energy is the penalty paid for the cancellation of MAI and ISI before transmission. It is expected from these observations that JT will demonstrate the best BER performance and TP-MAT the worst. This will be verified by the simulations that are following.

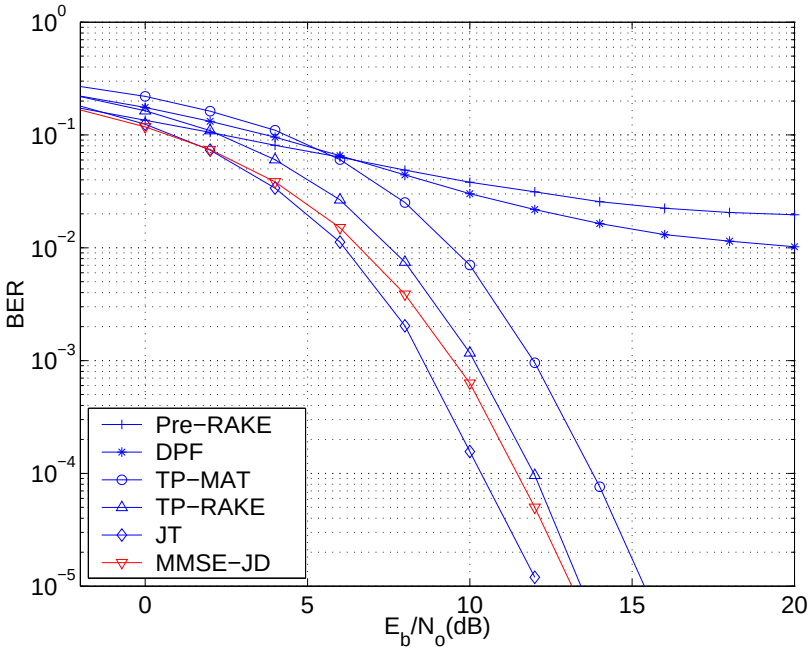

Figure 4.8: *Transmitter based precoding techniques and MMSE-JD vs* E_b/N_o

In Figure 4.8 the BER performance is shown versus E_b/N_o. The system is one of $K = 5$ users in a severe multipath environment. The best performance is displayed by JT and the worst by the pre-RAKE. In the blockwise techniques the end bits have been discarded from the calculation of BER. This is because the theoretical BER, as calculated from eq. (3.12) pressumes transmission of a single block of data without taking into account the end-bits interference. Thus, the

analytical and the simulation results can be in agreement. This can be justified from the fact that for large blocks the effect of the end bits is negligible. We examine first the region where BER is equal to 10^{-3}. TP-MAT is worse than TP-RAKE. This is because TP-MAT over-increases the required transmitted energy E_g, compared with TP-RAKE. The RAKE receiver utilised by TP-RAKE exploits the diversity principles and increases the SNR at the receiver output. In the same Figure the performance of the MMSE-JD receiver based multiuser detection is illustrated. We observe that MMSE-JD outperforms all the transmitter based precoding techniques except JT. JT completely eliminates the ISI and MAI within a block of data and selects the transmission vector with the minimum energy. This, in conjuction with the lack of any receiver based decorrelation that may increase the noise justifies the superiority of JT. This simulation does not include any channel coding such as convolutional or turbo coding techniques. Utilisation of such techniques would further reduce the BER, e.g. 10^{-1} would have been reduced down to 10^{-3}. By setting as minimum target BER=10^{-3}, with channel coding implemented, it is interesting to discuss the BER at the region of 10^{-1}. JT and receiver-based MMSE-JD clearly outperform the others, however the performance gap is not so large anymore. Pre-RAKE not only performs sufficiently but outperforms methods as TP-MAT and DPF.

4.8 Summary

In Chapter 4 recent developed transmitter based tecnhniques were described. Their algorithms were briefly described pointing out the different criteria that lead to different performance. It was shown that the blockwise techniques outperform the bitwise and that among them JT demonstrates a very good BER performance. It's even a better solution than the receiver based MMSE-JD. On the other hand, in Chapter 3 specific advantages of bitwise techniques were addressed. These advantages are summarised as the low computational cost and flexibility in implementation. Hence, it makes it essential to investigate and develop bitwise techniques that outperform the current ones and achieve a BER performance competitive with the one demonstrated by blockwise techniques. In the next two Chapters our research is towards this goal and two new bitwise algorithms are proposed.

Chapter 5
Inverse filters - Wiener solution

In this Chapter a new bitwise algorithm, named inverse filters (INVF) is proposed. Part of this work has been published in [103] In section 5.1 the origin of this technique is discussed. The adaptation to a CDMA system, the criteria and an analysis of the algorithm is presented in sections 5.2 and 5.3. Sections 5.4, 5.5 and 5.6 deal with the Wiener solution and the parameters associated with it. At last, section 5.7 presents some simulation results and compares INVF with other techniques in terms of performance and complexity.

5.1 INVF in stereophonic sound reproduction system

It's useful to present briefly the origins of the inverse filtering before describing their application and appropriate modification in a CDMA-TDD system. In [104–110] the problem of producing better approximations to the perfect reproduction of prerecorded acoustic signals was addressed. Let two channel stereophonic signals be recorded at two points Γ, Δ in an existing sound field. When these signals are replayed via two loudspeakers in a listening room,

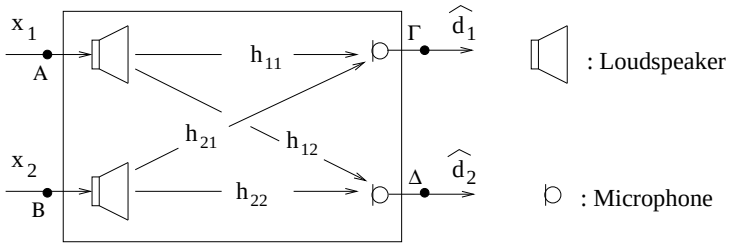

Figure 5.1: *A stereophonic sound reproduction system*

at points A and B as shown in Figure 5.1, the original signals are imperfectly reproduced at the ears of a listener. The imperfections in the reproduction arise from the following main causes:

- The signal played via the right channel is reproduced at both the right and the left ears of the listener. It is the same for the signal played via the left channel.
- The acoustic response of the listening room provides a reverberant field which is in addition to the reverberant field of the space in which the existing recordings were made.

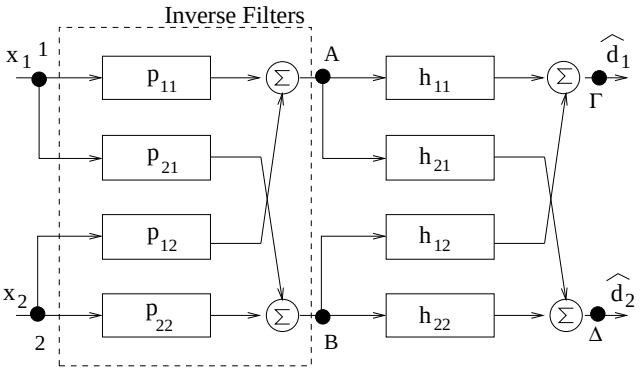

Figure 5.2: *Block diagram of sound reproduction system with inverse filters*

- The frequency response of the loudspeakers used for reproduction is imperfect.

In order to compensate for the above three factors it is necessary to introduce inverse filters p_{ij}, $i, j = 1, 2$, with impulse response $p_{ij}(n)$, before the loudspeakers. These filters act on the inputs to the loudspeakers, used for reproduction, and compensate for both the loudspeaker response and the room response. The block diagram of the described system is illustrated in Figure 5.2. The objective is to produce signals at the two microphones, located at Γ and Δ, which are exactly the signals input to the loudspeakers, i.e. $\hat{d}_1(n) = x_1(n)$ and $\hat{d}_2(n) = x_2(n)$. The analysis in [104] uses a "statistical" least squares technique without any power constraints for the determination of the inverse filters tap-coefficients and results in an adaptive solution referred to as the *multiple-error LMS*. This approach has the advantage of computing the filters *in situ* in a given listening space without resource to powerful computational facilities necessary for conventional fixed design. The adaptive solution will be further analysed in the next Chapter. In this Chapter the emphasis will be given in the calculation of a closed form Wiener solution and its properties.

In the following section the least squares technique will be adapted to a CDMA system with a single element antenna. The algorithm will be modified to keep the transmitted power limited to desired levels, adding the necessary power constraints. The technique will be first described for two users for simplicity reasons and then it will be extended to the generalised case of K users.

Inverse filters maintain the structure of a bitwise precoding scheme but the algorithm followed to calculate the pre-filter impulse responses is essentially different from the ZF decorrelating pre-filters [78] or pre-RAKE. A MMSE criterion is chosen and the power constraint has been

included in the algorithm so as to minimise the resulting transmitted power.

5.2 Least squares power constrained algorithm

In Figure 5.2 the sound is produced by two loudspeakers at points A and B in the space and received by two microphones at points Γ and Δ. In a CDMA system it is equivalent to having two antennas at the transmission point (BS for the downlink scheme) and two mobile units at different sites. The model of Figure 5.2 has to be modified for a single element antenna. Thus the channels h_{j1}, $j = 1, 2$, linking antenna A with receiver j and h_{j2}, $j = 1, 2$, linking antenna B with receiver j have to be reduced down to the channels h_1 and h_2 between the antenna and the mobile terminals. The resulted modified model is then as displayed in Figure 5.3 where the analogy with the bitwise general model of Figure 3.6 is obvious. Filters p_i correspond to the transmission pre-filters for bitwise transmission precoding as described in section 3.4.2. To

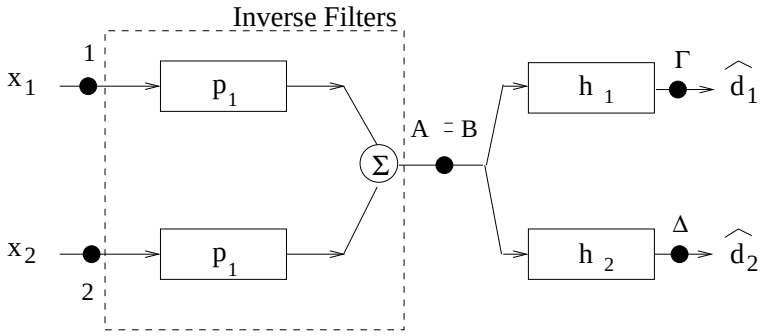

Figure 5.3: *Modified diagram to comply with a single antenna CDMA model*

make the model suitable for a two user CDMA system with transmitter precoding we must further replace the input signals x_1 and x_2 by the corresponding spread data $d_1^m c_1(n)$ and $d_2^m c_2(n)$, respectively. By including the matched filter receivers $c_k(Q-n)$, $k = 1, 2$, instead of the microphones, in the diagram a complete CDMA downlink model with bitwise precoding results. The new block diagram is as shown in Figure 5.4 where the power scaling factor $\sqrt{\mathcal{F}}$ has been also included. In Figure 5.4 the cascaded filters $h_k(n)$ and $c_k(Q-n)$ are substituted by an FIR filter of length $Z = Q + L - 1$ and impulse response $z_k(n) = h_k(n) * c_k(Q-n)$, also defined in eq. (4.37). Now the block diagram can be redrawn as illustrated in Figure 5.5. The noise v_{awgn}, included in Figure 5.4, is not included in Figure 5.5 because the noise is not pre-filtered by $p_k(n)$ and thus it cannot affect the solution for the tap-coefficients. The scaling factor $\sqrt{\mathcal{F}}$ has also been omitted and temporarily excluded from our analysis. The objective is to calculate the inverse filters impulse response in a MMSE sense.

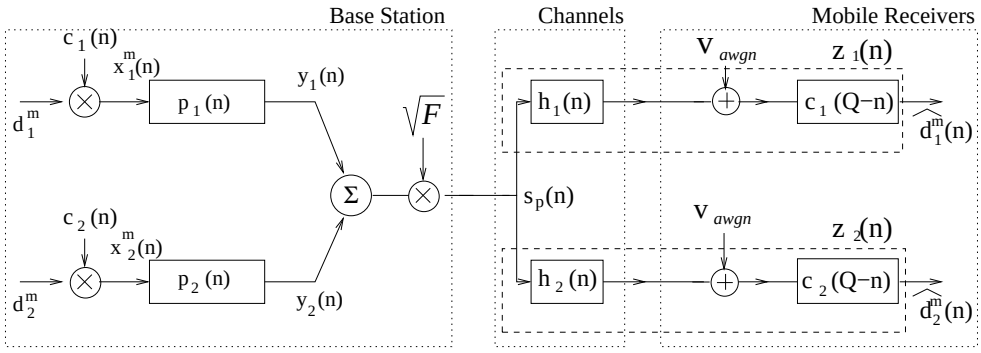

Figure 5.4: *Two users block diagram of an inverse filters system*

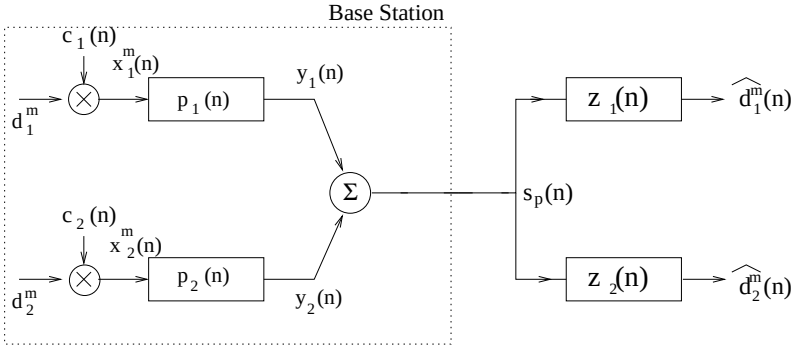

Figure 5.5: *Two users block diagram of a simplified inverse filters system*

To take the least squares approach to the design of the inverse filters matrix it helps greatly if the block diagram representation of the composite system as shown in Figure 5.5 is rearranged to an equivalent block diagram as shown in Figure 5.6. It has to be clear that this rearrangement is only to facilitate the mathematical analysis. Signals $r_{\mu\nu}(n)$, $\mu, \nu = 1, 2$ are defined as 'filtered reference signals' and are produced by passing the sequence of symbols $x_\nu^m(n)$ through the filters with impulse response $z_\mu(n)$. This 'transfer function reversal' approach is essentially the one taken by [107] in deriving the multiple error LMS algorithm and is used to determine the optimal, in mean squared error terms, finite impulse responses $\mathbf{p}_1$, $\mathbf{p}_2$, as in eq. (3.18).

We define the following vectors of the filtered reference signals:

$$\mathbf{r}_{\mu\nu}(n) = [r_{\mu\nu}(n) \cdots r_{\mu\nu}(n - P + 1)]^T, \quad \mu, \nu = 1 \ldots K \tag{5.1}$$

Following the block diagram in Figure 5.6 the output $\hat{d}_k^0$ (the superscript symbol index m has been replaced by 0 without loss of generality) of the kth user matched filter receiver can be

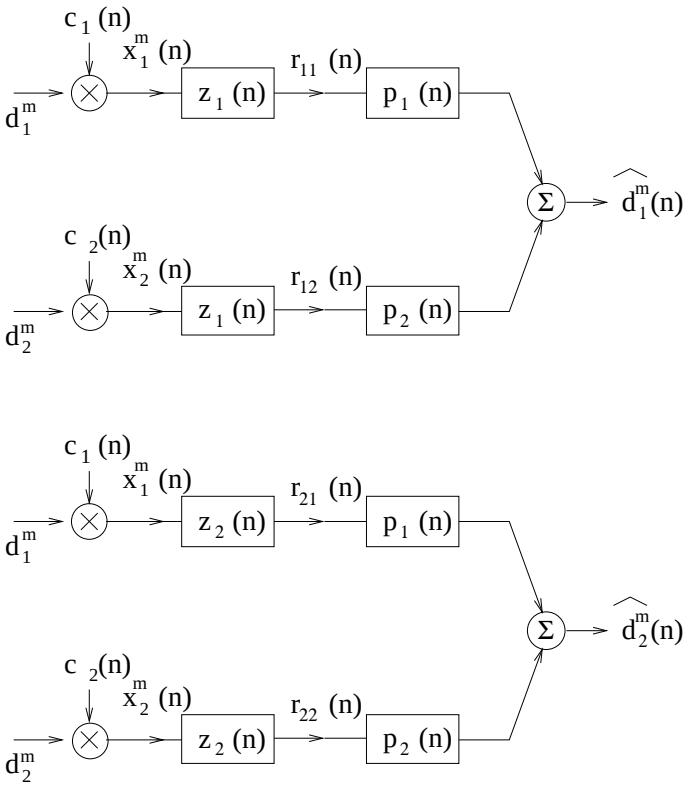

Figure 5.6: *Rearranged inverse filters block-diagram for two users*

expressed in a matrix-vector notation form:

$$\hat{d}_k^0 = [\mathbf{r}_{11}^T \mathbf{r}_{12}^T]\mathbf{p} \tag{5.2}$$

where $\mathbf{p}$ is a column arrangement of both inverse filters tap coefficients.

$$\mathbf{p} = [\mathbf{p}_1^T \mathbf{p}_2^T]^T \tag{5.3}$$

By arranging both estimate outputs in one vector $\hat{\mathbf{d}}_0$ the system illustrated in Figure 5.6 is described as:

$$\hat{\mathbf{d}}_0(n) = \mathbf{R}(n)\mathbf{p} \tag{5.4}$$

where the vector $\hat{\mathbf{d}}_0(n)$ and the matrix $\mathbf{R}(n)$ are denoted as:

$$\hat{\mathbf{d}}_0(n) = \begin{bmatrix} \hat{d}_1^0(n) \\ \hat{d}_2^0(n) \end{bmatrix}, \mathbf{R}(n) = \begin{bmatrix} \mathbf{r}_{11}^T(n) & \mathbf{r}_{12}^T(n) \\ \mathbf{r}_{21}^T(n) & \mathbf{r}_{22}^T(n) \end{bmatrix} \tag{5.5}$$

We now seek the optimal filter vector $\mathbf{p}$ to minimise the time averaged squared error between the actual and desired outputs. The desired outputs are sampled every symbol period $T_s^n = nQ+\Delta$, $n = 1, 2, \ldots$, where Δ is an imposed delay in the system which assists the equalisation of the multipath channels [111]. The cost function to be minimised is:

$$J = E[(\mathbf{d}_0 - \hat{\mathbf{d}}_0(T_s^n))^T(\mathbf{d}_0 - \hat{\mathbf{d}}_0(T_s^n))] \tag{5.6}$$

where $\mathbf{d}_0$ is the vector of desired data defined as $\mathbf{d}_0 = [d_1^0 d_2^0]^T$.

The problem now is that the resulted Wiener solution $\mathbf{p}_o$ for the inverse filters may increase to undesired levels the transmitted power compared with the unprecoding CDMA scheme. As explained in section 3.5 the usage of the power scaling factor $\sqrt{\mathcal{F}} < 1$ afterwards will cause a degradation in the SNR at the receiver point. Thus, it is wise to impose to the cost function the necessary power constraint term by means of Lagrange multipliers.

The average total transmitted power for the bitwise techniques has been calculated in section 3.5 as a function of the vector $\mathbf{p}$ that contains the tap-coefficients of all inverse filters. We reproduce here the equation.

$$E_g(\mathbf{p}) = \mathbf{p}^T\mathbf{U}^T \cdot \mathbf{U}\mathbf{p} \tag{5.7}$$

with $\mathbf{U}$ as defined in eq. (3.30). The $E_g(\mathbf{p})$ should not exceed the power that corresponds to the conventional CDMA scheme $\mathcal{E}_g$. Thus:

$$E_g(\mathbf{p}) \leq \mathcal{E}_g \tag{5.8}$$

The complete power constrained cost function to be minimised then takes the form:

$$J_c = E[(\mathbf{d}_0 - \hat{\mathbf{d}}_0(T_s^n))^T(\mathbf{d}_0 - \hat{\mathbf{d}}_0(T_s^n))] + \lambda\big(E_g(\mathbf{p}) - \mathcal{E}_g\big) \tag{5.9}$$

Recalling eq. (5.4) J_c can be written as:

$$J_c = E[(\mathbf{d}_0 - \mathbf{R}(T_s^n)\mathbf{p})^T(\mathbf{d}_0 - \mathbf{R}(T_s^n)\mathbf{p})] + \lambda\big(E_g(\mathbf{p}) - \mathcal{E}_g\big) \tag{5.10}$$

After expansion and use of the expectation operator, eq. (5.10) reduces to the quadratic form:

$$J_c = E[\mathbf{d}_0^T\mathbf{d}_0] - 2E[\mathbf{d}_0^T\mathbf{R}(T_s^n)]\mathbf{p} + \mathbf{p}^T E[\mathbf{R}^T(T_s^n)\mathbf{R}(T_s^n)]\mathbf{p} + \lambda\big(E_g(\mathbf{p}) - \mathcal{E}_g\big) \tag{5.11}$$

Taking the gradient $\vartheta/\vartheta\mathbf{p}$ of the power constraint term we have:

$$\frac{\vartheta\big(E_g(\mathbf{p})-\mathcal{E}_g\big)}{\vartheta\mathbf{p}}=\frac{\vartheta\big(\mathbf{p}^T\mathbf{U}^T\mathbf{U}\mathbf{p}\big)}{\vartheta\mathbf{p}}=2\mathbf{U}^T\mathbf{U}\mathbf{p} \tag{5.12}$$

The gradient $\vartheta/\vartheta\mathbf{p}$ of the cost function J_c is:

$$\frac{\vartheta J_c}{\vartheta\mathbf{p}}=-2E[\mathbf{R}^T(T_s^n)\mathbf{d}_0]+2E[\mathbf{R}^T(T_s^n)\mathbf{R}(T_s^n)]\mathbf{p}+2\lambda\mathbf{U}^T\mathbf{U}\mathbf{p} \tag{5.13}$$

The Wiener solution for the tap-coefficients of the pre-filters $\mathbf{p}_o$ is obtained by setting:

$$\left.\frac{\vartheta J_c}{\vartheta\mathbf{p}}\right|_{\mathbf{p}_o}=0 \tag{5.14}$$

Thus, from eq. (5.13) and eq. (5.14) we can write:

$$-2E[\mathbf{R}^T(T_s^n)\mathbf{d}_0]+2E[\mathbf{R}^T(T_s^n)\mathbf{R}(T_s^n)]\mathbf{p}_o+2\lambda\mathbf{U}^T\mathbf{U}\mathbf{p}_o = 0 \tag{5.15}$$

$$-E[\mathbf{R}^T(T_s^n)\mathbf{d}_0]+\big(E[\mathbf{R}^T(T_s^n)\mathbf{R}(T_s^n)]+\lambda\mathbf{U}^T\mathbf{U}\big)\mathbf{p}_o = 0 \tag{5.16}$$

Finally, the Wiener solution $\mathbf{p}_o$ is calculated as:

$$\mathbf{p}_o=\big[E[\mathbf{R}^T(T_s^n)\mathbf{R}(T_s^n)]+\lambda\mathbf{U}^T\mathbf{U}\big]^{-1}E[\mathbf{R}^T(T_s^n)\mathbf{d}_0] \tag{5.17}$$

The Wiener solution as shown in eq. (5.17) is valid even if users are transmitted with unequal powers. In that case, the desired output vector is $\mathbf{W}\mathbf{d}_0$ ($\mathbf{W}$ is the power matrix) and it is shown in Appendix A that the final solution $\mathbf{p}_o$ is not affected.

5.3 Generalisation

The least squares approach can easily be extended to deal with the case of multiple channels and multiple users as in Figure 5.7. Figure 5.8 shows how the rearranged block diagram of Figure 5.6 is extended in the general case for receiver μ. Eq. (5.4) is still valid but now the terms are redefined as follows:

$$\hat{\mathbf{d}}_0(n)=\begin{bmatrix}\hat{d}_1^0(n)\\ \vdots\\ \hat{d}_K^0(n)\end{bmatrix},\mathbf{R}(n)=\begin{bmatrix}\mathbf{r}_1^T(n)\\ \vdots\\ \mathbf{r}_K^T(n)\end{bmatrix}, \tag{5.18}$$

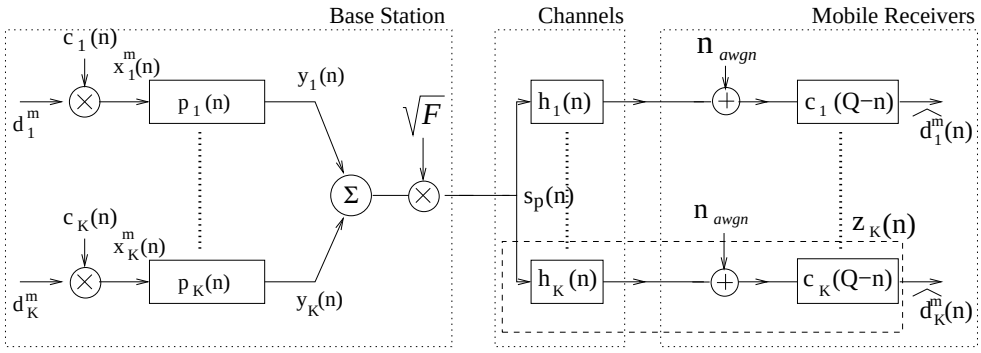

Figure 5.7: *Generalised block diagram of an inverse filters system*

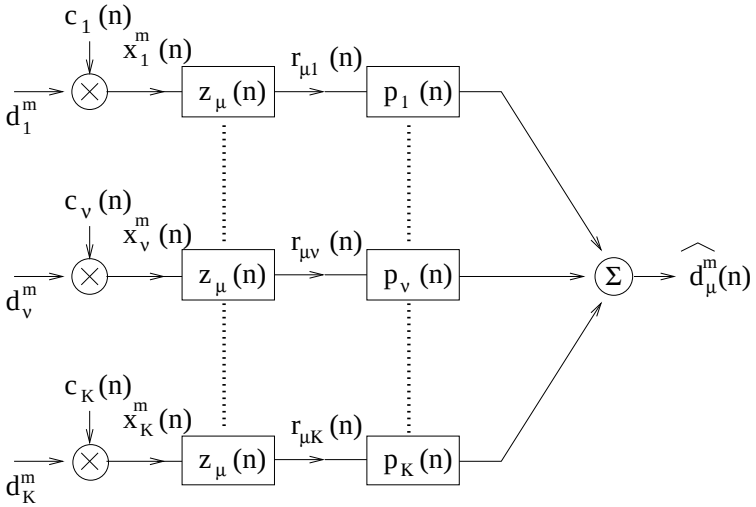

Figure 5.8: *Generalised rearranged block diagram for μ user.*

with $\mathbf{r}_k^T(n), k = 1 \dots K$, given as:

$$\mathbf{r}_k(n) = [\mathbf{r}_{k1}^T(n), \cdots, \mathbf{r}_{kK}^T(n)]^T \tag{5.19}$$

$\mathbf{r}_{\mu\nu}(n)$ is as in eq. (5.1) and $\mathbf{p}$ is as in eq. (3.28). The power constrained mean minimum squared error cost function J_c is as in eq. (5.9) and following the analysis presented in the previous section we get to the Wiener solution as described in eq. (5.17). An attempt to find a closed form solution for the Wiener solution takes place in the next section.

5.4 Wiener solution

In order to find the analytical Wiener solution $\mathbf{p}_o$, the expectation terms $E[\mathbf{R}^T(n)\mathbf{R}(n)]$ and $E[\mathbf{R}^T(n)\mathbf{d}_0]$ in eq. (5.17) must be calculated. As stated before $r_{\mu\nu}(n) = d_\nu^m c_\nu(n) * h_\mu(n) *$

$c_\mu(Q-n)$. Let $\gamma_{\mu\nu}(n) = c_\nu(n) * h_\mu(n) * c_\mu(Q-n)$ as also defined in eq. (4.33). The corresponding symbol in vector form is denoted as $\boldsymbol{\gamma}_{\mu\nu}$ of length $G_\gamma = 2Q + L - 2$ due to the convolution effect.

$$\boldsymbol{\gamma}_{\mu\nu} = [\gamma_{\mu\nu}(0) \cdots \gamma_{\mu\nu}(G_\gamma - 1)]^T \tag{5.20}$$

Vector $\mathbf{r}_{\mu\nu}(n)$ of length P, defined as in eq. (5.1), is given next as a function of the $N = 2M+1$ vector $\mathbf{d}_\nu$ accounting for the ISI effect that is introduced due to the pre-filters. M symbols transmitted before and after symbol d_ν^0 are taken into account. We recall here that the sampling time is $T_s^n = nQ + \Delta$, $n = 1, 2, \ldots$ and we further assume that $\Delta + Q \leq G_\gamma$, $\Delta + Q \geq P$ (these assumptions are only to assist the illustration of the Wiener solution as both P and Δ can be arbitrarily chosen). Then:

$$\mathbf{r}_{\mu\nu} = \boldsymbol{\Gamma}_{\mu\nu}\mathbf{d}_\nu \tag{5.21}$$

where the $P \times N$ matrix $\boldsymbol{\Gamma}_{\mu\nu}$ is:

$$\boldsymbol{\Gamma}_{\mu\nu} = \{[\boldsymbol{\Gamma}_{\mu\nu}]^{i,(j+M+1)}\} \quad ; \quad i = 1...P, j = -M...M$$

$$[\boldsymbol{\Gamma}_{\mu\nu}]^{i,(j+M+1)} = \begin{cases} \gamma_{\mu\nu}(\Delta + Q - i - jQ), & \text{for} \quad 0 \leq \Delta + Q - i - jQ \leq G_\gamma - 1 \\ 0, & \text{otherwise} \end{cases} \tag{5.22}$$

For instance, in the case of $Q = 4, P = 5, \Delta = 2, L = 3, M = 1$ eq. (5.21) takes the form:

$$\begin{bmatrix} r_{\mu\nu}(T_s^n) \\ \vdots \\ r_{\mu\nu}(T_s^n - P + 1) \end{bmatrix} = \begin{bmatrix} 0 & \gamma_{\mu\nu}(5) & \gamma_{\mu\nu}(1) \\ \gamma_{\mu\nu}(8) & \gamma_{\mu\nu}(4) & \gamma_{\mu\nu}(0) \\ \gamma_{\mu\nu}(7) & \gamma_{\mu\nu}(3) & 0 \\ \gamma_{\mu\nu}(6) & \gamma_{\mu\nu}(2) & 0 \\ \gamma_{\mu\nu}(5) & \gamma_{\mu\nu}(1) & 0 \end{bmatrix} \begin{bmatrix} d_\nu^{-1} \\ d_\nu^0 \\ d_\nu^1 \end{bmatrix} \tag{5.23}$$

By combining now eq. (5.18) and eq. (5.21) we obtain:

$$\mathbf{R}(T_s^n) = \begin{bmatrix} \mathbf{d}_1^T\boldsymbol{\Gamma}_{11}^T & \cdots & \mathbf{d}_K^T\boldsymbol{\Gamma}_{1K}^T \\ \vdots & \ddots & \vdots \\ \mathbf{d}_1^T\boldsymbol{\Gamma}_{K1}^T & \cdots & \mathbf{d}_K^T\boldsymbol{\Gamma}_{KK}^T \end{bmatrix} \tag{5.24}$$

We will consider again the simple case of two users to calculate the mean terms of the Wiener

solution.

$$E[\mathbf{R}^T(T_s^n)\mathbf{R}(T_s^n)] = E\left\{ \begin{bmatrix} \mathbf{\Gamma}_{11}\mathbf{d}_1 & \mathbf{\Gamma}_{21}\mathbf{d}_1 \\ \mathbf{\Gamma}_{12}\mathbf{d}_2 & \mathbf{\Gamma}_{22}\mathbf{d}_2 \end{bmatrix} \begin{bmatrix} \mathbf{d}_1^T\mathbf{\Gamma}_{11}^T & \mathbf{d}_2^T\mathbf{\Gamma}_{12}^T \\ \mathbf{d}_1^T\mathbf{\Gamma}_{21}^T & \mathbf{d}_2^T\mathbf{\Gamma}_{22}^T \end{bmatrix} \right\} =$$

$$\begin{bmatrix} \mathbf{\Gamma}_{11}E\{\mathbf{d}_1\mathbf{d}_1^T\}\mathbf{\Gamma}_{11}^T + \mathbf{\Gamma}_{21}E\{\mathbf{d}_1\mathbf{d}_1^T\}\mathbf{\Gamma}_{21}^T & \mathbf{\Gamma}_{11}E\{\mathbf{d}_1\mathbf{d}_2^T\}\mathbf{\Gamma}_{12}^T + \mathbf{\Gamma}_{21}E\{\mathbf{d}_1\mathbf{d}_2^T\}\mathbf{\Gamma}_{22}^T \\ \mathbf{\Gamma}_{12}E\{\mathbf{d}_2\mathbf{d}_1^T\}\mathbf{\Gamma}_{11}^T + \mathbf{\Gamma}_{22}E\{\mathbf{d}_2\mathbf{d}_1^T\}\mathbf{\Gamma}_{21}^T & \mathbf{\Gamma}_{12}E\{\mathbf{d}_2\mathbf{d}_2^T\}\mathbf{\Gamma}_{12}^T + \mathbf{\Gamma}_{22}E\{\mathbf{d}_2\mathbf{d}_2^T\}\mathbf{\Gamma}_{22}^T \end{bmatrix} \tag{5.25}$$

In Chapter 2 we mentioned that the data symbols are uncorrelated, $\mathbf{R}_d = \mathbf{I}$, which means that:

$$E\{d_\mu^{m_1} d_\nu^{m_2}\} = \begin{cases} 1, & \mu = \nu \quad \text{and} \quad m_1 = m_2 \\ 0, & \text{otherwise} \end{cases} \tag{5.26}$$

Thus:

$$E\{\mathbf{d}_\nu\mathbf{d}_\mu^T\} = \begin{cases} \mathbf{I}, & \text{if } \mu = \nu \\ \mathbf{0}, & \text{otherwise} \end{cases} \tag{5.27}$$

Hence eq. (5.25) takes the final form:

$$E[\mathbf{R}^T(T_s^n)\mathbf{R}(T_s^n)] = \begin{bmatrix} \mathbf{\Gamma}_{11}\mathbf{\Gamma}_{11}^T + \mathbf{\Gamma}_{21}\mathbf{\Gamma}_{21}^T & \mathbf{0} \\ \mathbf{0} & \mathbf{\Gamma}_{12}\mathbf{\Gamma}_{12}^T + \mathbf{\Gamma}_{22}\mathbf{\Gamma}_{22}^T \end{bmatrix} \tag{5.28}$$

In the same way we have

$$E[\mathbf{R}^T(T_s^n)\mathbf{d}_0] = [\bar{\boldsymbol{\gamma}}_{11}^T\bar{\boldsymbol{\gamma}}_{22}^T]^T \tag{5.29}$$

where $\bar{\boldsymbol{\gamma}}_{\mu\nu}$ is a P-length vector defined as:

$$\bar{\boldsymbol{\gamma}}_{\mu\nu} = [[\mathbf{\Gamma}_{\mu\nu}]^{1,(M+1)} \cdots [\mathbf{\Gamma}_{\mu\nu}]^{P,(M+1)}]^T \tag{5.30}$$

and $[\mathbf{\Gamma}_{\mu\nu}]^{i,(M+1)}$ is given by eq. (5.22).

Generalising equations (5.25) and (5.29) to the case of arbitrary number of users K we have:

$$E[\mathbf{R}^T(T_s^n)\mathbf{R}(T_s^n)] = \begin{bmatrix} \sum_{\mu=1}^K \mathbf{\Gamma}_{\mu 1}\mathbf{\Gamma}_{\mu 1}^T & \mathbf{0} & \mathbf{0} \\ \mathbf{0} & \ddots & \mathbf{0} \\ \mathbf{0} & \mathbf{0} & \sum_{\mu=1}^K \mathbf{\Gamma}_{\mu K}\mathbf{\Gamma}_{\mu K}^T \end{bmatrix} \tag{5.31}$$

and

$$E[\mathbf{R}^T(T_s^n)\mathbf{d}_0] = [\bar{\boldsymbol{\gamma}}_{11}^T \cdots \bar{\boldsymbol{\gamma}}_{KK}^T]^T \tag{5.32}$$

By replacing now the expectation terms in eq. (5.17) with the right-hand side of eq. (5.31) and eq. (5.32) the Wiener solution is almost determined in a closed form. What remains to be investigated is the right value for the parameter λ. This is the objective of the following two sections.

5.5 λ - In depth

The question raised is as to what is the best choice for the parameter λ in eq. (5.17). A numerical solution with reference to [102] is given and the performance of this solution is discussed. The performance graphs, in terms of system's average BER, given in this section are mostly based on the analytical eq. (3.12). The consistency between theory and simulation results will be shown in section 5.7.

5.5.1 Numerical solution

The problem described in section 5.2 can be restated in the following form:

$$\begin{aligned} \text{minimize :} \quad & E\left[\|\mathbf{d}_0 - \mathbf{R}(T_s^n)\mathbf{p}\|^2\right] \\ \text{subject to :} \quad & \|\mathbf{U}\mathbf{p}\|^2 \leq \mathcal{E}_g \end{aligned} \tag{5.33}$$

The objective function to be minimised is:

$$E[\mathbf{d}_0^T\mathbf{d}_0] - 2E[\mathbf{d}_0^T\mathbf{R}(T_s^n)]\mathbf{p} + \mathbf{p}^T E[\mathbf{R}^T(T_s^n)\mathbf{R}(T_s^n)]\mathbf{p} \tag{5.34}$$

After deletion of the constant term $E[\mathbf{d}_0^T\mathbf{d}_0]$ and the following substitutions

$$\begin{aligned} E[\mathbf{d}_0^T\mathbf{R}(T_s^n)] &= -\boldsymbol{\gamma} \\ E[\mathbf{R}^T(T_s^n)\mathbf{R}(T_s^n)] &= \boldsymbol{\Gamma} \end{aligned} \tag{5.35}$$

eq. (5.33) is rewritten as:

$$\begin{aligned} \text{minimize :} \quad & 2\boldsymbol{\gamma}\mathbf{p} + \mathbf{p}^T\boldsymbol{\Gamma}\mathbf{p} \\ \text{subject to :} \quad & \|\mathbf{U}\mathbf{p}\|^2 \leq \mathcal{E}_g \end{aligned} \tag{5.36}$$

This problem specifies minimisation of a convex quadratic function ($\mathbf{\Gamma}$ is positive semi-definite as a correlation matrix) over an ellipsoid whose surface is the set of signal vectors which have a transmitted power level $\mathcal{E}_g$. This is a trust-region-subproblem as occurs in nonlinear optimisation theory and the solution is determined with reference to the numerical optimisation techniques in [112, 113]. The gradient of the objective function is given by $2\boldsymbol{\gamma} + 2\mathbf{\Gamma}\mathbf{p}$ while the gradient to the constraint is, as shown in eq. (5.12), $2\mathbf{U}^T\mathbf{U}\mathbf{p}$. If the *Karush-Kuhn-Tucker* (KKT) conditions for the local optimum $\mathbf{p}_o$ are satisfied with Lagrange multiplier λ then the following holds:

$$\begin{aligned}(\mathbf{\Gamma} + \lambda\mathbf{U}^T\mathbf{U})\mathbf{p}_o + \gamma &= 0 && (5.37)\\ \sqrt{\mathcal{E}_g} - \|\mathbf{U}\mathbf{p}_o\| &\geq 0 && (5.38)\\ \lambda &\geq 0 && (5.39)\\ \lambda(\sqrt{\mathcal{E}_g} - \|\mathbf{U}\mathbf{p}_o\|) &= 0 && (5.40)\end{aligned}$$

To establish that $\mathbf{p}_o$ is a minimum, the second order sufficient condition requires positive curvature of the objective function at $\mathbf{p}_o$. This is described with the following equation:

$$\mathbf{x}^T\big(\mathbf{\Gamma} + \lambda\mathbf{U}^T\mathbf{U}\big)\mathbf{x} > \mathbf{0}, \quad \forall\,\mathbf{x} \in \big\{\mathbf{w}|\mathbf{w}^T\mathbf{p}_o = \mathbf{0}, \mathbf{w} \neq \mathbf{0}\big\} \tag{5.41}$$

The matrix $\mathbf{\Gamma}$ is positive semi-definite and so is $\mathbf{U}^T\mathbf{U}$ (both are correlation matrices). Therefore the quantity $\big(\mathbf{\Gamma} + \lambda\mathbf{U}^T\mathbf{U}\big)$ is positive definite for $\lambda > 0$. Eq. (5.41) will then be satisfied for any point on the constraint surface. When $\lambda = 0$, we obtain the unconstrained minimum of the objective function which must be a minimum based on the convexity implied by a positive semi-definite $\mathbf{\Gamma}$. These observations coupled with a non-zero constraint gradient at all points other than the origin result in the conclusion that the KKT conditions are satisfied with a unique λ and that the associated point $\mathbf{p}_o$ is a global optimum.

The optimum value for λ can be found with numerical optimization techniques. The lower bound for λ is zero. Before calculating an upper bound some notations are necessary to precede. For any matrix $\mathbf{X}$, $\check{\psi}(\mathbf{X})$ and $\tilde{\psi}(\mathbf{X})$ denote a minimum and maximum eigenvalue of matrix $\mathbf{X}$, respectively. The upper bound for λ can now be calculated by rearranging and taking the norm of each side of eq. (5.37) as shown in [113]. The calculations following are not intented to be a vigorous proof for the upper bound of λ. The norm used is the *spectral norm* $\|\mathbf{X}\|_s$ defined in [89] as the square root of the largest eigenvalue of the matrix product $\mathbf{X}^T\mathbf{X}$. For a vector $\mathbf{x}$ it

is $\|\mathbf{x}\|_s = \|\mathbf{x}\| = \sqrt{\mathbf{x}^T\mathbf{x}}$.

$$\|\left(\mathbf{\Gamma} + \lambda\mathbf{U}^T\mathbf{U}\right)^{-1}\boldsymbol{\gamma}\|_s = \|\mathbf{p}\|_s \tag{5.42}$$

which implies,

$$\frac{1}{\check{\psi}(\mathbf{\Gamma}) + \lambda\check{\psi}(\mathbf{U}^T\mathbf{U})}\|\boldsymbol{\gamma}\|_s \geq \|\mathbf{p}\|_s \tag{5.43}$$

which further implies,

$$\check{\psi}(\mathbf{\Gamma}) + \lambda\check{\psi}(\mathbf{U}^T\mathbf{U}) \leq \frac{\|\boldsymbol{\gamma}\|_s}{\|\mathbf{p}\|_s} \tag{5.44}$$

Hence,

$$\lambda \leq \frac{1}{\check{\psi}(\mathbf{U}^T\mathbf{U})}\left(\frac{\|\boldsymbol{\gamma}\|_s}{\|\mathbf{p}\|_s} - \check{\psi}(\mathbf{\Gamma})\right) \tag{5.45}$$

If a non-zero λ satisfies the KKT conditions, then the corresponding $\mathbf{p}_o$ must have $\|\mathbf{U}\mathbf{p}_o\|_s = \sqrt{\mathcal{E}_g}$. Then, if we write

$$\|\mathbf{U}\mathbf{p}_o\|_s \leq \|\mathbf{U}\|_s\|\mathbf{p}_o\|_s = \sqrt{\mathcal{E}_g} \tag{5.46}$$

and further proceed to (using $\|\mathbf{p}_o\|_s = \|\mathbf{p}_o\|$) :

$$\|\mathbf{p}_o\| = \frac{\sqrt{\mathcal{E}_g}}{\sqrt{\tilde{\psi}(\mathbf{U}^T\mathbf{U})}} \tag{5.47}$$

In case the eigenvalues of the correlation matrix $\mathbf{\Gamma}$ cannot be calculated the term $\check{\psi}(\mathbf{\Gamma})$ may be dropped out from eq. (5.45) which relaxes the upper bound. The new simplified upper bound for the parameter λ is then:

$$\lambda \leq \frac{\|\boldsymbol{\gamma}\|}{\sqrt{\mathcal{E}_g}}\frac{\sqrt{\tilde{\psi}(\mathbf{U}^T\mathbf{U})}}{\check{\psi}(\mathbf{U}^T\mathbf{U})} \tag{5.48}$$

The above analysis provides a range of possible values for λ parameter. The search for the right choice of λ starts from $\lambda = 0$. If the norm $\|\mathbf{U}\mathbf{p}_o\| \leq \sqrt{\mathcal{E}_g}$ then the solution is inside the constraint. Otherwise, an arbitrary λ can be tested for optimality by solving eq. (5.37) and then checking the power constraint. If $\|\mathbf{U}\mathbf{p}_o\| = \sqrt{\mathcal{E}_g}$, then $\mathbf{p}_o$ is the solution we are looking for. This procedure suggests a bisection algorithm for solving eq. (5.36). For such an algorithm a converge precision has to be determined and it is denoted as ε. The bisection algorithm

proceeds as follows [113]:

$$
\begin{aligned}
&1. \quad \text{set } \lambda_{low} = 0 \text{ and } \lambda_{high} = \frac{\|\boldsymbol{\gamma}\|}{\sqrt{\mathcal{E}_g}} \frac{\sqrt{\tilde{\psi}(\mathbf{U}^T\mathbf{U})}}{\check{\psi}(\mathbf{U}^T\mathbf{U})} \\
&2. \quad \text{set } \lambda = \tfrac{1}{2}(\lambda_{low} + \lambda_{high}) \\
&3. \quad \text{if } (\lambda_{high} - \lambda_{low}) \leq \varepsilon \text{ exit procedure, otherwise go to 4.} \\
&4. \quad \text{solve } (\boldsymbol{\Gamma} + \lambda \mathbf{U}^T\mathbf{U})\mathbf{p}_o + \boldsymbol{\gamma} = 0 \text{ for } \mathbf{p} \\
&5. \quad \text{if } \|\mathbf{U}\mathbf{p}\| \geq \sqrt{\mathcal{E}_g}, \text{ then set } \lambda_{low} = \lambda, \text{ otherwise set } \lambda_{high} = \lambda \\
&6. \quad \text{go to step 2}
\end{aligned}
\tag{5.49}
$$

The complexity of this algorithm is determined by the desired accuracy and the cost of the linear system solution in step 4. At least $log_2 \frac{\|\boldsymbol{\gamma}\|}{\sqrt{\mathcal{E}_g}} \frac{\sqrt{\tilde{\psi}(\mathbf{U}^T\mathbf{U})}}{\check{\psi}(\mathbf{U}^T\mathbf{U})} - log_2\varepsilon$ iterations are required to converge to the desired precision [102]. If the eigenvalues of $\boldsymbol{\Gamma}$ are known the number of iterations can be reduced. The structure of the linear system in step 4 is more helpful. As $\lambda > 0$ in each iteration, $(\boldsymbol{\Gamma} + \lambda\mathbf{U}^T\mathbf{U})$ must be symmetric positive definite which suggests the Cholesky factorization to solve the system quickly.

5.5.2 Performance results

In graph 5.9(a) the average total energy transmitted per symbol E_g versus λ if no power scaling takes place is shown. The system under consideration is one of 5 users with spreading gain of 16 in a multipath environment with $E_b/N_o = 10$dB. We observe that E_g is very high for $\lambda \sim 0$ and is radically reduced as λ increases. When $\|\mathbf{c}_k\| = 1$ then the energy transmitted of a corresponding conventional CDMA system is $\mathcal{E}_g = 5$. In the inverse filters scheme, for the particular scenario, $E_g = 5$ is achieved for $\lambda = 0.1077$, as shown in the graph. This result is in agreement with the convergence of the bisection algorithm in (5.49). In Figure 5.9(b) the performance in terms of the system's average BER versus λ is illustrated. The solid line shows the BER when the resulted signal $\mathbf{s}_p$ after pre-filtering is transmitted without any scaling. For λ very small, where the transmitted power is nearly uncontrolled, the performance is very good but gets very poor as λ increases, due to over-reduction of the power as shown in Figure 5.9(a). The dashed line shows how the BER evolves versus λ for the same system when the power is scaled with scaling factor $\sqrt{\mathcal{F}}$. Now the energy is kept constant at $E_g = 5$. The crossing point with the unscaled graph is at $\lambda = 0.1077$ as expected. The interesting thing is that the performance is getting better for a $\lambda \sim 0.05$ which is other than the one the numerical solution suggests. This does not create a contradiction as no power scaling was

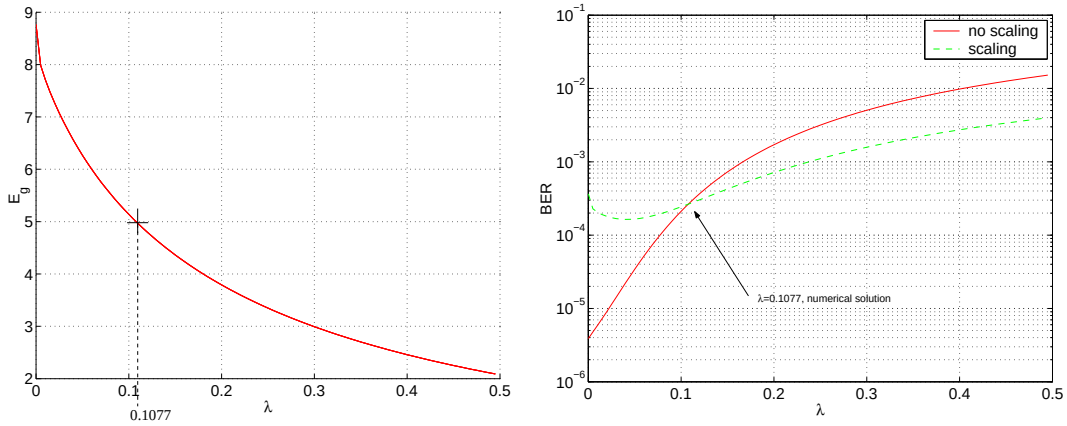

(a) *Unscaled transmitted signal vs* λ. K=5, Q=16, E_b/N_o=10dB.

(b) *BER vs* λ *for scaled and non-scaled transmitted signal.* K=5, Q=16, E_b/N_o=10dB.

Figure 5.9: *Transmitted energy and BER vs* λ *for INVF.*

imposed in the numerical solution. It means that by letting the pre-filters to achieve $E_g > \mathcal{E}_g$ and then scaling the resulted signal back to the desired power we can have a better average BER. This observation is becoming more intense if we repeat the experiment for $E_b/N_o = 15$dB as shown in Figure 5.10. In the next section we investigate how λ affects a variety of the system's characteristics and we try to determine some criteria for choosing it.

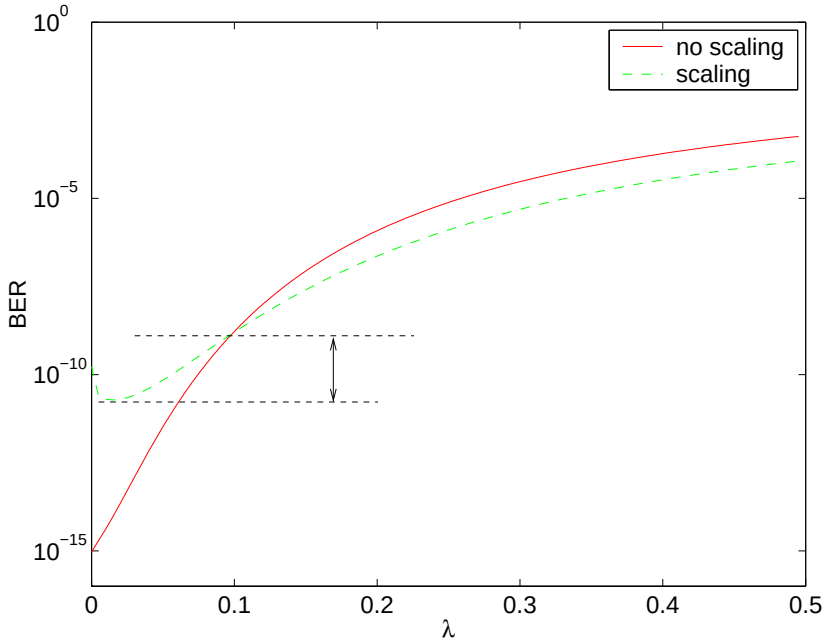

Figure 5.10: *BER vs* λ *for scaled and non-scaled* $\mathbf{s}_p$. K=5, Q=16, E_b/N_o=15dB.

5.6 Observations on λ parameter

Last section gave a numerical solution for λ but it also showed that the converged value is not necessary the optimum. By setting λ to zero the Wiener solution is unconstrained, as given in [104] but the power of the produced signal is prohibitive. λ selection determines the trade off between reducing the mean squared error and the transmitted energy that the Wiener solution achieves. In the following the effect of λ on the performance, the performance spread and the transmitted energy will be examined. In all the graphs in this section the total energy transmitted per symbol is ensured to be the reference power of a corresponding conventional CDMA system. This is achieved, as already have been explained, by multiplying the precoded signal with a scaling factor $\sqrt{\mathcal{F}}$.

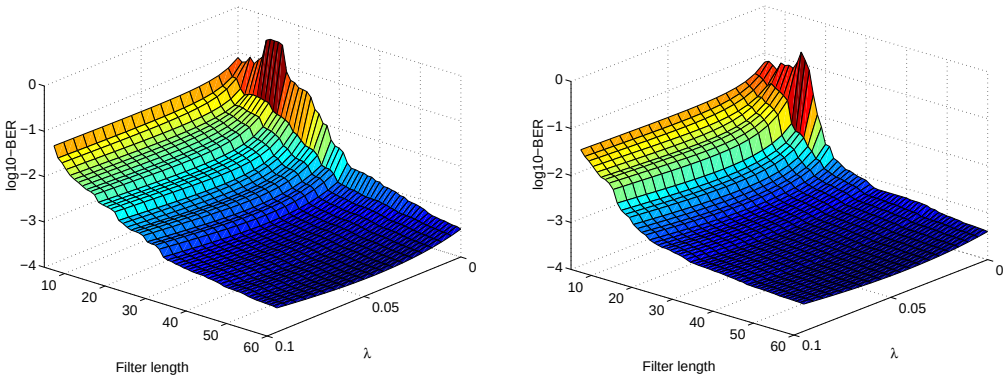

(a) *Multipath channel* **(b)** *AWGN channel*

Figure 5.11: *BER vs λ & P. K=5, Q=16, $E_b/N_o = 10$dB.*

5.6.1 BER vs λ & filter length

In Figure 5.11(a) the BER performance versus λ and filter length P is displayed for a system of $K = 5$ users and $Q = 16$ when E_b/N_o is set to 10dB. The channel is set to be multipath, while in Figure 5.11(b) is AWGN. In both graphs for a constant λ the performance is getting better as the filter length is increased. For the Gaussian channel the performance versus filter length reaches a lower bound (levels off) for a smaller number of taps compared to the multipath environment with channel length $L = 11$ chips. This is expected as more taps are needed to achieve the channel equalisation. In these graphs the initial value for λ is 0.0001. We

can't set λ to zero because the resulting matrix to be inverted becomes $\left[E[\mathbf{R}^T(T_s^n)\mathbf{R}(T_s^n)]\right]$ which has a very large eigenvalue ratio and is nearly singular. The bad condition of matrix $\left[E[\mathbf{R}^T(T_s^n)\mathbf{R}(T_s^n)]\right]$, when λ is small, leads to an increased transmitted power in order to achieve elimination of MAI and ISI. In this case the scaling factor used before final transmission reduces the SNR at the receiver point as explained in Chapter 3 and results in poor performance. This factor in conjunction with the fact that a small pre-filter length makes it more difficult to equalise the channel explains why the selection of the right λ plays a critical role to the system's BER when filter length is kept small. On the other hand the performance versus λ is nearly flat for large filter length, at a complexity cost. For a heavy loaded system of $K = 12$ as shown in graph 5.12, the performance, which is not so good anymore, is more immune to λ choice.

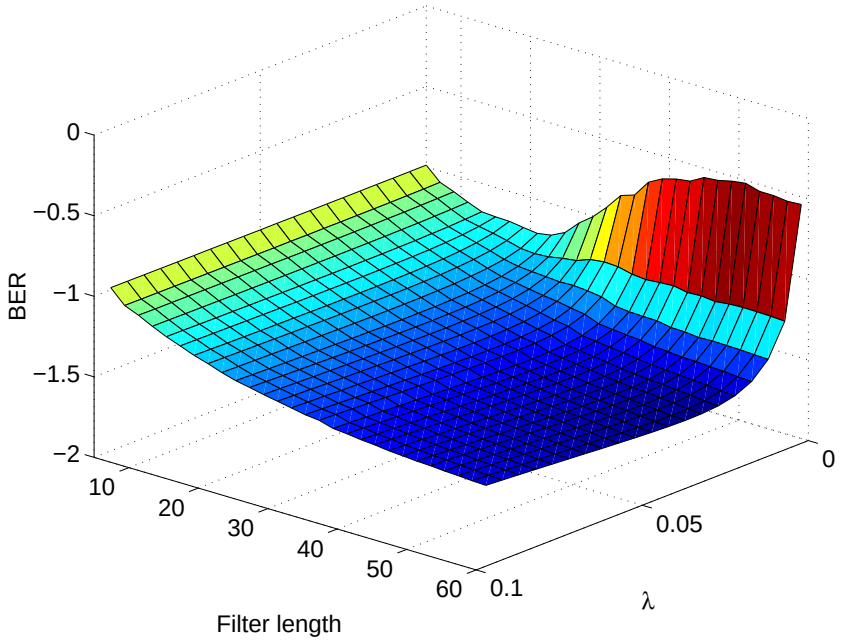

Figure 5.12: *BER vs λ & P. $K = 12$, $Q = 16$, $E_b/N_o = 10$dB.*

In Figure 5.13 the solid lines show how λ affects the BER for a system of $K = 5$ users and $E_b/N_o = 10$dB for four different sets of 5 random codes when the pre-filter length $P = 16$. The experiment is repeated for four new sets of 5 randomly generated spreading codes when $P = 32$ and this is shown in the same Figure by the dashed lines. All graphs follow a similar pattern. There is a range for λ which gives almost the optimum BER performance with a variety of spreading codes and pre-filter lengths. We observe that for $E_b/N_o = 10$dB this range is $\gtrapprox 0.05$. This gives a degree of freedom about the choice of λ. The discussion over the

relationship between BER, λ and E_b/N_o is in the next section.

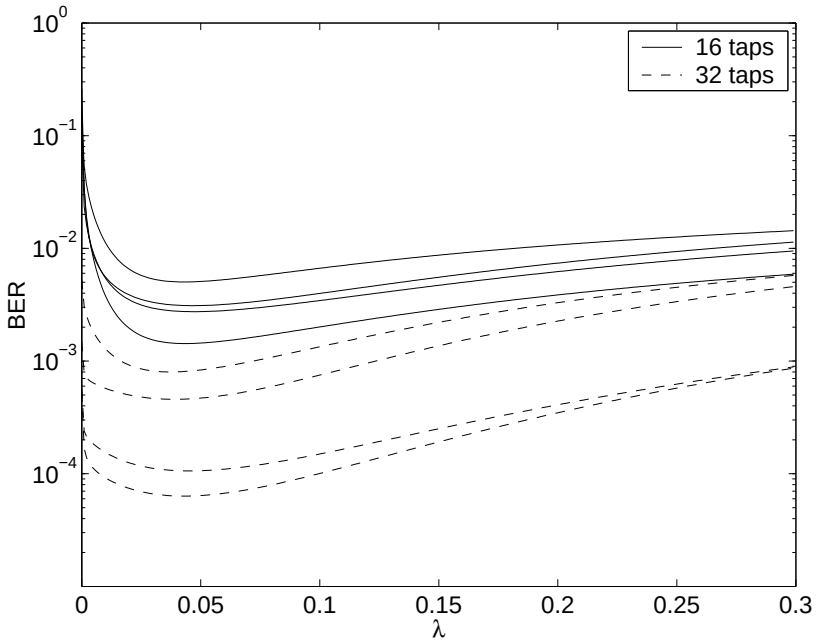

Figure 5.13: *BER vs* λ. $K = 5$, $Q = 16$, $E_b/N_o = 10$*dB.*

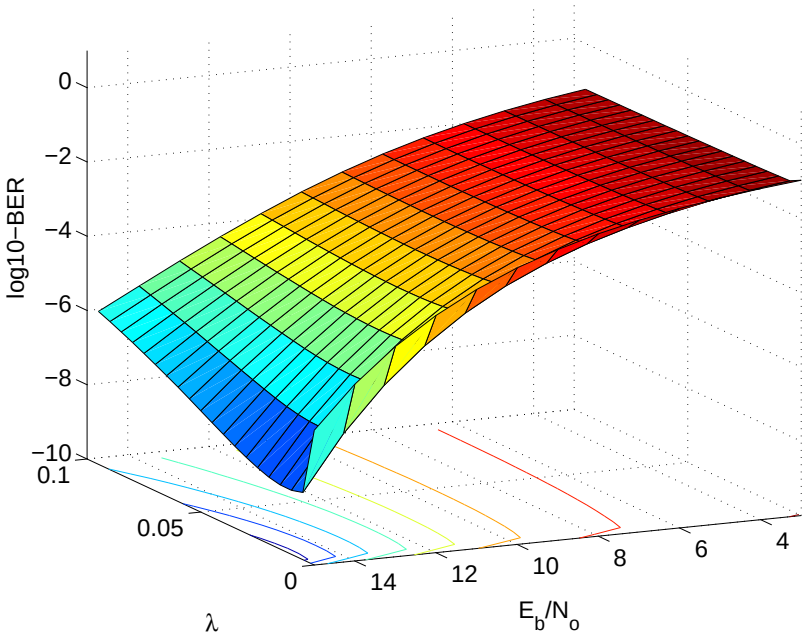

Figure 5.14: *BER vs* E_b/N_o *&* λ. $K = 5$, $Q = 16$, $P = 32$.

5.6.2 BER vs λ & E_b/N_o

Since λ is the power control term it is expected that the best value for it is a function of E_b/N_o. In Figure 5.14 the performance in terms of BER versus different choices of λ and E_b/N_o is shown. The CDMA system is one of 5 users with random selected codes and pre-filter length set to 32 taps. Channels are always multipath with the profile given in table 2.3. From the contour diagram in the xy plane we can draw the conclusion that for low E_b/N_o there is a wide range where the BER versus λ is nearly flat. The flat range begins around the value of $0.04-0.05$ for λ. In contrast, for E_b/N_o higher than 12dB the BER is a more sensitive function of λ and the best performance is shifted to smaller λ values ($\simeq 0.025$). We assume here that for a telecommunication system the average E_b/N_o encountered is 10dB and, therefore, our conclusions are drawn relied on the 10dB line. In the next two figures these remarks are more clear.

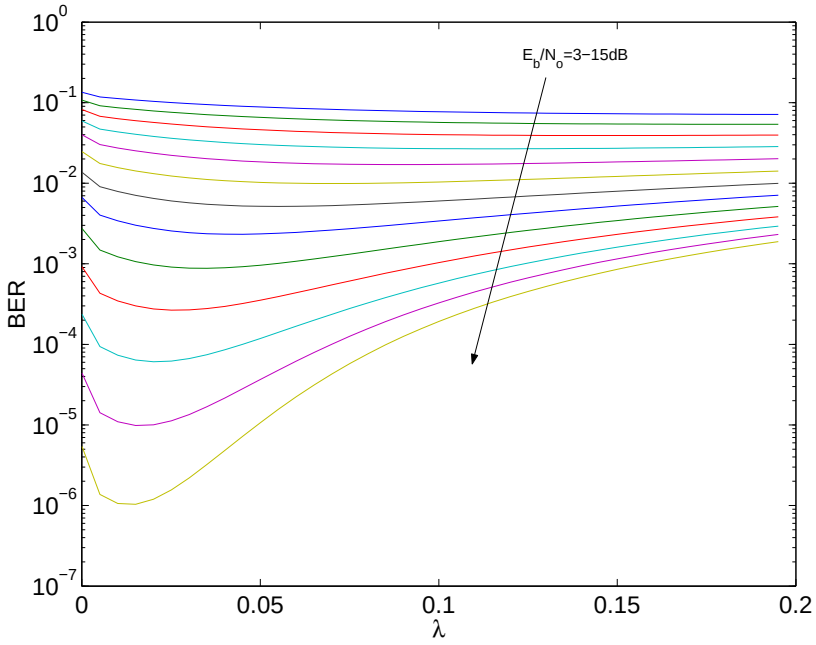

Figure 5.15: *BER vs* λ. $P = 32$, $K = 5$, $Q = 16$.

From Figure 5.15 we observe the relationship between the BER of a 5 users system and λ for E_b/N_o that varies from 3 to 15dB. The channels used follow the profile that is presented in table 2.3. Again it is shown that the higher the E_b/N_o the closer to zero the best value for λ is shifted. On the other hand, for $E_b/N_o \lessapprox$ 12dB the graphs are almost flat. Similar results are drawn for the case that the system under consideration is loaded up to 12 users while the spreading gain remains to $Q = 16$, as shown in Figure 5.16. These results hold on even for

different length of pre-filters, e.g. $P = 16$, as was illustrated in Figure 5.13. In an effort to explain this behavior we could say that as the E_b/N_o gets higher the need for power constraint is fading and the Wiener solution should be shifted to deal mostly with the MAI and less with the power. Hence, the necessity for power control is not so important and the Wiener solution is set "free" to deal with multiple access and intersymbol interference as λ approaches zero. The natural transmitted power in that case increases, of course, but the scaling factor normalises it. These conclusions come in agreement with the ones drawn from Figure 5.10 in section 5.5.

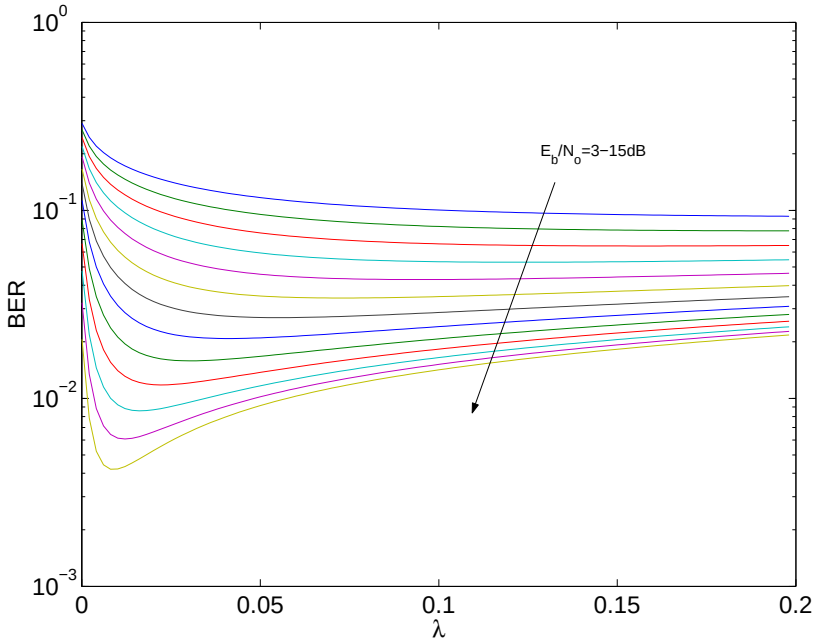

Figure 5.16: *BER vs* λ. $P = 32$, $K = 12$, $Q = 16$.

5.6.3 Performance spread vs λ

A critical issue in CDMA systems is to provide all users with equivalent performance, assuming that users are transmitted with equal powers. That means that the SNIR ϕ_k, as defined in eq. (3.10) must be approximately the same for every user. In zero forcing solutions for precoding, e.g. joint transmission and transmitter precoding, this is ensured by the algorithm's nature. Under zero forcing criteria the MAI and ISI is completely eliminated and the demodulated data, at the receiver output, are only a scaled version of the transmitted ones. This scalar is the same for all K users and thus the performance is equal for all. However, this in not the case for the MMSE and power constraint algorithm we introduced with the inverse filters. Now, there is residual MAI and ISI due to the trade off between MAI and ISI elimination and limited power

transmission. In other words, by constraining the transmitted power we force the system to include MAI in situations where eliminating it would require inappropriate power levels. This leads to differences among the users' performance, as is clearly shown in the Figures 5.17 and 5.18.

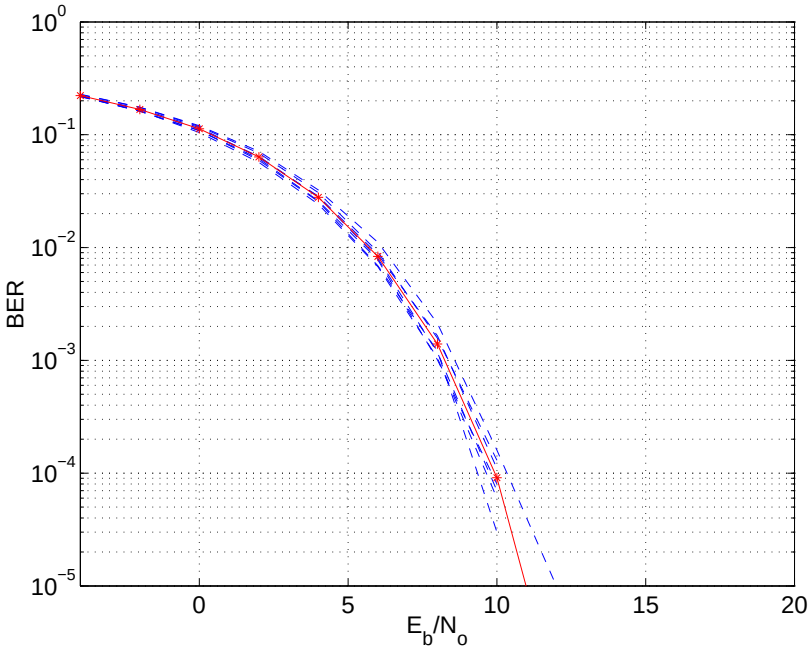

Figure 5.17: *Individual users and average BER, K=7, Q=16, $\lambda = 0.05$.*

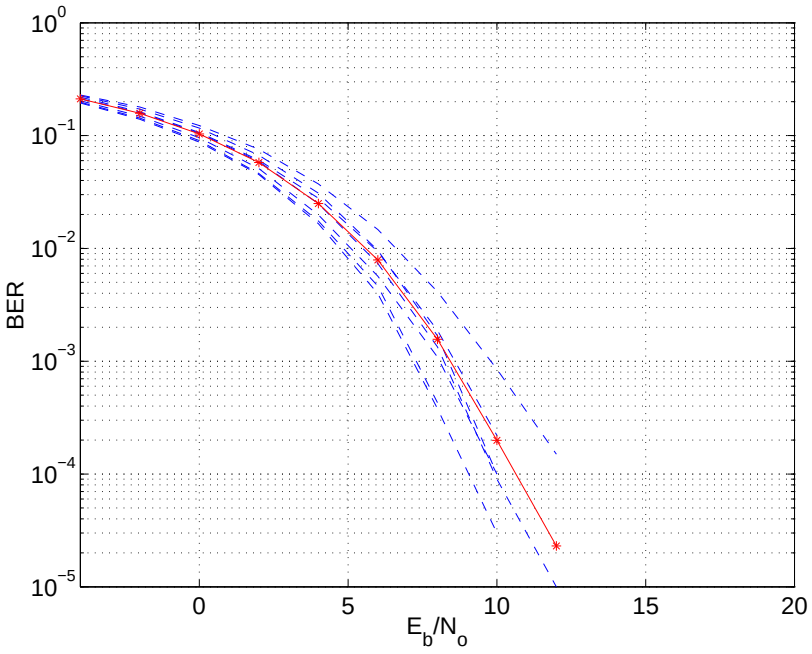

Figure 5.18: *Individual users and average BER, K=7, Q=16, $\lambda = 0.15$.*

In Figure 5.17 the BER versus E_b/N_o is illustrated for a system of $K = 7$ users, when $\lambda = 0.05$ and $P = 32$. This time, the graphs are produced by means of Monte-Carlo simulations. The solid line corresponds to the average BER of the system while the dashed lines are the individual performances for each one of the seven users. The same system is depicted in Figure 5.18, but now the Wiener solution is calculated with λ set to 0.15. It is obvious that in the first case the users are almost equivalent in performance while in the later there is a 'performance spread' among the users, which becomes more significant for higher E_b/N_o.

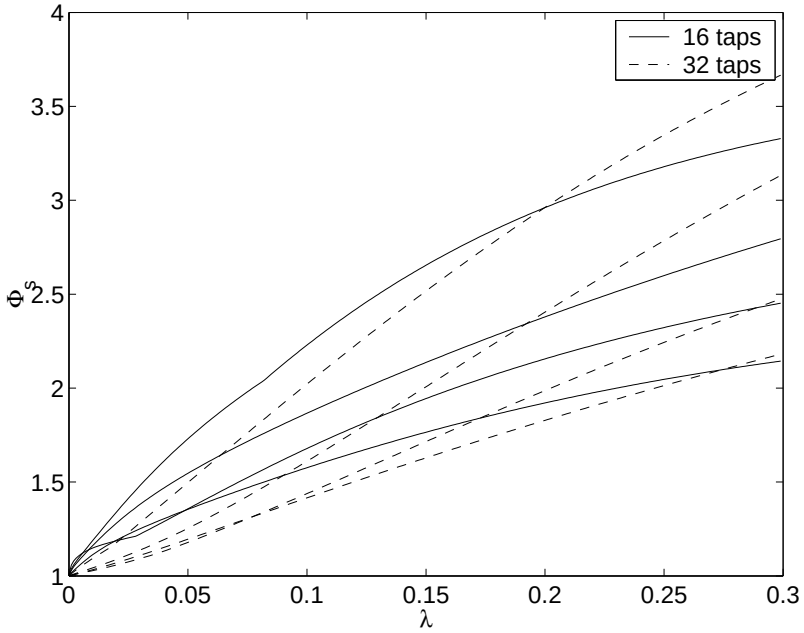

Figure 5.19: *SNIR spread vs* λ. $K = 5$, $Q = 16$, $L = 11$, $E_b/N_o = 10$*dB.*

To achieve a deeper insight of how λ affects the system we recall the performance spread Φ_s^x as defined in eq. (3.13). This gives a good idea of the "gap" between the best and the worst performance in a system of K users, when equal powers are considered. In Figure 5.19 the performance spread versus λ value is shown for a system of 5 users and $E_b/N_o = 10$dB when filter length is set to 16 or 32 taps. The solid lines represent analytical results for 4 sets of 5 different random spreading codes when $P = 16$. The dashed lines represent analytical results for 4 new sets of 5 randomly generated codes when $P = 32$. In both cases the results are similar. An important conclusion that can be drawn from these graphs is that large values of λ result in significant differences in the users' performance while small values result in similar performance.

Φ_s^8 is illustrated as a function of two variables, λ & filter length P for $K = 5$ in the Figure

5.20. It is apparent that across any filter length, inequalities among users' performance are more intense as λ increases. The Φ_s^8 is larger for small filter lengths due to insufficient precoding/pre-equalisation. In figures 5.21(a) and 5.21(b) Φ_s versus E_b/N_o & λ is shown for $P = 16$ and $P = 32$ respectively. The graphic representation in the two Figures has nearly the same pattern. For any yz plane the performance spread increases with the E_b/N_o. This is consistent with the remarks from Figures 5.17 and 5.18 and it is explained as follows.

AWGN is assumed to be the same for all users in a cell and thus the differences among users performance is due to MAI and ISI. Therefore, for low E_b/N_o, the overwhelming interference is the noise and the system is more likely to have a performance spread close to unity. On the other hand, for high E_b/N_o MAI and ISI (mostly MAI) are the dominant disturbances and these result in larger Φ_s. The solution is a small λ under the restriction of not increasing too much the power.

The graphs of this section proved that there is more to say than the numerical solution given for the parameter λ in section 5.5. These remarks are given in a summary next.

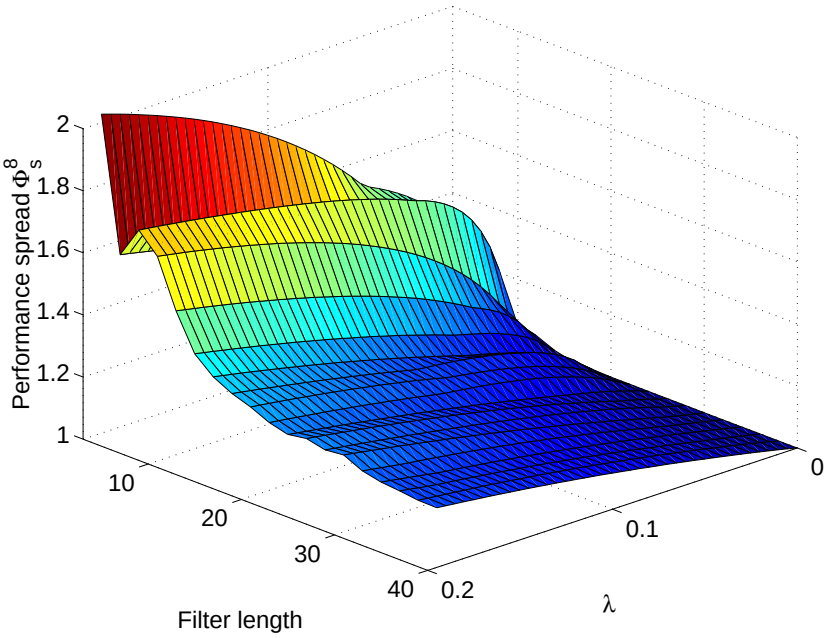

Figure 5.20: *SNIR spread vs λ & P. $K = 5$, $Q = 16$, $E_b/N_o = 8$dB.*

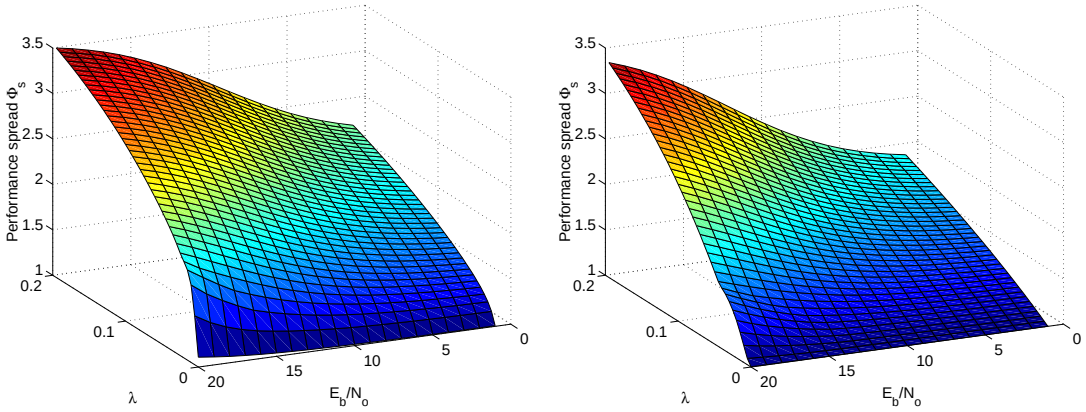

(a) K=5, Q=16, $P = 16$

(b) K=5, Q=16, $P = 32$.

Figure 5.21: Φ_s *vs* λ *&* E_b/N_o

5.6.4 Discussion

The bisection algorithm given in eq. (5.49) converges to the λ that satisfies two criteria simultaneously. It minimises the mean squared error and ensures that the averaged transmitted power per symbol is the desired one. But analytical and simulated results show that by relaxing the criteria better results can be achieved. By letting the power of $\mathbf{s}_p$ to exceed the desired level and then scaling it to $\mathcal{E}_g$ the BER performance can be significantly improved. Depending on the conditions (e.g. E_b/N_o) the Wiener solution trades off between power constraint and ISI-MAI cancellation. High $E_b/N_o \gtrapprox 12$dB requires small λ (e.g.. $\lambda \lessapprox 0.025$) to allow the suppression of the dominant MAI and ISI and keep the unscaled power to reasonable limits. For these range of E_b/N_o the BER is sensitive to λ choice. Things are more clear when $E_b/N_o \lessapprox 12$dB for a variety of scenarios. Now the BER performance is almost flattened versus λ for $\lambda \geq 0.05$. This gives a degree of freedom, which is restricted by the need to keep the performance among different users in the same levels. The performance spread is increased proportionally with λ. Consequently, of the available range of λ values we choose the smallest ($\lambda \simeq 0.05$). In addition, it is shown that the longer the tap-vector of the pre-filters (P), the less sensitive is the system's characteristics to λ parameter. However, it is desirable to keep P small for complexity reasons. In conclusion, a rough empirical rule could be proposed for the choice of λ based on

the knowledge of E_b/N_o:

$$E_b/N_o \begin{cases} \lessapprox 12\text{dB} & \text{then } \lambda \simeq 0.05 \\ \gtrapprox 12\text{dB} & \text{then } \lambda \lessapprox 0.025 \end{cases} \tag{5.50}$$

5.7 Simulation results-Comparison

In this section the results are produced by means of Monte Carlo simulations. We compare the INVF with the methods described in Chapter 4. Complexity comparison takes place and it is also shown how the analytical performance calculated in Chapter 3 is consistent with the simulation results. The basic assumptions for the simulations are the same as presented in section 2.5, which we repeat briefly here.

BPSK data symbols d_k^m are spread by random binary spreading codes $\mathbf{c}_k$ of length $Q = 16$ and transmitted synchronously over the mobile channel. Variations of the received power due to path loss and log-normal fading are assumed to be eliminated by power control. Each of the users is assumed to be transmitted with equal energy which is normalised to have unit amplitude. The codes are also normalised to have unit power. The scheme of unequal powers will also be addressed. The mobile radio channels are different for each user and the tap weights are normalised to $\|\mathbf{h}_k\| = 1$. The delay profile adopted is the one of the channel A case in [114], which is line with the UMTS European system and has a delay spread of $L = 11$ chips. Their impulse response is given in table 2.3 of section 2.5.1. The channels are assumed to be stationary with no Doppler effects. Perfect knowledge of the downlink channel is presumed in the BS. For the DPF and INVF methods the delay, Δ, in sampling the output at the receiver is set to half the pre-filter length [111].

In Figure 5.22 the BER performance versus the length of the pre-filters for the DPF and INVF is displayed for a CDMA system of 5 users and $E_b/N_o = 10$dB. The parameter λ in INVF is set to 0.05 as derived from the previous section. Analytical curves are displayed along with the simulation results. It is obvious that the performance of INVF dramatically exceeds the performance of DPF. For a filter length close to the number of users, DPF encounters near rank deficiency of the matrices to be inverted [78]. This is mirrored in the graph by the mismatch of the analytical and the simulated results for small filter lengths. Furthermore, according to the algorithm presented in [78] the pre-filter length for DPF is restricted to $P \leq \Delta + Q$ whereas the length for the INVF can be arbitrarily chosen. It is worth noting how closely the analytical

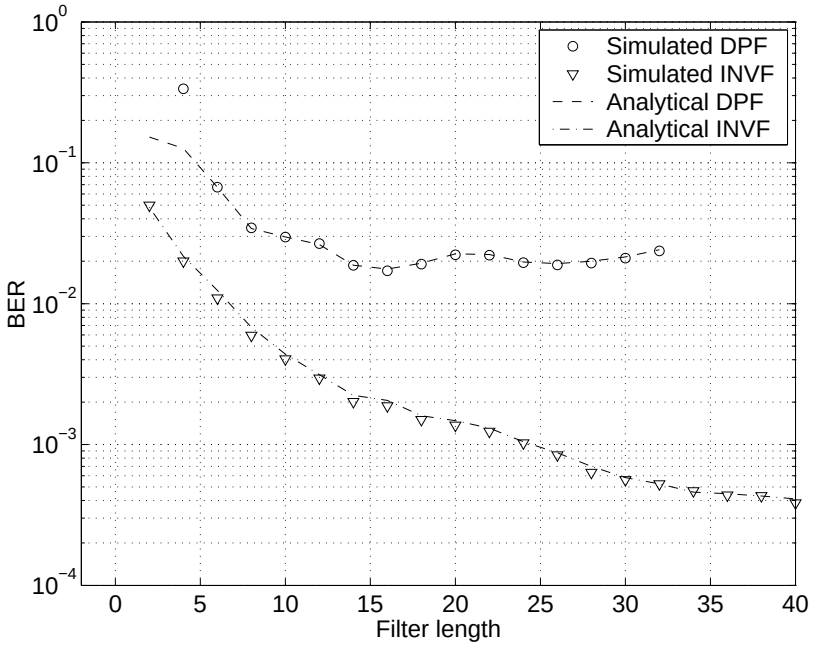

Figure 5.22: *BER vs* P. $K = 5$, $E_b/N_o = 10$*dB,* $Q = 16$. $\lambda = 0.05$ *for INVF.*

graphs correspond to the simulation results. The improved performance of INVF over the DPF is expected due to the power constraint incorporated in the algorithm and the MMSE approach adopted in comparison with the ZF one of DPF.

In the next two figures the BER versus E_b/N_o of INVF is shown and compared with pre-RAKE, TP, JT and DPF in a severe multipath propagation environment. A system of $K = 5$ and one of $K = 14$ is considered in Figure 5.23 and Figure 5.24 respectively. In Figure 5.23 TP is illustrated for both a matched filter (TP-MAT) and a RAKE (TP-RAKE) receiver versions. TP-RAKE is omitted in Figure 5.24 to ease the congestion of the graph. In these simulations the end-bits of the block transmitting techniques are being discarded for the sake of consistency with the analytical results in chapter 3. Their contribution to the performance deterioration is negligible. For $K = 5$, JT and INVF have the same performance and by far outperform the other techniques. For $K = 14$ INVF is the best technique for reasonable E_b/N_o with a significant error floor in performance when $P = 32$. By increasing the number of taps to $P = 90$ taps and selecting $\lambda = 0.003$, ideal for $E_b/N_o = 20$dB, INVF performance is further improved and becomes consistently better than JT. However, the penalty is a degradation in the low E_b/N_o ratio region, when compared with the ($P = 32, \lambda = 0.05$)-graph and it results in a crossing point at about 12dB. This is due to the fact that $\lambda = 0.003$, selected for the case of $P = 90$, is not the best choice for $E_b/N_o = 10$dB, according to our conclusions in expression

(5.50). The above leads to the idea that if the base station knows the noise power at the receiver it can optimise the performance for high loaded systems by selecting the appropriate λ value, from a data base. In figures 5.23 and 5.24 the markers represent the simulation results while the dashed lines the analytical ones as derived based on eq. (3.11). Theory and simulations are in remarkable agreement in both graphs.

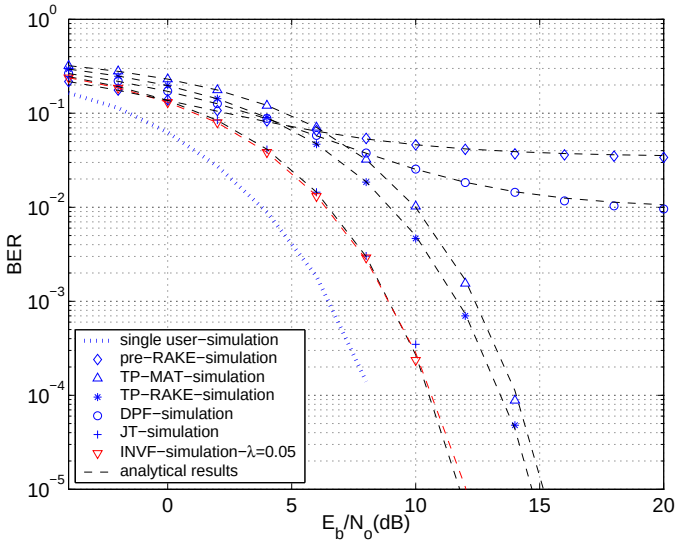

Figure 5.23: *BER vs* E_b/N_o. $K = 5$, $Q = 16$, $L = 11$.

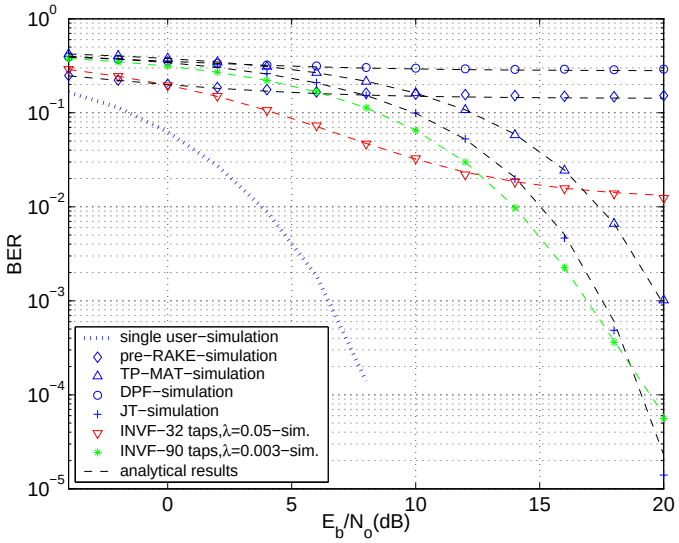

Figure 5.24: *BER vs* E_b/N_o. $K = 14$, $Q = 16$.

The BER versus the number of users is shown in Figure 5.25. For every number of users the system's BER is averaged over 60 different sets of random codes to smooth out the effect of

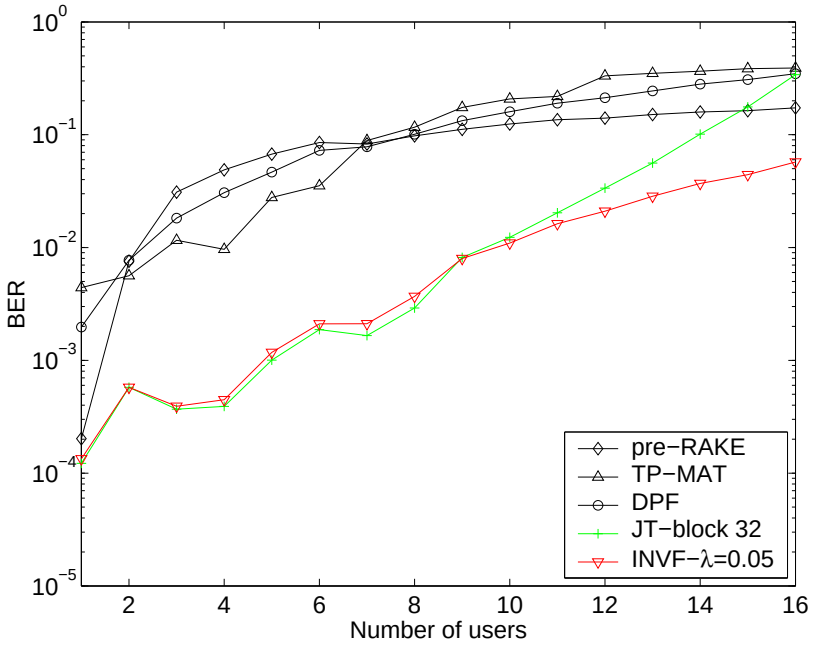

Figure 5.25: *BER vs* K. $E_b/N_o = 10$*dB,* $Q = 16$. $P = 32$ *for INVF and DPF.* $\lambda = 0.05$ *for INVF.*

codes with low or high crosscorrelation. E_b/N_o is set to 10dB and for INVF and DPF the pre-filters have a length of $P = 32$ taps. It is clear that INVF outperform TP, Pre-RAKE and DPF. INVF exhibits better performance than JT for a heavily loaded CDMA system. For a system loaded to a number of users less than half the spreading gain INVF and JT are competitive in terms of performance but it worths examining the computational cost of the two methods. The block length for JT is set to $N = 32$ bits. The matrices that need to be inverted for both JT and INVF algorithms have the same dimensions. Thus, we examine the multiplications needed per symbol per user after any matrix inversion has been completed. Recalling the computational cost as issued for blockwise and bitwise techniques in Chapter 3, table 5.1 is obtained. INVF

Algorithm	Size of matrix to be inverted when channel changes	Number of Multiplications per symbol (excluding inversions)
JT	$NK \times NK = 160 \times 160$	$N^2KQ = 81920$
INVF	$PK \times PK = 160 \times 160$	$PQ = 512$

The numerical examples correspond to the case of $N = 32$, $K = 5$, $Q = 16$, $P = 32$.

Table 5.1: *INVF vs JT computational cost comparison*

requires a lot less computational cost than JT. The block length of JT can by reduced at the

cost of capacity loss if N is too small, due to incorrect precoding of the end-bits of the block. Moreover, the blocks to be transmitted in a real CDMA system are much longer than the 32 length used in Figure 5.25.

The degree of deterioration in performance due to severity in multipath channels is shown in Figures 5.26 and 5.27. Only JT and INVF are shown as they both outperform the other

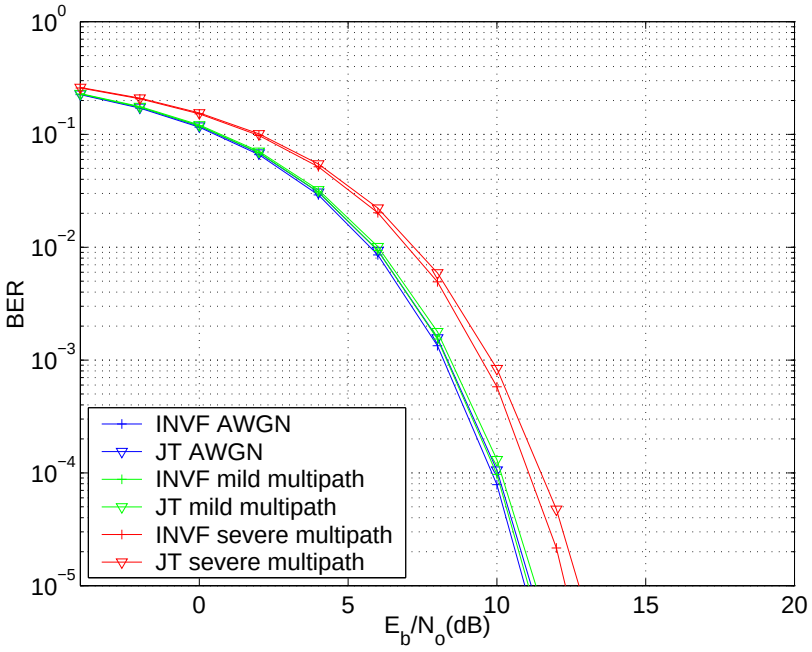

Figure 5.26: *Channel's effect for spreading codes set 1.*

techniques and compete in performance terms. For each algorithm the BER is shown for a AWGN channel along with the BER for a mild and a severe multipath channels. The system chosen is one of $K = 6$ users and the filters length is set to $P = 40$ taps. For JT the end bits are discarded. The difference between the two graphs is the set of spreading codes used (denoted as spreading codes set 1 and 2). The severe multipath channels follow the same pattern as shown in table 2.3, while for the mild channel is as in table 5.2. As observed from both graphs, deterioration in performance occurs to the same extent for both algorithms and as expected is more significant and apparent when a severe multipath environment is considered. The difference in performance among the two Figures reflects the effect that different random codes can have on a system.

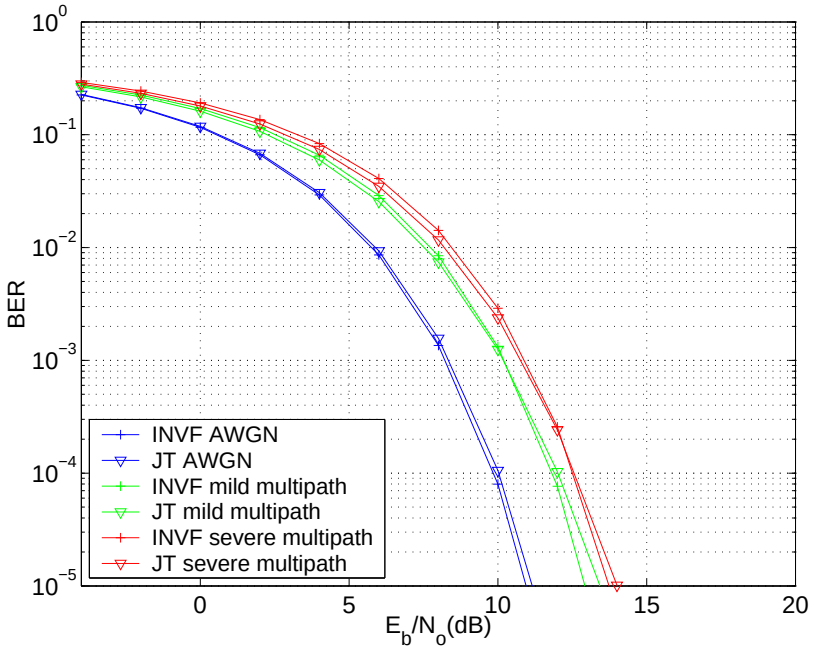

Figure 5.27: *Channel's effect for spreading codes set 2.*

Delay in μsec	**Tap Coefficients for channel**					
	User 1	User 2	User 3	User 4	User 5	User 6
0.0	0.998054	-0.995696	0.999707	-0.861355	-0.891757	0.901384
0.26	-0.062311	0.083777	-0.007458	0.507978	0.070835	-0.431625
0.52	0.000000	0.000000	0.000000	0.000000	0.000000	0.000000
0.78	0.002369	-0.039639	-0.023048	-0.005155	0.446937	0.034736

Table 5.2: *Mild multipath channel's profile*

In section 5.2 we stated that differences in transmission power among the users do not affect the Wiener solution (this is proved in Appendix A). The scenario of different transmission powers occurs in the downlink when different quality of services are required for each user. In Figure 5.28 the dashed lines correspond to the individual performances of each user when transmitted with equal powers $w_k^2 = 1$. The simulation BER curves are almost overlaping with each other. In the same graph we show the INVF simulation performance for $K = 3$ users, when $(w_2/w_1)^2 = 4$ and $(w_3/w_1)^2 = 9$ with $w_1^2 = 1$. From the graph it is obvious that user-1 performance is not affected compared with the case of $w_k^2 = 1$, $k = 1, 2, 3$. On the other hand users 2 and 3 display performance improved according to the transmission power. This means that the Wiener solution is near-far resistant.

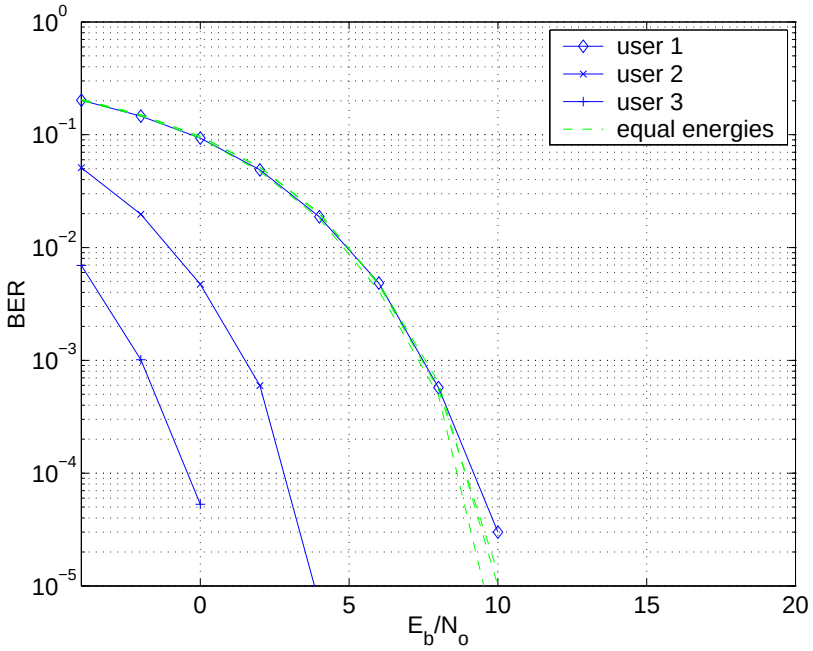

Figure 5.28: *BER vs* E_b/N_o. $K = 3$, $Q = 16$.

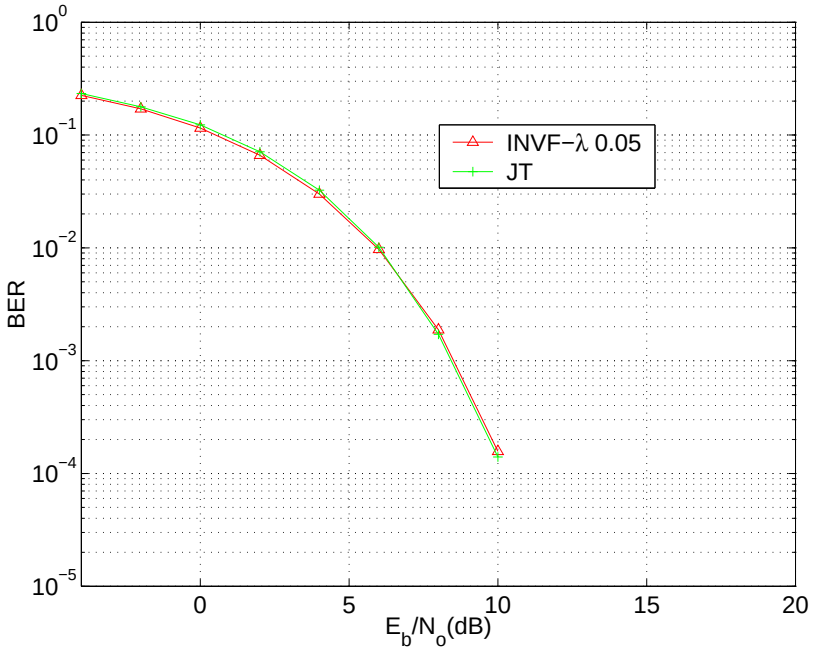

Figure 5.29: *BER vs* E_b/N_o. $K = 3$, $Q = 16$ *for complex channels.*

So far, throughout this thesis the simulations and the theoretical analysis are using the channel profiles as described in tables 2.3 or 5.2. Although these channels follow the delay profile of an urban channel, in line with UMTS, their tap-coefficients have real values and the power is

equivantly distributed among them, which is not very realistic. The channel tap-coefficients in a real system are complex numbers and they can follow a Rayleigh distribution, time varying with a Doppler frequency. Figure 5.29 displays the average BER of three users. The techniques compared are the INVF and JT. Each tap-coefficient is time varying and complex. The real and imaginary part are simulated independently as sum of sinus [115, 116] with a selected Doppler frequency. The power of tap-coefficient has a Rayleigh distribution. Each one of the three channels is initialised with different phases to achieve uncorrelated results. We let the channels run for 20 seconds, with Doppler frequencies of 30-90 Hz. We lock them and then run the BER simulation for INVF and JT. The set of channels was for both graphs the same for the sake of fair comparison and they are demonstrated in table 5.3.

Delay in μsec	**Tap Coefficients for channel**		
	User 1	User 2	User 3
0.00	-0.242974-j0.303296	0.220272-j0.342193	-0.612400+j0.730495
0.26	-0.125466-j0.063417	-0.099331-j0.277136	-0.444251-j0.669437
0.52	0.000000-j0.000000	0.000000-j0.000000	0.000000-j0.000000
0.78	0.010125+j0.036019	-0.066840+j0.004550	-0.048003+j0.264531
1.04	0.174803+j0.117559	-0.071114+j0.103831	-0.238124-j0.123369
1.30	0.000000-j0.000000	0.000000-j0.000000	0.000000-j0.000000
1.56	0.000000-j0.000000	0.000000-j0.000000	0.000000-j0.000000
1.82	0.027070+j0.011528	-0.107521-j0.036790	-0.089175-j0.084012
2.08	0.000000-j0.000000	0.000000-j0.000000	0.000000-j0.000000
2.34	0.000000-j0.000000	0.000000-j0.000000	0.000000-j0.000000
2.60	0.074906+j0.012934	-0.006503-j0.048724	0.052034-j0.031326

Table 5.3: *Complex multipath channel's profile*

5.8 Summary

In this Chapter a new technique was proposed called inverse filters originating from the stereophonic sound reproduction systems. The algorithm was appropriately modified and the power constraint was added to it. The Wiener solution was calculated and given in a closed form, while the power constraint parameter λ was thoroughly investigated. The technique is bitwise and outperforms DPF, TP-MAT and TP-RAKE. INVF also outperforms JT for heavily loaded systems, while the methods are competitive when $K \leq Q/2$ for sufficiently large data-block length. However, INVF requires significantly less computational cost than JT. The simulation BER curves for a variety of precoding techniques, produced in this Chapter, were in ultimate

agreement with the analytical ones as derived from the analysis in Chapter 3. INVF can be easily adjusted to any existing CDMA-TDD system with slowly varying propagation channels.

Chapter 6
Multichannel adaptive algorithms

In this Chapter we will examine adaptive transmitter based techniques that reduce MAI and ISI in a TDD system. Part of this work has been published in [117]. Section 6.1 presents the motivation that inspired the study of adaptive techniques and the link with the Wiener solution for INVF, as given in Chapter 5. Section 6.2 introduces filtered-X. The adaptive multichannel techniques are described in section 6.3. In sections 6.4 and 6.5 there is a discussion about convergence speed and BER performance.

6.1 Motivation

The fundamental basis that precoding techniques rely on is that the base station (transmitter) has knowledge of all the downlink channels plus the receiver structure (filters matched to the spreading codes) of the mobile stations. In Chapter 4 and Chapter 5 the methods presented use this knowledge to implement algorithms that calculate directly a precoded signal which is ISI and MAI resistant prior to transmission. These algorithms include inversion of one or more matrices, which contributes to the complexity and computational cost. Pre-RAKE doesn't involve any matrix inversion but its performance for a multiuser scheme is rather poor. A matrix inversion free technique is then sought.

In conventional receiver based equalisation or multiuser detection systems *adaptive techniques* [11, 69–74, 89] are commonly used to converge to the tap-coefficients that remove the interference and increase the signal to noise ratio. Therefore the matrix inversion needed for the receiver based ZF, eq. (2.38), or MMSE, eq. (2.42), is avoided. The objective is to find such an approach which is feasible for the transmitter based techniques. This idea implies that the adaptive filters are placed before the channels, within the BS. In active control of sound and vibration technology an adaptive feedforward technique, named *filtered-X*, is extensively used to pre-equalise the sound produced by a loudspeaker and compensate for any distortion caused by the channel between the microphone and the loudspeaker. Obviously, such an approach

presumes that the controller, which adaptively sets the pre-filter taps, is provided with the error sensed at the microphone with a feedback link. An adaptation of this method to a CDMA system implies that the mobile terminal should receive a training sequence and provide the BS with the error at its output. However, in wireless telecommunications the feedback from the receiver to the transmitter in conjunction with the necessary training sequences result in bandwidth usage and waste of capacity. Hence, this is not the solution that designers are in favor of. It would have been ideal if there was no need for the mobile to feed back any error to the BS , but yet the error was known to the BS.

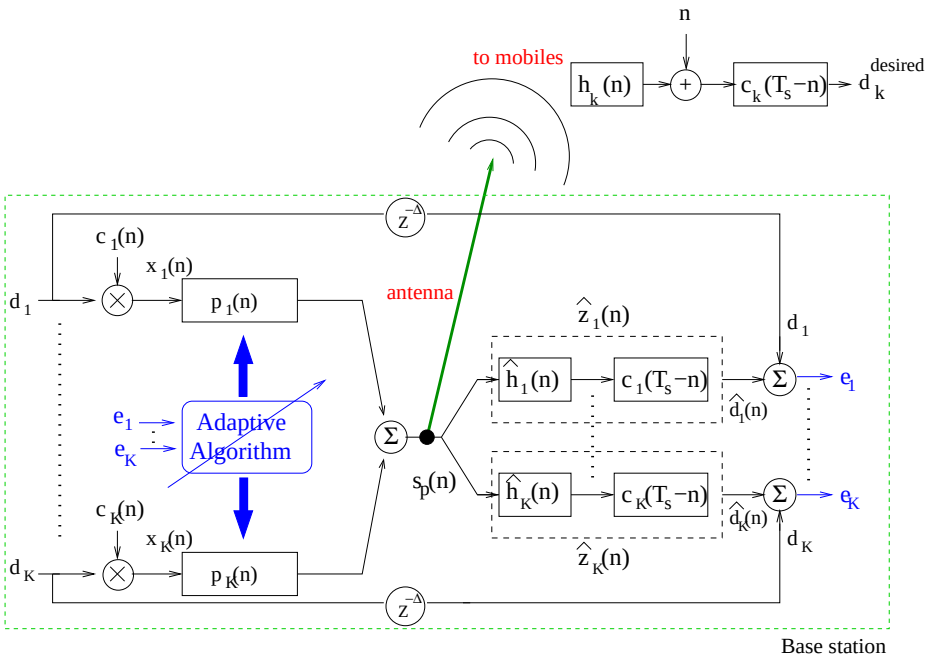

Figure 6.1: *Block diagram of emulation in the BS*

This is feasible under the TDD scenario according to which the BS along with the knowledge of the receivers structure is feasible to have an estimate $\hat{h}_k(n)$, $k = 1 \dots K$, of kth user's channel $h_k(n)$, from the last uplink burst. There is nothing to prevent then the BS from emulating the actual system, in a cell, in an internal block. The block diagram of the emulation that takes place in the BS is shown in Figure 6.1. It is similar to the block diagram suggested for the INVF with the addition of the adaptive algorithm block and the error feedback lines. The BS station initialises the tap-coefficients of the pre-filters and then starts transmission. The resulting $s_p(n)$ signal is sent to the BS antenna element and an internal block that emulates the real receivers and their corresponding channels. By emulating the system, the BS can estimate the output $\hat{d}_k(n)$ sampled from the mobile. The errors $e_k = \hat{d}_k - d_k$, $k = 1 \dots K$, are fed back

to the adaptive algorithm and after a number of transmissions the algorithm converges to the coefficients that minimise the sum of the squares of K error signals. If the same cost function is used the converged solution should be, ideally, the Wiener solution for INVF. Instead of a single error as in the conventional adaptation process, a vector of errors

$$\mathbf{e} = [e_1 \dots e_K]^T \tag{6.1}$$

is sent now back to the adaptive block. Therefore, an independent adaptive algorithm for each user's pre-filter is not effective. A *joint adaptive* approach should be followed for the simultaneous convergence of all the filters $\mathbf{p}_k$. This is achieved with the *multichannel* (MC) adaptive algorithms for feedforward control as will be explained in a later section.

These algorithms were originally used and investigated for active noise control and sound reproduction systems. These systems consist generally by a number of I source signals, a number of J actuators (typically loudspeakers) and a number of K "error" sensors (typically microphones). In the CDMA systems we examine in the current thesis the source signals are the K spread spectrum signals addressed to each user, the actuator is one single element antenna (although this could be generalised for a multiple antenna array) and the the "error" sensors the K matched filter receivers.

6.2 Filtered-X LMS

It is considered as essential to present a short introduction to the origin and principles of the monochannel filtered-X algorithm as introduced in [111]. The classic problem of the adaptive inverse modeling of a noisy plant is illustrated in Figure 6.2(a). The plant noise can be represented as additive noise at the plant output. This noise is an additive input to the adaptive filter and is not correlated with the desired-response input to the system. The result of the plant noise is therefore to cause the adaptive solution to be generally different from that of a close approximation to the delayed inverse.

The problem of plant noise led to the development of the filtered-X algorithm, which allows adaptation of the inverse filter placed forward of the plant in the cascade sequence. This approach is partially illustrated in Figure 6.2(b), where plant noise doesn't appear in the adaptive filter input. Consequently, this noise will have no effect on the converged solution for the inverse filter provided that the adapting input can be derived properly. Assuming an FIR model,

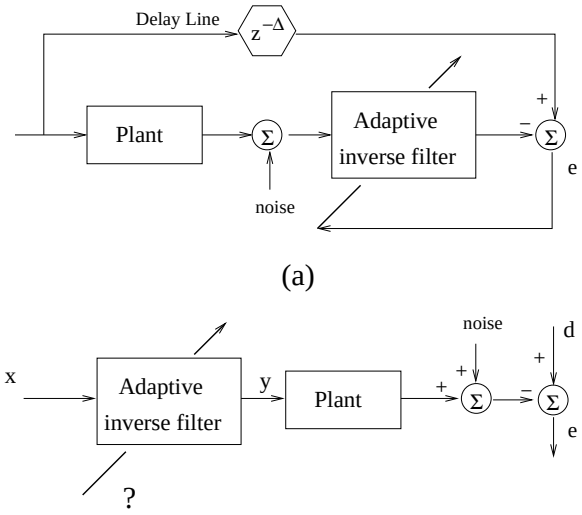

Figure 6.2: *Adaptive inverse modeling of a noisy plant*

the mean square of error e in Figure 6.2(b) is a quadratic function of the adaptive filter weights and the adaptation has the potential for smooth convergence with a unimodal performance surface. The classic least mean squares (LMS) algorithm cannot be used unless an appropriate "desired" signal is derived to be compared with the adaptive filter output y. The signals d and e are not sufficient because e is the error at the plant output, not at the adaptive filter output. If e is used directly with the LMS algorithm to adapt the inverse filter, the adaptive process is very likely to be unstable or, if not, to converge to an irrelevant solution [111].

The correct approach of the problem as shown in Figure 6.2(b) is shown in Figures 6.3(a)-(c). In Figure 6.3(a) the noise plant is neglected for the moment and the plant is commuted with the LMS filter , whereupon the LMS algorithm can be directly applied. Adjusting the weights to minimise the mean square error e will yield the correct set of weights to minimise the e in Figure 6.2(b) with plant noise neglected. Next the system diagrammed in Figure 6.3(b) is regarded. Here the adaptive filter and the plant are cascaded as originally in Figure 6.2(b). The objective is that the adaptive process shown in Figure 6.3(c) produce the same set of weights as the systems illustrated in Figure 6.3(a) and (b). Then, the filtered-X algorithm is a viable solution to the adaptation problem of Figure 6.2(b). Comparing the systems of Figure 6.3(a) and (b) it is clear that the input signal vectors available to the LMS algorithms in both systems are identical at all times. However, the errors e are not necessarily identical to each other at all times. They would be identical if the adaptive FIR filter weight vectors were identical to each other at all times and if the plant and the adaptive filter were commutable. For the same

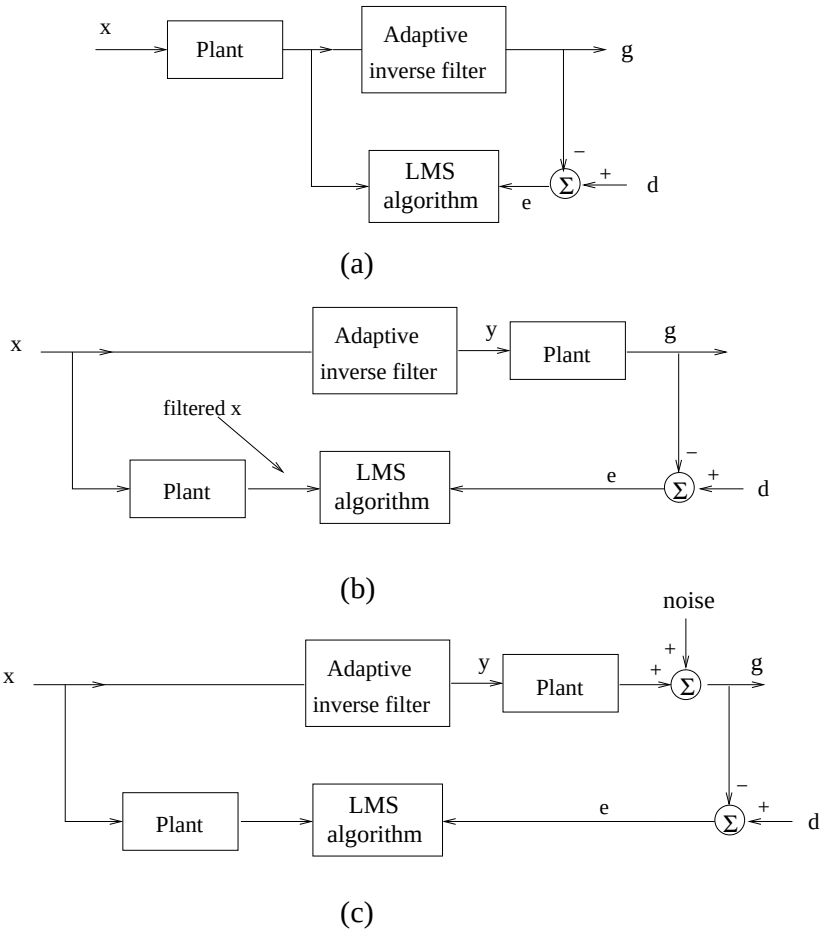

Figure 6.3: *Development of filtered-X algorithm*

input, the same output results when the positions of two cascaded filters are commutable. They would be commutable if the plant were linear and if the time variations of the impulse responses of both the plant and the adaptive filter took place with time constants long compared to the combined memory times or time constants of the adaptive filter and the plant. Thus assuming slow adaptation plant and that the adaptive filters are commutable, the weight vectors of the systems in Figures 6.3(a) and (b) undergo the same changes if the are identically initialised. Hence, the adaptive process in Figure 6.3(b) is suitable for the problem in Figure 6.2(b). In Figure 6.3(c) the noise plant is added again to the system. The expected value of the adaptive weight vector will be the same with the noiseless system in Figure 6.3(b). However it will of course cause some misadjustment to the weight vector.

6.3 Multichannel algorithms

The filtered-X technique refers to a single input single output feedforward adaptive system. Multichannel/multiuser feedforward adaptive algorithms have also been developed. The most popular of them are the *multichannel least mean squares* (MC-LMS)[1] and *multichannel recursive least squares* (MC-RLS). Originally in the derivation of these algorithms the power constraint term was omitted. However, in recent publications control output constraints have been incorporated into MC-LMS method. The cost function for the derivation of the adaptive algorithms can be taken directly from Chapter 5 with or without the power constraint term, denoted as J_c and J respectively. These techniques adapted to a CDMA system will be described along with a reference to some alternative versions.

6.3.1 Multichannel LMS

The multichannel LMS algorithm [107] provides a multichannel generalisation of Widrow's filtered-X LMS algorithm [111]. It is widely used and it is the benchmark to which most adaptive filtering algorithms are compared. In this algorithm, the gradient of the instantaneous sum of squared error signals is computed as a function of each coefficient in the adaptive filters. Thus, the method of steepest descent can be used to descend toward the minimum on the performance surface of the quadratic form in eq. (5.11). The values of the pre-filter taps weight vector are iteratively updated by an amount proportional to the negative of the gradient of the quadratic performance surface.

The complete cost function to be minimised is as in eq. (5.11) without the power constraint term:

$$J = E[\mathbf{d}_0^T \mathbf{d}_0] - 2E[\mathbf{d}_0^T \mathbf{R}(T_s^n)]\mathbf{p} + \mathbf{p}^T E[\mathbf{R}^T(T_s^n)\mathbf{R}(T_s^n)]\mathbf{p} \tag{6.2}$$

The gradient $\vartheta J/\vartheta \mathbf{p}$ of eq. (6.2) is:

$$\begin{aligned} \frac{\vartheta J}{\vartheta \mathbf{p}} &= -2E[\mathbf{R}^T(T_s^n)\mathbf{d}_0] + 2E[\mathbf{R}^T(T_s^n)\mathbf{R}(T_s^n)]\mathbf{p} \\ &= -2E\left[\mathbf{R}^T(T_s^n)\big(\mathbf{d}_0 - \mathbf{R}(T_s^n)\mathbf{p}\big)\right] \\ &= -2E\left[\mathbf{R}^T(T_s^n)\big(\mathbf{d}_0 - \hat{\mathbf{d}}_0(T_s^n)\big)\right] \end{aligned} \tag{6.3}$$

[1] Multichannel LMS can also be found in the bibliography as *Multiple error LMS* emphasising in the vector error feedback

By defining the instantaneous error vector $\mathbf{e}(T_s^n)$ between the desired data and the estimated data as:

$$\mathbf{e}(T_s^n) = \mathbf{d}_0 - \hat{\mathbf{d}}_0(T_s^n) \tag{6.4}$$

and substituting in eq. (6.3) the gradient is expressed as:

$$\frac{\vartheta J}{\vartheta \mathbf{p}} = -2E[\mathbf{R}^T(T_s^n)\mathbf{e}(T_s^n)] \tag{6.5}$$

If each pre-filter taps vector is now adjusted at every sample time (T_s^n) by an amount proportional to the negative instantaneous value of the gradient, a modified form of the well-known LMS algorithm is produced:

$$\mathbf{p}(T_s^n) = \mathbf{p}(T_s^{n-1}) + \mu\mathbf{R}^T(T_s^n)\mathbf{e}(T_s^n) \tag{6.6}$$

where μ is the step-size parameter of the algorithm. The error vector $\mathbf{e}$ is known to the BS due to the emulation of the real system as explained in section 6.1.

Recalling equations (5.18) and (5.19) we can 'break' eq. (6.6) down to the corresponding update step for the specific pre-filter of each user:

$$\mathbf{p}_k(T_s^n) = \mathbf{p}_k(T_s^{n-1}) + \mu\big[\mathbf{r}_{1k}(T_s^n)\cdots\mathbf{r}_{Kk}(T_s^n)\big]\mathbf{e}(T_s^n) \tag{6.7}$$

where $\mathbf{r}_{\mu\nu}(n)$ as in eq. (5.1).

The representation of eq. (6.7) for individual pre-filters can be realised as shown in Figure 6.4. The block diagram corresponds to the 2-users case. Both in Figures 6.1 and 6.4 $\hat{z}_k(n) = \hat{h}_k * c_k(Q-n)$ means that an estimate $\hat{h}_k(n)$ of the downlink channel $h_k(n)$ is available. Under ideal conditions perfect knowledge of the channels is available and thus the internal emulation reflects the actual system. The detailed block diagram of the MC-LMS algorithm in Figure 6.4 is given for simplicity reasons only for user 2. The analogy with the filtered-X, which is the monochannel version of MC-LMS, is obvious. Spread signal $d_2c_2(n)$ is passing in parallel through the corresponding pre-filter $p_2(n)$ and $\hat{z}_1$, $\hat{z}_2$ to produce the 'reference signals' $r_{12}(n)$, $r_{22}(n)$. Each sample, taken in chip rate, is stored in a corresponding P-length buffer. Estimated errors e_1, e_2 multiply the contents of the r_{12}, r_{22} signal buffers, respectively. The MC-LMS algorithm is applied then, every Q chips, to update the coefficients of the adaptive pre-filters. The algorithm is very simple and doesn't require excessive computational cost. A drawback of

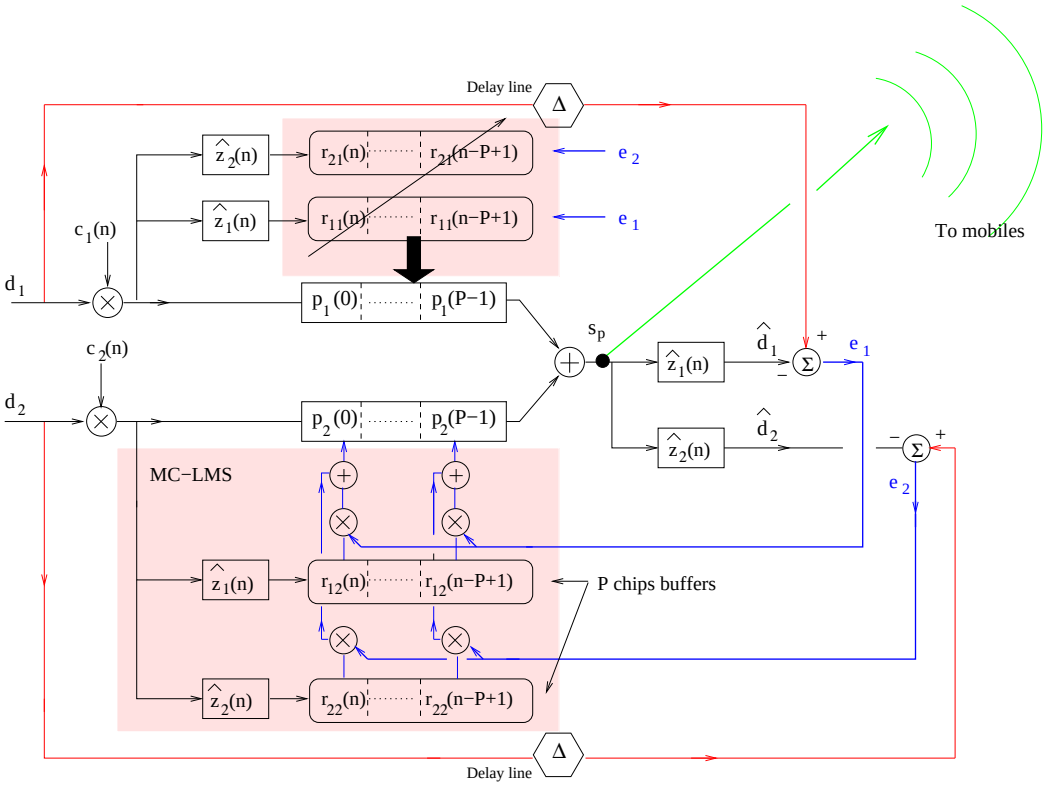

Figure 6.4: *Detailed MC-LMS algorithm for two users*

MC-LMS is its slow convergence rate. In a theoretical analysis of MC-LMS, given in [118], an upper bound for the step-size parameter has been calculated as:

$$0 \leq \mu \leq \frac{2}{3K\text{trace}\left(E\left[\mathbf{R}^T(T_s^n)\mathbf{R}(T_s^n)\right]\right)} \tag{6.8}$$

$E\left[\mathbf{R}^T(T_s^n)\mathbf{R}(T_s^n)\right]$ has been calculated in a closed form in eq. (5.31). These bounds guarantee convergence of the algorithm to finite values.

6.3.2 Multichannel LMS with power constraints

The MC-LMS uses the method of steepest descent to minimise the sum of the mean squared error signals with no constraint on the magnitude of the resulting transmission signal $s_p(n)$. After convergence the total average transmitted energy per symbol is calculated and then scaled with the appropriate scaling factor $\sqrt{\mathcal{F}}$, eq. (3.32). The objective is to achieve an average transmission power per symbol equal to $\mathcal{E}_g$, corresponding to a classic CDMA system. In [119, 120] the steepest descent algorithm is modified to incorporate the power constraint, aiming

to render the scaling factor unnecessary. The developed techniques are named *leakage* and *rescaled* MC-LMS algorithms.

6.3.2.1 Leakage algorithm

The leakage algorithm [119], tries to minimise the square moduli of the error signals $\mathbf{e}^T\mathbf{e}$ subject to the constraint that $\mathbf{u}^T\mathbf{u}$ is less than some upper limit W_{max}, with $\mathbf{u}$ the control signals. The cost function is:

$$E\big[\mathbf{e}^T\mathbf{e}\big] + \lambda(\mathbf{u}^T\mathbf{u} - W_{max}) \tag{6.9}$$

This cost function is not in accordance with the block diagram given in Figure 6.1 and certain modifications need to be done. In our system the control signals $\mathbf{u}$ are replaced by the pre-filtered spread signals $\mathbf{c}_k * \mathbf{p}_k$, $k = 1 \dots K$. The total average power per symbol $\|\mathbf{Up}\|^2 = \big(\mathbf{p}^T\mathbf{U}^T\mathbf{Up}\big)$ replaces $\mathbf{u}^T\mathbf{u}$, while the error vector $\mathbf{e}(T_s^n)$ is as defined in eq. (6.4). Furthermore W_{max} is replaced by $\mathcal{E}_g$ and the power constrained cost function is

$$J_c = J + \lambda\big(\mathbf{p}^T\mathbf{U}^T\mathbf{Up} - \mathcal{E}_g\big) \tag{6.10}$$

with J as in eq. (6.2). By usage of equations (5.12) and (6.5) the derivative $\vartheta J_c/\vartheta\mathbf{p}$ is given by:

$$\frac{\vartheta J_c}{\vartheta\mathbf{p}} = -2E[\mathbf{R}^T(T_s^n)\mathbf{e}(T_s^n)] + 2\lambda\mathbf{U}^T\mathbf{Up} = -2\big(E[\mathbf{R}^T(T_s^n)\mathbf{e}(T_s^n)] - \lambda\mathbf{U}^T\mathbf{Up}\big) \tag{6.11}$$

Equation (6.11) can now be used as the basis for an adaptive algorithm using the method of steepest descent such that the vector of pre-filter taps at the n iteration, denoted as $\mathbf{p}(T_s^n)$, is given by:

$$\mathbf{p}(T_s^n) = \mathbf{p}(T_s^{n-1}) + \mu\big(\mathbf{R}^T(T_s^n)\mathbf{e}(T_s^n) - \lambda\mathbf{U}^T\mathbf{Up}(T_s^{n-1})\big) \tag{6.12}$$

After manipulating the right-hand part of (6.12) the following update equation[2] is derived

$$\mathbf{p}(T_s^n) = \big(\mathbf{I} - \lambda\mu\mathbf{U}^T\mathbf{U}\big)\mathbf{p}(T_s^{n-1}) + \mu\big(\mathbf{R}^T(T_s^n)\big) \tag{6.13}$$

[2] In [119] the update equation given is :

$$\mathbf{p}(T_s^n) = \big(1 - \lambda\mu\big)\mathbf{p}(T_s^{n-1}) + \mu\big(\mathbf{R}^T(T_s^n)\big)$$

which is a form of the MC-LMS with leakage [121]. μ is the step-size parameter of the algorithm. The addition of leakage keeps the output power under control by continual removal, or leakage, of a small value of the weights, which represents a compromise between biasing the pre-filters weights from the original optimum solution (when cost function is J) and bounding the output power [120]. Therefore the final performance of the control algorithm significantly depends on the value of the leakage coefficient and it is not guaranteed that the final solution will be within the constraint.

It is possible to increase the performance of the leakage algorithm by applying a time-varying leakage coefficient $\lambda(T_s^n)$. The value of $\lambda(T_s^n)$ is changed during adaptation and made dependent on the value of $\|\mathbf{Up}(T_s^n)\|^2$, which is calculated in every updating step. A method of scheduling $\lambda(T_s^n)$ on $\|\mathbf{Up}(T_s^n)\|^2$ is proposed in [119] and is given in eq. (6.14). According to that $\lambda(T_s^n)$ is set to zero if $\|\mathbf{Up}(T_s^n)\|^2$ is less than 90% of $\mathcal{E}_g$ and then it is increased in proportion to the value of $\|\mathbf{Up}(T_s^n)\|^2$ above this value.

$$\lambda(T_s^n) = \begin{cases} 0 & \|\mathbf{Up}(T_s^n)\|^2 \leq 0.9\mathcal{E}_g \\ \frac{\|\mathbf{Up}(T_s^n)\|^2 - 0.9\mathcal{E}_g}{\mathcal{E}_g} & \|\mathbf{Up}(T_s^n)\|^2 \geq 0.9\mathcal{E}_g \end{cases} \tag{6.14}$$

6.3.2.2 Rescaling algorithm

An alternative way to solve this problem is to use the idea of the active set method (a gradient projection method focused on the solution of the Kuhn-Tucker equations), which is widely used in the field of constrained optimisation to solve the nonlinear programming problem. The active set method is an iterative procedure that involves two phases: the first phase calculates a feasible point (a weight vector satisfies the constraint); the second phase generates an iterative sequence of feasible points that converge to the solution. The search direction for generating the sequence of feasible points is calculated by projecting the gradient along the constraint boundary if the constraint is violated. Depending on the quadratic nature of the objective function and the strictly convex property of the constraint set, the algorithm should converge to the minimum under the constraints. The algorithm so obtained is called the rescaling algorithm and is given in [120] for a single-input single-output problem, which corresponds to the filtered-X. Here, we generalise this method to the multichannel/multiuser case. According to this algorithm the weight vector $\mathbf{p}$ and output signal $s_p(n)$ are rescaled after updating as follows:

$$\mathbf{p}(T_s^n) = \mathbf{p}(T_s^{n-1}) + \mu \mathbf{R}^T(T_s^n)\mathbf{e}(T_s^n) \tag{6.15}$$

if $E_g(T_s^n) = \mathbf{p}(T_s^n)\mathbf{U}^T\mathbf{U}\mathbf{p}(T_s^n) \geq \mathcal{E}_g$, then

$$\mathbf{p}(T_s^n) = \mathbf{p}(T_s^n)\sqrt{\mathcal{E}_g / E_g(T_s^n)} \tag{6.16}$$

$$s_p(T_s^n) = s_p(T_s^n)\sqrt{\mathcal{E}_g / E_g(T_s^n)} \tag{6.17}$$

The original MC-LMS algorithm uses the estimated gradient $\mathbf{R}^T(T_s^n)\mathbf{e}(T_s^n)$ as the weight update vector, which, however, sometimes makes the output power per symbol greater than the desired $\mathcal{E}_g$ after convergence. The rescaling algorithm remedies the problem by projecting the estimated gradient into the constraint set to obtain the new updated vector, which is simply obtained in eq. (6.17) by rescaling the control weight vector and control output after the updating.

6.3.3 Multichannel RLS

For the learning of FIR filters using linear adaptive filtering algorithms, it is well known that classic recursive-least-squares algorithms [89] produce a faster convergence speed than stochastic gradient descent techniques, such as the basic least mean squares algorithm [111]. This conclusion remains valid for the feedforward control systems like active noise control. The filtered-X monochannel RLS algorithm for active noise control has been introduced in [122, 123]. In [106] the filtered-X RLS is upgraded to deal with a multichannel/multiuser scheme. To update the coefficients of the adaptive filters, the multichannel RLS algorithm uses an approach similar to the multichannel LMS algorithm, in the update eq. (6.6), but a gain matrix is used to multiply the error signals, instead of directly using the $r_{\mu\nu}(n)$, $\mu, \nu = 1 \ldots K$ filtered-reference signals. MC-RLS algorithm combines a decorrelation of the filtered-reference signals (reducing the effect of the eigenvalue spread in the filtered-reference signals correlation matrix) and a minimisation of a weighted sum of the past squarred errors.

Each input sample in the input vector of the classical RLS algorithm is replaced by a $P \times K$ matrix, to produce the MC-RLS filtered-reference matrix $\mathbf{V}(n)$, whose dimensions are $KP \times K$:

$$\mathbf{V}(n) = \begin{bmatrix} \mathbf{r}_{11}(n) & \cdots & \mathbf{r}_{K1}(n) \\ \vdots & \ddots & \vdots \\ \mathbf{r}_{1K}(n) & \cdots & \mathbf{r}_{KK}(n) \end{bmatrix} \tag{6.18}$$

The number of rows in $\mathbf{V}(n)$ [3]reflects the total number of coefficients in all the adaptive filters (degrees of freedom in the system), while the number of columns reflects the number of error signals to be minimised by the adaptive filters. The P-length weight vector (adaptive filter) in the classical RLS algorithm is replaced by KP vector $\mathbf{p}$, eq. (3.28), that contains the weights of all filter-taps. Error vector $\mathbf{e}$, defined in eq. (6.1), replaces the scalar error of the classic RLS. Then the multichannel RLS algorithm is:

$$\begin{aligned}
\mathbf{M}(0) &= \delta^{-1}\mathbf{I}, \quad \mathbf{I}: \ K \times K \text{ identity matrix} && (6.19)\\
\mathbf{p}(0) &= \mathbf{0} && (6.20)\\
\mathbf{K}(T_s^n) &= \theta^{-1}\mathbf{M}(T_s^{n-1})\mathbf{V}(T_s^n) \\
&\quad \left[\mathbf{I} + \theta^{-1}\mathbf{V}^T(T_s^n)\mathbf{M}(T_s^{n-1})\mathbf{V}(T_s^n)\right]^{-1} && (6.21)\\
\mathbf{e}(T_s^n) &= \mathbf{d}(T_s^n) - \mathbf{R}(T_s^n)\mathbf{p}(T_s^{n-1}) && (6.22)\\
\mathbf{p}(T_s^n) &= \mathbf{p}(T_s^{n-1}) + \mathbf{K}(T_s^n)\mathbf{e}(T_s^n) && (6.23)\\
\mathbf{M}(T_s^n) &= \theta^{-1}\mathbf{M}(T_s^{n-1}) - \theta^{-1}\mathbf{K}(T_s^n)\mathbf{V}^T(T_s^n)\mathbf{M}(T_s^{n-1}) && (6.24)
\end{aligned}$$

The factor θ in equations (6.20) and (6.24) is a "forgetting factor" (typically $0.9 \leq \theta \leq 1.0$) that enables RLS-type algorithms to track the statistics of the input signals (filtered-reference signals in this case) if they are time varying. δ is a small positive constant [89].

In the MC-RLS presented there was no power constraint incorporated. Therefore after setting the filter coefficients we must scale the transmitted signal $s_p(n)$ with a factor $\sqrt{\mathcal{F}}$ to achieve the desired average total transmitted energy per symbol. An effort to use the rescaling MC-LMS principles in the MC-RLS by means of simulations resulted in an unstable algorithm.

Both the unconstrained MC-LMS and MC-RLS algorithms are derived from the unconstrained cost function J, presented in eq. (6.2). They try to converge adaptively to the unconstrained Wiener solution, as in eq. (5.17) for $\lambda = 0$. In other words, both algorithms compute recursively the value of the inverse of a time-averaged correlation matrix $[\mathbf{R}^T(T_s^n)\mathbf{R}(T_s^n)]$. However instability can occur if the correlation matrix is ill-conditioned. In multichannel systems, the ill-conditioning may be caused by some coupling between the different "channels" or between the difference reference signals, or simply by the finite numerical resolution. In MC-RLS this

[3]In [106] vector $\mathbf{p}$ is defined as $\mathbf{p} = [p_1(0)\ldots p_K(0)\ldots p_K(P-1)\ldots p_K(P-1)]$ and thus matrix $\mathbf{V}(n)$ has a different representation. The matrix content remains the same but the arrangement of the rows is different to conform with the $\mathbf{V}(n)$ definition.

is reflected as will be shown in Figure 6.10 by the fact that the average mean-squared-error during convergence doesn't level off, even when it achieves very small values. These potential problems can be avoided by adding a small amount of noise to the filtered-reference signals $r_{\mu\nu}(n)$. This causes a bias to the solution found by the RLS-based algorithms and slows down the convergence, but it improves the numerical stability of the algorithms.

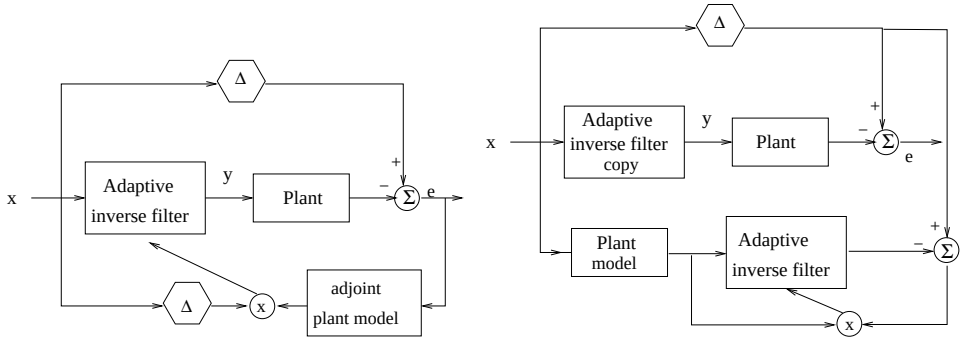

(a) Adjoint block diagram using filtered-X LMS algorithm

(b) Modified block diagram using filtered-X LMS algorithm

Figure 6.5: *Alternative MC techniques*

6.3.4 Alternative MC adaptive techniques

The multichannel LMS and RLS algorithms as described are not the only adaptive algorithms for multichannel/multiuser systems. In [124] a low computational alternative to the MC-LMS was introduced, named as *adjoint MC-LMS*. Instead of filtering the reference signals $d_k c_k(n)$ by filters $\hat{z}_k(n)$, as in Figure 6.4, it is the error signals $e_k(n)$ that are filtered by an adjoint (time reverse) version of the $\hat{z}_k(n)$, $\hat{z}'_k(n)$. In Figure 6.5(a) an illustration of a monochannel adjoint filtered-X LMS is given. The corresponding adjoint MC-RLS was introduced and described in [106]. Another version of the MC-LMS, called *modified MC-LMS*, is given in [125, 126]. The modified MC-LMS algorithm performs a commutation of the $\hat{z}_k(n)$ and the adaptive filters, so that that the adaptive filters try to predict the estimation of the $d_k(n)$ signals (instead of the original $d_k(n)$). The block diagram of a monochannel MC-LMS is depicted in Figure 6.5(b). Similarly to the modified MC-LMS the *modified MC-RLS*, was developed in [106]. Other known time domain feedforward adaptive algorithms for the multichannel/multiuser scheme are the multichannel filtered-X fast transerval-filter (FTF) with its modified and adjoint versions.

An elaborate explanation of these methods can be found in [106]. The reader can find more information, including theoretical analysis, about multichannel algorithms as applied in the stereophonic sound reproduction area in [105, 107–110, 118, 127]. In this thesis we apply MC-LMS, power constrained MC-LMS and MC-RLS in the scenario of CDMA-TDD to control the MAI and ISI, adaptively and before transmission. In the next sections the performance and the efficiency of these techniques is discussed.

6.4 Convergence speed

An important and essential characteristic of the adaptive algorithms is the convergence speed. The leakage MC-LMS algorithm used in the following simulations is the one with the time varying leakage coefficient $\lambda(T_s^n)$ as shown in eq. (6.14). The reason is that a constant leakage coefficient doesn't guarantee that after convergence the power will be consistent with the initial constraint. The propagation channels used in the following simulations correspond to the severe multipath profile channels given in table 2.3.

6.4.1 MC-LMS, leakage MC-LMS, rescaling MC-LMS

In Figure 6.6 we present the convergence of one user within a system of $K = 3$ users when the pre-filter length is $P = 16$. The mean-squared error versus iterations displayed is an ensemble averaging of 100 independent trials of the experiment. Two different step-size parameters μ have been chosen, and the algorithm applied is the MC-LMS. The same user is represented in both curves. As expected $\mu = 0.02$ results to a smaller mean-squared error compared to the case of $\mu = 0.1$ at the cost of slower convergence. The fact that no power constraint is included in MC-LMS leads to an increase in transmit power. In both schemes the scaling factor needed to normalise the power to $\mathcal{E}_g$ (power corresponds to classic CDMA transmission) after convergence is $\sqrt{\mathcal{F}} \simeq 0.6$, which negatively affects the BER performance at the receiver's output as we will see.

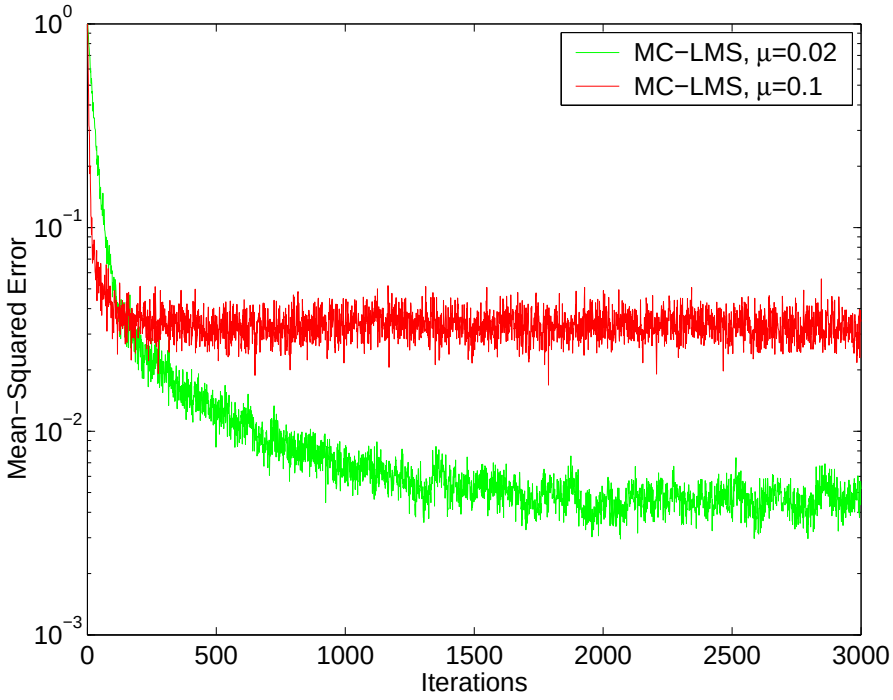

Figure 6.6: *Convergence speed with different μ parameter. Ensemble of 100 trials.* $Q = 16$, $K = 3$, $P = 16$.

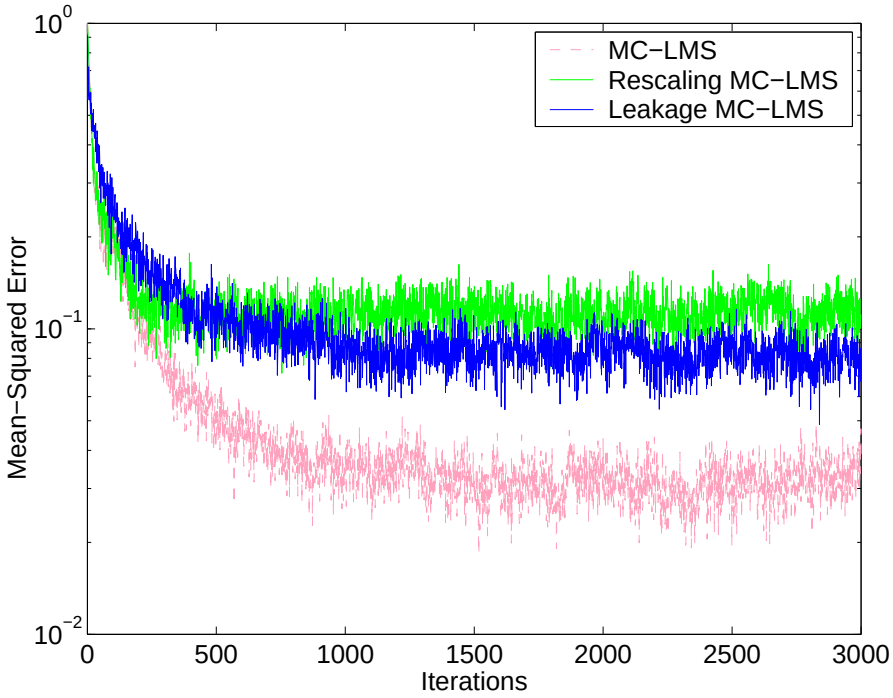

Figure 6.7: *Convergence speed comparison for $\mu = 0.02$. Ensemble of 100 trials.* $Q = 16$, $K = 3$, $P = 16$, $\mu = 0.02$.

In Figure 6.7 the convergence speed of the MC-LMS, leakage MC-LMS and rescaling MC-LMS is compared. Again a system of $K = 3$ users with $P = 16$ taps is under consideration. The same step-size parameter $\mu = 0.02$ is used for all algorithms and the same user is picked up for our analysis. For leakage MC-LMS and rescaling MC-LMS the average total power per symbol E_g, after convergence, is as desired ($\mathcal{E}_g = 3$, for 3 users with $\|\mathbf{c}_k\|^2 = 1$), which makes the scaling factor necessary ($\sqrt{\mathcal{F}} = 1.0$). A scaling factor of $\sqrt{\mathcal{F}} \simeq 0.6$ is required for the MC-LMS. From the curves we observe that the least mean-squared error achieved by the unconstrained MC-LMS which is expected as the tap coefficients can take any value in order to reduce MAI and ISI, due to the lack of restrictions. The rescaling MC-LMS achieves the fastest convergence of all but the worst mean-squared error. From a simple observation on the qcurves it is easy to be misled to the conclusion that MC-LMS may display the best performance due to the smallest mean-squared error. However, it will be shown later that this is not true, under the requirement that all methods are normalised to transmit the same average power per symbol.

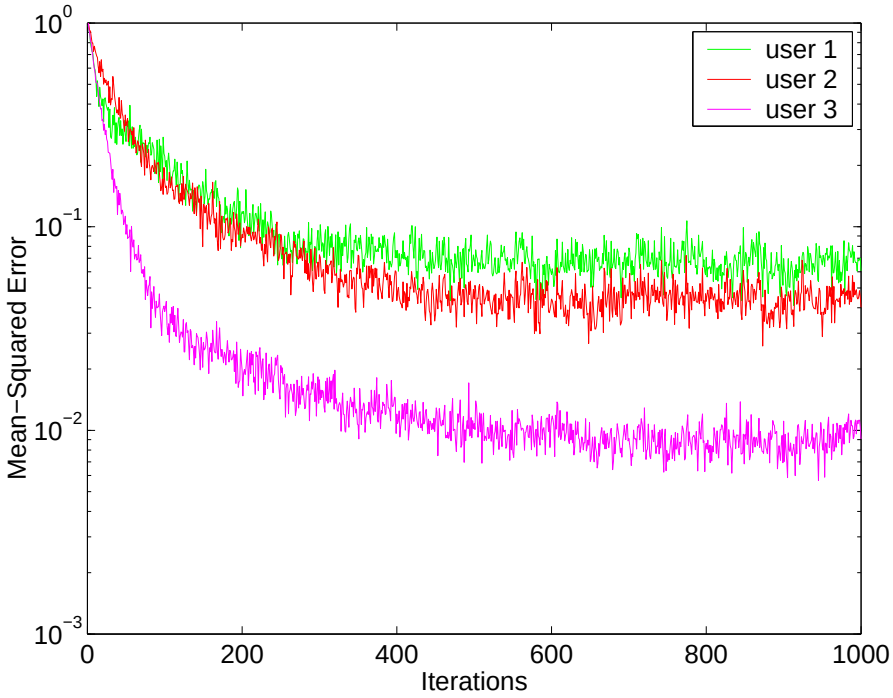

Figure 6.8: *Mean-squared error among all users. MC-LMS. $K = 3$, $P = 32$*

In Figures 6.8 and 6.9 the mean-squared error versus iterations is given for all 3 users for MC-LMS and leakage MC-LMS algorithms respectively. An ensemble averaging of 100 independent trials is shown by the graphs. The same spreading codes are used for both graphs, a filter length $P = 32$ has been chosen and the step-size parameter is set to $\mu = 0.02$. We

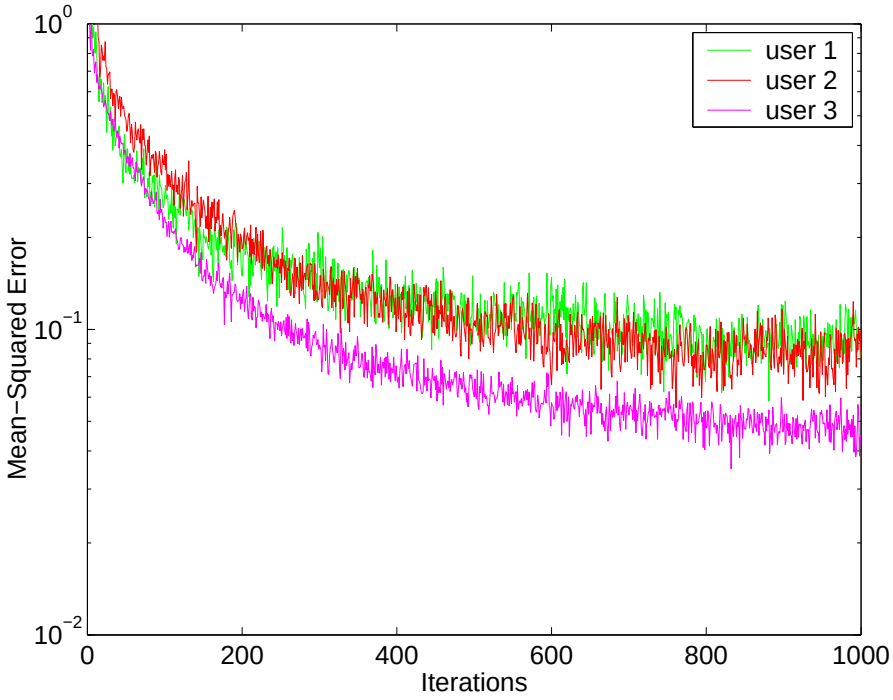

Figure 6.9: *Mean-squared error among all users. Leakage MC-LMS.* $K = 3$, $P = 32$

note that MC-LMS results in intensified differences among user's converged mean-squared error compared with the leakage MC-LMS. The MC-LMS converges to tap-weights that increase the transmitted power to a level that a scaling factor of $\sqrt{\mathcal{F}} \simeq 0.7$ is needed to normalise it. We compare now the curves that corresponds to MC-LMS-$\mu = 0.02$-$P = 16$ in Figure 6.6 and the ones of 6.8 for MC-LMS-$\mu = 0.02$-$P = 32$. In these two graphs the same set of spreading codes has been used and the same $\mu = 0.02$. For $P = 32$ we have a faster convergence at the cost of deteriorated mean-squared error, which is often true for adaptive filters which are unable to keep up.

6.4.2 MC-RLS

The parameters to be selected in the MC-RLS algorithm, described in equations (6.19) to (6.24), are the forgetting factor θ and δ, which initialise matrix $\mathbf{M}(0)$. In what follows the forgetting factor is consistently set to $\theta = 1$.

In Figure 6.10 we examine the mean-squared error versus the number of iterations for a various values of δ for one of the system's user. The curve shown is an ensemble averaging of 50 independent examples. The system considered is one of $K = 3$ users and pre-filter length

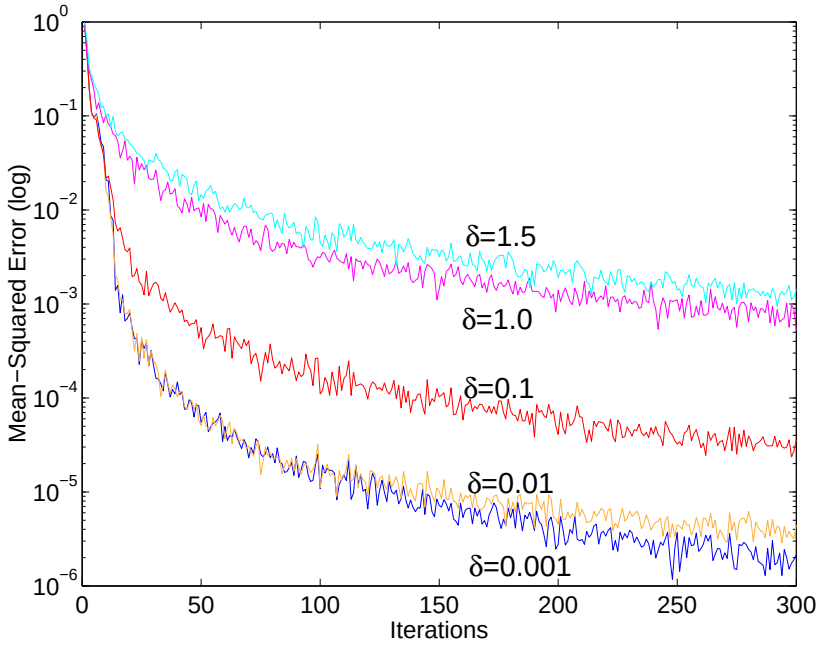

Figure 6.10: *Convergence speed.*

$P = 16$. For a small $\delta \sim 10^{-2}$ the mean-squared error reaches values of 10^{-4} order within a few iterations (less than 50). As δ increases (up to 1.5) convergence is slowing down and after 50 iterations the mean-squared error reaches an order 10^{-2}. The same pattern of curves is followed by the other two users. For all schemes, convergence speed outperforms by far the MC-LMS with or without power constraints which is expected. This occurs at the cost of excess computational cost compared with the MC-LMS. In Figure 6.10 it is also shown that despite the very low average values that the mean-squared error can reach, it doesn't level off but carries on reducing. This is due to the very high eigenvalue ratio (nearly singular) of matrix $\mathbf{R}^T(T_s^n)\mathbf{R}(T_s^n)$ as explained in section 6.3.3.

MC-RLS, as presented in section 6.3.3, doesn't incorporate any power constraints. Therefore it is important to investigate the evolution of the average total energy per symbol E_g as the convergence proceeds. In Figure 6.11 E_g is displayed versus iterations as MC-RLS is proceeding for a variety of δ values. The same training sequence is used for all curves. The system considered is the same with the one given for Figure 6.10. Given that $\|\mathbf{c}_k\|^2 = 1$, the desired energy of a conventional CDMA system is $\mathcal{E}_g = 3$. The graph shows that for small values of δ after only a few iterations E_g exceeds the desired levels and stabilises there. As δ increases the unscaled transmitted power E_g starts from levels close to $\mathcal{E}_g$ and slowly increases with the iterations. It is clear that in every case a scaling factor $\sqrt{\mathcal{F}} \leq 1.0$ is needed before final trans-

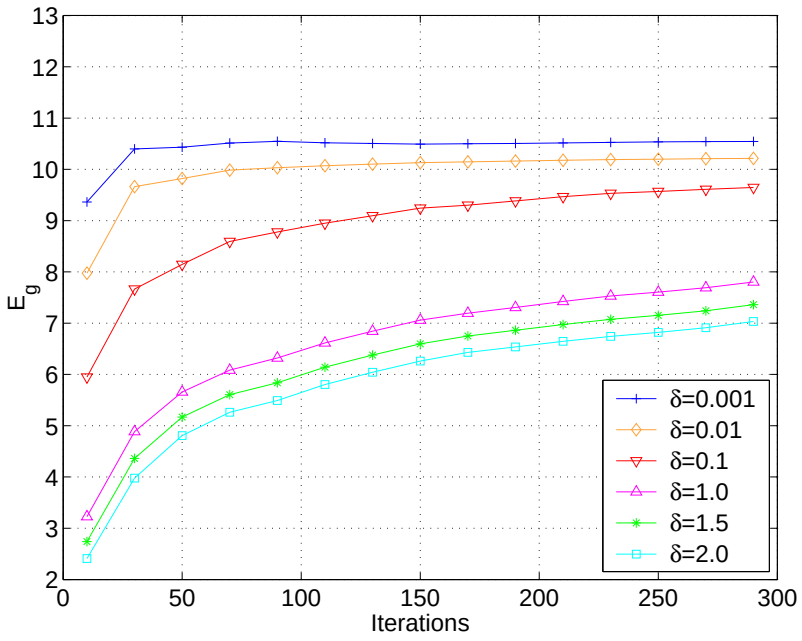

Figure 6.11: *MC-RLS.* $K = 3$, $P = 16$

mission to the users. The value of $\sqrt{\mathcal{F}}$ is critical as it results in a decrease of the SNR at the receivers outputs and it is obvious by Figure 6.11 that it is affected by two factors. These factors are the δ parameter and the time the convergence process is ceased and the pre-filter weights are locked. The question raises as to what value is the best choice. On one hand small δ may raise excessively the transmitted power but it achieves a very small mean-squared error after only a few iterations and on the other higher values of δ do not give an unreasonable boost to the transmitted power at the cost of increasing the mean-squared error, as shown in Figure 6.10.

To answer the question the following experiment was realised. For a particular δ value MC-RLS algorithm was run for 300 iterations and every 10 iterations the tap-weights were locked. The average total transmitted energy E_g per symbol is calculated and the appropriate scaling factor is used to normalise the power to $\mathcal{E}_g$. Then, transmission to the users for the scenario of $E_b/N_o = 10$dB occurred by means of Monte Carlo simulations. Hence, the system's BER could be evaluated. The same experiment was repeated for different values of δ and the same training sequence was always used for fair comparison. The results are illustrated in Figure 6.12. It is shown that for a $\delta \simeq 1.0$ the best BER is achieved after 50 iterations. For more than 50 iterations the BER is deteriorated as the transmitted energy is increased and $\sqrt{\mathcal{F}}$ plays a critical role. However, the deterioration is not severe (we can consider the performance versus iterations flat) and this gives a flexibility to the number of iterations selected. It is important,

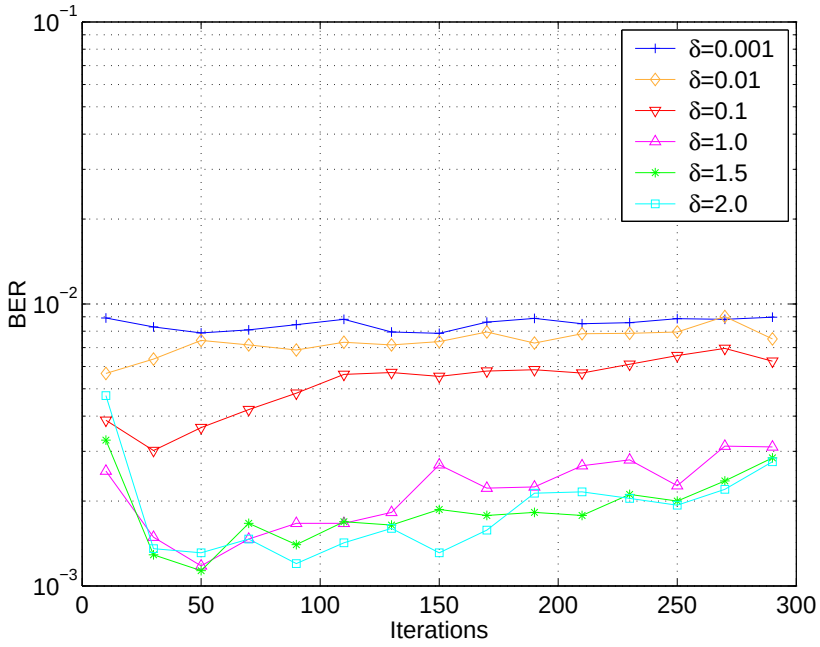

Figure 6.12: *MC-RLS.* $K = 3$, $P = 16$

though to let an initial minimum number of iterations to allow for the algorithm to converge to a sufficient mean-squared error as shown in Figure 6.10.

After 50 iterations, when the best BER performance occurred for $\delta = 1.0$ the mean-squared error for our 3-users system, with $P = 16$, was of order 10^{-2}. The same conclusions were drawn for a system of $K = 5$ users and $P = 32$. Therefore, we define as sufficient mean-squared error value for MC-RLS the 10^{-2} and as minimum number of iterations the number of iterations required to achieve this level of mean-squared error.

6.4.3 UMTS-TDD block sizes

In a UMTS TDD system downlink with spreading code $Q = 8$ each slot can be a vector of 320 symbols per slot ($0.66msec$). That gives sufficient time for the MC-RLS algorithm to converge to the desired tap-coeffiecients.

6.5 BER performance-Simulation results

In this section the BER versus E_b/N_o after the tap-weights of the pre-filters have been adaptively determined is discussed. The results are produced by means of Monte Carlo simulations.

The effect of the choice of parameters used in the algorithms is also examined. The basic assumptions for the simulations are the ones presented in section 2.5.1. All users are transmitted through the severe multipath profile channels as given in table 2.3.

6.5.1 MC-LMS, leakage MC-LMS, rescaling MC-LMS

In Figure 6.13 the system's average BER is shown against E_b/N_o. The simulated system is one of $K = 3$ users with pre-filter length set to $P = 16$. For all the adaptive algorithms the same step-size parameter $\mu = 0.02$ has been selected and the same training sequence. Convergence is stopped after 400 iterations. For the leakage MC-LMS algorithm the time varying leakage coefficient $\lambda(T_s^n)$ is used. It is shown that the leakage MC-LMS outperforms the rescaling and the unconstrained MC-LMS. This is in contrast with Figure 6.7 where the leakage LMS converges to a larger mean-squared error than the unconstrained MC-LMS. The explanation is that the leakage MC-LMS converges to tap weights that do not increase the transmitted power above the allowed level. Thus, no scaling factor is required afterwards. On the other hand, MC-LMS increases the E_g in order to achieve better cancellation of MAI and ISI and consequently a scaling factor $\sqrt{\mathcal{F}} \leq 1.0$ is necessary. Hence, the final BER performance is deteriorated. Equivalent observations can be made for a system of 5 users and pre-filters length set to $P = 32$, as illustrated in Figure 6.14.

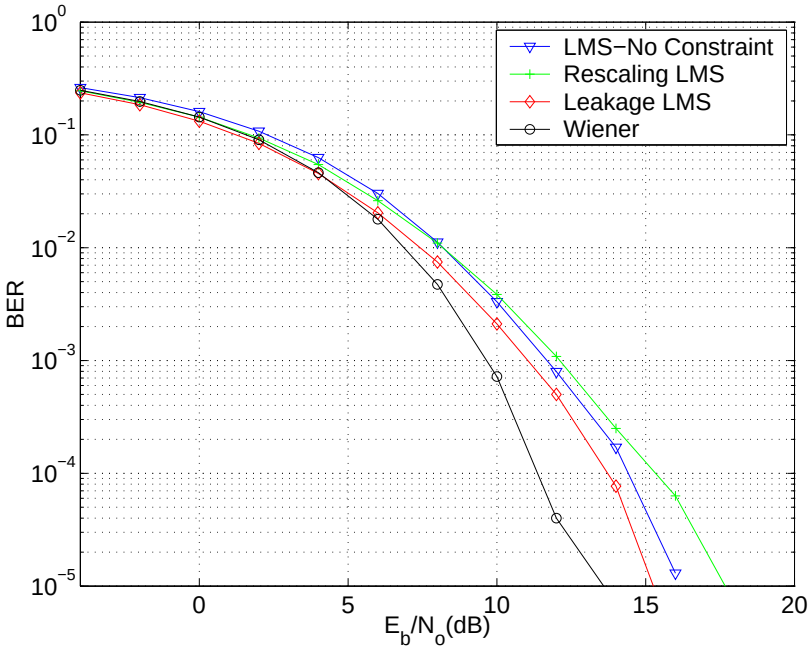

Figure 6.13: *BER versus E_b/N_o. $K = 3$, $P = 16$, $\mu = 0.02$, 400 iterations.*

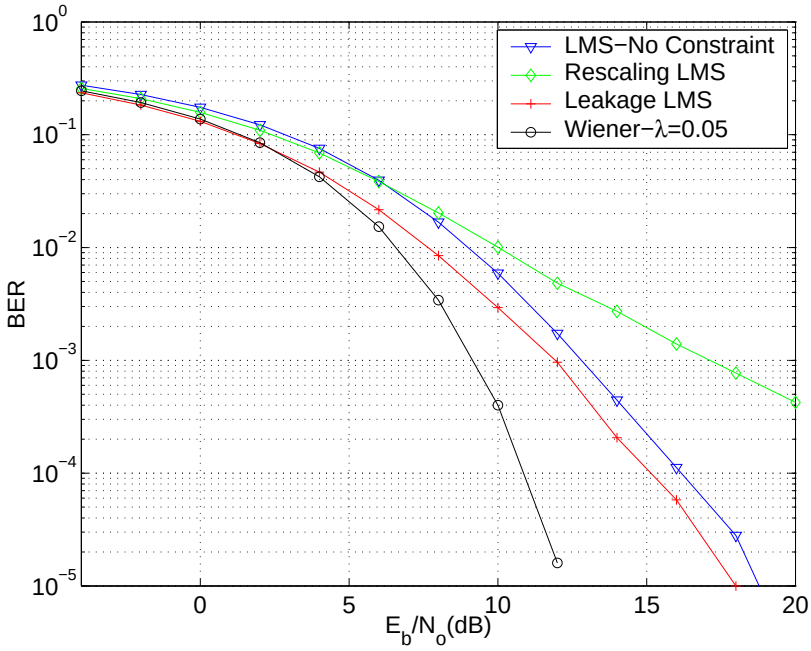

Figure 6.14: *BER versus* E_b/N_o. $K = 5$, $P = 32$, $\mu = 0.005$, *1500 iterations.*

6.5.2 MC-RLS

The next two figures illustrate the BER versus E_b/N_o when the multichannel adaptive algorithm implemented is the MC-RLS. The results are shown for different values of the δ parameter, while the forgeting factor is consistently set to $\theta = 1.0$. The curves are in consistency with the results in Figure 6.12. Figure 6.15 shows a system of $K = 3$ users and $P = 16$. For $\delta \simeq 1.0$ the BER curve is very close to the Wiener solution as given for the INVF in section 5.4. Parameter λ for Wiener solution is set to 0.05. As δ gets smaller the performance is getting worse. The same observations are valid for Figure 6.16, where the system chosen is one of $K = 5$ users and $P = 32$ pre-filters length. The MC-RLS doesn't reach the Wiener solution as the initial cost function from which the two techniques are derived is essentially different. Wiener solution incorporates a power constraint term while MC-RLS does not. The scaling factor is used instead. MC-RLS algorithm was let to run for 50 and 70 iterations for the system of 3 and 5 users respectively.

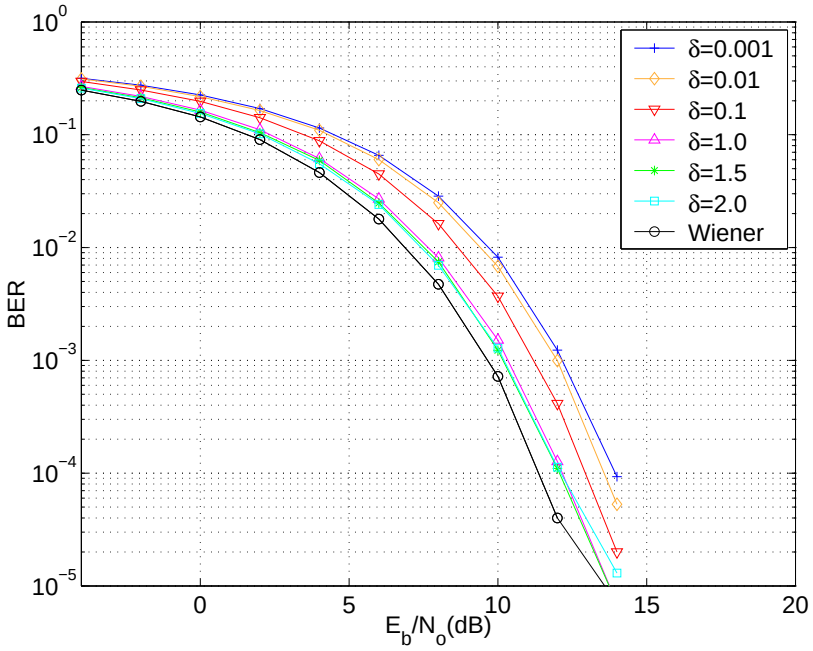

Figure 6.15: *BER vs E_b/N_o for MC-RLS. $K = 3$, $P = 16$. $\theta = 1.0$, $\lambda = 0.05$ for INVF.*

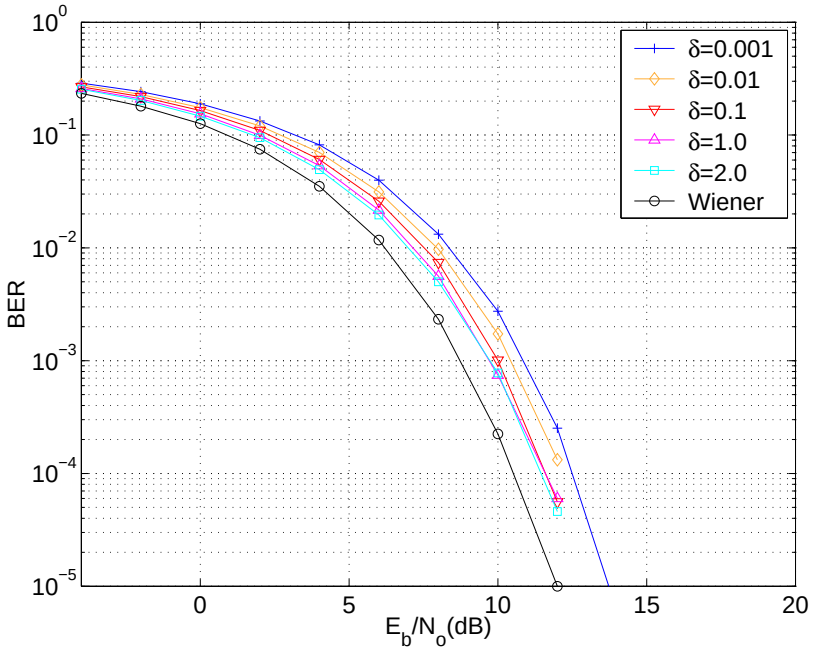

Figure 6.16: *BER vs E_b/N_o for MC-RLS. $K = 5$, $P = 32$. $\theta = 1.0$, $\lambda = 0.05$ for INVF.*

6.5.3 Comparison-Discussion

In Figure 6.17 the bit error rate performance of a $K = 5$ users system is displayed versus the length of the pre-filters for DPF, INVF, leakage MC-LMS and MC-RLS techniques. The E_b/N_o is set to 10dB and $\Delta = P/2$. Step-size parameter for leakage MC-LMS is set as $\mu = 0.005$ and for MC-RLS $\theta = 1.0$ and $\delta = 1.0$. Tap-coefficients for the adaptive algorithms are locked after 1500 iterations for MC-LMS and 50 for MC-RLS. The MC-RLS, for $\theta = 1.0$, and leakage MC-LMS, for $\mu = 0.005$ display far better performance than the DPF, whose taps are determined according to [78]. Wiener solution, leakage MC-LMS and MC-RLS display similar performance for small P. However, as the pre-filter length is increased the difference in performance becomes distinguished with MC-RLS outperforming constistently the leakage MC-LMC. As expected the best performance is associated with the Wiener solution. We recall, at this point that MC-RLS doesn't overlap with the Wiener solution because they originate from different cost functions. Furthermore, INVF and adaptive algorithms allow for an arbitrary selection of P while DPF restricts the pre filters to a length of $P \leq \Delta + Q$.

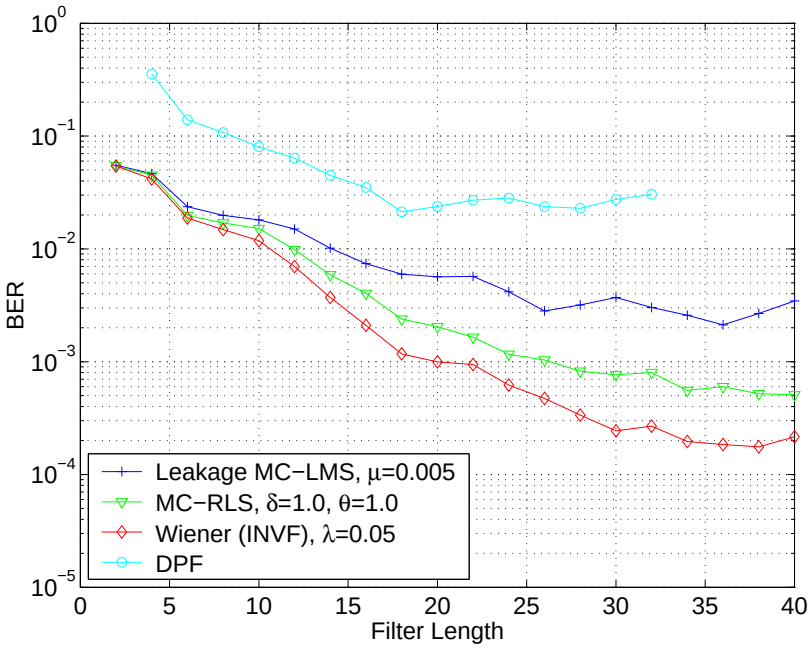

Figure 6.17: *BER versus Filter Length for $E_b/N_o = 10$dB, $K = 5$ users*

In Figure 6.18 the BER performance versus E_b/N_o is displayed for $K = 5$ users CDMA system with DPF, Pre-RAKE, JT, INVF and feedforward adaptive precoding techniques. The set of spreading codes is different from the one used in the previous figures. The pre-filter

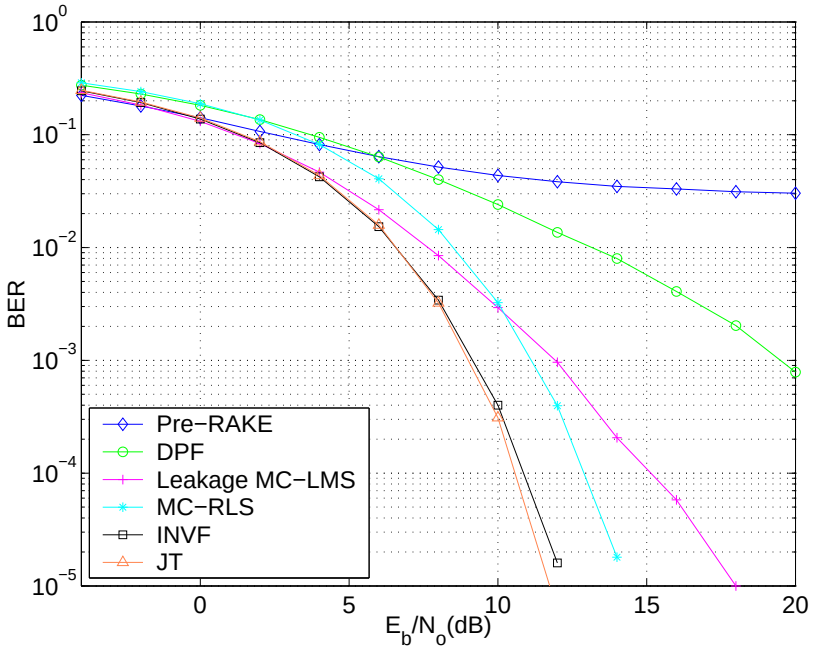

Figure 6.18: *BER versus* E_b/N_o, $K = 5$ *users*

taps have a length of $P = 32$ chips and the delay Δ imposed in the system is 16 chips. Both MC-RLS and leakage MC-LMS outperform pre-RAKE, DPF techniques. Leakage MC-LMS outperforms MC-RLS for low E_b/N_o because the noise is the dominant interference and the power constraint is very critical. On the contrary, when E_b/N_o is high the major interference is MAI and ISI and MC-RLS copes better as it converges fast to a very low mean-squared error. The INVF and the JT have almost the same performance and outperform all the others.

6.6 Summary

In this Chapter adaptive techniques were proposed for the determination of the pre-filters in the bitwise precoding approach. The crucial idea was that the BS can emulate the actual system in a cell, due to knowledge of downlink channels and the receivers structure, in an internal block. The errors at the output of the receivers are used by the adaptive algorithms in order to calculate the pre-filters tap-weights. Multichannel LMS and RLS feedforward adaptive algorithms were studied from the sound and stereo-phonics reproduction systems. They are an extension of the monochannel filtered-X LMS technique for active noise control introduced in [111]. Certain modifications to versions of the power constraint filtered-X LMS had to be done to apply them to our multiuser/multichannel CDMA system. The algorithms derived were the

adaptive leakage and the rescaling MC-LMS. The leakage MC-LMS appears to display the best performance, in terms of BER, among the LMS algorithms as shown by means of Monte Carlo simulations. MC-RLS is the one that approaches the Wiener solution and outperforms any other MC adaptive technique. MC-LMS exhibits a slow convergence speed compared with MC-RLS but the computational cost is significantly reduced. MC-RLS only needs a few iterations to converge to a sufficient mean-squared error, e.g. 50 iterations for $P = 32$. Adaptive techniques have the advantage of excluding completely matrix inversion (MC-LMS with or without power constraint) or reducing the dimension of the matrices needed to be inverted (MC-RLS).

Chapter 7
Summary - Conclusions

The aim of the work presented in this thesis was to simplify the user equipment in a DS-CDMA system by removing the MUD techniques and implementing linear precoding of the signal prior transmission. This final Chapter summarises in section 7.1 the main topics and conclusions contained within this thesis. Finally, section 7.2 presents the limitations of this work and proposes areas that this work can be extended to.

7.1 Summary and thesis contributions

The lack of orthogonality among the users' spreading codes in a DS-CDMA poses limitations on the system due to the presence of multiple access interference. However, in 3G cellular systems limitations should be minimised as much as possible due to the requirement for high quality and demanding services. Numerous multiuser detection techniques have been proposed and applied that mitigate the MAI and ISI and restore sufficiently the transmitted signal, de-coupling the multiplexed users. MUD algorithms often have high computational cost, require channel estimation and presume that the spreading codes of all active users are known to the receiver. All these requirements are easy to satisfy at the BS where the resources are readily available but not at the mobile terminal, where size, power consumption, weight, and hardware are of great concern and are often limited. Hence, MUD techniques are very successful when applied on the BS for the reverse link, but they can't be implemented on the mobile terminals for the forward link so easily. This gave birth to the idea of precoding (pre-distorting) the signal to be transmitted in such a way that the MAI and ISI are reduced if not completely cancelled prior to transmission. The receiver structure at the user equipment is then simplified when compared to a multiuser detection receiver, and can be a conventional matched filter (which only requires knowledge of the desired user's spreading code). Thus no channel estimation or adaptive equaliser is required at the mobile receiver. Techniques which only require a matched filter receiver also enhance the downlink system capacity since no system resources have to be allocated for the transmission of training signals on the downlink. The basic assumption

for achieving a correct precoding is base station knowledge of the downlink channel. This is feasible in a TDD scheme if the time elapsing between uplink and downlink transmissions is small compared to the coherence time of the mobile radio channel. Then, the downlink channel is highly correlated with the uplink one and it can be estimated by the uplink burst. These conditions may be valid for the WCDMA-TDD mode (air interface for the 3G) in a personal communication system with low mobility users such as pedestrians in an outdoor environment or in a wireless local area network. Throughout this work the channels are assumed to be stationary during transmission without variations.

In Chapter 2 the discrete-time model and the vector-matrix description of a CDMA downlink system was derived. A few air interface structure characteristics were briefly described to give an idea of the complexity that a modern cellular communications system has. The conventional RAKE receiver was described and it was explained that its inability to use multiuser information is responsible for its poor performance. Algorithms that perform a joint detection and utilise the cross-correlation of the spreading codes should be employed instead. Such algorithms are called multiuser detection algorithms and can be linear, non-linear, optimal or suboptimal. The ZF-JD and MMSE-JD linear multiuser detection techniques are described along with a discussion on their complexity and requirements. It is shown that they are too demanding to be applied on a mobile terminal for many applications and hence, the need for precoding techniques emerges.

The motivation and the scheme under which a linear precoding technique can give the desired results are given in Chapter 3. The theoretical BER performance of any linear precoding technique that assumes a simple matched filter or a RAKE receiver is analytically calculated. The SNIR spread is introduced as a metric to measure the differences in performance among different users under the condition that signals of equal power are addressed to each one of them. Ideal values for the SNIR spread are close to unity. The linear precoding techniques are classified, according to their realisation, to bitwise and blockwise. The former's implementation is by individually filtering the spread data before transmission and the later is by applying a transformation matrix on a block of data prior to transmission. Bitwise techniques display a lighter computational cost than the blockwise ones in addition to the fact that they are easier to apply to an existing system. Furthermore the end block-bits in the blockwise schemes are not correctly precoded in the case of a multipath environment. An important conclusion of Chapter 3 was that the optimum precoding technique is one that minimises the MAI and ISI and max-

imises the scaling factor $\sqrt{F}$, which is used to scale and normalise the transmitted power. That conclusion implies the use of a power constraint.

In Chapter 4 the state of the art for the linear precoding techniques is given. The most representative and popular blockwise and bitwise techniques are used as reference. Bitwise pre-RAKE method includes pre-RAKE diversity combining at the transmitter. Although the pre-RAKE method reduces the multipath channel effects, it unfortunately doesn't reduce the multiuser interference. One alternative transmitter based multiuser detection is TP. Nevertheless this technique does not adequately deal with the issue of constrained transmission power resulting in poor noise performance and requires a RAKE receiver for reasonable performance. Another recently published transmitter precoding technique is JT, according to which a common transmit signal for all users is determined in the base station. DPF is a bitwise algorithm and the tap-coefficients of the pre-filters are calculated using zero forcing without power constraint which tends to increase the transmitted power. In the BER performance comparison that follows it is shown that the blockwise JT and TP outperform the bitwise DPF and pre-RAKE at the cost of complexity. That conclusion triggers the idea of further research on the bitwise techniques.

A new bitwise technique that uses an MMSE approach with the necessary power constraint incorporated is introduced in Chapter 5. The method originates from the unconstrained inverse filters applied for active noise control in stereophonic sound reproduction. It is appropriately modified for application in a CDMA system. The Wiener solution for the filter-taps is calculated in a closed form. The power constraint is included using the Lagrange multiplier λ. Small values for λ result in sufficient cancellation of MAI and ISI but over-increase the transmitted power. On the other hand, large values do control the power but increase the SNIR spread. A numerical solution along with an empirical solution is proposed for the value of the parameter λ. The performance of INVF, in terms of BER, is demonstrated and compared with the state of the art techniques from the previous Chapter. The simulation results are in remarkable agreement with the analytical ones as developed in Chapter 3. INVF outperforms DPF, TP-MAT and TP-RAKE. INVF also outperforms JT for heavily loaded systems, while the methods are competitive when $K \leq Q/2$ for sufficiently large data-block length. However, INVF requires significantly less computational cost than JT.

All the techniques, apart from the pre-RAKE, that were mentioned till now require the inversion of matrices for the tap-coefficients calculation, which implies large complexity. In Chapter

6 adaptive multichannel feed-forward algorithms are applied at the transmitter of a CDMA system. The algorithms are an extension of the well known single-channel filtered-X method for noise control. MC-LMS, MC-RLS are implemented and the results are discussed. Certain modifications to versions of power constrained filtered-X LMS had to be made to apply them to our multiuser/multichannel CDMA system. The algorithms derived were the adaptive leakage and rescaling MC-LMS. MC-RLS is the one that approaches the Wiener solution and outperforms any other MC adaptive techniques. MC-LMS exhibits a slow convergence speed compared with MC-RLS but the computational cost is significantly reduced. Adaptive techniques have the advantage of excluding completely matrix inversion (MC-LMS with or without power constraint) or reducing the dimensions of the matrices that need to be inverted (MC-RLS).

7.2 Limitations of the work and scope for further research

7.2.1 Time varying channels

Throughout this thesis we assumed that the transmitter (BS) has a perfect knowledge of the downlink channel due to reciprocity. In the reciprocity method we use the fact that the transmit and receiver channels are at the same frequency and at the same time are identical according to the principle of reciprocity [128]. In TDD systems receive and transmit are separated in time but not in frequency. In principle we can then rely on the reciprocity and use the estimates of the uplink channel as estimates of the downlink channel. However, for time varying channels the reciprocity will only be valid if the duplexing time is much shorter than the coherence time. The accuracy of the transmit channel estimation depends on the channel characteristics. Doppler spread induced by the motion of subscribers or scatterers has a strong influence on time processing algorithms. The Doppler spread is large in macro-cells which serve high mobility subscribers and it increases with higher operating frequencies. Doppler spread is also present in low mobility (microcell) or fixed wireless networks due to mobility of scatterers.

Thus, in real systems perfect knowledge of the downlink channel is realistic under certain conditions only. It is important to examine the precoding algorithms for time varying channels and investigate for what Doppler frequencies they can still give sufficient results and when do they collapse.

7.2.2 Channel estimation

Another interesting topic is to combine the precoding algorithms with the channel estimation algorithms needed to estimate the uplink channel. In the bibliography there are plenty of channel estimation algorithms for the uplink CDMA system.

7.2.3 Space-time techniques

One more open issue concerning the work done in this thesis is the ultility of multiple antennas. With multiple antennas, received and transmitted signals can be separated not only with temporal processing but also with spatial processing. The combination of spatial and temporal processing is called *space-time processing*. Space-time processing is a tool for improving the overall efficiency of a digital cellular radio system by exploiting the use of multiple antennas. Space time processing improves the signal to interference ratio through co-channel interference cancellation, mitigates fading through improved receive diversity, offers higher signal to noise ratio through array gain and reduces intersymbol interference through spatial equalisation. These improvements can have a significant impact on the overall performance of a wireless network.

Space-time processing using multiple antennas can be applied at the base station, the subscriber unit or at both locations. The differences in propagation environment, physical limitations and cost constraints result in different choices of type and number of antennas. Base stations can employ multiple antenna elements more easily because the size and cost constraints are less restrictive. Figure 7.1 shows how INVF is modified for the case of a two-element antenna on the BS and a single-element one on each mobile. Obviously, the number of pre-filters now has doubled and the computational cost for calculating the tap-coefficients is expected to be increased.

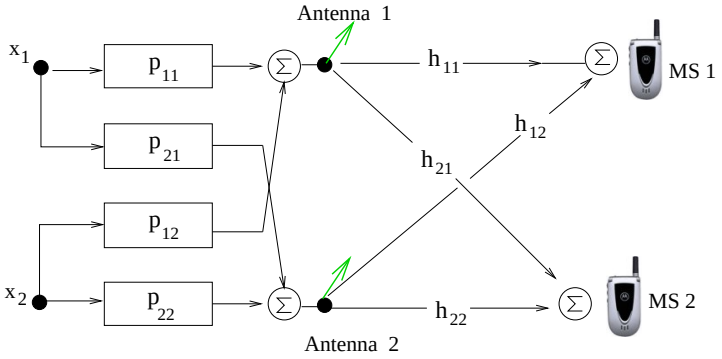

Figure 7.1: *Space-time INVF extension*

References

[1] W.H. Press, S.A. Teukolsky, W.T. Vetterling, and B.P. Flannery, *Numerical Recipes in C, The Art of Scientific Computing*, Cambridge University Press, second edition, 1992.

[2] T. Ojanpera and R. Prasad, *WCDMA, Towards IP Mobility and Mobile Internet*, Personal Communications Series. Artech House Publishers, 2001.

[3] W.W. Erdman, "A decade of progress," *IEEE Commun. Mag.*, vol. 31, pp. 48–51, Dec. 1993.

[4] J.E. Padgett, C.G. Gunther, and T. Hattori, "Overview of wireless personal communications," *IEEE Commun. Mag.*, vol. 33, pp. 28–41, Jan. 1995.

[5] Lal Chand Godara, *Handbook of Antennas in Wireless Communications*, CRC Press, 2002.

[6] D.J. Goodman, "Second generation wireless information networks," *IEEE Trans. on Veh. Technol.*, vol. 40, pp. 366–374, 1991.

[7] L.C. Godara, M.J. Ryan, and N. Padovan, "Third generation mobile communication systems: overview and modelling considerations," *Annals of Telecommunications*, vol. 54, no. 1-2, pp. 114–136, 1999.

[8] B. Sklar, "Rayleigh fading channels in mobile digital communication systems part I:characterization," *IEEE Commun. Mag.*, pp. 90–100, Jul. 1997.

[9] B. Sklar, "Rayleigh fading channels in mobile digital communication systems part II: Mitigation," *IEEE Commun. Mag.*, pp. 102–109, Jul. 1997.

[10] R. Ertel, P. Cardiery, K.W. Sowerby, T.S. Rappaport, and J.H. Reed, "Overview of spatial channel models for antenna array communication systems," *IEEE Personal Communications*, pp. 114–136, Feb. 1998.

[11] John G. Proakis, *Digital Communications*, Electrical Engineering. McGraw-Hill, 3rd edition, 1995.

[12] A. Paulraj and C.B. Papadias, "Space-time processing for wireless communications," *IEEE Signal Processing Mag.*, pp. 49–83, Nov. 1997.

[13] R.C. Dixon, *Spread Spectrum*, John Wiley & Sons, 1976.

[14] W.C.Y. Lee, "Overview of cellular CDMA," *IEEE Trans. on Veh. Technol.*, vol. 40, no. 2, pp. 291–301, May 1991.

[15] K.S. Gilhousen, I.M. Jacobs, L.A. Weaver R Padovani, A. Viterbi, and C.E. Wheatley, "On the capacity of a cellular CDMA system," *IEEE Trans. on Veh. Technol.*, vol. 40, no. 2, pp. 303– 312, May 1991.

[16] A.J. Viterbi, *CDMA: principles of spread spectrum communication*, Addison-Wesley, 1995.

[17] E. Nikula, A.Toskala, E. Dahlman, Girald L., and A. Klein, "FRAMES multiple access for umts and imt-2000," *IEEE Personal Communications*, pp. 16–24, Apr. 1998.

[18] "Multiplexing and Channel Coding (FDD)," *3GPP Technical Specifications 25.212*.

[19] "Spreading and Modulation (FDD)," *3GPP Technical Specifications 25.213*.

[20] "Physical Layer Procedures (FDD)," *3GPP Technical Specifications 25.214*.

[21] "Physical Layer Measurements (FDD)," *3GPP Technical Specifications 25.215*.

[22] T. Ojanpera and R. Prasad, *WCDMA: Towards IP Mobility and Mobile Internet*, Artech House, 2000.

[23] J. Laiho, A. Wacker, and T. Novosad, *Radio Network Planning and Optimization for UMTS*, John Wiley and Sons Ltd, 2001.

[24] Harri Holma and Antti Toskala, *WCDMA for UMTS: Radio Access for Third Generation Mobile Communications*, John Wiley and Sons Ltd, 2002.

[25] Z. Zvonar and D. Brady, "On multiuser detection in asynchronous CDMA flat Rayleigh fading channels," *Personal, Indoor and Mobile Radio Communications 1992, PIMRC '92*, pp. 123–127, 1992.

[26] S. Verdú, "Minimum probabilty of error for asynchronous gaussian multiple access channels," *IEEE Trans. on Inform. Theory*, vol. IT-32, no. 1, pp. 85–96, Jan. 1986.

[27] Z. Zvoran and D. Brady, "Suboptimum multiuser detector for synchronous CDMA frequency-selective Rayleigh fading channels," *Proc. Global Telecommunications Conference, Communication Theory Mini-Conference*, pp. 82–86, Dec. 1992.

[28] A. Klein, *Multi-user detection of CDMA signals-algorithms and their application to cellular mobile radio*, Fortschritt-Berichte VDI, 1996.

[29] "Selection procedures for the choice of radio transmission technologies of the UMTS (UMTS 30.03 version 3.2.0)," .

[30] Recommendation ITU-R M.687, *Future Public Land Mobile Telecommunication Systems (FPLMST)*, 1998.

[31] Recommendation ITU-R M.1034, *Requirements for the radio interface(s) for Future Public Land Mobile Telecommunication Systems (FPLMTS)*, 1998.

[32] ETSI ETR 291, "Systems requirements for the UMTS," Tech. Rep., ETSI, May 1996.

[33] ETSI UMTS 21.01, "Requirements for the UMTS terrestial radio access system (UTRA)," Tech. Rep., ETSI, May 1997.

[34] Recommendation ITU-R M.1035, *Framework for the radio interface(s) and radio sub-system functionality for Future Public Land Mobile Telecommunication Systems (FPLMTS)*, 1998.

[35] K.G. Beauchamp, *Walsh Functions and their Applications*, London: Academic Press, 1975.

[36] R.L. Pickholtz, D.L. Schilling, and L.B. Milstein, "Theory of Spread-Spectrum Communications—A Tutorial"," *IEEE Trans. Commun.*, vol. 30, no. 5, pp. 855–884, May 1982.

[37] R.L. Pickholtz, L.B. Milstein, and D.L. Schilling, "Spread spectrum for mobile communications," *IEEE Trans. on Veh. Technol.*, vol. 40, no. 2, pp. 313–321, May 1991.

[38] M.K. Simon, J.K. Omura, R.A. Scholtz, and B.K. Levitt, *Spread Spectrum Communications Handbook*, New York: McGraw-Hill, revised edition, 1994.

[39] R.L. Peterson, R.E. Ziemer, and D.E. Borth, *Introduction to Spread Spectrum Communications*, Englewood Cliffs, NJ: Prentice Hall, 1995.

[40] K. Kärkkäinen, *Code Families and their Performance Measures for CDMA and Military Spread-Spectrum Systems*, Ph.D. thesis, Ph.D. Dissertation, University of Oulu, Finland, 1996.

[41] F. Adachi, M. Sawahashi, and K. Okawa, ," .

[42] S. Lin and J. Costello, *Error Control Coding: Fundamentals and Applications*, Englewood Cliffs, NJ: Prentice Hall, 1983.

[43] R.D. Cideciyan, E. Eleftheriou, and M. Rupf, "Concatenated Reed-Solomon/convolutional coding for data transmission in CDMA-based cellular systems," *IEEE Trans. Commun.*, vol. 45, no. 10, pp. 1291–1303, Oct. 1997.

[44] S. Benedetto, D. Divsalar, and J. Hagenauer, "Concatenated coding techniques and iterative decoding: Sailing toward channel capacity," *IEEE J. Select. Areas Commun.*, vol. 16, no. 2, Feb. 1998.

[45] ," *Proc. of International Symbosium on Turbo Codes and Related Topics, Brest, France*, Sep. 1997.

[46] P. Jung, J. Plechinger, M. Doetsch, and F. Berens, "Pragmatic approach to rate compatible punctured turbo-codes for mobile radio applications," *Proc. in 6th International Conference on Advances in Communications and Control: Telecommunications/Signal Processing,Corfu*, pp. 23–27, Jun. 1997.

[47] C. Berrou, A. Glavieux, and P. Thitimajshima, "Near shannon limit error-correcting coding and decoding: Turbo codes," *IEEE International Conference on Communications, ICC'93, Geneva*, vol. 1, pp. 1064–1070, May 1993.

[48] J.M. Holtzman, *CDMA Power Control for Wireless Networks*, Norwell, MA:Kluwer, 1992.

[49] V.K. Garg, K. Smolic, and J.E. Wilkes, *Applications of Code-Division Multiple Access (CDMA) in Wireless/Personal Communications*, NJ:Prentice Hall, 1996.

[50] R. Price and P.E. Green, "A communication technique for the multipath channels," *Proceedings of the IRE*, vol. 46, pp. 555–569, Mar. 1958.

[51] G.L. Turin, "Introduction to spread-spectrum antimultipath techniques and their application to urban digital radio," *Proc. IEEE*, vol. 68, no. 3, pp. 328–353, Mar. 1980.

[52] S. Moshavi and Bellcore, "Multi-user detection for ds-CDMA communications," *IEEE Communications Magazine*, pp. 124–136, Oct. 1996.

[53] Z. Xie, R.T. Short, and C.K. Rushforth, "A family of suboptimum detectors for coherent multiuser communications," *IEEE J. Select. Areas Commun.*, vol. 8, no. 4, pp. 683–690, May 1990.

[54] A. Duel-Hallen, J.H., and Z. Zvonar, "Multiuser detection for CDMA systems," *IEEE Personal Communications*, vol. 2, no. 2, pp. 46–58, Apr. 1995.

[55] Sergio Verdú, *Multiuser Detection*, Cambridge University Press, 1 edition, 1998.

[56] H.V. Poor and S. Verdú, "Probability of error in MMSE multiuser detection," *IEEE Trans. on Inform. Theory*, vol. 43, no. 3, pp. 858–871, May 1997.

[57] R. Lupas and S. Verdu, "Linear multiuser detectors for synchronous code division multiple access channels," *IEEE Trans. on Inform. Theory*, vol. 35, no. 1, pp. 123–136, Jan. 1989.

[58] Z. Zvoran and D. Brady, "Multiuser detection in single-path fading channels," *IEEE Trans. Commun.*, vol. 42, no. 3, pp. 1729–1739, Mar. 1994.

[59] U. Madhow and M.L. Honig, "MMSE interference suppression for direct-sequence spread-spectrum CDMA," *IEEE Trans. Commun.*, vol. 42, no. 12, pp. 3178–3188, Dec. 1994.

[60] Z. Zvoran and D. Brady, "Suboptimal multiuser detector for frequency-selective Rayleigh fading synchronous CDMA channels," *IEEE Trans. Commun.*, vol. 43, no. 3, pp. 154–157, Mar. 1995.

[61] A. Klein, G.K. Kaleh, and P.W. Baier, "Zero forcing and minimum mean-square-error equalization for multiuser detection in code-division multiple-access channels," *IEEE Trans. on Veh. Technol.*, vol. 45, no. 2, pp. 276–286, May 1996.

[62] A. Klein and P.W. Baier, "Linear unbiased data estimation in mobile radio systems applying CDMA," *IEEE J. Select. Areas Commun.*, vol. 11, no. 7, pp. 1058–1066, Sep 1993.

[63] H.C. Huang and S.C. Schwartz, "A comparative analysis of linear multiuser detectors for fading multipath channels," *Proc. of the IEEE GLOBECOM Conf.*, pp. 11–15, 1994.

[64] Z. Zvonar and D. Brady, "Linear multipath-decorrelating receivers for CDMA frequency-selective fading channels," *IEEE Trans. Commun.*, vol. 44, no. 6, pp. 650–653, Jun. 1996.

[65] Z. Zvoran, "Combined multiuser detection and diversity reception for wireless CDMA systems," *IEEE Trans. on Veh. Technol.*, vol. 45, no. 1, pp. 205–211, Feb. 1996.

[66] M.K. Varanasi and B. Aazhang, "Multistage detection in asynchronous code-division multiple-access communications," *IEEE Trans. Commun.*, vol. 38, no. 4, pp. 509–519, Apr. 1990.

[67] J.M. Holtzman, "DS/CDMA successive interference cancellation," *Spread Spectrum Techniques and Applications,IEEE ISSSTA '94*, vol. 1, pp. 69–78, 1994.

[68] R.M. Buehrer, N.S. Correal-Mendoza, and B.D. Woerner, "A simulation comparison of multiuser receivers for cellular CDMA," *IEEE Trans. on Veh. Technol.*, vol. 49, no. 4, pp. 1065–1085, Jul. 2000.

[69] P. B. Rapajic and D.K. Borah, "Performance study of the adaptive MMSE maximum likelihood CDMA receiver," *Personal, Indoor and Mobile Radio Communications 1998, PIMRC '98*, vol. 3, pp. 1285–1289, 1998.

[70] D. K. Borah and P. B. Rapajic, "Adaptive weighted least squares CDMA multiuser detection," *IEEE Vehicular Technology Conference Spring Tokyo2000*, vol. 1, pp. 92–96, 2000.

[71] H. Elders-Boll, M. Herper, and A. Busboom, "Adaptive receivers for mobile DS-CDMA communication systems," *IEEE Vehicular Technology Conference 1997*, vol. 3, pp. 2128–2132, 1997.

[72] P. B. Rapajic and D.K. Borah, "Adaptive receiver structures for asynchronous CDMA systems," *IEEE J. Select. Areas Commun.*, vol. 17, no. 12, pp. 2110–2122, Dec. 1994.

[73] P. B. Rapajic and B.S. Vucetic, "Adaptive receiver structures for asynchronous CDMA systems," *IEEE J. Select. Areas Commun.*, vol. 12, no. 4, pp. 685–697, May 1994.

[74] S. Verdú, "Adaptive Multiuser Detection," *Spread Spectrum Techniques and Applications,IEEE ISSSTA '94*, vol. 1, pp. 43–50, 1994.

[75] D.G.M. Cruickshank, "Optimal and adaptive FIR filter receivers for DS-CDMA," *IEEE PIMRC '94*, pp. 1339–1343, Sep. 1994.

[76] R. Esmailzadeh, E. Sourour, and M. Nakagawa, "Pre-rake diversity combining in time division duplex CDMA mobile communications," *IEEE Trans. on Veh. Technol.*, vol. 48, no. 3, pp. 795–801, May 1999.

[77] R. Esmailzadeh, M. Nakagawa, and E.A. Sourour, "Time-division duplex CDMA," *IEEE Personal Communications*, vol. 4, pp. 51–56, Apr. 1997.

[78] M. Brandt-Pearce and A. Dharap, "Transmitter-based multiuser interference rejection for the down-link of a wireless CDMA system in a multipath environment," *IEEE J. Select. Areas Commun.*, vol. 18, no. 3, pp. 407–417, Mar. 2000.

[79] B. R. Vojčić and W. M. Jang, "Transmitter precoding in synchronous multiuser communications," *IEEE Trans. Commun.*, vol. 46, no. 10, pp. 1346–1355, Oct. 1998.

[80] M. Meurer, P.W. Baier, T. Weber, Y. Lu, and A. Papathanasiou, "Joint transmission:advantageous downlink concept for CDMA mobile radio systems using time division duplexing," *IEE Electronics Letters*, vol. 36, pp. 900–901, May 2000.

[81] A. Papathanasiou, M. Meurer, T. Weber, and P.W. Baier, "A novel multiuser transmission scheme requiring no channel estimation and no equalization at the mobile stations for the downlink of TD-CDMA operating in the TDD mode," *IEEE Vehicular Technology Conference Fall 2000*, pp. 203–210, 2000.

[82] G.R. Walsh, *Methods of optimization*, John Wiley & Sons Inc., 1975.

[83] L. Scharf, *Statistical signal processing : detection, estimation, and time series analysis*, Addison-Wesley series in electrical and computer engineering. Addison-Wesley Pub. Co, 1991.

[84] A.N. Barreto and G. Fettweis, "Capacity increase in the downlink of spread spectrum systems through joint signal precoding," *in Proc. ICC*, vol. 4, pp. 1142–1146, 2001.

[85] M. Joham and W. Utschick, "Downlink processing for mitigation of intracell interference in DS-CDMA systems," *IEEE 6th Int. Symp. on Spread-Spectrum Tech. & Applic.,New Jersey,USA*, pp. 15–19, Sep. 2000.

[86] F. Kowalewski, "Joint predistortion and transmit diversity," *IEEE Global Telecommunications Conference '00*, vol. 1, pp. 245–249.

[87] Z. Tang and S. Cheng, "Pre-decorrelating single user detection for CDMA systems," *IEEE Vehicular Technology Conference '94,IEEE 44th*, vol. 2, pp. 767–769, 1994.

[88] Z. Tang and S. Cheng, "Interference cancellation for DS-CDMA systems over flat fading channels through pre-decorrelating," *PIMRC'94*, pp. 435–438, 1994.

[89] S. Haykin, *Adaptive Filter Theory*, Prentice Hall, 1991.

[90] R. Esmailzadeh and M. Nakagawa, "Pre-RAKE diversity combination for direct sequence spread spectrum communications systems," *International Conference on Communications*, vol. 1, pp. 463–467, Geneva 1993.

[91] S. Georgoulis and D.G.M. Cruickshank, "Pre-equalization, transmitter precoding and joint transmission techniques for time division duplex CDMA," *IEE 3G 2001 Conference on Mobile Telecommunications Technologies*, pp. 257–261, Mar. 2001.

[92] R. Irmer F. Wathan and G. Fettweis, "On transmitter-based interference mitigation in TDD-downlink with frequency selective fading channel environment," *Proc. Asia-Pacific Conference on Communications (APCC), Bandung, Indonesia*, Sep. 2002.

[93] R. Irmer A.N. Barreto and G.Fettweis, "Transmitter precoding forSpread-Spectrum signals in frequency-selective fading channels," *Proc. 3G Wireless 2001*, pp. 939–944, Jun. 2001.

[94] W. Wang, X. Wu, and Q. Yin, "A novel space-time pre-multiuser downlink transmission scheme suitable for TDD-CDMA systems," *IEEE Vehicular Technology Conference 2001-Spring*, vol. 2, pp. 185–189, 2001.

[95] U. Ringel, R. Irmer, and G. Fettweis, "Transmit diversity for frequency selective channels in UMTS-TDD," *Spread Spectrum Techniques and Applications, IEEE ISSSTA '02*, vol. 3, pp. 802–806, 2002.

[96] A. Morgado, A. Gameiro, and J. Fernandes, "Constrained space-time zero-forcing pre-equalizer for the downlink channel of UMTS-TDD," *Personal, Indoor and Mobile Radio Communications 2002, PIMRC '02*, vol. 3, pp. 1122–1126, 2002.

[97] A. Gameiro, A. Morgado, and J. Fernandes, "Space-time pre-equaliser for the downlink channel of UMTS-TDD," *IEE 3G 2001 Conference on Mobile Telecommunications Technologies*, pp. 99–103, 2001.

[98] A. Morgado, P.Pinho, A. Gameiro, and J. Fernandes, "Pre-equalisation technique for the interference cancellation in the UMTS-TDD downlink channel," *IEEE Vehicular Technology Conference 2001-Fall*, vol. 2, pp. 878–881, 2001.

[99] A.N. Barreto and G. Fettweis, "Performance improvement in DS-spread spectrum CDMA systems using a pre- and a post-RAKE," *Proc. of 2000 International Zurich Seminar on Broadband Communications*, pp. 39–46, 2000.

[100] W.M. Jang, B.R. Vojčić, and R.L. Pickholtz, "Joint transmitter-receiver optimization in synchronous multiuser communications over multipath channels," *IEEE Trans. Commun.*, vol. 46, no. 2, pp. 269–278, Feb. 1998.

[101] R. Irmer and G.Fettweis, "Combined transmitter and receiver optimization for multiple antenna frequency-selective channels," *Proc. WPMC'02, Honolulu, Hawaii*, Oct. 2002.

[102] E.S. Hons, A.K. Khandani, and W. Tong, "An optimized transmitter precoding scfheme for synchronouds DS-CDMA," *in Proc. ICC*, , no. 3, pp. 1818–1822, 2002.

[103] S. Georgoulis and D.G.M. Cruickshank, "Transmitter based inverse filters for MAI and ISI mitigation in a TDD/CDMA downlink," *IEEE Vehicular Technology Conference 2002-Fall*, vol. 2, pp. 618–622, Sep. 2002.

[104] P.A. Nelson, H. Hamada, and S. Elliott, "Adaptive inverse filters for stereophonic sound reproduction," *IEEE Trans. Signal Processing*, vol. 40, no. 7, pp. 1621–1632, Jul. 1992.

[105] F. Yu and M. Bouchard, "Multichannel active noise control algorithms using inverse filters," *in Proc. ICASSP'00*, vol. 2, pp. 825–828, 2000.

[106] M. Bouchard and S. Quednau, "Multichannel recursive-least-squares algorithms and fast-transversal-filter algorithms for active noise control and sound reproduction systems," *IEEE Trans. Speech Audio Processing*, vol. 8, no. 5, pp. 606–618, Sep. 2000.

[107] S.J. Elliott, I.M. Stothers, and P.A. Nelson, "A multiple error LMS algorithm and its application to the active control of sound and vibration," *IEEE Trans. on Acoust., Speech, Signal Processing*, vol. 35, no. 10, pp. 1423–1434, Oct. 1987.

[108] P.A. Nelson, F. Orduña-Bustamante, and H. Hamada, "Inverse filters design and equalization zones in multichannel sound reproduction," *IEEE Trans. Speech Audio Processing*, vol. 3, no. 3, pp. 185–192, May 1995.

[109] S.J. Elliott and P.A. Nelson, "Algorithm for multichannel LMS adaptive filtering," *Electronics Letters*, vol. 21, no. 21, pp. 979–981, Oct. 1985.

[110] M. Miyoshi and Y. Kaneda, "Inverse filtering of room acoustics," *IEEE Trans. on Acoust., Speech, Signal Processing*, vol. 36, no. 2, pp. 145–152, Feb. 1988.

[111] Bernard Widrow, *Adaptive Signal Processing*, Prentice-Hall, 1985.

[112] J. Nocedal and S.J. Wright, *Numerical Optimization*, Springer Series in Operations research, Springer-Verlag, New York, 1999.

[113] Y. Ye, "On affine scaling algorithms for nonconvex quadratic programming," *Mathematical Programming*, vol. 56, pp. 285–300, 1992.

[114] Simon R.Saunders, *Antennas and Propagation for Wireless Communication Systems*, Wiley, 1999.

[115] M. Patzold, U. Killat, F. Laue, and Y. Li, "On the statistical properties of deterministic simulation models for mobile fading channels," *IEEE Trans. on Veh. Technol.*, vol. 47, no. 1, pp. 254–269, Feb. 1998.

[116] M. Patzold, U. Killat, Y. Shi, and F. Laue, "A deterministic method for the derivation of a discrete WSSUS multipath fading channel model," *Telecommunication Systems*, vol. 7, no. 2, pp. 165–175, Mar.-Apr. 1996.

[117] S. Georgoulis and D.G.M. Cruickshank, "Multichannel LMS and RLS algorithms for cancelling MAI and ISI before transmission in TDD/CDMA downlink," *Spread Spectrum Techniques and Applications, IEEE ISSSTA '02*, vol. 2, pp. 681–685, Sep. 2002.

[118] S. C. Douglas, "Analysis of the multiple-error and block least-mean-square adaptive algorithms," *IEEE Trans. Circuits and Syst.*, vol. 42, no. 2, pp. 92–101, Feb. 1995.

[119] S. Elliott and K.H. Baek, "Effort constraints in adaptive feedforward control," *IEEE Signal Processing Lett.*, vol. 3, no. 1, pp. 7–9, Jan. 1996.

[120] X. Qiu and C.H. Hansen, "A study of time-domain FXLMS algorithms with control output constraint," *The Journal of the Acoustical Society of America*, pp. 2815–2823, Jun. 2001.

[121] S.J. Elliott, C.C. Boucher, and P.A. Nelson, "The behavior of a multiple channel active control system," *IEEE Trans. Signal Processing*, vol. 40, pp. 1041–1052, 1991.

[122] S.M. Kuo and D.R. Morgan, *Active Noise Control Systems: Algorithms and DSP Implementations*, New York, Wiley, 1996.

[123] T. Auspitzer, D. Guicking, and S.J. Elliott, "Using a fast-recursive-least-squares algorithm in a feedback-controller," *IEEE ASSP Workshop Applications Signal Processing Audio Acoustics*, pp. 61–64, 1995.

[124] E. A. Wan, "Adjoint LMS:An efficient alternative to the filtered-X LMS and multiple error LMS algorithms," *in Proc. ICASSP'96*, pp. 1842–1845.

[125] S.C. Douglas, "Fast exact filtered-x LMS and LMS algorithms for multichannel active noise control," *Proc. Int. Conf. Acoustics Speech, Signal Processing '97, Munich, Germany*, pp. 399–402, 1997.

[126] E. Bjarnarson, "Active noise cancellation using a modified form of the filtered-x LMS and multiple error LMS algorithms," *Proc. 6th Eur. Signal Processing Conf., Munich, Germany*, vol. 2, pp. 1053–1056, 1992.

[127] S. C. Douglas and W. Pan, "Exact expectation analysis of the lms adaptive filter," *IEEE Trans. Signal Processing*, vol. 43, no. 12, pp. 2863–2871, Dec. 1995.

[128] R.K. Wangsness, *Electromagnetic fields*, John Wiley & Sons Inc., 1986.

Appendix A
Wiener solution for unequal powers

In the case of two users with unequal powers the block diagram of the transmitter is modified as shown in Figure A.1. Each symbol m of user k is transmitted with power $(w_k^m)^2$. To simplify the analysis we assume equal transmission power for all symbols of the same user and we drop m from w_k^m. w_k, $k = 1 \dots K$ is the transmission energies for user k. The w_k multipliers

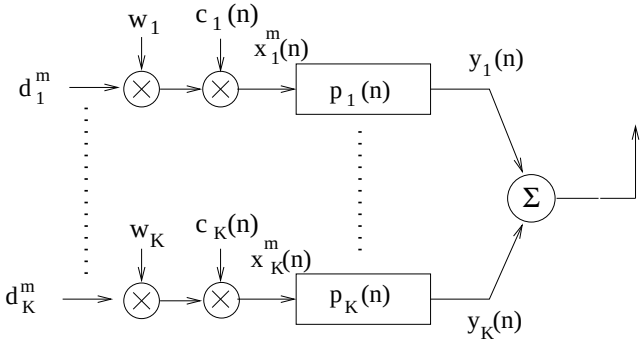

Figure A.1: *Two users with unequal powers block diagram*

in Figure A.1 can be "transfered" in the pre-filters of the users scaling the tap-coefficients. Therefore, we substitute tap-coefficients vector $\mathbf{p}$ with $\mathbf{W}_p\mathbf{p}$ where $\mathbf{W}_p$ a diagonal matrix of $KP \times KP$ dimensions:

$$\mathbf{W}_p = \text{blockdiag}\big(\mathbf{W}_{p1}, \dots, \mathbf{W}_{pK}\big) \tag{A.1}$$

$\mathbf{W}_{pk}$, $k = 1 \dots K$ is defined as a $P \times P$ diagonal matrix:

$$\mathbf{W}_{pk} = \{[\mathbf{W}_{pk}]^{i,j}\} \quad ; \quad i = 1 \dots P, j = 1 \dots P$$

$$[\mathbf{W}_{pk}]^{i,j} = \begin{cases} w_k & i = j \\ 0 & i \neq j \end{cases} \tag{A.2}$$

Now the cost function 5.10 is written as:

$$J = E[(\mathbf{W}\mathbf{d}_0 - \mathbf{R}(T_{ss})\mathbf{W}_p\mathbf{p})^T(\mathbf{W}\mathbf{d}_0 - \mathbf{R}(T_{ss})\mathbf{W}_p\mathbf{p})] + \lambda\big(E_g(\mathbf{p}) - \mathcal{E}_g\big) \tag{A.3}$$

where $\mathbf{W}$ is a diagonal $K \times K$ matrix with diagonal elements $[\mathbf{W}]^{i,i} = w_i$, $i = 1 \dots K$. The average total transmission power per symbol is:

$$E_g = \big(\mathbf{U}\mathbf{W}_p\mathbf{p}\big)^T \mathbf{U}\mathbf{W}_p\mathbf{p} \tag{A.4}$$

and its gradient:

$$\frac{\vartheta\big(E_g(\mathbf{p}) - \mathcal{E}_g\big)}{\vartheta\mathbf{p}} = \frac{\vartheta\big(\mathbf{p}^T\mathbf{W}_p^T\mathbf{U}^T\mathbf{U}\mathbf{W}_p\mathbf{p}\big)}{\vartheta\mathbf{p}} = 2\mathbf{W}_p^T\mathbf{U}^T\mathbf{U}\mathbf{W}_p\mathbf{p} \tag{A.5}$$

The gradient $\vartheta/\vartheta\mathbf{p}$ of the new cost function J_c is:

$$\frac{\vartheta J_c}{\vartheta\mathbf{p}} = -2\mathbf{W}_p^T E[\mathbf{R}^T(T_{ss})\mathbf{W}\mathbf{d}_0] + 2\mathbf{W}_p E[\mathbf{R}^T(T_{ss})\mathbf{R}(T_{ss})]\mathbf{W}_p\mathbf{p} + 2\lambda\mathbf{W}_p^T\mathbf{U}^T\mathbf{U}\mathbf{W}_p\mathbf{p} \tag{A.6}$$

It is easy to prove that:

$$E[\mathbf{R}^T(T_{ss})\mathbf{W}\mathbf{d}_0] = E[\mathbf{R}^T(T_{ss})\mathbf{d}_0]\mathbf{W}_p \tag{A.7}$$

Hence A.6 is rewritten :

$$\begin{aligned} -\mathbf{W}_p^T E[\mathbf{R}^T(T_{ss})\mathbf{d}_0]\mathbf{W}_p + \big(\mathbf{W}_p^T E[\mathbf{R}^T(T_{ss})\mathbf{R}(T_{ss})]\mathbf{W}_p + \lambda\mathbf{W}_p^T\mathbf{U}^T\mathbf{U}\mathbf{W}_p\big)\mathbf{p} &= 0 \\ -\mathbf{W}_p^T E[\mathbf{R}^T(T_{ss})\mathbf{d}_0]\mathbf{W}_p + \mathbf{W}_p^T\big(E[\mathbf{R}^T(T_{ss})\mathbf{R}(T_{ss})] + \lambda\mathbf{U}^T\mathbf{U}\big)\mathbf{W}_p\mathbf{p} &= 0 \end{aligned} \tag{A.8}$$

Eventually, the equation is reduced to eq. (5.13) and the solution is:

$$\mathbf{p}_o = \big[E[\mathbf{R}^T(T_{ss})\mathbf{R}(T_{ss})] + \lambda\mathbf{U}^T\mathbf{U}\big]^{-1} E[\mathbf{R}^T(T_{ss})\mathbf{d}_0] \tag{A.9}$$

which proves that differen transmission power per user doesn't affect the Wiener solution.

Appendix B
Publications

- S.Georgoulis and D.G.M. Cruickshank, "Pre-equalization, transmitter precoding and joint transmission techniques for time division duplex CDMA," *3G 2001 Conference*, London, pp. 257–261, Mar. 2001.

- S.Georgoulis and D.G.M. Cruickshank, " Multichannel LMS and RLS Algorithms for Cancelling MAI and ISI before Transmission in TDD/CDMA Downlink," *ISSSTA 2002*, Prague, Sep. 2002.

- S.Georgoulis and D.G.M. Cruickshank, "Transmitter Based Inverse Filters for MAI and ISI Mitigation in a TDD/CDMA Downlink ," *IEEE VTC 2002-Fall*, Vancouver, vol.: 2, pp. 681-685, Sep. 2002.

- S.Georgoulis and D.G.M. Cruickshank, "Inverse Filters for Transmitter based Interference Mitigation in TDD/CDMA," accepted for publication in *IEEE Transactions on Wireless Communications.*

- S.Georgoulis and D.G.M. Cruickshank, "Adaptive Techniques for Transmission in TDD Downlink ," submitted to *AEI European Transactions on Telecommunications*

- Contributing author in textbook entitled "Next Generation Mobile Access Technologies: Implementing TDD", Dr. Harald Haas & Professor Stephen McLaughlin. Due to be published in 2003.

PRE-EQUALISATION, TRANSMITTER PRECODING AND JOINT TRANSMISSION TECHNIQUES FOR TIME DIVISION DUPLEX CDMA

S. Georgoulis and D.G.M. Cruickshank
University of Edinburgh
Department of Electronics and Electrical Engineering
email: sg@ee.ed.ac.uk, dgmc@ee.ed.ac.uk

Abstract— **In this paper we consider options for moving receiver complexity from the terminal to the base station in a mobile communications system downlink. We compare pre-equalisation, transmitter precoding and joint transmission techniques carried out at the base station with equalisation and joint detection at the user equipment receiver for synchronous CDMA over frequency selective fading channels. All the transmitter based methods assume knowledge of the channel at the transmitter. This is feasible under the Time Division Duplex (TDD) mode of the 3G UMTS system where the channel is assumed to be the same on uplink and downlink and can be estimated from the uplink at the base station. The advantage over the well known receiver-based equalisation and multiuser detection techniques is that reduction of the mobile receiver complexity is achieved.**

I. INTRODUCTION

Direct-sequence code-division-multiple access (DS-CDMA) is expected to gain a significant share of the cellular market. This technique, already being used in current IS-95 systems, is also going to be employed in the next generation of mobile communication systems currently under standardisation. Another technique that has been increasingly popular is Time Division Duplexing (TDD)[1] in which the same carrier is used for both up-and downlink in different time slots. This technique is employed in the European cordless system DECT and will be used in part of the frequency range allocated to third generation systems.

In a CDMA scheme the major encountered problems are the multiple access interference (MAI) due to simultaneous usage of the bandwidth by all users and intersymbol interference (ISI) due to multipath fading channels. Multipath fading often causes a major limitation to CDMA system performance since it destroys the orthogonality among the spreading sequences. In the absence of MAI the conventional approach to data detection is to employ an independent, single user RAKE receiver[2] which equalises the channel. In the absence of multipath (i.e. additive white Gaussian noise channel) the linear [3] and nonlinear[4] multiuser detection techniques are well studied and analysed. However for data detection in systems applying CDMA the two problems of equalisation and signal separation have to be solved simultaneously.

Linear suboptimal multiuser detectors for frequency-selective Rayleigh fading channels include the multipath decorrelating detector developed in[5] and the RAKE decorrelating detector[6]. The latter technique,also known as linear unbiased data estimation for discrete time CDMA systems, reduces intersymbol and multiple access interference based on zero-forcing (ZF)or mean minimum square error (MMSE)algorithms. This scheme, which *jointly detects*(JT) all the users, gives improved results over the standard RAKE receiver, but the receiver requires knowledge of all the users CDMA codes, the channel's impulse response and the algorithm includes inversion of a fairly large matrix. This results in high mobile receiver complexity on the downlink which is highly undesirable.

Recently, work has been done on algorithms that exploit the fact that in a TDD scheme the downlink channel is known to the transmitter. In the case of TDD the same channel impulse responses are valid for both the uplink and the downlink, if -and this assumed in what follows- the time elapsing between uplink and downlink transmissions is sufficiently small compared to the coherence time of the mobile radio channel. In these algorithms, the multiuser detection and equalisation can be carried out at the transmitter. The receiver structure at the user equipment is then simplified when compared with a multiuser receiver, and can be a conventional matched filter (which only requires knowledge of the desired users code) or a RAKE receiver (which requires knowledge of the desired users code and the propagation channel). Techniques which only require a matched filter receiver also enhance the system capacity since no system resources have to be allocated for the transmission of training signals on the downlink.

One such transmitter technique is *Pre-equalisation* [7], [8] which includes pre-RAKE diversity combining at the transmitter. In the downlink the desired user's signal is maximal ratio combined while other user's signals are not. Under this scenario the receiver is just a fixed filter matched to the desired user's code and the receiver is not required to implement any channel estimation or adaptive equaliser.

Another transmitter based technique is *Transmitter precoding* as proposed in [9]. In this technique, the objective is to carry out multiple access interference cancellation at the transmitter rather than the receiver. In this case, a RAKE receiver is required for sufficient performance under severe multipath.

An alternative transmitter based multiuser detection scheme is *Joint transmission*, proposed in [10]. In this approach a common transmit signal for all users is determined in the base station and each signal is assumed to pass through a different multipath channel. After having passed through the mobile radio channel this signal is filtered by a filter matched to the user's code, yielding the desired data.

In this paper we derive an implementation and simulation of the above transmitter-based multiuser detection

and equalisation systems using the vehicular A channel proposed in UMTS [11]. We compare the various transmitter based approaches with each other and with their equivalent receiver based approach (joint detection).

Basic assumptions are that during the downlink all the users are synchronised and they are transmitted with equal powers. The scheme is also free from intercell interference.

The system model and a brief review of the receiver-based technique are given in section II. The transmitter based techniques are explained in section III. In section IV the simulation results are presented and the different downlink processing schemes are compared.

II. SYSTEM MODEL

A. System Description

Under the considered scenario a base station (BS) with one antenna element transmits synchronously over frequency selective Rayleigh channels to K mobile stations (MS) located in the same cell. The downlink or forward link within one cell is presented in fig. 1. The discrete-time transmission model is described as follows.

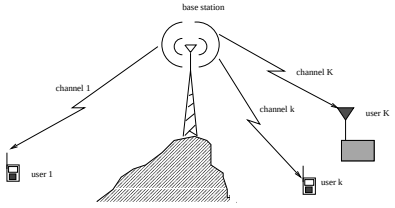

Fig. 1. Base station(BS) and downlink scenario

The base station transmits blocks of N symbols d^k for the k_{th} user:

$$\underline{\mathbf{d}}^{(\mathbf{k})} = (d_1^k \cdots d_N^k)^T, \tag{1}$$

The symbols d^k are BPSK and they are spread by a spreading code $\underline{\mathbf{c}}^{(\mathbf{k})}$ of length Q which denotes that the different codes consist of Q chips:

$$\underline{\mathbf{c}}^{(\mathbf{k})} = (c_1^k \cdots c_Q^k)^T \tag{2}$$

The symbol interval is T_s and the chip interval T_c:

$$T_c = \frac{T_s}{Q} \tag{3}$$

The k_{th} channel is characterised by an impulse response which is sampled at the chip rate:

$$\underline{\mathbf{h}}^{(\mathbf{k})} = (h_1^k \cdots h_W^k)^T \tag{4}$$

where W is the length of the channel. Assuming that the i_{th} symbol of power w_i^j is transmitted for the user j_{th}, the total downlink signal is described as:

$$\sum_{j=1}^{K} \underline{\mathbf{c}}^{(\mathbf{j})} \sqrt{w_i^j}\, d_i^j \tag{5}$$

Therefore the noiseless received signal at the k_{th} MS will be a superposition of all users filtered by the k_{th} channel $\underline{\mathbf{h}}^{(\mathbf{k})}$:

$$\underline{\mathbf{e}}_{\mathbf{i}}^{(\mathbf{k})} = \sum_{j=1}^{K} \underline{\mathbf{c}}^{(\mathbf{j})} \sqrt{w_i^j}\, d_i^j * \underline{\mathbf{h}}^{(\mathbf{k})} \tag{6}$$

The received vector $\underline{\mathbf{e}}_{\mathbf{i}}^{(\mathbf{k})}$ for i_{th} transmitted data symbol is of length $(Q+W-1)$ as a result of the convolution in eq. 6. In this paper all the signals are transmitted with equal power and w_i^k is normalised to have unit amplitude.

For transmission of a block of N-data bits the aforementioned received vector in the k_{th} MS $\underline{\mathbf{e}}_{\mathbf{i}}^{(\mathbf{k})}$ is extended to the vector $\underline{\mathbf{e}}^{\mathbf{k}}$ of length $(NQ+W-1)$ and the latter is expressed as in eq. 10 after forming the vector $\underline{\mathbf{d}}$ of length (KN):

$$\underline{\mathbf{d}} = (\underline{\mathbf{d}}^{(\mathbf{1})^{\mathbf{T}}} \cdots \underline{\mathbf{d}}^{(\mathbf{K})^{\mathbf{T}}})^{\mathbf{T}}, \tag{7}$$

the matrix $\underline{\mathbf{C}}$ of size $(QN) \times (KN)$:

$$\underline{\mathbf{C}} = (C_{i,j}); \qquad i = 1...NQ, j = 1...KN$$

$$C_{Q(n-1)+q,N(k-1)+n} = \begin{cases} c_q^{(k)} & for \quad q = 1 \ldots Q, n = 1 \ldots N, \\ & k = 1 \ldots K \\ 0 & otherwise \end{cases} \tag{8}$$

and the matrix $\underline{\mathbf{H}}^{(\mathbf{k})}$ of size $(QN+W-1) \times (QN)$:

$$\underline{\mathbf{H}}^{(\mathbf{k})} = (H_{i,j}^k); \quad i = 1 \ldots NQ+W-1, \quad j = 1 \ldots QN$$

$$H_{i,j}^k = \begin{cases} h_{i-j+1}^k & for \quad 1 \le i-j+1 \le W \\ 0 & otherwise \end{cases} \tag{9}$$

Then :

$$\underline{\mathbf{e}}^{\mathbf{k}} = \underline{\mathbf{H}}^{\mathbf{k}} \underline{\mathbf{C}}\, \underline{\mathbf{d}} + \underline{\mathbf{n}} = \underline{\mathbf{A}}\, \underline{\mathbf{d}} + \underline{\mathbf{n}} \tag{10}$$

where $\underline{\mathbf{H}}^{\mathbf{k}} \underline{\mathbf{C}} = \underline{\mathbf{A}}$ and $\underline{\mathbf{n}}$ is a $(QN+W-1)$ vector of zero mean complex AWGN whose real and imaginary parts are independent. The covariance matrix is

$$\underline{\mathbf{R}}_{\mathbf{n}} = E\left(\underline{n}\, \underline{n}^{*^T}\right) = \sigma^2 \mathbf{I} \tag{11}$$

.

The noiseless case of Q equal to 3, W equal to 2, N equal to 2 and K equal to 2 has been used in eq. 12:

$$\begin{bmatrix} e_1^k \\ e_2^k \\ e_3^k \\ e_4^k \\ e_5^k \\ e_6^k \\ e_7^k \end{bmatrix} = \begin{bmatrix} h_1^k & & & & & & \\ h_2^k & h_1^k & & & & & \\ & h_2^k & & & & & \\ & & \ddots & & & & \\ & & & h_1^k & & & \\ & & & h_2^k & h_1^k & & \\ & & & & h_2^k & & \end{bmatrix} \begin{bmatrix} c_1^1 & & c_1^2 & \\ c_2^1 & & c_2^2 & \\ c_3^1 & & c_3^2 & \\ & c_1^1 & & c_1^2 \\ & c_2^1 & & c_2^2 \\ & c_3^1 & & c_3^2 \end{bmatrix} \begin{bmatrix} d_1^1 \\ d_2^1 \\ d_1^2 \\ d_2^2 \end{bmatrix} \tag{12}$$

It is important for fairness to ensure that the systems under consideration transmit equal powers. For the system described above the transmitted energy is given as:

$$trace\left\{\underline{\mathbf{e}}^{*^T} \cdot \underline{\mathbf{C}}\right\} \tag{13}$$

B. Linear Unbiased Estimation

In the *linear unbiased estimation algorithm* [6] the estimate of the combined data vector $\underline{\mathbf{d}}$ is determined by the zero forcing technique and defined by

$$\hat{\underline{\mathbf{d}}} = arg \quad \min_{\underline{\mathbf{d}}} \left((\underline{\mathbf{e}} - \underline{\mathbf{A}} \cdot \underline{\mathbf{d}})^{*^{\mathbf{T}}} \mathbf{R}_{\mathbf{n}}^{-\mathbf{1}} (\underline{\mathbf{e}} - \underline{\mathbf{A}} \cdot \underline{\mathbf{d}}) \right) \tag{14}$$

According to the estimation theory and with $\mathbf{R_n}$ as in eq. 11 the estimate becomes

$$\hat{\underline{\mathbf{d}}} = \left(\underline{\mathbf{A}}^{*^{\mathbf{T}}} \cdot \underline{\mathbf{A}} \right)^{-\mathbf{1}} \cdot \underline{\mathbf{A}}^{*^{\mathbf{T}}} \cdot \underline{\mathbf{e}} \tag{15}$$

As a presupposition for this algorithm, the matrix $\underline{\mathbf{A}}^{*^{\mathbf{T}}} \cdot \underline{\mathbf{A}}$ has to be non-singular which is not always the case. However when considered real world time-variant channel impulse responses $\underline{\mathbf{h}}^{(\mathbf{k})}$ and when choosing the user-specific CDMA codes $\underline{\mathbf{c}}^{(\mathbf{k})}$ this matrix is singular with a probability equal to zero. Linear unbiased estimation can be considered as a bank of K RAKE receivers followed by a decorrelator[12].

III. TRANSMITTER BASED TECHNIQUES

From eq. 15 it is obvious that the receiver requires knowledge of all the user codes and an estimate of the channel impulse response to perform the aforementioned algorithm in addition to the need for inversion of a fairly large matrix. This scheme has an increased complexity in contrast with the increased demand for less complex portable units. Therefore, current research has been focused on algorithms that take place on the base station exploiting the fact that in a TDD scheme the downlink channel is known to the transmitter.

A. Transmitter Pre-coding

In [9] it is shown that when a RAKE receiver is employed, both multiple access and intersymbol interference can be eliminated by means of a suitable transmitter precoding scheme. A linear transformation matrix $\underline{\mathbf{T}}$ of the data $\underline{\mathbf{d}}$ to be transmitted is used and thus the received signal is given as:

$$\underline{\mathbf{e}}^{\mathbf{k}} = \underline{\mathbf{H}}^{\mathbf{k}} \underline{\mathbf{C}} \left(\underline{\mathbf{T}}\, \underline{\mathbf{d}} \right) + \underline{\mathbf{n}} = \underline{\mathbf{A}} \left(\underline{\mathbf{T}}\, \underline{\mathbf{d}} \right) + \underline{\mathbf{n}} \tag{16}$$

The output vector $\underline{\mathbf{y}}$ of a bank of K RAKE receivers for a block of N transmitted data is given by

$$\underline{\mathbf{y}} = \underline{\mathbf{A}}^{*^{\mathbf{T}}} \underline{\mathbf{A}} (\underline{\mathbf{T}}\, \underline{\mathbf{d}}) + \underline{\mathbf{n}}' \tag{17}$$

The mean-squared error criterion J defined as :

$$J = E_{b,n} \{ \parallel \underline{\mathbf{d}} - \left((\underline{\mathbf{A}}^{*^{\mathbf{T}}} \underline{\mathbf{A}}) \cdot (\underline{\mathbf{T}}\, \underline{\mathbf{d}}) + \underline{\mathbf{n}}' \right) \parallel^{\mathbf{2}} \} \tag{18}$$

The optimum precoding transformation $\underline{\mathbf{T}}$, which minimises J is

$$\underline{\mathbf{T}} = \left(\underline{\mathbf{A}}^{*^{\mathbf{T}}} \underline{\mathbf{A}} \right)^{-\mathbf{1}} \tag{19}$$

In order to maintain the transmitted energy equal to the case of no-precoding as given by eq. 13 we modify the precoding transformation as :

$$\underline{\mathbf{T}} = \sqrt{\mathcal{F}} \left(\underline{\mathbf{A}}^{*^{\mathbf{T}}} \underline{\mathbf{A}} \right)^{-\mathbf{1}} \tag{20}$$

where the factor $\sqrt{\mathcal{F}}$

$$\mathcal{F} = \frac{trace\{ \underline{\mathbf{C}}^{*^{T}} \underline{\mathbf{C}} \}}{trace\{ (\underline{\mathbf{C}}\, \underline{\mathbf{T}})^{*^{T}} \underline{\mathbf{C}}\, \underline{\mathbf{T}} \}} \tag{21}$$

The schematic diagram of pre-coding scheme is given in fig. 2. The required RAKE receiver does not achieve the simplest mobile unit which is a filter matched to the user's spreading code. The latter aim is achieved in the following algorithm.

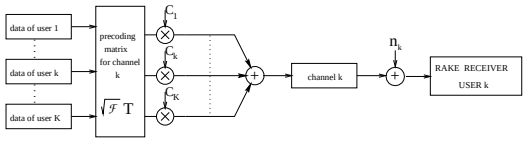

Fig. 2. Block diagram of transmitter pre-coding

B. Joint Transmission

The main idea of this approach as proposed in [10] is that the BS determines a common signal $\underline{\mathbf{s}}$ for all MSs. This signal after having passed through the mobile radio channels, yields the data sent for each MS by simple filtering. Blocks of N-data symbols are transmitted and the filters at each MS are matched to a specific spreading code of length Q. It is assumed that the common signal $\underline{\mathbf{s}}$ is of length NQ .

All the active channels in a cell and the vectors received at every MS must be taken into account. Thus, a $\left[K(NQ+W-1)\right] \times NQ$ matrix $\underline{\mathbf{H}}$ is defined:

$$\underline{\mathbf{H}} = \left(\underline{\mathbf{H}}^{(\mathbf{1})^{\mathbf{T}}} \cdots \underline{\mathbf{H}}^{(\mathbf{k})^{\mathbf{T}}} \cdots \underline{\mathbf{H}}^{(\mathbf{K})^{\mathbf{T}}} \right)^{\mathbf{T}} \tag{22}$$

where $\underline{\mathbf{H}}^{(\mathbf{k})}$ is as in eq. 9. The K received signals $\underline{\mathbf{e}}^{(\mathbf{k})}$ of eq. 10 are arranged in a $K(NQ+W-1)$ vector $\underline{\mathbf{e}}$ as:

$$\underline{\mathbf{e}} = \left(\underline{\mathbf{e}}^{(\mathbf{1})^{\mathbf{T}}} \cdots \underline{\mathbf{e}}^{(\mathbf{k})^{\mathbf{T}}} \cdots \underline{\mathbf{e}}^{(\mathbf{K})^{\mathbf{T}}} \right)^{\mathbf{T}} \tag{23}$$

The total received vector $\underline{\mathbf{e}}$ is concisely expressed as:

$$\underline{\mathbf{e}} = \underline{\mathbf{H}}\, \underline{\mathbf{s}} \tag{24}$$

The requirement that in every MS the filtered $NQ + W - 1$ vector $\underline{\mathbf{e}}^{(\mathbf{k})}$ yields the data vector $\underline{\mathbf{d}}^{\mathbf{k}}$ as defined in eq. 1 is jointly expressed for all K users as:

$$\underline{\mathcal{C}}^{*^{\mathbf{T}}}\, \underline{\mathbf{e}} = \underline{\mathbf{d}} \tag{25}$$

$\underline{\mathcal{C}}$ is the CDMA code matrix :

$$\underline{\mathcal{C}} = \mathbf{blockdiag} \left[\underline{\mathcal{C}}^{(\mathbf{1})} \cdots \underline{\mathcal{C}}^{(\mathbf{k})} \cdots \underline{\mathcal{C}}^{(\mathbf{K})} \right] \tag{26}$$

$$\underline{\mathcal{C}}^{(k)} = \left(\mathcal{C}_{i,j}^{(k)} \right); \qquad i = 1 \ldots NQ + W - 1, j = 1 \ldots NK$$

$$\mathcal{C}_{i,j}^{(k)} = \begin{cases} c_{i-Q(j-1)}^{(k)} & for 1 \le i - Q(j-1) \le Q \\ 0 & otherwise \end{cases} \tag{27}$$

Eq. 24 and eq 25 give :

$$\underline{\mathcal{C}}^{*^{\mathbf{T}}}\,\underline{\mathbf{H}}\,\underline{\mathbf{s}} = \underline{\mathbf{d}} \tag{28}$$

In [10] it is assumed that $QN \geq KN$ and the underdetermined system of eq. 28 has many solutions. The given solution in eq. 29 is the one of minimum energy $\| \underline{\mathbf{s}} \|^2 /2$ which is optimum in the sense that the transmit power is minimised.

$$\underline{\mathbf{s}} = \underline{\mathbf{H}}^{*^{\mathbf{T}}}\,\underline{\mathcal{C}}\,(\underline{\mathcal{C}}^{*^{\mathbf{T}}}\,\underline{\mathbf{H}}\,\underline{\mathbf{H}}^{*^{\mathbf{T}}}\,\underline{\mathcal{C}})^{-\mathbf{1}}\,\underline{\mathbf{d}} \tag{29}$$

The common signal $\underline{\mathbf{s}}$ is scaled by a factor $\sqrt{\mathcal{F}}$:

$$\mathcal{F} = \frac{trace\{\underline{\mathbf{C}}^{*^{T}}\,\underline{\mathbf{C}}\}}{\| \underline{s} \|^2} \tag{30}$$

to equalise the transmitted energy for the systems under comparison in this paper. The schematic diagram of the pre-coding scheme is given in fig. 3.

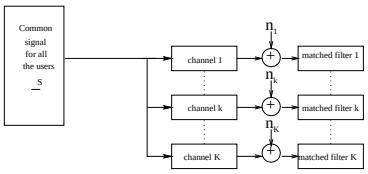

Fig. 3. Block diagram of joint transmission scheme

This scheme is appropriate for point to multipoint links in contrast with the transmitter pre-coding. However, for a simple one path AWGN channel the joint transmission algorithm reduces down to transmitter precoding. Under this method the MS requires knowledge only of one user spreading code which achieves minimum complexity.

C. Pre-Rake

A different approach of the problem of reducing the complexity of the MS receiver is presented in [8]. The schematic diagram for this scheme is presented in fig. 4. The BS filters the signal to be sent to user k with the

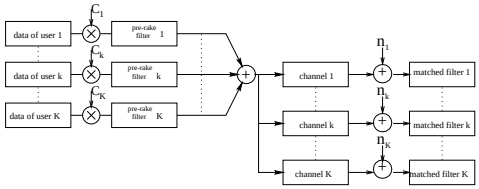

Fig. 4. Block diagram of pre-RAKE scheme

time inverted complex conjugate of the up-link channel impulse response of the same user. Then in the down-link the desired user's signal is maximal ratio combined by the channel itself while other user's signals are not. The result is a strong peak at the output of the channel which is equivalent to the RAKE receiver's output. Therefore the receiver of the MS does not need to estimate the channel impulse response and can be a conventional matched filter to the user's spreading code $\underline{\mathbf{c}}^{(\mathbf{k})}$.

To maintain equal transmission power as eq. 13 we scale the data of k_{th} user with the factor:

$$\frac{1}{\sqrt{\sum_{i=1}^{W} \|h_i^k\|^2}} \tag{31}$$

IV. SIMULATION RESULTS

In this section the transmitter based techniques, described above, are compared with the receiver based joint detection(linear unbiased estimate technique). Random binary spreading codes $\underline{\mathbf{c}}^{(\mathbf{k})}$ of length $Q = 31$ are multiplied by the BPSK data symbols $\underline{\mathbf{d}}^{(\mathbf{k})}$ and transmitted in blocks of $N = 3$ synchronously over the mobile channel. Variations of the received power due to path loss and lognormal fading are assumed to be eliminated by power control. Each of the users is assumed to be transmitted with equal energy which is normalised to have unit amplitude. The chip interval is equal to $T_c = 0.26\mu sec$ and for the correspondent continuous-time system a raised cosine pulse shaping[2] is used with a factor $\beta = 0.22$ and $\tau = T_c/2$.

$$\frac{\sin(\frac{\pi t}{\tau}) \cdot \cos(\frac{\pi \beta t}{\tau})}{(\frac{\pi t}{\tau}) \cdot (1 - 4(\frac{\beta t}{\tau})^2)} \tag{32}$$

Due to pulse shaping interchip interference has been taken into account.

A mobile radio channel is given by its channel impulse response $\underline{\mathbf{h}}^{(\mathbf{k})}$, which is derived from the COST/GSM models. The delay power profile of the vehicular environment A from [11] is adopted where the length of the channel is $W = 11$ chips. The tap coefficients experience independent Rayleigh fading with the Classic Doppler spectrum.

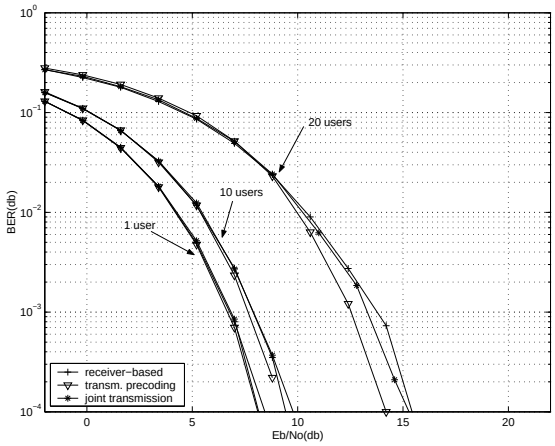

Fig. 5. BER versus SNR for AWGN channel, K=1,10,20, Random codes Q=31

It is assumed for both the receiver and transmitter based processings that the channels impulse response are constant during the N-data block transmission. Perfect knowledge of the channel in the middle of the $(N * Q)$-chip sequence is presumed for the receiver based estimate. In contrast, the channel impulse response that had

been valid during the last transmission is used by the transmitter based methods to modify the next transmitted signal.

In fig. 5 the performance in terms of BER versus SNR for the aforementioned techniques in the case of AWGN channel is presented. The graphs for a single,10 and 20 user scenario are displayed. As expected the performance is similar for all the cases. The pre-rake technique is omitted since it is based on maximum ratio combining of uncorrelated channel impulse responses which is not consistent with an AWGN channel.

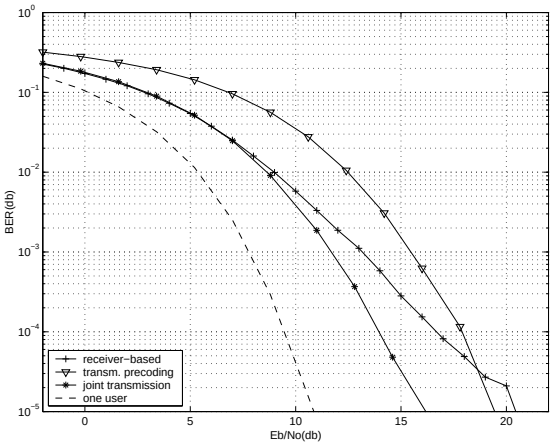

Fig. 6. BER versus SNR. K=10, Random codes Q=31, W=11, Doppler Frequency=0 Hz

In fig. 6 the case of time invariant multipath channel is considered and $K = 10$. Joint transmission appears to have similar behaviour with joint detection for low SNR while it shows significant improvement for higher signal to noise ratio. The transmitter precoding technique is outperformed by both the former algorithms.

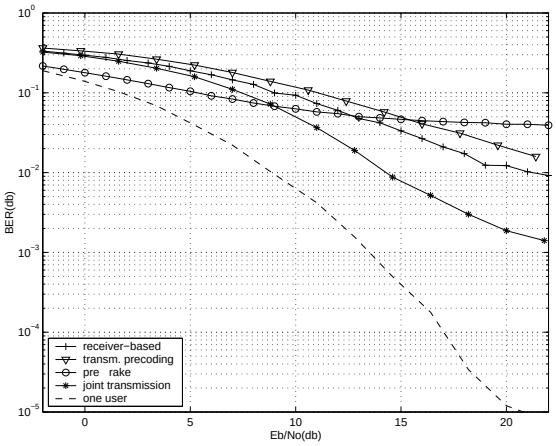

Fig. 7. BER versus SNR. K=20, Random codes Q=31, W=11, Doppler Frequency=300 Hz

In the case of fig. 7 a time variant channel with a Doppler frequency of 300 Hz has been simulated and the number of users in the cell has been increased to 20. For high noise conditions pre-rake technique outperforms all the discussed techniques, while for large SNR values it gives poor results. This is expected as pre-rake leads to enhancement of multiple access interference. The performance for the other methods follows the results that were concluded in the former paragraph.

In terms of complexity the joint transmission method requires much more time and computational resources since the matrices that it uses are of dimension $[K(NQ+W-1)\times NQ]$. For typical values of $K = 20, N = 3, Q = 31, W = 11$ $\underline{\mathbf{H}}$ of eq. 22 turns out to be a (2060×93) matrix.

V. CONCLUSION

In this paper a review of three transmitter based methods that reduce both intersymbol and multiple access interference has been provided. A simulation comparison with well-known receiver based technique was then presented where the joint transmission method showed very good results for frequency selective Rayleigh channels. All the methods exploit the fact that for the TDD scenario the channel is assumed to be the same for the uplink and the downlink. The extra complexity in terms of computational load and channel estimators is removed to the BS where resources can be sufficient. Space-time transmitter based techniques are now under investigation.

References

[1] G.J.R. Povey. Capacity of a cellular time division dublex CDMA sysyem. *IEE Proc. in Commun.*, 141(5):351–355, Oct. 1994.

[2] John G. Proakis. *Digital Communications*. Electrical Engineering. McGraw-Hill, 3rd edition, 1995.

[3] R. Lupas and S. Verdu. Linear multiuser detectors for synchronous code division multiple access channels. *IEEE Trans. on Information Theory*, 35(1):123–136, Jan. 1989.

[4] M.K. Varanasi and B. Aazhang. Near-optimum detection in synchronous code-division multiple access systems. *IEEE Trans. on Communications*, 39(5):725–736, May 1991.

[5] Z. Zvoran and D. Brady. Suboptimal multiuser detector for frequency-selective Rayleigh fading synchronous CDMA channels. *IEEE Trans. on Communications*, 43(3):154–157, Mar. 1995.

[6] A. Klein and P.W. Baier. Linear unbiased data estimation in mobile radio systems applying CDMA. *IEEE Journal on Selected Areas in Communications*, 11(7):1058–1066, Sep 1993.

[7] R. Esmailzadeh and M. Nakagawa. Pre-RAKE diversity combination for direct sequence spread spectrum communications systems. *International Conference on Communications*, 1:463–467, Geneva 1993.

[8] R. Esmailzadeh, E. Sourour, and M. Nakagawa. Pre-rake diversity combining in time division duplex CDMA mobile communications. *IEEE Trans. on Vehicular Technology*, 48(3):795–801, May 1999.

[9] B. R. Vojčić and W. M. Jang. Transmitter precoding in synchronous multiuser communications. *IEEE Trans. on Communications*, 46(10):1346–1355, Oct. 1998.

[10] M. Meurer, P.W. Baier, T. Weber, Y. Lu, and A. Papathanasiou. Joint transmission:advantageous downlink concept for CDMA mobile radio systems using time division duplexing. *IEE Electronics Letters*, 36:900–901, May 2000.

[11] Selection procedures for the choice of radio transmission technologies of the UMTS (UMTS 30.03 version 3.2.0).

[12] H.C. Huang and S.C. Schwartz. A comparative analysis of linear multiuser detectors for fading multipath channels. *Proc. of the IEEE GLOBECOM Conf.*, pages 11–15, 1994.

Multichannel LMS and RLS Algorithms for Cancelling MAI and ISI before Transmission in TDD/CDMA Downlink

S.L. Georgoulis and D.G.M. Cruickshank
Department of Electronics and Electrical Engineering, The University of Edinburgh
The King's Buildings, Mayfield Rd., Edinburgh, EH9 3JL, UK
emails: sg@ee.ed.ac.uk, dgmc@ee.ed.ac.uk

Abstract— **In this paper a novel transmitter based multiuser detection scheme for the TDD/CDMA downlink is presented. The method assumes knowledge of the channel at the transmitter. This is feasible under the Time Division Duplex (TDD) mode where the channel is assumed to be the same on uplink and downlink and can be estimated from the uplink at the base station. The portable unit's structure is significantly simplified since no channel estimation, equalisation or multiuser detection is required. The novelty is that the base station performs an emulation of the mobile receiver and adaptively sets the filters that pre-equalise the transmitted signals, reducing multiple access and multipath intersymbol interference. The theoretical analysis is supported with simulation results which show that the proposed technique increases the system's capacity, compared with other recently published methods and maintains low computational cost.**

Keywords— **code division multiple access, TDD, interference cancellation, transmitter based, multiuser detection, multichannel RLS, multichannel LMS**

I. Introduction

Direct sequence code division multiple access (DS-CDMA) is now gaining a significant share of the cellular market. Another technique that has been increasingly popular is Time Division Duplex (TDD) in which the same carrier is used for both up-and downlink in different time slots. This technique is employed in the European cordless system DECT and will be used in part of the frequency range allocated to third generation mobile systems in Europe.

In a CDMA scheme the major problems encountered are the multiple access interference (MAI) due to simultaneous usage of the bandwidth by many users and intersymbol interference (ISI) due to multipath fading channels. Multipath fading is a major limitation on CDMA system performance since it destroys the orthogonality among the spreading sequences. Therefore for sufficient data detection in systems applying CDMA the two problems of equalisation and signal separation have to be solved simultaneously for good performance.

Linear suboptimal multiuser detectors for frequency-selective Rayleigh fading channels have been extensively studied in literature [1],[2]. These techniques, reduce intersymbol and multiple access interference but the receiver requires knowledge of the CDMA spreading code and the channel impulse response of every user and the algorithms include inversion of fairly large matrices. This results in high mobile receiver complexity on the downlink which is highly undesirable.

Recently, work has been done on algorithms that exploit the fact that in a TDD scheme the downlink channel is known to the transmitter. In the case of TDD the same channel impulse responses are valid for both the uplink and the downlink, if – and this is assumed in what follows – the time elapsing between uplink and downlink transmissions is sufficiently small compared to the coherence time of the mobile radio channel. In these algorithms, the multiuser detection and channel equalisation can be carried out at the transmitter. This is achieved with *linear precoding* of the transmitted signal. The receiver structure at the user equipment is then simplified when compared to a multiuser detection receiver, and can be a conventional matched filter (which only requires knowledge of the desired user's spreading code). Thus no channel estimation or adaptive equaliser implementation is required at the mobile receiver. Techniques which only require a matched filter receiver also enhance the system capacity since no system resources have to be allocated for the transmission of training signals on the downlink.

One previously developed transmitter technique is *Pre-equalisation* [3] which includes pre-RAKE diversity combining at the transmitter. In the downlink the desired user's signal is maximal ratio combined while other user's signals are not. Under this scenario the receiver is just a fixed filter matched to the desired user's code. Although the pre-RAKE method reduces the multipath channel effects, it unfortunately doesn't reduce the multiuser interference even if used in conjunction with orthogonal sequences as shown in [3], [4].

To achieve a sufficient performance the transmitted signals in the downlink must be jointly optimised based on the spreading code and the channel impulse response of every user. Such transmitter based multiuser detection schemes are *Transmitter precoding* (TP), described in [5] and *Joint transmission* (JT), proposed in [6]. Both JT and TP jointly precode blocks of data and require a matched filter receiver. For a large block-length the computational cost is increased since these algorithms include inversion of matrices whose dimensions are proportional to the number of users and the block length and as it will be shown the complexity per symbol transmitted is extensive. Furthermore, in the case of multipath channel and presuming that the data is transmitted continually, the first and last bits are not correctly precoded which leads to a capacity loss. Thus, a bitwise technique that overcomes these drawbacks should be sought.

Such a bitwise technique was first introduced in [7] as *decorrelating pre-filters* (DPF). A conventional matched filter is assumed in the mobile station. According to this technique the spread data is pre-filtered before transmission in an effort to orthogonalise them with respect to each other. The tap coefficients of the pre-filters are calculated with a zero-forcing (ZF) algorithm.

In this work we propose *inverse filters* (INVF) for the equalisation of the response of multichannel/multiuser systems and the structure is the same as [7]. The mobile receiver is a conventional matched filter. The intention is to equalise the multipath channels and minimise the crosscorrelation of the users. The key is that the whole system in a cell is emulated by the base station as the channels of the active users and their receivers structure are assumed

to be known. The coefficients of the pre-filters are then adaptively calculated using the multichannel least mean square (MC-LMS) or recursive least squares (MC-RLS) algorithms. The developed algorithm uses a minimum mean squared error (MMSE) criterion which results in a solution which is different from DPF and gives an improved performance. Furthermore, the proposed algorithm is free of the data-block techniques drawbacks.

The system model is given in section II. Section III presents a theoretical analysis and in section IV the simulation results are presented along with a comparison to recently published methods. The conclusions are discussed in section V.

II. System model

The system considered is a wireless multiuser direct sequence TDD-CDMA system with K active users in a cell communicating through a common base station (BS). The BS has one antenna element and transmits synchronously over frequency selective channels to K mobile stations (MS).

The discrete time transmission model sampled at chip rate $1/T_c$ is described as follows. BPSK data d_k for user k,$k \in \{1, \cdots, K\}$ is spread with the spreading code $c_k(n)$. The spreading code consists of Q chips of duration T_c and it is described by the vector

$$\mathbf{c}_k = [c_k^1 \cdots c_k^Q]^T \tag{1}$$

which is normalised such that $\|\mathbf{c}_k\| = 1$. The symbol interval is T_s and the chip interval T_c so as $T_c = T_s/Q$. The k_{th} channel is characterised by its impulse response $h_k(n)$. It can be considered as an FIR filter whose tap coefficients are the vector $\mathbf{h}_k$ normalised to $\|\mathbf{h}_k\| = 1$.

$$\mathbf{h}_k = [h_k^1 \cdots h_k^W]^T \tag{2}$$

where W is the length of the channel when sampled at the chip rate. Assuming that symbol d_k is transmitted with power w_k, the total downlink signal for the conventional downlink scenario is described as:

$$\sum_{k=1}^{K} c_k(n)\sqrt{w_k}d_k \tag{3}$$

Therefore the received signal e_j at the j_{th} MS is a superposition of all users filtered by the j_{th} channel $h_j(n)$:

$$e_j(n) = \sum_{k=1}^{K} \left(c_k(n)\sqrt{w_k}d_k\right) * h_j(n) + v(n) \tag{4}$$

For the rest of the paper the w_k is normalised to have unit total power for all $k \in \{1 \ldots K\}$. $v(n)$ is zero mean AWGN whose covariance is:

$$E\left(v^2(n)\right) = N_o/2 \tag{5}$$

The multipath channel length is assumed to be less than a symbol's period and thus ISI is extended only to the next transmitted symbol. Throughout our analysis the users are synchronous which is realistic for the downlink and they are transmitted with equal power. Once more the methods presented in this paper rely on transmitter (BS) knowledge about all users spreading codes and channels which is satisfied for the TDD mode if the channel's dynamics are sufficiently slow. This means that the multipath profile remains essentially constant during transmission.

III. Analysis of proposed system

In the proposed system the data of user k after being spread is pre-filtered by an FIR filter of length P, with a discrete time impulse response $p_k(n)$, as shown in fig. 1. The produced signals are then summed to $s(n)$ and transmitted from the antenna element. Vector $\mathbf{p}_k$ of P length represents the tap coefficients of the k_{th} user specific FIR filter.

$$\mathbf{p}_k = [p_k^1 \cdots p_k^P]^T \tag{6}$$

The mobile receiver has been reduced to $c_k(T_s - n)$ which is a time inverse of the spreading code assigned to each individual user. It is equivalent to the conventional matched filter detector in CDMA, optimal for a single user over a flat-fading channel.

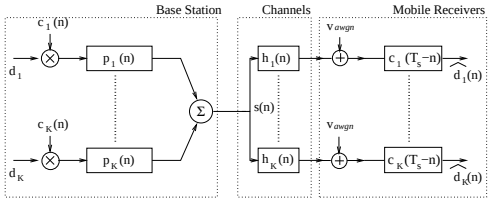

Fig. 1. Block diagram of the proposed system

If vectors $\mathbf{p}_k$, eq. (6), are arranged in a KP-length vector $\mathbf{p}$ as below

$$\mathbf{p} = [\mathbf{p}_1^T \cdots \mathbf{p}_k^T \cdots \mathbf{p}_K^T]^T \tag{7}$$

we can write the system's average total energy per transmitted symbol $Eg(\mathbf{p})$ as a function of $\mathbf{p}$, which is necessary for the derivation of the power constrained solution.

$$Eg(\mathbf{p}) = \mathbf{p}^T\mathbf{U}^T \cdot \mathbf{U}\mathbf{p} \tag{8}$$

$\mathbf{U}$ a matrix of size $K(Q+P-1) \times KP$:

$$\mathbf{U} = blockdiag\left(\mathbf{U}_1, \cdots, \mathbf{U}_K\right)$$

and $\mathbf{U}_k$ is a matrix of dimension $(Q+P-1) \times P$:

$$\mathbf{U}_k = \{U_k^{i,j}\}; \quad i = 1 \ldots Q+P-1, \quad j = 1 \ldots P$$

$$U_k^{i,j} = \begin{cases} c_k^{i-j+1} & for \quad 1 \le i-j+1 \le Q \\ 0 & otherwise \end{cases} \tag{9}$$

The same architecture for the transmitter has been previously proposed in [7] as 'decorrelating pre-filters'. The coefficients of the filter taps are determined with a ZF technique solving K systems of equations which involves the inverse of matrices. The DPF algorithm is briefly presented below:

$$\max_{p_k}\left(c_k(n) * p_k(n) * h_k(n) * c_k(T_s - n)\right)|_{n=T_{ss}}$$

subject to constraints:

$$\begin{aligned} \left(c_l(n) * p_l(n) * h_k(n) * c_k(T_s - n)\right)|_{n=T_{ss}} &= 0 \;\forall\; l \neq k \\ \|\mathbf{p}_k * \mathbf{c}_k\| &= 1 \end{aligned} \tag{10}$$

where T_{ss} is the decision sample. The second constraint allows for the desired power normalisation. Each user is individually normalised to achieve a specified received SNR in contrast with the global normalisation derived in eq. (27).

In the current work an emulation of all channels and receivers is performed in the BS exploiting the fact that the channels have been estimated in the BS during the last uplink burst and thus the whole downlink system is known. The BS uses the MC-LMS or MC-RLS algorithms [8] to adaptively converge to the optimal, in MMSE terms, taps of the inverse filters. The Wiener solution that includes the necessary power constraint is also stated. Inverse filters consist of a simple addition of an array of FIR filters to the existing BS system. The analysis that follows is similar to the analysis in [9] for stereophonic sound reproduction.

A. MMSE power constrained solution

The block diagram of the emulation that takes place in the BS is shown in fig. 2. After pre-filtering the spread sig-

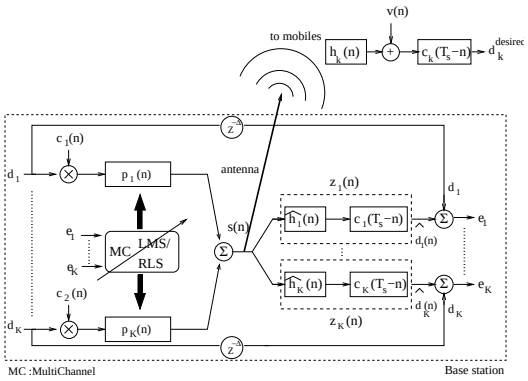

Fig. 2. Block diagram of emulation in the BS

nal of k_{th} user becomes $d_k c_k(n) * p_k(n)$ and the transmitted signal $s(n)$ is the superposition of all the users :

$$s(n) = \sum_{k=1}^{K} d_k(n) c_k(n) * p_k(n) \tag{11}$$

This signal is sent to the BS antenna element and an internal block that emulates the real receivers and their corresponding channels. The BS has an estimation $\hat{h}_k(n)$ of the downlink channels $h_k(n)$ and the remote receivers $c_k(T_s - n)$ are also known to the BS. By emulating the system, the BS can estimate the output $\hat{d}_k(n)$ sampled from the mobile:

$$\hat{d}_k(n) = s(n) * \hat{h}_k(n) * c_k(T_s - n) \tag{12}$$

The error in estimation $e_k = d_k - \hat{d}_k$ is fed back to the adaptive multichannel algorithm to determine the pre-filter taps. For simplicity we substitute the cascaded filters $\hat{h}_k(n)$ and $c_k(T_s - n)$ with an FIR filter of length $Z = Q + W - 1$ and impulse response $z_k(n) = \hat{h}_k(n) * c_k(T_s - n)$. Eq. (12) becomes:

$$\hat{d}_k(n) = s(n) * z_k(n) \tag{13}$$

After rearrangement, the system can be equivalently illustrated as in fig. 3 for the μ_{th} receiver. It has to be clear

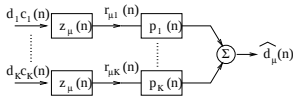

Fig. 3. Rearranged diagram of μ_{th} receiver

that this approximation is only to facilitate the mathematical analysis. Signals $r_{\mu\nu}(n)$,$\mu, \nu \in \{1 \dots K\}$, are defined as filtered reference signals and are produced by passing the signal $d_\nu c_\nu(n)$ through the filters with impulse response $z_\mu(n)$.

$$r_{\mu\nu}(n) = d_\nu c_\nu(n) * z_\mu(n) \tag{14}$$

This 'transfer function reversal' approach is essentially the one taken by [10] in deriving the multiple error LMS algorithm. This block diagram arrangement can now be used to determine the optimal, in minimum mean squared error terms, finite impulse response filters, $\mathbf{p}_k$. The fact that noise $v(n)$ is not included in the rearranged diagram doesn't affect the solution because the noise is not filtered by the inverse filters.

We define the following vectors of the filtered reference signals:

$$\mathbf{r}_{\mu\nu}(n) = [r_{\mu\nu}(n) \cdots r_{\mu\nu}(n - P + 1)]^T, \quad \mu, \nu = 1 \dots K \tag{15}$$

Following then the block diagram in fig. 3 the filtered reference signals are passing from the pre-filters $\mathbf{p}$, as in eq. (7), to yield the estimate desired data. The outputs $\hat{\mathbf{d}}(n)$ can be written in matrix form as:

$$\hat{\mathbf{d}}(n) = \mathbf{R}(n)\mathbf{p} \tag{16}$$

where the vector $\hat{\mathbf{d}}(n)$ and the matrix $\mathbf{R}(n)$ are denoted as:

$$\hat{\mathbf{d}}(n) = \begin{bmatrix} \hat{d}_1(n) \\ \vdots \\ \hat{d}_K(n) \end{bmatrix}, \mathbf{R}(n) = \begin{bmatrix} \mathbf{r}_{11}^T(n) & \cdots & \mathbf{r}_{1K}^T(n) \\ \vdots & \ddots & \vdots \\ \mathbf{r}_{K1}^T(n) & \cdots & \mathbf{r}_{KK}^T(n) \end{bmatrix} \tag{17}$$

We now seek the optimal filter vector $\mathbf{p}$ to minimise the time averaged squared error between the actual and desired outputs. The desired outputs are sampled at the symbol period $T_s^n = nT_s + \Delta$, $n = 1, 2, \dots$, where Δ is an imposed delay to the system which assists the equalisation of the multipath channels [11]. In the final cost function we must include, using Lagrange multipliers, that the average transmitted power per symbol should not exceed E_{max}. Thus the cost function to be minimised is:

$$J = E[(\mathbf{d} - \hat{\mathbf{d}}(T_s^n))^T (\mathbf{d} - \hat{\mathbf{d}}(T_s^n))] + \lambda\big(Eg(\mathbf{p}) - E_{max}\big) \tag{18}$$

where E denotes the expectation and $\mathbf{d}$ is the vector of desired data, defined as $\mathbf{d} = [d_1 \cdots d_K]^T$. The vector $\hat{\mathbf{d}}$ is replaced by the right part of eq. (16) and by using the expectation operator eq. (18) is expanded to the quadratic form:

$$\begin{aligned} J \;=\; & E[\mathbf{d}^T\mathbf{d}] - 2E[\mathbf{d}^T\mathbf{R}(T_s^n)]\mathbf{p} + \mathbf{p}^T E[\mathbf{R}^T(T_s^n)\mathbf{R}(T_s^n)]\mathbf{p} + \\ & \lambda\big(Eg(\mathbf{p}) - E_{max}\big) \end{aligned} \tag{19}$$

From vector gradient theory and eq. (8) we find that $\partial Eg(\mathbf{p})/\partial \mathbf{p} = 2\mathbf{U}^T\mathbf{U}\mathbf{p}$. Therefore the Wiener solution for the taps of the inverse filters $\mathbf{p}_o$ is given by

$$\mathbf{p}_o = \left[E[\mathbf{R}^T(T_s^n)\mathbf{R}(T_s^n)] + \lambda \mathbf{U}^T\mathbf{U}\right]^{-1} E[\mathbf{R}^T(T_s^n)\mathbf{d}] \tag{20}$$

B. Adaptive solution

An alternative technique to the direct solution of eq. (20), without any matrix inversion is to use the MC-LMS algorithm [10] which provides a multichannel generalisation of Widrow's filtered-x LMS algorithm [11]. Thus the method of steepest descent can be used to descend toward the minimum on the performance surface of the quadratic form in eq. (19). The values of the pre-filter taps weight vector are iteratively updated by an amount proportional to the negative of the gradient of the quadratic performance surface. The gradient of eq. (19) without the power constraint term becomes:

$$\frac{\partial J}{\partial \mathbf{p}} = -2E[\mathbf{R}^T(T_s^n)\mathbf{d}] + 2E[\mathbf{R}^T(T_s^n)\mathbf{R}(T_s^n)]\mathbf{p} \tag{21}$$

By defining the instantaneous error vector as:

$$\mathbf{e}(T_s^n) = \mathbf{d} - \hat{\mathbf{d}}(T_s^n) = \mathbf{d} - \mathbf{R}(T_s^n)\mathbf{p} \tag{22}$$

and substituting in eq. (21) the gradient is expressed as:

$$\frac{\partial J}{\partial \mathbf{p}} = -2E[\mathbf{R}^T(T_s^n)\mathbf{e}(T_s^n)] \tag{23}$$

If each pre-filter taps vector is now adjusted at every sample time by an amount proportional to the negative instantaneous value of the gradient, a modified form of the well-known LMS algorithm is produced:

$$\mathbf{p}(T_s^n) = \mathbf{p}(T_s^{n-1}) + \mu \mathbf{R}^T(T_s^n)\mathbf{e}(T_s^n) \tag{24}$$

where μ is the step-size parameter of the algorithm.

A second adaptive algorithm to calculate the taps $\mathbf{p}_k$ for the pre-filters is the MC-RLS described in [8]. Let $KP \times K$ matrix $\mathbf{V}(n)$ be:

$$\mathbf{V}(n) = \begin{bmatrix} \mathbf{r}_{11}(n) & \cdots & \mathbf{r}_{K1}(n) \\ \vdots & \ddots & \vdots \\ \mathbf{r}_{1K}(n) & \cdots & \mathbf{r}_{KK}(n) \end{bmatrix} \tag{25}$$

Then the multichannel RLS algorithm is:

$$\begin{aligned}
\mathbf{M}(0) &= \delta^{-1}\mathbf{I}, \quad \mathbf{I}: \ K \times K \text{ Identity matrix} \\
\mathbf{p}(0) &= \mathbf{0} \\
\mathbf{K}(T_s^n) &= \theta^{-1}\mathbf{M}(T_s^{n-1})\mathbf{V}(T_s^n) \\
&\quad \left[\mathbf{I} + \theta^{-1}\mathbf{V}^T(T_s^n)\mathbf{M}(T_s^{n-1})\mathbf{V}(T_s^n)\right]^{-1} \\
\mathbf{e}(T_s^n) &= \mathbf{d}(T_s^n) - \mathbf{R}(T_s^n)\mathbf{p}(T_s^{n-1}) \\
\mathbf{p}(T_s^n) &= \mathbf{p}(T_s^{n-1}) + \mathbf{K}(T_s^n)\mathbf{e}(T_s^n) \\
\mathbf{M}(T_s^n) &= \theta^{-1}\mathbf{M}(T_s^{n-1}) - \theta^{-1}\mathbf{K}(T_s^n)\mathbf{V}^T(T_s^n)\mathbf{M}(T_s^{n-1})
\end{aligned} \tag{26}$$

where θ, $0.9 \leq \theta \leq 1.0$, is the forgetting factor and δ a small positive constant.

After setting the filter coefficients we must scale the transmitted signal $s(n)$ with a factor $\sqrt{\mathcal{F}}$ to achieve the desired average total transmitted energy per symbol and this is done for all the techniques in the following section for the sake of fair comparison. As the reference power Eg^{CDMA} we use the one of a corresponding CDMA system without any precoding.

$$\mathcal{F} = \frac{Eg^{CDMA}}{\sum_{k=1}^{K} \|\mathbf{c}_k * \mathbf{p}_k\|^2} \tag{27}$$

where the denominator is the total transmitted power per symbol for the proposed system.

IV. Simulation results

In this section the performance of the adaptive inverse filters is shown and compared to the pre-RAKE, JT, TP and DPF. BPSK data symbols d_k are spread by random binary spreading codes $\mathbf{c}_k$ of length $Q = 16$ and transmitted synchronously over the mobile channel. Variations of the received power due to path loss and log-normal fading are assumed to be eliminated by power control. Each of the users is assumed to be transmitted with equal energy which is normalised to have unit amplitude. The codes are also normalised to have unit power. A normalised mobile radio channel is given by its channel impulse response $\mathbf{h}_k$, which is derived from the UMTS models. The delay profile, adopted, is the one of the vehicular environment A described in [12], with channel length $W = 11$. In the current paper the channels are assumed to be stationary with no Doppler effects. Perfect knowledge of the channels is presumed for the receiver based estimate. Thus the emulation in the BS under this ideal scenario reflects the real system. Equal average transmitted energies per symbol for all the compared systems has been forced for a fair comparison.

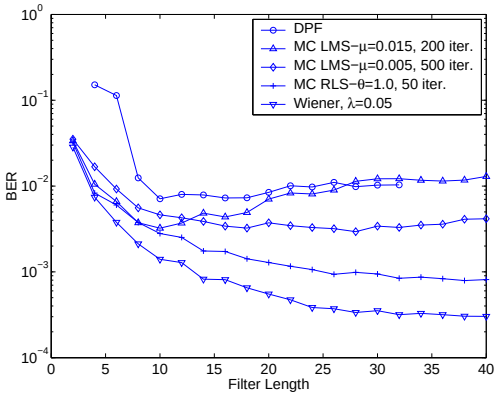

Fig. 4. BER versus Filter Length for $E_b/N_o = 8dB$, $K = 5$ users

In fig. 4 the bit error rate performance of a $K = 5$ users system is displayed versus the length of the pre-filters for DPF and adaptive INVF. The E_b/N_o is set to $8dB$ and $\Delta = P/2$. The MC-RLS, for $\theta = 1.0$, and MC-LMS, for $\mu = 0.005$ display by far better performance than the filters whose taps are determined according to [7]. For $\mu = 0.015$ the convergence is faster as shown in the next figure but the performance is not as good as with $\mu = 0.005$. Furthermore, DPF restricts the pre filters to a length $P \leq \Delta + Q$.

In fig. 5 the convergence speed of one user for the various adaptive algorithms is presented. The system has

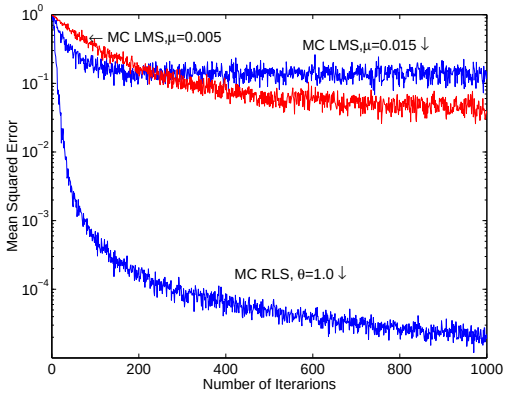

Fig. 5. Mean squared error of user 1 vs iterations for 32 taps filters

$K = 5$ users, pre-filters length is set to $P = 32$, delay to $\Delta = 16$ and an ensemble of 50 experiments is given for every algorithm. By choosing a large step-size parameter $\mu = 0.015$ MC-LMS achieves a faster convergence at the cost of deteriorated performance while smaller $\mu = 0.005$ cancels sufficiently MAI and ISI at the cost of slower convergence. It is shown that after 50 transmitted bits MC-RLS reaches a very small mean squared error at a cost of increased complexity per iteration. The MC-RLS does not exactly reach the Wiener solution as shown in fig. 4 because it increases the transmitted power and by using normalisation factor $\sqrt{\mathcal{F}}$ we decrease the signal to noise ratio.

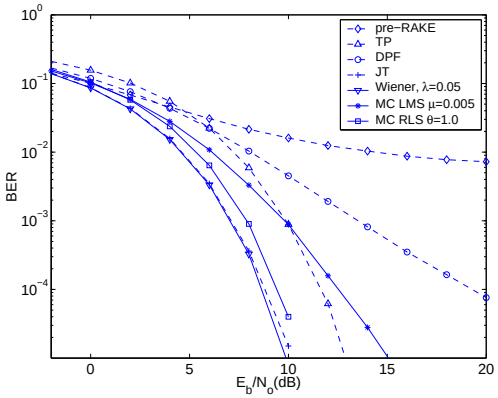

Fig. 6. BER vs E_b/N_o, $P = 32$, $\Delta = 16$, $K = 5$ users

In fig. 6 the BER performance versus E_b/N_o is displayed for a CDMA system of $K = 5$ users. The pre-filter taps have a length of $P = 32$ chips and the delay Δ imposed in the system is 16 chips. For TP and JT the length N of data block is set to 20. The performance of the Wiener solution along with the one after convergence of the adaptive algorithms is shown in the same figure. Both multichannel RLS and LMS outperform pre-RAKE, DPF and TP techniques. The Wiener solution and the joint transmission have almost the same performance. The advantage of the proposed technique is that the calculation takes place only once at the beginning of the transmission since it doesn't handle blocks of data and thus it is characterised as bitwise.

Ignoring the inversion of matrices required for data block techniques, and the adaptation process required for converging to the Wiener solution of INVF it can be proven that for JT and a block of length N data the multiplications required per symbol transmission are $NQ(KN)^2/KN$ whereas for the INVF is PQ. For instance, a system of $N = 20, Q = 16, K = 5, P = 32$ requires 32000 multiplications under JT and only 512 under INVF. Furthermore, with JT, assuming that blocks are transmitted continually, a decrease of the block length results in a capacity loss as data block techniques do not precode correctly the end bits.

V. Conclusions

A novel technique, called inverse filters, that exploits the knowledge of the downlink channel in TDD was presented. The technique takes the structure presented in [7] and develops the MMSE solution for individually pre-filtering the spread data before transmission. An emulation of the system is performed in the BS and the necessary pre-filters taps are calculated adaptively. The process takes place once before transmission instead of being repeated for every block of data and no matrix inversion is required. The performance exceeds that of pre-RAKE, DPF and TP, while it is equivalent to JT for large data blocks, which suffers from extensive computational cost and complexity. Space time techniques and efforts to make the adaptation process faster are under investigation.

References

[1] Sergio Verdú, *Multiuser Detection*, Cambridge University Press, 1 edition, 1998.

[2] A. Duel-Hallen, J.H., and Z. Zvonar, "Multiuser detection for CDMA systems," *IEEE Personal Communications*, vol. 2, no. 2, pp. 46–58, Apr. 1995.

[3] R. Esmailzadeh, E. Sourour, and M. Nakagawa, "Pre-rake diversity combining in time division duplex CDMA mobile communications," *IEEE Trans. on Vehicular Technology*, vol. 48, no. 3, pp. 795–801, May 1999.

[4] S. Georgoulis and D.G.M. Cruickshank, "Pre-equalization, transmitter precoding and joint transmission techniques for time division duplex CDMA," *IEE 3G 2001 Conference on Mobile Telecommunications Technologies*, pp. 257–261, Mar. 2001.

[5] B. R. Vojčić and W. M. Jang, "Transmitter precoding in synchronous multiuser communications," *IEEE Trans. on Communications*, vol. 46, no. 10, pp. 1346–1355, Oct. 1998.

[6] M. Meurer, P.W. Baier, T. Weber, Y. Lu, and A. Papathanasiou, "Joint transmission:advantageous downlink concept for CDMA mobile radio systems using time division duplexing," *IEE Electronics Letters*, vol. 36, pp. 900–901, May 2000.

[7] M. Brandt-Pearce and A. Dharap, "Transmitter-based multiuser interference rejection for the down-link of a wireless CDMA system in a multipath environment," *IEEE Journal on Selected Areas in Communications*, vol. 18, no. 3, pp. 407–417, Mar. 2000.

[8] M. Bouchard and S. Quednau, "Multichannel recursive-least-squares algorithms and fast-transversal-filter algorithms for active noise control and sound reproduction systems," *IEEE Trans. on Speech and Audio Processing*, vol. 8, no. 5, pp. 606–618, Sep. 2000.

[9] P.A. Nelson, H. Hamada, and S. Elliott, "Adaptive inverse filters for stereophonic sound reproduction," *IEEE Trans. on Signal Processing*, vol. 40, no. 7, pp. 1621–1632, Jul. 1992.

[10] S.J. Elliott, I.M. Stothers, and P.A. Nelson, "A multiple error LMS algorithm and its application to the active control of sound and vibration," *IEEE Trans. on Acoustics, Speech and Signal Processing*, vol. 35, no. 10, pp. 1423–1434, Oct. 1987.

[11] Bernard Widrow, *Adaptive Signal Processing*, Prentice-Hall, 1985.

[12] "Selection procedures for the choice of radio transmission technologies of the UMTS (UMTS 30.03 version 3.2.0)," .

Transmitter Based Inverse Filters for MAI and ISI Mitigation in a TDD/CDMA Downlink

S.L. Georgoulis and D.G.M. Cruickshank
Department of Electronics and Electrical Engineering, The University of Edinburgh
email: sg@ee.ed.ac.uk, dgmc@ee.ed.ac.uk

Abstract— **Recently research has been focused on techniques that simplify the mobile receiver structure in a CDMA system by means of signal precoding. These methods assume knowledge of the channel at the transmitter which is feasible in a time division duplex (TDD) system where the channel is assumed to be the same on uplink and downlink. In this paper a novel algorithm based on pre-filtering the spread signal in the base station is described. The pre-filter taps are determined with a MMSE criterion and the necessary power constraint. We shall show that this technique increases the system capacity with a low computational cost compared with existing schemes. The portable unit's structure is reduced to the conventional receiver for a single user in an AWGN channel, a matched filter. Thus no channel estimation, equalisation or multiuser detection is required at the mobile. The theoretical analysis is supported with simulation results where the performance is compared to other recently published methods.**

I. Introduction

In a CDMA scheme the major impairements are the multiple access interference (MAI) due to simultaneous usage of the bandwidth by many users and intersymbol interference (ISI) due to multipath fading channels. In the state of the art for CDMA systems the *multiuser detection* problem in multipath environment has been studied extensively and a number of solutions have been proposed in [1], [2], [3]. These techniques are all receiver based, they usually require channel estimation, knowledge of all the active user spreading codes and they have considerable computational cost. This contrasts with the desire to keep portable units simple and power efficient.

An alternative to multiuser detection is to precode the transmitted signal such that the ISI and MAI effects are minimised before transmission. The extra computational cost is transfered to the base station where power and computational resources are more readily available. Recently, work has been done on algorithms that exploit the fact that in a TDD scheme the downlink channel is known to the transmitter if the time elapsing between uplink and downlink transmissions is sufficiently small compared to the coherence time of the mobile radio channel. The receiver structure is then simplified when compared to a multiuser detection receiver and can be a conventional filter matched to the desired user's spreading code. Such techniques also enhance the system capacity since no system resources have to be allocated for the transmission of training signals on the downlink.

To achieve a sufficient performance the transmitted signals in the downlink must be jointly optimised based on the spreading code and the channel impulse response of every user. Such transmitter based multiuser detection schemes are *transmitter precoding* (TP), described in [4] and *joint transmission* (JT), proposed in [5]. TP was described in [4] for both the case of a RAKE and a matched filter receiver but in this paper we consider only techniques that require a matched filter. Both JT and TP jointly precode blocks of data. For a large block-length the computational cost is increased since these methods require inversion of matrices whose dimensions are proportional to the number of users and the block length and as will be shown, the complexity per symbol transmitted is extensive. Furthermore, in the case of multipath channels and presuming that the data is transmitted continually, the first and last bits in a block are not correctly precoded which leads to a capacity loss. Thus, a bitwise technique that overcomes these drawbacks should be sought.

One straightforward bitwise transmitter technique is *pre-RAKE* [6] which includes pre-RAKE diversity combining at the transmitter. Although the pre-RAKE method reduces the multipath channel effects, it unfortunately doesn't reduce the multiuser interference as shown in [6], [7]. A second bitwise technique is introduced in [8] as *decorrelating pre-filters* (DPF). According to this technique the spread data is pre-filtered before transmission in an effort to orthogonalise users with respect to each other. The taps of the pre-filters are calculated with the ZF algorithm and this tends to increase unacceptably the transmitted power. In this work we propose *inverse filters* (INVF) for multichannel/multiuser systems and the structure is the same as in [8]. This time, the tap-coefficients have been determined using an MMSE approach with the necessary power constraint included. The solution is different from DPF and gives an improved performance and as a bitwise technique it eliminates the data-block techniques drawbacks.

The system model is given in section II. In section III a brief description of transmitter based techniques is given and in section IV the theoretical analysis of the inverse filters is developed. The simulation results are presented in section V along with a comparison to recently published methods. The conclusions are discussed in section VI.

II. System Model

The system considered is a wireless multiuser direct sequence TDD-CDMA system with K active users in a cell communicating through a common base station (BS). The BS has one antenna element and transmits synchronously (which is realistic for the downlink) over frequency selective channels to K mobile stations (MS). The discrete time transmission model sampled at the chip rate $1/T_c$ is described as follows.

The m_{th} symbol for user k, $k\epsilon\{1\cdots K\}$, is the BPSK modulated data d_k^m spread with the spreading code $c_k(n)$, $d_k^m c_k(n)$. The spreading code consists of Q chips and it is described by the vector $\mathbf{c}_k = [c_k(0)\cdots c_k(Q-1)]^T$ which is normalised such that $\|\mathbf{c}_k\| = 1$. The symbol interval is T_s so $T_c = T_s/Q$.

The k_{th} channel is characterised by its impulse response $h_k(n)$. It can be considered as an FIR filter whose chip spaced tap-coefficients are the vector $\mathbf{h}_k = [h_k(0) \cdots h_k(W-1)]^T$, where W is the delay spread of the channel when sampled at the chip rate. Assuming that the m_{th} symbol of power w_k^m is transmitted for the k_{th} user, the total transmitted downlink signal for the conventional CDMA downlink scenario is described as:

$$s(n) = \sum_{k=1}^{K} \sqrt{w_k^m}\, d_k^m\, c_k(n) \tag{1}$$

In this work all the users are transmitted with equal power and thus w_k^m is normalised to one.

Let $\mathbf{d}_k$ be a vector sequence of $N = 2M+1$ transmitted bits for user k

$$\mathbf{d}_k = [d_k^{-M} \cdots d_k^0 \cdots d_k^M]^T \tag{2}$$

The vector $\mathbf{d}$ of length KN is a block of data that contains the bits of all the users and is defined as :

$$\mathbf{d} = \left[\mathbf{d}_1^T \cdots \mathbf{d}_k^T \cdots \mathbf{d}_K^T\right]^T \tag{3}$$

By defining now the $NQ \times N$ matrix $\mathbf{C}_k$

$$\mathbf{C}_k = \{C_k^{i,j}\} \quad ; \quad i = 1...NQ, j = 1...N$$

$$C_k^{i,j} = \begin{cases} c_k(i - Q(j-1) - 1) & for \quad 0 \le i - Q(j-1) - 1 \le Q-1 \\ 0 & otherwise \end{cases} \tag{4}$$

and the $NQ \times NK$ matrix $\mathbf{C}$ as $\mathbf{C} = \left[\mathbf{C}_1 \cdots \mathbf{C}_k \cdots \mathbf{C}_K\right]$ the NQ-length vector form for signal $\mathbf{s}$, in eq. (1), for a conventional CDMA downlink system is $\mathbf{s} = \mathbf{C}\mathbf{d}$. The received signal $e_k(n)$ at the k_{th} MS in a vector form is of length $NQ + W - 1$ and is written as $\mathbf{e}_k = \mathbf{H}_k\mathbf{s} + \mathbf{v}$, where matrix $\mathbf{H}_k$ is of size $(NQ + W - 1) \times (NQ)$:

$$\mathbf{H}_k = \{H_k^{i,j}\} \quad ; \quad i = 1 \ldots NQ + W - 1, j = 1 \ldots NQ$$

$$H_k^{i,j} = \begin{cases} h_k(i-j) & for \quad 0 \le i - j \le W - 1 \\ 0 & otherwise \end{cases} \tag{5}$$

and $\mathbf{v}$ is a $NQ + W - 1$ vector of zero mean AWGN and covariance matrix $\mathbf{V}_n = E(\mathbf{v}\,\mathbf{v}^T) = \sigma^2\mathbf{I}$.

The receiver is restricted to be a conventional filter matched to the spreading code of the desired user. Its impulse response is $c_k(Q-n)$ and its output vector is $\hat{\mathbf{d}}_k = \mathbf{B}_k^T\mathbf{e}_k$, where the $(NQ + W - 1) \times N$ matrix $\mathbf{B}_k$ is defined as $\mathbf{B}_k = \left[\mathbf{C}_k^T\ \mathbf{O}\right]^T$ and $\mathbf{O}$ is a $N \times (W-1)$ zero matrix.

The multipath channel length is assumed to be less than one symbol period and thus ISI is extended only to the next transmitted symbol. Once more the methods presented in this paper rely on transmitter (BS) knowledge about all users spreading codes and channels which is satisfied for the BS using a TDD mode if the channel's dynamics are sufficiently slow. This means that the multipath profile remains essentially constant during transmission.

III. Transmitter Based Techniques

A. Data-block and bitwise techniques

Transmitter precoding is introduced in [4]. The author seeks a linear transformation matrix $\mathbf{T}$ to apply to the block of transmitted data $\mathbf{d}$ in order to minimise MAI and ISI. By applying a MMSE criterion over the noise and the transmitted bits the resulting $KN \times KN$-size $\mathbf{T}$ matrix is given by:

$$\mathbf{T} = \left\{[\mathbf{T}_1^T \cdots \mathbf{T}_k^T \cdots \mathbf{T}_K^T]^T\right\}^{-1}$$

where $\mathbf{T}_k$ is a $N \times KN$ matrix given by $\mathbf{T}_k = \mathbf{B}_k^T\mathbf{H}_k\mathbf{C}$. After being precoded the data is spread and the transmitted signal $\mathbf{s}$ becomes:

$$\mathbf{s} = \mathbf{C}\mathbf{T}\mathbf{d} = \boldsymbol{\mathcal{T}}_{TP}\,\mathbf{d} \tag{6}$$

In joint transmission [9] a common signal $\mathbf{s}$, which gives the desired data at the output of every user's receiver is sought for transmission. As shown in [9], $\mathbf{s}$ is:

$$\mathbf{s} = \mathbf{H}^T\mathbf{B}\left(\mathbf{B}^T\mathbf{H}\,\mathbf{H}^T\mathbf{B}\right)^{-1}\mathbf{d} = \boldsymbol{\mathcal{T}}_{JT}\mathbf{d} \tag{7}$$

The $K(NQ + W - 1) \times NQ$ matrix $\mathbf{H}$ is defined as an arrangement of $\mathbf{H}_k$ matrices, $\mathbf{H} = \left[\mathbf{H}_1^T \cdots \mathbf{H}_k^T \cdots \mathbf{H}_K^T\right]^T$ and the $K(NQ + W - 1) \times KN$ block diagonal matrix $\mathbf{B}$ is $\mathbf{B} = blockdiag\left(\mathbf{B}_1, \cdots, \mathbf{B}_k, \cdots, \mathbf{B}_K\right)$.

In the bitwise techniques, including our new algorithm, the data of each user k after being spread is pre-filtered by an FIR filter of length P with a discrete time impulse response $p_k(n)$ as shown in fig. 1. The produced signals are then summed and transmitted from the antenna element. The taps of the pre-filters are determined by the adopted technique. Vector $\mathbf{p}_k$ represents the tap-coefficients of the k_{th} user specific FIR pre-filter.

$$\mathbf{p}_k = [p_k(0) \cdots p_k(P-1)]^T \tag{8}$$

Pre-RAKE [6] is a straight forward algorithm where the BS filters the k_{th} user's signal with the time inverted uplink channel impulse response of the same user. In the downlink the desired user's signal is maximal ratio combined by the channel itself while other user's signals are not. The result is a strong peak at the output of the channel which is equivalent to the RAKE receiver's output.

DPF, as presented in [8], calculates the pre-filter tap-coefficients with a zero forcing algorithm as presented below.

$$\max_{\mathbf{p}_k}\left(c_k(n) * p_k(n) * h_k(n) * c_k(Q-n)\right)|_{n=T_{ss}}$$

subject to constraints:

$$\begin{aligned} \left(c_l(n) * p_l(n) * h_k(n) * c_k(Q-n)\right)|_{n=T_{ss}} &= 0 \ \forall\ l \neq k \\ \|\mathbf{p}_k * \mathbf{c}_k\| &= 1 \end{aligned} \tag{9}$$

where T_{ss} is the decision sample. The second constraint allows for the desired power normalisation. Each user is individually normalised to achieve a specified received SNR in contrast with the global normalisation derived in eq. (11).

The average total transmitted energy E_g per symbol for a precoding algorithm is given by:

$$E_g = \begin{cases} \frac{trace\{\boldsymbol{\mathcal{T}}^T\boldsymbol{\mathcal{T}}\}}{N} & \text{block techniques} \\ \sum_{k=1}^{K} \|\mathbf{c}_k * \mathbf{p}_k\|^2 & \text{bitwise techniques} \end{cases} \quad (10)$$

where $\boldsymbol{\mathcal{T}}$ is $\boldsymbol{\mathcal{T}}_{TP}$ or $\boldsymbol{\mathcal{T}}_{JT}$ in accordance with the algorithm used. For a flat fading AWGN channel $\boldsymbol{\mathcal{T}}_{TP}$ and $\boldsymbol{\mathcal{T}}_{JT}$ are the same matrices.

B. Power scaling factor

In the above methods, ignoring noise and assuming a unit gain channel the aim is $\hat{d}_k^m = d_k^m$. Depending on the method employed, a certain transmit power is required for interference elimination which is usually greater than the one required for a conventional spreading. Thus, the transmitted signal $\mathbf{s}$ must be scaled with the appropriate factor $\sqrt{\mathcal{F}}$ to maintain the average transmitted power per symbol to the same level for all the techniques. The reference power used is the one for the corresponding conventional CDMA system, $\mathcal{E}_g$. If $\mathcal{F} < 1.0$, the scaling results in a decrease in the SNR at the receiver decision point. With this in mind, the optimum precoding technique is one that minimises the MAI and ISI and maximises $\mathcal{F}$. If the unscaled total transmission power per symbol produced by any algorithm is denoted as E_g, eq. (10), then $\mathcal{F}$ is given by

$$\mathcal{F} = \mathcal{E}_g / E_g \quad (11)$$

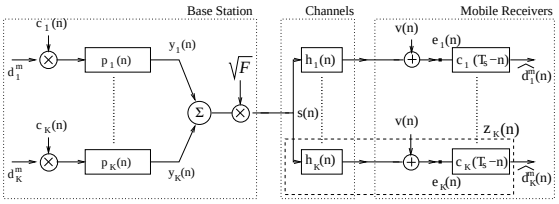

Fig. 1. Block diagram of a bitwise system

IV. Proposed System

The proposed method in this paper maintains the structure in [8] but the algorithm followed to calculate the tap-coefficients is essentially different. A MMSE criterion is chosen and the power constraint has been included in the algorithm so as to minimise the resulting transmitted power. If vectors $\mathbf{p}_k$, (8), are arranged in a KP-length vector $\mathbf{p}$ as below

$$\mathbf{p} = [\mathbf{p}_1^T \cdots \mathbf{p}_k^T \cdots \mathbf{p}_K^T]^T \quad (12)$$

the energy $E_g^{invf}(\mathbf{p})$ of the transmitted signal $\mathbf{s}$ as a function of $\mathbf{p}$ is given by:

$$E_g^{invf}(\mathbf{p}) = \mathbf{p}^T \mathbf{U}^T \cdot \mathbf{U}\mathbf{p} \quad (13)$$

where $\mathbf{U}$ is a matrix of size $K(Q+P-1) \times KP$:

$$\mathbf{U} = blockdiag\left(\mathbf{U}_1, \cdots, \mathbf{U}_k, \cdots \mathbf{U}_K\right)$$

and $\mathbf{U}_k$ is a matrix of dimension $(Q+P-1) \times P$:

$$\mathbf{U}_k = \{U_k^{i,j}\}; \quad i = 1 \ldots Q+P-1, \quad j = 1 \ldots P$$

$$U_k^{i,j} = \begin{cases} c_k(i-j) & for \quad 0 \le i-j \le Q-1 \\ 0 & otherwise \end{cases} \quad (14)$$

The analysis that follows is similar to the non-power constrained analysis for adaptive inverse filters in [10].

A. New least squares power constrained algorithm

As stated before the BS is assumed to have exact knowledge of the downlink channels $h_k(n)$ and the remote receiver $c_k(Q-n)$ structure for all active users. For simplicity we substitute the cascaded filters $h_k(n)$ and $c_k(Q-n)$ with an FIR filter of length $Z = Q+W-1$ and impulse response $z_k(n) = h_k(n) * c_k(Q-n)$, as shown in fig. 1.

After rearrangement, the system can equivalently be illustrated as in fig. 2 for the μ_{th} receiver. This rearrangement is only to facilitate the mathematical analysis. Signals $r_{\mu\nu}(n)$,$\mu, \nu \epsilon \{1 \cdots K\}$ are defined as filtered reference signals and are produced by passing the sequence of symbols $d_k^m c_k(n)$ through the filters with impulse response $z_\mu(n)$. This block diagram arrangement can now be used to determine the optimal, in MMSE terms, finite impulse response filters, $\mathbf{p}_k$. The fact that noise is not included in the rearranged diagram doesn't affect the solution because the noise is not filtered by the inverse filters. The power constraint term imposed in the solution gives good noise performance.

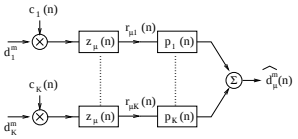

Fig. 2. Rearranged system diagram

We define the following vectors of the filtered reference signals:

$$\mathbf{r}_{\mu\nu}(n) = [r_{\mu\nu}(n) \cdots r_{\mu\nu}(n-P+1)]^T, \quad \mu, \nu = 1 \ldots K \quad (15)$$

Following the block diagram in fig. 2 the filtered reference signals are passed through the pre-filters $\mathbf{p}$, (12), to yield the estimate desired data. The outputs $\hat{\mathbf{d}}_0(n)$ can be written in matrix form as:

$$\hat{\mathbf{d}}_0(n) = \mathbf{R}(n)\mathbf{p} \quad (16)$$

where the vector $\hat{\mathbf{d}}_0(n)$ and the matrix $\mathbf{R}(n)$ are denoted as:

$$\hat{\mathbf{d}}_0(n) = \begin{bmatrix} \hat{d}_1^0(n) \\ \vdots \\ \hat{d}_K^0(n) \end{bmatrix}, \mathbf{R}(n) = \begin{bmatrix} \mathbf{r}_{11}^T(n) & \cdots & \mathbf{r}_{1K}^T(n) \\ \vdots & \ddots & \vdots \\ \mathbf{r}_{K1}^T(n) & \cdots & \mathbf{r}_{KK}^T(n) \end{bmatrix} \quad (17)$$

We now seek the optimal filter vector $\mathbf{p}$ to minimise the time averaged squared error between the actual and desired outputs. The desired outputs are sampled every symbol period

$T_{ss} = nQ + \Delta$, $n = 1, 2, \ldots$, where Δ is an imposed delay to the system which assists the equalisation of the multipath channels [11]. In the final cost function we must include, using Lagrange multipliers, the constraint that the average transmitted power per symbol should not exceed $\mathcal{E}_g$, which is equal to the corresponding conventional CDMA system. The cost function to be minimised is:

$$J = E[(\mathbf{d}_0 - \hat{\mathbf{d}}_0(T_{ss}))^T(\mathbf{d}_0 - \hat{\mathbf{d}}_0(T_{ss}))] + \lambda\left(E_g^{invf}(\mathbf{p}) - \mathcal{E}_g\right) \quad (18)$$

where E denotes the expectation, $\mathbf{d}_0$ is the vector of desired data defined as $\mathbf{d}_0 = [d_1^0 \cdots d_k^0 \cdots d_K^0]^T$ and E_g^{invf} is as in eq. (13). After expansion and use of eq. (16), eq. (18) reduces to the quadratic form:

$$\begin{aligned} J &= E[\mathbf{d}_0^T\mathbf{d}_0] - 2E[\mathbf{d}_0^T\mathbf{R}(T_{ss})]\mathbf{p} + \mathbf{p}^T E[\mathbf{R}^T(T_{ss})\mathbf{R}(T_{ss})]\mathbf{p} \\ &+ \lambda\left(E_g^{invf}(\mathbf{p}) - \mathcal{E}_g\right) \end{aligned} \quad (19)$$

From vector gradient theory and eq. (13) we find that $\vartheta E_g^{invf}(\mathbf{p})/\vartheta\mathbf{p} = 2\mathbf{U}^T\mathbf{U}\mathbf{p}$. Therefore the Wiener solution for the taps of the pre-filters $\mathbf{p}_o$ is given by

$$\mathbf{p}_o = \left[E[\mathbf{R}^T(T_{ss})\mathbf{R}(T_{ss})] + \lambda\mathbf{U}^T\mathbf{U}\right]^{-1} E[\mathbf{R}^T(T_{ss})\mathbf{d}_0] \quad (20)$$

B. Wiener solution

In order to find the analytical Wiener solution $\mathbf{p}_o$, the expectation terms $E[\mathbf{R}^T(T_{ss})\mathbf{R}(T_{ss})]$ and $E[\mathbf{R}^T(T_{ss})\mathbf{d}_0]$ in eq. (20) must be calculated. As stated before $r_{\mu\nu}(n) = d_\nu^m c_\nu(n) * h_\mu(n) * c_\mu(Q-n)$. Let $\gamma_{\mu\nu}(n) = c_\nu(n) * h_\mu(n) * c_\mu(Q-n)$. The corresponding symbol in vector form is denoted as $\boldsymbol{\gamma}_{\mu\nu}$ of length $G = 2Q + W - 2$ due to the convolution effect.

$$\boldsymbol{\gamma}_{\mu\nu} = [\gamma_{\mu\nu}(0) \cdots \gamma_{\mu\nu}(G-1)]^T \quad (21)$$

Vector $\mathbf{r}_{\mu\nu}(n)$ of length P, defined in eq. (15), is given next as a function of the $N = 2M + 1$ vector $\mathbf{d}_\nu$, as in eq. (2), accounting for the ISI effect that is imposed by the pre-filters (M bits transmitted before and after the d_ν^0 bit of interest). By assuming that $\Delta + Q \leq G$, $\Delta + Q \geq P$ (these assumptions are only to assist the description of the Wiener solution as both P and Δ can be arbitrarily chosen) we write:

$$\mathbf{r}_{\mu\nu} = \boldsymbol{\Gamma}_{\mu\nu}\mathbf{d}_\nu \Leftrightarrow \mathbf{r}_{\mu\nu}^T = \mathbf{d}_\nu^T\boldsymbol{\Gamma}_{\mu\nu}^T \quad (22)$$

where the $P \times N$ matrix $\boldsymbol{\Gamma}_{\mu\nu}$ is:

$$\boldsymbol{\Gamma}_{\mu\nu} = \{\Gamma_{\mu\nu}^{i,(j+M+1)}\} \quad ; \quad i = 1 \ldots P, j = -M \ldots M$$

$$\Gamma_{\mu\nu}^{i,(j+M+1)} = \begin{cases} \gamma_{\mu\nu}(\Delta + Q - i - jQ) & for \quad 0 \leq \Delta + Q - i - jQ \leq G - 1 \\ 0 & otherwise \end{cases} \quad (23)$$

Since sampling takes place every Q chips and $W \leq Q$ it is sufficient to take into account the effect of $M = 2$ bits, in general. Substituting now eq. (22) into eq. (17) and assuming that:

$$E\{d_\mu^{m_1} d_\nu^{m_2}\} = \begin{cases} 1 & \mu = \nu \quad and \quad m_1 = m_2 \\ 0 & otherwise \end{cases} \quad (24)$$

it is proved that:

$$E[\mathbf{R}^T(T_{ss})\mathbf{R}(T_{ss})] = \begin{bmatrix} \sum^K & & & & \\ & \sum^K & \mathbf{0} & \ddots & \mathbf{0} \\ & \mathbf{0} & \sum^K & & \\ & \ddots & & \ddots & \\ & \mathbf{0} & & & \sum^K \end{bmatrix} \quad (25)$$

where $\sum^K = \sum_{k=1}^K \boldsymbol{\Gamma}_{\mu k}\boldsymbol{\Gamma}_{\mu k}^T$, and

and

$$E[\mathbf{R}^T(T_{ss})\mathbf{d}_0] = [\bar{\boldsymbol{\gamma}}_{11}^T \cdots \bar{\boldsymbol{\gamma}}_{KK}^T]^T \quad (26)$$

where $\bar{\boldsymbol{\gamma}}_{\mu\nu}$ is a P-length vector defined as:

$$\bar{\boldsymbol{\gamma}}_{\mu\nu} = [\Gamma_{\mu\nu}^{1,(M+1)} \cdots \Gamma_{\mu\nu}^{P,(M+1)}] \quad (27)$$

and $\Gamma_{\mu\nu}^{i,(M+1)}$ is given by eq. (23). By replacing now the expectation terms in eq. (20) with the righthand side of eq. (25) and eq. (26) the Wiener solution is fully determined in a closed form.

V. Simulation Results

In this section the performance of INVF is shown and compared to pre-RAKE, TP, JT and DPF. The BER performance we refer to is the averaged BER over all the users. BPSK data symbols d_k^m are spread by random binary spreading codes $\mathbf{c}_k$ of length $Q = 16$ chips and transmitted synchronously over the mobile channel. Variations of the received power due to path loss and log-normal fading are assumed to be eliminated by power control. The codes are also normalised to $\|\mathbf{c}_k\| = 1$. The mobile radio downlink channels are different for each user, their delay spread is $W = 11$ chips and the tap weights are normalised to $\|\mathbf{h}_k\| = 1$. Furthermore it is assumed that they are stationary with no Doppler effects and that the BS has perfect knowledge of their impulse response. For the DPF and INVF methods the delay, Δ, in sampling the output at the receiver is set to half the pre-filter length [11].

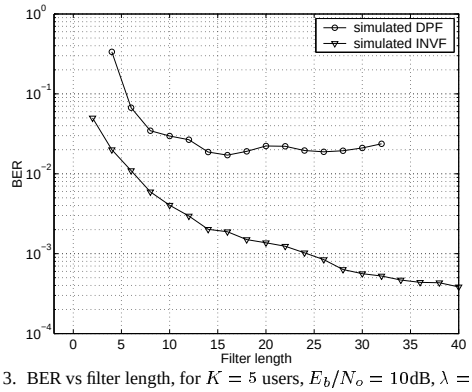

Fig. 3. BER vs filter length, for $K = 5$ users, $E_b/N_o = 10$dB, $\lambda = 0.05$.

In fig. 3 the BER performance versus the length of the pre-filter for the DPF and INVF is displayed for a CDMA system

of $K = 5$, $Q = 16$ and $E_b/N_o = 10$dB. The parameter λ in INVF is set to 0.05 for reasons that will be explained below. The performance of INVF dramatically exceeds the performance of DPF. According to the algorithm presented in [8] the pre-filter length for DPF is restricted to $P \leq \Delta + Q$ whereas the length for the INVF can be arbitrarily chosen.

A question arises as to what is the best choice for the parameter λ in eq. (20). Since λ is the power control term it is expected that the best value for it is a function of E_b/N_o. Fig. 4 shows how λ affects the BER for a system of $K = 5$, $Q = 16$ and $E_b/N_o = 10$dB for four different sets of 5 random codes when pre-filter length $P = 16, 32$. There is a range for λ which gives almost the optimum BER performance with a variety of spreading codes and pre-filter lengths. This gives a degree of freedom about the choice of λ. When $E_b/N_o = 10$dB λ is set to 0.05 which gives near optimum BER performance.

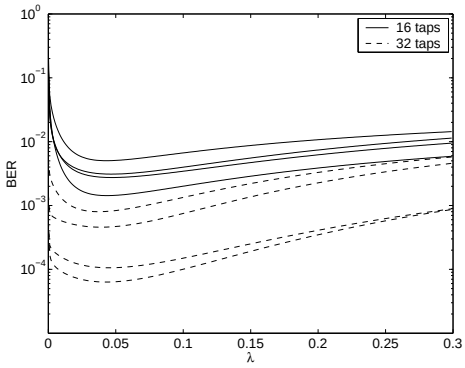

Fig. 4. INVF BER performance vs λ for $K = 5$, $E_b/N_o = 10$dB. Solid lines represent 4 sets of 5 random spreading codes when $P = 16$. Dashed lines represent 4 new sets of 5 randomly generated codes when $P = 32$.

In fig. 5 the BER versus the number of users is shown. The system's BER is averaged over 60 different sets of random codes to smooth out the effect of codes with low or high crosscorrelation. E_b/N_o is set to 10 dB, $Q = 16$. It is clear that INVF outperforms TP, Pre-RAKE and DPF. As mentioned before the block techniques, when used for data that is transmitted continually, do not account correctly for the end-bits of the block. Thus, these bits reduce the performance of the system. The problem is alleviated by increasing the length of the block at the cost of higher complexity. In fig. 5 the performance of JT is shown for blocks of $N = 1, 3$ and 20 data. INVF achieves better performance than JT for a heavily loaded CDMA system. When the number of users is less than half the spreading factor JT and INVF display equivalent performance, as illustrated in fig. 5, for a JT block length $N = 20$ bits. Ignoring the complexity of inverting the appropriate matrices, since it occurs only when the channel changes, we consider the multiplications required per transmitted symbol. Regarding eq. (7) the computational complexity per symbol for JT is $NQ(KN)^2/KN$ whereas for INVF it is PQ. Consequently, the complexity of INVF is far less as shown in table I.

VI. Conclusions

In this paper a new technique was proposed called inverse filters. The technique takes the structure presented in [8] and develops the power constrained MMSE solution. The performance of the INVF technique is dramatically better when compared with the ZF solution of DPF and also when compared with TP and pre-RAKE. JT achieves the INVF performance only for large blocks of data which results in a large computational cost for JT. Moreover for heavily loaded systems ($K \geq Q/2$), INVF gives superior performance to all the techniques. Inverse filters can be easily adjusted to any existing TDD/CDMA system with slowly varying propagation channels.

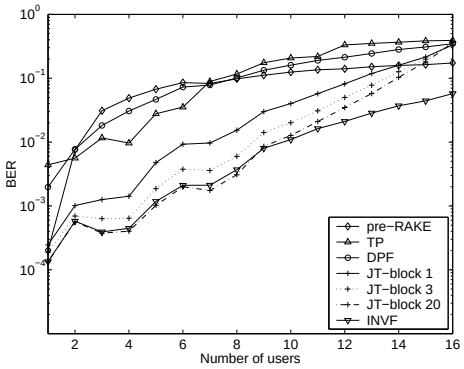

Fig. 5. $E_b/N_o = 10$dB, $N = 20$ for TP, $P = 32$ for INVF, DPF, $\lambda = 0.05$.

TABLE I

Computational Cost Comparison

Algorithm	Multiplications/symbol (excluding inversions)	Size of matrix to be inverted when channel changes
JT	$N^2KQ = 32000$	$NK \times NK = 100 \times 100$
INVF	$PQ = 512$	$PK \times PK = 160 \times 160$

Numerical examples for the case of $N = 20$, $K = 5$, $Q = 16$, $P = 32$.

References

[1] A. Klein, *Multi-user detection of CDMA signals-algorithms and their application to cellular mobile radio*, Fortschritt-Berichte VDI, 1996.

[2] Sergio Verdú, *Multiuser Detection*, Cambridge University Press, 1 edition, 1998.

[3] A. Duel-Hallen, J.H., and Z. Zvonar, "Multiuser detection for CDMA systems," *IEEE Personal Communications*, vol. 2, no. 2, pp. 46–58, Apr. 1995.

[4] B. R. Vojčić and W. M. Jang, "Transmitter precoding in synchronous multiuser communications," *IEEE Trans. on Communications*, vol. 46, no. 10, pp. 1346–1355, Oct. 1998.

[5] M. Meurer, P.W. Baier, T. Weber, Y. Lu, and A. Papathanasiou, "Joint transmission:advantageous downlink concept for CDMA mobile radio systems using time division duplexing," *IEE Electronics Letters*, vol. 36, pp. 900–901, May 2000.

[6] R. Esmailzadeh, E. Sourour, and M. Nakagawa, "Pre-rake diversity combining in time division duplex CDMA mobile communications," *IEEE Trans. on Vehicular Technology*, vol. 48, no. 3, pp. 795–801, May 1999.

[7] S. Georgoulis and D.G.M. Cruickshank, "Pre-equalization, transmitter precoding and joint transmission techniques for time division duplex CDMA," *IEE 3G 2001 Conference on Mobile Telecommunications Technologies*, pp. 257–261, Mar. 2001.

[8] M. Brandt-Pearce and A. Dharap, "Transmitter-based multiuser interference rejection for the down-link of a wireless CDMA system in a multipath environment," *IEEE Journal on Selected Areas in Communications*, vol. 18, no. 3, pp. 407–417, Mar. 2000.

[9] A. Papathanasiou, M. Meurer, T. Weber, and P.W. Baier, "A novel multiuser transmission scheme requiring no channel estimation and no equalization at the mobile stations for the downlink of TD-CDMA operating in the TDD mode," *IEEE Vehicular Technology Conference Fall 2000*, pp. 203–210, 2000.

[10] P.A. Nelson, H. Hamada, and S. Elliott, "Adaptive inverse filters for stereophonic sound reproduction," *IEEE Trans. on Signal Processing*, vol. 40, no. 7, pp. 1621–1632, Jul. 1992.

[11] Bernard Widrow, *Adaptive Signal Processing*, Prentice-Hall, 1985.

Transmitter Based Inverse Filters for Reducing MAI and ISI in TDD/CDMA Downlink

S.L. Georgoulis and D.G.M. Cruickshank

Abstract

Inverse filters (INVF) are introduced as a new transmitter based precoding scheme for the TDD/CDMA downlink. MAI and ISI are significantly reduced while the mobile station's (MS) structure is reduced to a filter matched to the user's spreading code. The method assumes knowledge of the channel at the transmitter which is feasible under Time Division Duplex (TDD). The new algorithm uses a MMSE criterion with power constraint. When compared with existing schemes, INVF increase the system performance while maintaining a low computational cost. The theoretical analysis is supported with simulation results. Analytical BER for any precoding algorithm is also calculated.

I. Introduction

Recently, work has been done on transmitter based algorithms that implement a *linear precoding* of the transmitted signal in a CDMA system aiming to reduce the multiple access interference (MAI) and intersymbol interference (ISI) prior to transmission. The algorithms utilise the fact that in a TDD scheme the downlink channel is known to the transmitter if the time elapsing between uplink and downlink transmissions is sufficiently small compared to the coherence time of the mobile radio channel. The receiver structure at the user equipment is then simplified to be a conventional matched filter, which only requires knowledge of the desired user's spreading code. Thus no channel estimation or adaptive equaliser is required at the mobile receiver. The extra computational cost is transfered to the base station (BS) where power and computational resources are more readily available. Such an approach also enhances the downlink system capacity since no system resources have to be allocated for the transmission of training signals on the downlink.

One straight forward transmitter technique is *pre-RAKE* [1] which includes pre-RAKE diversity combining at the transmitter but doesn't reduce the multiuser interference, as shown in [1], [2].

Authors are with the Institute for Digital Communications, School of Engineering and Electronics, The University of Edinburgh, Edinburgh EH9 3JL, UK. Emails:sg@ee.ed.ac.uk, dgmc@ee.ed.ac.uk

To achieve a better performance the transmitted signals in the downlink must be jointly optimised based on the spreading code and the channel impulse response of every user. These alternative techniques are derived following a zero-forcing (ZF) or minimum mean-squared error (MMSE) criteria and are classified as blockwise or bitwise, based on their realisation block diagram. The bitwise ones demonstrate less computational cost and additional advantages.

A new bitwise method is proposed in this paper, called *inverse filters* (INVF). The developed algorithm is an MMSE approach with the necessary power constraint included. The performance is superior to the previous developed bitwise and blockwise techniques when compared under a common framework.

The system model is given in section II. A discussion about blockwise and bitwise techniques along with the theoretical calculation of the BER is given in section III. Section IV presents a theoretical analysis of INVF. Section V deals with a comparison between recently published methods by means of simulations. The conclusions are drawn in section VI.

II. System Model

The system considered is a multiuser direct sequence TDD-CDMA with K active users in a cell communicating through a common BS. The BS has one antenna element and transmits synchronously over frequency selective channels to K MSs. The discrete time transmission model that follows is sampled at the chip rate $1/T_c$. For the sake of clarity we state that for any vector $\mathbf{x}$, $\|\mathbf{x}\|^2$ denotes the inner product $\mathbf{x}^T\mathbf{x}$ and for any matrix $\mathbf{X}$, $X^{i,j}$ denotes the element in the i_{th} row and j_{th} column.

The m_{th} symbol $d_k^m c_k(n)$ for user k, $k\epsilon\{1\cdots K\}$, is the BPSK modulated data d_k^m spread with the spreading code $c_k(n)$. The spreading code consists of Q chips and it is described by the vector $\mathbf{c}_k = [c_k(0)\cdots c_k(Q-1)]^T$, which is normalised such that $\|\mathbf{c}_k\| = 1$. The symbol interval is T_s so as $T_c = T_s/Q$. The k_{th} channel is characterised by its impulse response $h_k(n)$. It is considered as a finite impulse response filter (FIR) whose chip spaced tap coefficients are the vector $\mathbf{h}_k = [h_k(0)\cdots h_k(W-1)]^T$, where W is the delay spread. Assuming that the m_{th} symbol of power w_k^m is transmitted for the k_{th} user, the total transmitted downlink signal for the conventional CDMA downlink scenario is described as $s(n) = \sum_{k=1}^{K}\sqrt{w_k^m}d_k^m c_k(n)$. To simplify the analysis

we will assume that all the users are transmitted with equal power and thus w_k^m is normalised to one. Furthermore, data d_k^m are assumed to be independent from bit to bit and between users:

$$E\{d_\mu^{m_1} d_\nu^{m_2}\} = \begin{cases} 1 & \text{for } \mu = \nu \text{ and } m_1 = m_2 \\ 0 & \text{otherwise} \end{cases} \quad (1)$$

Let $\mathbf{d}_k$ be a vector sequence of $N = 2M+1$ transmitted bits for user k, $\mathbf{d}_k = [d_k^{-M} \cdots d_k^0 \cdots d_k^M]^T$. The vector $\mathbf{d}$ of length KN contains the bits of all the users and is defined as $\mathbf{d} = \left[\mathbf{d}_1^T \cdots \mathbf{d}_k^T \cdots \mathbf{d}_K^T\right]^T$. By defining now the $NQ \times N$ matrix $\mathbf{C}_k$ as $\mathbf{C}_k = blockdiag(\mathbf{c}_k \ldots \mathbf{c}_k)$ and the $NQ \times NK$ matrix $\mathbf{C}$ as $\mathbf{C} = \left[\mathbf{C}_1 \cdots \mathbf{C}_k \cdots \mathbf{C}_K\right]$, the NQ-length vector form $\mathbf{s}$ for signal $s(n)$, for a conventional CDMA downlink system and its corresponding total energy per transmitted symbol $\mathcal{E}_g$ is $\mathbf{s} = \mathbf{C}\mathbf{d}$ and $\mathcal{E}_g = trace\{\mathbf{C^T C}\}/N = K$, for $\|\mathbf{c}_k\| = 1$, respectively.

The receiver is a filter matched to the spreading code of the desired user with impulse response $c_k(Q-n)$. AWGN $\mathbf{v}$, with correlation matrix $\sigma^2\mathbf{I}$, is added to the received signal. The multipath channel length is assumed to be less than one symbol period and thus ISI is extended only to the next transmitted symbol. Throughout our analysis the users are synchronous (realistic for the downlink) and the BS has exact knowledge about all users spreading codes and channels which is satisfied for the TDD mode if the channel's dynamics are sufficiently slow. This means that the multipath profile remains essentially constant during transmission as, for example, in a personal communication system with low mobility users such as pedestrians in an outdoor environment.

III. Transmitter Based Techniques

In blockwise techniques a linear transformation matrix $\mathcal{T}$ is applied to the block of transmitted data $\mathbf{d}$ in order to minimise MAI and ISI. The transmitted vector $\mathbf{s}_p$ is written then as:

$$\mathbf{s}_p = \mathcal{T}\mathbf{d} \quad (2)$$

Matrix $\mathcal{T}$ is of dimension $NQ \times KN$ and is a function of the spreading codes and the channel impulse responses. Recently developed blockwise precoding algorithms are *joint transmission* JT [3] and *transmitter precoding* TP [4]. For a large block-length the computational cost is increased since these methods require inversion of matrices whose dimensions are proportional to the number of users and the block length. Furthermore, in the case of multipath channels and presuming that

the data are transmitted continuously, the first and last bits in a block are not correctly precoded which leads to a capacity loss.

In the bitwise techniques, like INVF, the data of user k after being spread are pre-filtered by an FIR filter of length P with impulse response $p_k(n)$ as shown in Fig. 1. Filtering is applied at the chip level and the higher computation required for data-block techniques is eliminated. Pre-filters do not modify the original CDMA structure directly as it is a simple addition of an array of FIR filters to the existing BS transmission system. The taps of the pre-filters are determined according to the adopted criteria. Bitwise techniques are the Pre-RAKE [1] and the ZF *decorrelating pre-filters* (DPF) [5]. It is essential for the derivation of theoretical BER to describe the bitwise techniques in the matrix form of eq. (2). This description is straight forward for the blockwise approach.

Vector $\mathbf{p}_k = [p_k(0) \cdots p_k(P-1)]^T$ represents the tap-coefficients of the k_{th} user specific FIR pre-filter. The transmitted symbol is now expanded to $d_k^m c_k(n) * p_k(n) = d_k^m g_k(n)$. Written in vector form, $g_k(n)$ has a length of $G = Q + P - 1$ chips and is denoted as $\mathbf{g}_k = [g_k(0) \cdots g_k(G-1)]^T$. Since the technique is bitwise we define as desired data-bits the d_k^0. The pre-filters impose intersymbol interference on the system and we must take into account M transmitted bits before and after the desired one. The right choice for M is $M = \langle (G-Q)/Q \rangle$ where $\langle x \rangle$ denotes that x is rounded up to the nearest integer. Let $y_k(n)$ be the signal at the output of the k_{th} pre-filter as shown in Fig. 1. The G-length transmitted vector for user k, $\mathbf{y}_k$, is written as $\mathbf{y}_k = \mathbf{G}_k \mathbf{d}_k$, where the $G \times N$, ($N = 2M + 1$), matrix $\mathbf{G}_k$ is:

$$\mathbf{G}_k = \{G_k^{i,(j+M+1)}\} \quad ; \quad i = 1...G, j = -M...M$$

$$G_k^{i,(j+M+1)} = \begin{cases} g_k(i - jQ - 1) & \text{for} \quad 0 \leq i - jQ - 1 \leq G - 1 \\ 0 & \text{otherwise} \end{cases} \tag{3}$$

The transmitted signal $\mathbf{s}_p$ can be written as the G-length vector $\mathbf{s}_p = \sum_{k=1}^{K=1} \mathbf{y}_k = \mathbf{G}\mathbf{d}$, where the $G \times NK$ matrix $\mathbf{G}$ is defined as $\mathbf{G} = \left[\mathbf{G}_1 \cdots \mathbf{G}_k \cdots \mathbf{G}_K\right]$. It is obvious that matrix $\mathbf{G}$ corresponds to $\mathcal{T}$ in eq. (2).

Now that $\mathcal{T}$ is defined for all precoding schemes we can proceed to a general analytical calculation of BER performance. It is similar to the one followed in [6] for receiver based linear multiuser detection techniques. The output vector $\hat{\mathbf{d}}_k$ at the receiver's matched filter can be expressed as

$\hat{\mathbf{d}}_k = \underbrace{\mathbf{B}_k^T \mathbf{H}_k \boldsymbol{\mathcal{T}}}_{\mathbf{A}_k} \mathbf{d} + \mathbf{B}_k^T \mathbf{v}$. Matrices $\mathbf{B}_k$ and $\mathbf{H}_k$ contain the columns of $\mathbf{c}_k$ and $\mathbf{h}_k$ associated with the k_{th} user's matched filter receiver and channel respectively. $\mathbf{A}_k$ is a $N \times KN$ matrix with elements $\{A_k^{i+M+1,j}\}$, $i = -M \ldots M,\ \ j = 1 \ldots KN$. Each component $\hat{d}_k^m, m = -M \ldots M$, in $\hat{\mathbf{d}}_k$ consists of three contributions, the first determined by the desired symbol d_k^m, the second determined by ISI and MAI and the third determined by additive noise. Thus, vector $\hat{\mathbf{d}}_k$ can be expressed as $\hat{\mathbf{d}}_k = \underbrace{diag\mathbf{A}_k\mathbf{d}}_{desired\,symbol} + \underbrace{\overline{diag}\mathbf{A}_k\mathbf{d}}_{ISI\,and\,MAI} + \underbrace{\mathbf{B}_k^T\mathbf{v}}_{noise}$. Matrix $diag\mathbf{A}_k$ is diagonal and contains only the diagonal elements of the matrix $\mathbf{A}_k$ while $\overline{diag}\mathbf{A}_k = \mathbf{A}_k - diag\mathbf{A}_k$ represents a matrix with zero diagonal elements containing all but the diagonal elements of $\mathbf{A}_k$. The covariance matrix of the noise term, is equal to $\mathbf{B}_k^T\mathbf{B}_k\sigma^2$ which equals to $\sigma^2\mathbf{I}$ after considering that $\|\mathbf{c}_k\| = 1$.

A performance measure is the signal-to-noise-plus-interference ratio (SNIR) $\phi(\hat{d}_k^m)$ of $\hat{d}_k^m$ at the receiver's output. In the analysis below we consider the bit $\hat{d}_k^0$, to allow for both the case of block and bitwise transmission. Taking into account the assumption in eq. (1) $\phi(\hat{d}_k^0)$ takes the form:

$$\phi(\hat{d}_k^0) = \frac{\left(A_k^{M+1,j'}\right)^2}{\sum_{\substack{j=1 \\ j\neq j'}}^{KN}\left(A_k^{M+1,j}\right)^2 + \sigma^2}, \quad j' = M + 1 + N(k-1) \tag{4}$$

By further assuming that the ISI and MAI follow a Gaussian distribution the error probability P_e for the detected BPSK bit $\hat{d}_k^0$ is given by applying the Q function $P_e(\hat{d}_k^0) = Q\left(\sqrt{\phi(\hat{d}_k^0)}\right)$. For a system of K users the average theoretical error probability is $\bar{P}_e(\hat{d}^0) = \left(\sum_{k=1}^{K} P_e(\hat{d}_k^0)\right)/K$.

IV. Proposed System

The precoding techniques, ignoring noise and assuming a unit gain channel, aim at $\hat{d}_k^m = d_k^m$. A certain transmit power is required for interference elimination which is usually greater than the one required for a conventional spreading. Thus, the transmitted signal $\mathbf{s}_p$ must be scaled with the appropriate factor $\sqrt{\mathcal{F}}$ to maintain the average transmitted power per symbol to the same level for all the techniques. The reference power used is the one for the corresponding conventional CDMA system, $\mathcal{E}_g$. If $\mathcal{F} < 1.0$, the scaling results in a decrease in the signal-to-noise ratio (SNR) at the receiver decision point. With this in mind, the optimum precoding technique is one that minimises the MAI and ISI and maximises $\mathcal{F}$, which implies the necessity of a power constraint. If the unscaled total transmission power per symbol produced by any algorithm is denoted as E_g, then $\mathcal{F}$ is given by $\mathcal{F} = \mathcal{E}_g/E_g$. To incorporate power constraint in the bitwise algorithm the E_g

must be expressed as a function of $\mathbf{p}$, which is a KP-length vector of pre-filter taps defined as $\mathbf{p} = [\mathbf{p}_1^T \cdots \mathbf{p}_k^T \cdots \mathbf{p}_K^T]^T$. It can be shown that:

$$E_g(\mathbf{p}) = \mathbf{p}^T \mathbf{U}^T \cdot \mathbf{U}\mathbf{p} \tag{5}$$

where matrix $\mathbf{U} = blockdiag\left(\mathbf{U}_1, \cdots, \mathbf{U}_k, \cdots \mathbf{U}_K\right)$ is of dimension $K(Q+P-1) \times KP$ and matrix $\mathbf{U}_k$ is of dimension $(Q+P-1) \times P$ and is defined as:

$$\mathbf{U}_k = \{U_k^{i,j}\}; \quad i = 1 \ldots Q+P-1, \quad j = 1 \ldots P$$

$$U_k^{i,j} = \begin{cases} c_k(i-j) & \text{for} \quad 0 \le i-j \le Q-1 \\ 0 & \text{otherwise} \end{cases} \tag{6}$$

Equation (5) is used in what follows to develop the INVF algorithm using MMSE criterion with power constraint[1] in order to determine vector $\mathbf{p}$. The method is essentially different from the ZF-DPF although they follow the same block diagram.

For simplicity we substitute the cascaded filters $h_k(n)$ and $c_k(Q-n)$ with an FIR filter of length $Z = Q + W - 1$ and impulse response $z_k(n) = h_k(n) * c_k(Q-n)$, as shown in Fig. 1. After rearrangement (only to facilitate the mathematical analysis), the system can equivalently be illustrated as in Fig. 2 for the μ_{th} receiver. Signals $r_{\mu\nu}(n)$ are defined as 'filtered reference signals' and are produced by passing the sequence of symbols $d_\nu^m c_\nu(n)$ through the filters with impulse response $z_\mu(n)$. This approach is essentially the one followed by [8] for stereophonic sound reproduction systems. This block diagram arrangement is used to determine the optimal, in MMSE terms, FIR filters, $\mathbf{p}_k$. The fact that noise is not included in the analysis doesn't affect the solution because the noise is not filtered by the inverse filters. The power constraint term imposed in the solution gives good noise performance.

Vectors $\mathbf{r}_{\mu\nu}(n) = [r_{\mu\nu}(n) \cdots r_{\mu\nu}(n-P+1)]^T$ correspond to the filtered reference signals. Following the block diagram in Fig. 2 the $r_{\mu\nu}(n)$ are passed through the pre-filters $\mathbf{p}$ to yield the estimated desired data. The outputs $\hat{\mathbf{d}}_0(n)$ can be written in matrix form as:

$$\hat{\mathbf{d}}_0(n) = \mathbf{R}(n)\mathbf{p} \tag{7}$$

[1] Power constraint has also been included in the technique developed in [7] but it is blockwise and is not examined further.

$$\hat{\mathbf{d}}_0(n) = \begin{bmatrix} \hat{d}_1^0(n) \\ \vdots \\ \hat{d}_K^0(n) \end{bmatrix}, \mathbf{R}(n) = \begin{bmatrix} \mathbf{r}_{11}^T(n) & \cdots & \mathbf{r}_{1K}^T(n) \\ \vdots & \ddots & \vdots \\ \mathbf{r}_{K1}^T(n) & \cdots & \mathbf{r}_{KK}^T(n) \end{bmatrix} \tag{8}$$

We now seek the optimal filter vector $\mathbf{p}$ to minimise the time averaged squared error between the actual and desired outputs. The desired outputs are sampled every symbol period $T_{ss} = nQ + \Delta$, $n = 1, 2, \ldots$, where Δ is an imposed delay to the system which assists the equalisation of the multipath channels. In the final cost function we must include, using Lagrange multipliers, the constraint that E_g, eq. (5) should not exceed the reference transmitted power per symbol $\mathcal{E}_g$. The cost function to be minimised is:

$$J = E[(\mathbf{d}_0 - \hat{\mathbf{d}}_0(T_{ss}))^T(\mathbf{d}_0 - \hat{\mathbf{d}}_0(T_{ss}))] + \lambda\big(E_g(\mathbf{p}) - \mathcal{E}_g\big) \tag{9}$$

where E denotes the expectation and $\mathbf{d}_0$ is the vector of desired data defined as $\mathbf{d}_0 = [d_1^0 \cdots d_k^0 \cdots d_K^0]^T$. By using eq. (7) and after expansion eq. (9) takes the quadratic form:

$$J = E[\mathbf{d}_0^T\mathbf{d}_0] - 2E[\mathbf{d}_0^T\mathbf{R}(T_{ss})]\mathbf{p} + \mathbf{p}^T E[\mathbf{R}^T(T_{ss})\mathbf{R}(T_{ss})]\mathbf{p} + \lambda\big(E_g(\mathbf{p}) - \mathcal{E}_g\big) \tag{10}$$

From vector gradient theory we find that $\vartheta E_g(\mathbf{p})/\vartheta\mathbf{p} = 2\mathbf{U}^T\mathbf{U}\mathbf{p}$. Therefore, the Wiener[2] solution for the taps of the pre-filters $\mathbf{p}_o$ is given by

$$\mathbf{p}_o = \big[E[\mathbf{R}^T(T_{ss})\mathbf{R}(T_{ss})] + \lambda\mathbf{U}^T\mathbf{U}\big]^{-1} E[\mathbf{R}^T(T_{ss})\mathbf{d}_0] \tag{11}$$

In order to complete the analysis, the expectation terms $E[\mathbf{R}^T(T_{ss})\mathbf{R}(T_{ss})]$ and $E[\mathbf{R}^T(T_{ss})\mathbf{d}_0]$ in eq. (11) must be calculated. As stated before $r_{\mu\nu}(n) = d_\nu^m c_\nu(n) * h_\mu(n) * c_\mu(Q-n)$. Let $\gamma_{\mu\nu}(n) = c_\nu(n) * h_\mu(n) * c_\mu(Q-n)$. The corresponding symbol in vector form is denoted as $\boldsymbol{\gamma}_{\mu\nu} = [\gamma_{\mu\nu}(0) \cdots \gamma_{\mu\nu}(G_\gamma - 1)]^T$ of length $G_\gamma = 2Q + W - 2$ due to the convolution effect. Vector $\mathbf{r}_{\mu\nu}(n)$, of length P, is given next as a function of the $N = 2M+1$ vector $\mathbf{d}_\nu$ accounting for the ISI effect. To assist the illustration of the Wiener solution it is assumed that $\Delta + Q \leq G_\gamma$, $\Delta + Q \geq P$ (in fact they can be arbitrarily chosen). In eq. (12) $\boldsymbol{\Gamma}_{\mu\nu}$ is a $P \times N$ matrix and $\mathbf{r}_{\mu\nu}$ is written as:

$$\mathbf{r}_{\mu\nu} = \boldsymbol{\Gamma}_{\mu\nu}\mathbf{d}_\nu \tag{12}$$

[2]The assumption that users are transmitted with powers $w_k^m = 1$ doesn't affect the final Wiener solution. For different powers Wiener solution is still $\mathbf{p}_o$ and the received powers will be proportionally different.

$$\mathbf{\Gamma}_{\mu\nu} = \{\Gamma_{\mu\nu}^{i,(j+M+1)}\} \quad ; \quad i = 1...P, j = -M...M$$

$$\Gamma_{\mu\nu}^{i,(j+M+1)} = \begin{cases} \gamma_{\mu\nu}(\Delta + Q - i - jQ) & \text{for} \quad 0 \leq \Delta + Q - i - jQ \leq G_\gamma - 1 \\ 0 & \text{otherwise} \end{cases} \tag{13}$$

By combining eq. (8) and eq. (12) we obtain:

$$\mathbf{R}(T_{ss}) = \begin{bmatrix} \mathbf{d}_1^T \mathbf{\Gamma}_{11}^T & \cdots & \mathbf{d}_K^T \mathbf{\Gamma}_{1K}^T \\ \vdots & \ddots & \vdots \\ \mathbf{d}_1^T \mathbf{\Gamma}_{K1}^T & \cdots & \mathbf{d}_K^T \mathbf{\Gamma}_{KK}^T \end{bmatrix} \tag{14}$$

Taking into account the assumption in eq. (1) it is proved that:

$$E[\mathbf{R}^T(T_{ss})\mathbf{R}(T_{ss})] = \begin{bmatrix} \sum_{\mu=1}^K \mathbf{\Gamma}_{\mu 1}\mathbf{\Gamma}_{\mu 1}^T & \mathbf{0} & \mathbf{0} \\ \mathbf{0} & \ddots & \mathbf{0} \\ \mathbf{0} & \mathbf{0} & \sum_{\mu=1}^K \mathbf{\Gamma}_{\mu K}\mathbf{\Gamma}_{\mu K}^T \end{bmatrix} \tag{15}$$

$$E[\mathbf{R}^T(T_{ss})\mathbf{d}_0] = [\bar{\boldsymbol{\gamma}}_{11}^T \cdots \bar{\boldsymbol{\gamma}}_{KK}^T]^T \tag{16}$$

where $\bar{\boldsymbol{\gamma}}_{\mu\nu}$ is a P-length vector defined as $\bar{\boldsymbol{\gamma}}_{\mu\nu} = [\Gamma_{\mu\nu}^{1,(M+1)} \cdots \Gamma_{\mu\nu}^{P,(M+1)}]$. $\Gamma_{\mu\nu}^{i,(M+1)}$ is given by eq. (13). By replacing now the expectation terms in eq. (11) with the right-hand side of eq. (15) and eq. (16) the Wiener solution is fully determined in a closed form.

V. Simulation Results

In this section the performance of the INVF is shown and compared to pre-RAKE, TP, JT and DPF. The BER performance, we refer to, is the averaged BER over all the users. BPSK data symbols d_k^m are spread by random binary spreading codes $\mathbf{c}_k$ of length $Q = 16$ and transmitted synchronously over the mobile channel. The mobile radio channels are different for each user and the tap weights are normalised such that $\|\mathbf{h}_k\| = 1$. The delay profile adopted is consistent with the UMTS European system and has a delay spread of $W = 11$ chips. In the current paper the channels are assumed to be stationary with no Doppler effects. Perfect knowledge of the downlink channel is presumed in the base station transmitter. For the DPF and INVF methods the delay Δ in sampling the output at the receiver is set to half the pre-filter length.

The Wiener solution as stated in eq. (11) contains the power control term $\lambda \mathbf{U}^T\mathbf{U}$. A question arises as to what is the best choice for the parameter λ. Since λ is the power control term it is

expected that the best value for it is a function of E_b/N_o. Figure 3 shows how λ affects the BER for a variety of schemes. There is a range for λ which gives almost the optimum BER performance with a variety of spreading codes and pre-filter lengths. This gives a degree of freedom about the choice of λ. A critical issue, in CDMA systems is to provide all users with equivalent performance under the assumption that signals of equal powers are addressed to them. That means that the SNIR ϕ_k must be approximately the same for every user. By defining the SNIR spread as $\Phi_s = max\{\phi_i\}/min\{\phi_j\} \quad i,j \epsilon \{1 \cdots K\}$ we have a measure of the variety among the K individual performances. Ideal values for Φ_s are close to unity. In Fig. 4 it is shown that large values of λ result in significant differences in the users performance while small values result in similar performance. A small value of λ minimises the contribution of the power control term in eq. (11) and the Wiener solution cancels MAI and ISI for all users at the cost of increasing the transmitted energy. This is reflected in a reduction of the receiver's output SNR when the transmitted power is normalised by $\mathcal{F} \leq 1$. In the contrast, a large value of λ enhances the power control so as $\mathcal{F} \geq 1$ but the penalty is a degradation in the SNIR spread. In Fig. 4 it is shown that for $E_b/N_o = 10$dB ideal values for λ are close to 0.05.

In Fig. 5 the BER versus the number of users is shown. The BER is averaged over 60 different sets of random codes to smooth out the effect of codes with low or high crosscorrelation. It is clear that INVF (P is set to 32) outperforms TP, Pre-RAKE and DPF. The effect of the data-block length N on JT is also illustrated. The problem is alleviated by increasing N at the cost of higher complexity. When $N = 32$, INVF achieves better performance than JT for a heavily loaded CDMA system and equivalent for $K \leq Q/2$. However, INVF displays significantly reduced complexity in terms of multiplications required per transmitted symbol Ω. Ignoring the complexity of inverting the appropriate matrices (it is identical for $N = P = 32$), since it occurs only when the channel changes, it can be shown that $\Omega^{INVF} = PQ = 512$ and $\Omega^{JT} = N^2KQ = 81920$, for $K = 5$.

The BER performance versus E_b/N_o for $K = 5, 14$ is shown in Fig. 6. In the JT curves the end-bits are being discarded to give the most optimistic performance. For $K = 5$ JT and INVF have similar performance. For $K = 14$ INVF is the best technique for reasonable E_b/N_o with a significant error floor in performance when $P = 32$. By increasing the number of taps to $P = 90$ taps and selecting $\lambda = 0.003$, ideal for $E_b/N_o = 20$dB, INVF performance is further improved and

becomes constantly better than JT. However, the penalty is a degradation, in the low E_b/N_o ratio region. This is due to the fact that $\lambda = 0.003$, selected for the case of $P = 90$, is not near optimum for $E_b/N_o = 10$dB. The above leads to the idea that if the base station knows the noise power at the receiver it can optimise the performance for high loaded systems by selecting the appropriate λ value. Theory and simulations are in remarkable agreement in the graph.

VI. Conclusions

Inverse filters were proposed as a new efficient bitwise transmitter based pre-coding technique. The technique takes the structure of DPF and develops the power constrained MMSE solution for individually pre-filtering the spread data before transmission. The performance of the INVF exceeds the one of Pre-RAKE, DPF and TP. It is competitive or better than JT but displays a lower computational cost. INVF can be easily adjusted to any existing TDD/CDMA system with slowly varying propagation channels.

References

[1] R. Esmailzadeh and M. Nakagawa, "Pre-RAKE diversity combination for direct sequence spread spectrum communications systems," *International Conference on Communications*, vol. 1, pp. 463–467, Geneva 1993.

[2] S. Georgoulis and D.G.M. Cruickshank, "Pre-equalization, transmitter precoding and joint transmission techniques for time division duplex CDMA," *IEE 3G 2001 Conference on Mobile Telecommunications Technologies*, pp. 257–261, Mar. 2001.

[3] A. Papathanasiou, M. Meurer, T. Weber, and P.W. Baier, "A novel multiuser transmission scheme requiring no channel estimation and no equalization at the mobile stations for the downlink of TD-CDMA operating in the TDD mode," *IEEE Vehicular Technology Conference Fall 2000*, pp. 203–210, 2000.

[4] B. R. Vojčić and W. M. Jang, "Transmitter precoding in synchronous multiuser communications," *IEEE Trans. on Communications*, vol. 46, no. 10, pp. 1346–1355, Oct. 1998.

[5] M. Brandt-Pearce and A. Dharap, "Transmitter-based multiuser interference rejection for the down-link of a wireless CDMA system in a multipath environment," *IEEE Journal on Selected Areas in Communications*, vol. 18, no. 3, pp. 407–417, Mar. 2000.

[6] A. Klein, *Multi-user detection of CDMA signals-algorithms and their application to cellular mobile radio*, Fortschritt-Berichte VDI, 1996.

[7] A.N. Barreto and G. Fettweis, "Capacity increase in the downlink of spread spectrum systems through joint signal precoding," *in Proc. ICC*, vol. 4, pp. 1142–1146, 2001.

[8] P.A. Nelson, H. Hamada, and S. Elliott, "Adaptive inverse filters for stereophonic sound reproduction," *IEEE Trans. on Signal Processing*, vol. 40, no. 7, pp. 1621–1632, Jul. 1992.

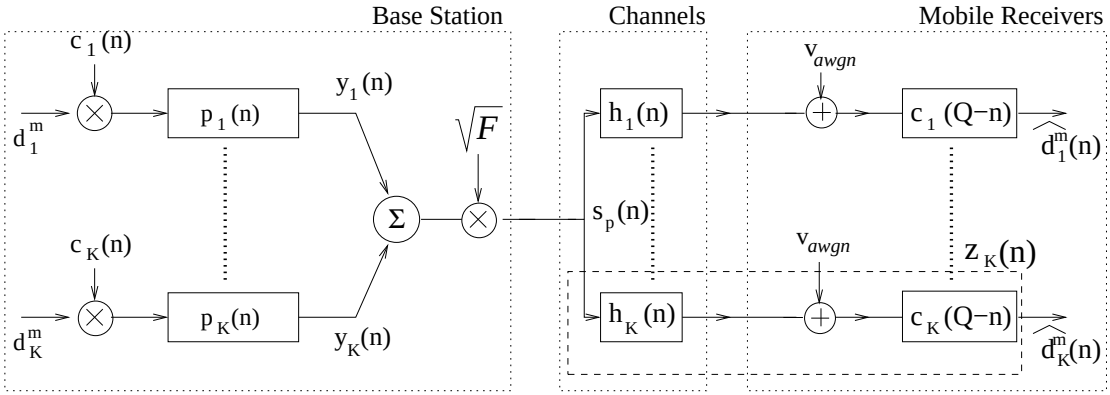

Fig. 1. Block diagram of a bitwise system

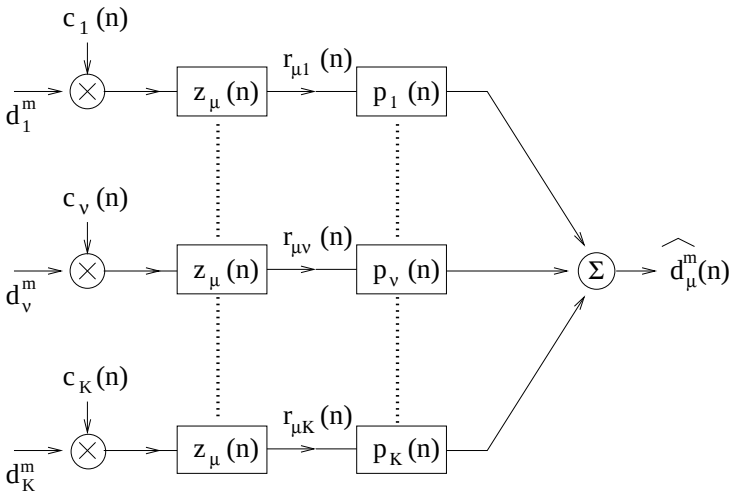

Fig. 2. Rearranged system diagram

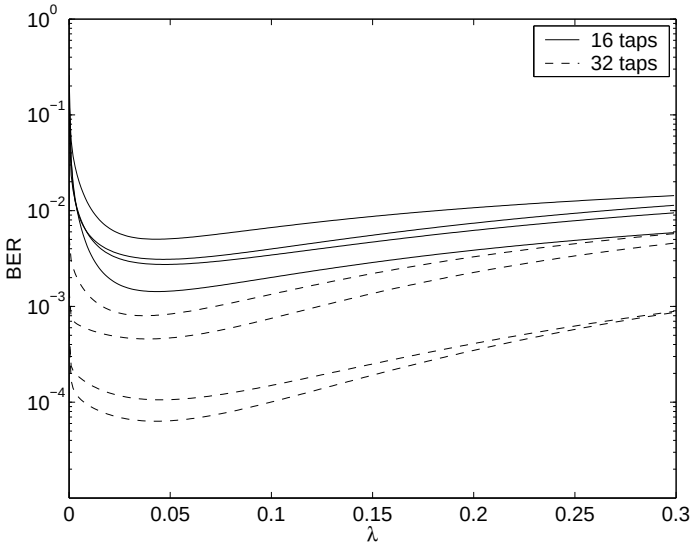

Fig. 3. BER performance for INVF vs λ for $K = 5$, $Q = 16$, $W = 11$, $E_b/N_o = 10$dB. The solid lines represent analytical results for 4 sets of 5 different random spreading codes when $P = 16$. The dashed lines represent analytical results for 4 new sets of 5 randomly generated codes when $P = 32$.

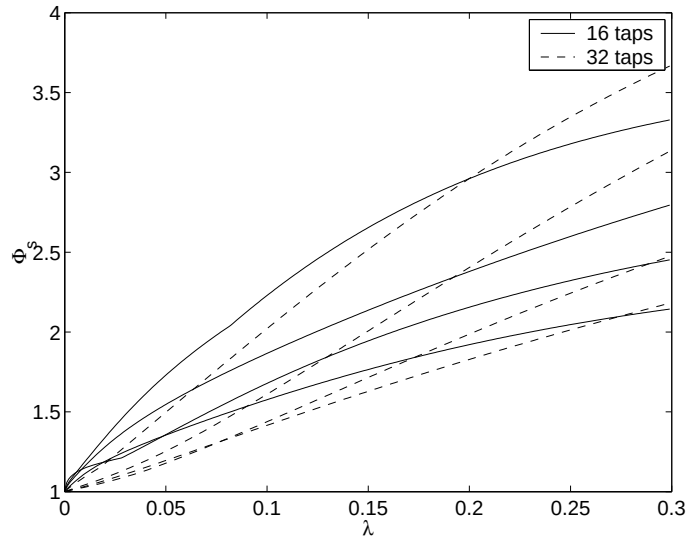

Fig. 4. SNIR spread vs λ for $K = 5$, $Q = 16$, $W = 11$, $E_b/N_o = 10$dB. The solid lines represent analytical results for 4 sets of 5 different random spreading codes when $P = 16$. The dashed lines represent analytical results for 4 new sets of 5 randomly generated codes when $P = 32$.

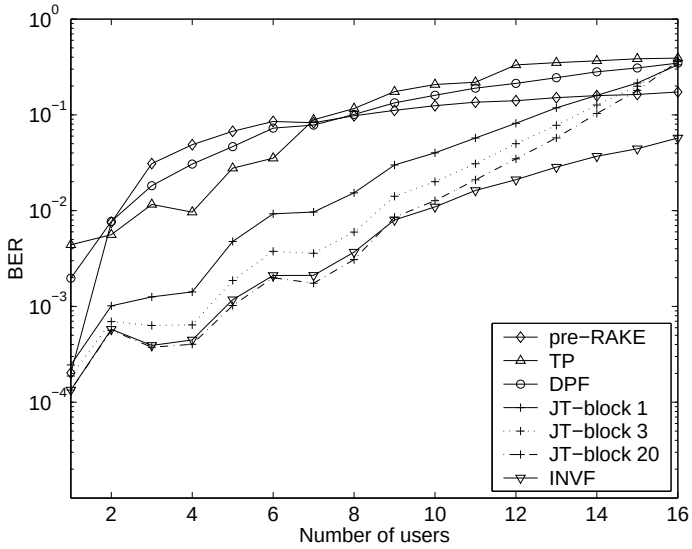

Fig. 5. Simulated BER performance vs number of users for $E_b/N_o = 10$dB, $Q = 16$, $W = 11$. For TP the length of the transmitted blocks has been set to $N = 32$. A length $P = 32$ has been selected for INVF and DPF and $\lambda = 0.05$ for INVF.

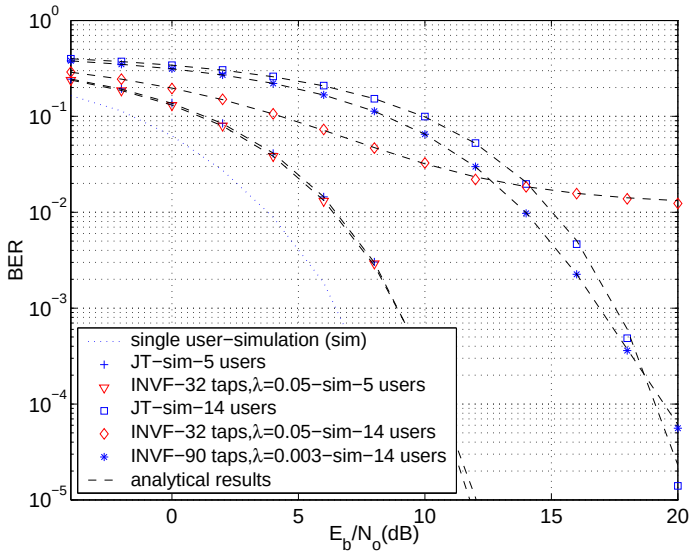

Fig. 6. BER vs E_b/N_o for $K = 5, 14$ users. System parameters are $Q = 16$, $W = 11$. The markers correspond to the simulation results and the dashed lines to the corresponding analytical ones.